

Sommaire

Liste des figures.....XII

Liste des tableaux.....XV

INTRODUCTION1

1^{ÈRE} PARTIE.....5

Chapitre 1 : Phytodisponibilité des éléments traces dans les sols – généralités.....7

I. Origine et teneurs des éléments traces dans les sols 7

II. Deux catégories d'éléments traces : essentiels ou non-essentiels 8

III. Toxicité des éléments traces 9

III.1. Fraction phytodisponible 9

III.2. Phytotoxicité des éléments traces.....10

Chapitre 2 : Caractérisation expérimentale des interactions physico-chimiques éléments traces - racines..... 15

I. Transfert racinaire des éléments traces15

I.1. Les voies apoplasmiques et symplasmiques15

I.2. Localisation des éléments traces dans les racines.....16

II. Le compartiment apoplasmique18

II.1. La lamelle moyenne et les parois apoplasmiques18

II.2. Composition chimique des parois apoplasmiques.....20

II.3. Capacité de complexation de l'apoplasme racinaire24

III. Les membranes plasmiques.....26

III.1. Composition chimique des membranes plasmiques26

III.2. Capacité de complexation des membranes plasmiques.....27

IV. Spéciation des éléments traces dans les racines28

<i>Chapitre 3 : Modélisation des interactions éléments traces - racines</i>	31
I. Le modèle électrostatique.....	31
I.1. Principales hypothèses et applications	32
I.2. Principales limites.....	33
II. Les modèles de complexation.....	34
II.1. Principales hypothèses communes.....	34
II.2. Le TBLM.....	36
II.3. Les modèles basés sur les substances humiques	37
II.4. Limites des modèles de complexation	38
 <i>Chapitre 4 : Objectifs et stratégies de recherche</i>	 41
I. Hypothèse de travail	41
II. Objectifs.....	41
III. Modèles expérimentaux	42
III.1. Le cuivre : élément trace modèle	42
III.2. La tomate et le blé : espèces végétales modèles.....	43
IV. Approches expérimentales et modélisation	43
 2^{ÈME} PARTIE	 57
 <i>Chapitre 5 : Origine des propriétés de complexation des racines</i>	 59
I. Introduction.....	62
II. Material and methods	64
II.1. Plant growth.....	64
II.2. Isolation of root cell walls	64
II.3. Determination of the cation exchange capacity of roots and cell walls	65
II.4. Characterization of the acidic properties of roots and cell walls by potentiometric titration	65
II.5. Identification of the chemical structure of roots and cell walls by solid-state ¹³ C-NMR spectroscopy	66

III.	Results.....	67
III.1.	Loss of mineral elements during the isolation procedure.....	67
III.2.	Cation exchange capacity of roots and cell walls	68
III.3.	Acidic properties of roots and cell walls	68
III.4.	¹³ C-NMR spectra of roots and cell walls.....	70
IV.	Discussion.....	72
IV.1.	Efficiency of the cell wall isolation procedure.....	72
IV.2.	Limited contribution of cell walls to the total binding capacity of roots.....	74
IV.3.	Distinct acidic properties of roots and cell walls related to the chemical nature of binding sites	75
V.	Conclusion.....	77

Chapitre 6 : Rôle des acides aminés dans la complexation du cuivre au sein du continuum parois apoplasmiques – membranes plasmiques

I.	Introduction.....	88
II.	Material and methods	89
II.1.	Plant growth and isolation of root cell walls.....	89
II.2.	Experimental batches of copper sorption on roots and cell walls	90
II.2.a.	Experiment 1	90
II.2.b.	Experiment 2	90
II.2.c.	Experiment 3	91
II.3.	Copper speciation in roots and cell walls by X-ray absorption spectroscopy	91
II.4.	Identification of Cu binding functional groups by NMR	91
II.5.	Modeling copper sorption on roots, cell walls and plasma membranes	92
III.	Results.....	93
III.1.	Copper speciation in roots and cell walls	93
III.2.	Identification of functional groups involved in Cu binding by ¹³ C-NMR	96
III.3.	Modeling the acidic properties of roots, cell walls and plasma membranes.....	99
III.4.	Copper sorption on roots, cell walls and plasma membranes.....	101
III.5.	Modeling copper sorption on roots, cell walls and plasma membranes	101

IV.	Discussion.....	104
IV.1.	Dual copper coordination with carboxyl and amine groups.....	104
IV.2.	High-affinity copper complexation.....	105
IV.3.	Relative contribution of cell walls and plasma membranes.....	106
IV.4.	Interspecific comparison.....	107
IV.5.	The HLScale under-estimates the contribution of amino acids	107
V.	Conclusion.....	108
VI.	Supporting information	109
 3^{ÈME} PARTIE		123
 <i>Chapitre 7 : Développement d'un modèle de prédiction de la complexation du cuivre dans les racines.....</i>		
I.	Introduction.....	128
II.	Experimental approach.....	130
II.1.	Plant root material.....	130
II.2.	Potentiometric titration	130
II.3.	Copper sorption experiments.....	130
III.	Modeling approach.....	131
IV.	Results and discussion.....	133
IV.1.	Ability of WHAM-THP to predict root acidic properties.....	133
IV.2.	Ability of WHAM-THP to predict copper binding on roots.....	136
IV.2.a.	Root copper binding affinity	136
IV.2.b.	Influence of ionic strength.....	138
IV.2.c.	Proton competition.....	140
IV.2.d.	Calcium and zinc competition	142
IV.3.	Perspectives for the application of WHAM-THP in predictive ecotoxicology ..	144
V.	Supporting information.....	146
 CONCLUSION ET PERSPECTIVES		160

Liste des figures

- Figure 1 : Courbe dose-réponse d'un élément essentiel (A) et d'un élément uniquement toxique (B ; d'après Adriano 2001 (modifiée))..... 9
- Figure 2 : Diminution de la biomasse de l'origan (*Origanum vulgare* subsp. *Hirtum*) avec l'augmentation de la concentration en Cu dans le sol.....10
- Figure 3 : Symptômes de rhizotoxicité.....11
- Figure 4 : Coupe d'une racine présentant les deux voies de transfert des minéraux depuis la solution de sol jusqu'au xylème (site internet biologie-forums.com).....15
- Figure 5 : Localisation des ET dans les racines.....17
- Figure 6 : Représentation schématique d'une cellule végétale entourée des parois apoplasmiques (A) (site internet phschool.com) ; image MET (microscope électronique à transmission) de parois apoplasmiques racinaires d'*Arabidopsis thaliana* (B).18
- Figure 7 : Représentation 3D de l'apoplasme racinaire d'une jeune cellule (site internet : wpclipart.com).....19
- Figure 8 : Structure chimique des principaux constituants des parois apoplasmiques (monomères à gauche et polymères respectifs à droite ; Sarkar et al. 2009).....22
- Figure 9 : Formation de gel pectique par l'intermédiaire de structures en « egg-box » (d'après Carpita and Gibeaut 1993).23
- Figure 10 : Schéma représentant l'adsorption des ET (ici Pb) au sein de chaînes de polymères pectiques (Krzyszowska 2011).....25
- Figure 11 : Représentation schématique d'une membrane plasmique (extrait de Taiz and Zeiger 2006).....27
- Figure 12 : Capacité de l'activité de Cu^{2+} en solution (a) et de l'activité de Cu^{2+} à la surface des membranes plasmiques (b) à décrire l'élongation racinaire relative chez *Vigna unguiculata* L. Walp (Kopittke et al. 2011b).33
- Figure 13 : Représentation schématique des équilibres chimiques qui existent entre le cation métallique, les constituants du sol et de la solution de sol et les sites réactifs situés à la surface de l'organisme (ici dénommés Biotic Ligand, Thakali et al. 2006a).34
- Figure 14 : Courbe dose-réponse présentant l'évolution du taux d'élongation racinaire d'*Hordeum vulgare* en fonction de la quantité de sites occupés par du Ni (Thakali et al. 2006a).....35
- Figure 15 : Elongation racinaire prédite avec (i) le TMM (considération de la concentration totale en Cu du sol), (ii) le FIAM (considération de l'activité de Cu^{2+} libre dans la solution de sol) et (iii) le TBLM (avec prise en compte de la compétition avec le proton) en fonction de l'élongation racinaire mesurée chez l'orge (*Hordeum vulgare* cv. *Regina*, exposé à des sols présentant différents niveaux de contamination en Cu ainsi que des propriétés physico-chimiques variées ;Thakali et al. 2006a).....37
- Figure 16 : Percentage of the mass of copper (Cu), iron (Fe), calcium (Ca), phosphorus (P) and potassium (K) in roots lost in cell walls after the 30-d isolation procedure for wheat (filled bars) and tomato (empty bars).67

Figure 17 : Cation exchange capacity (CEC) of roots (filled bars) and cell walls (empty bars) of wheat and tomato.....	68
Figure 18 : Potentiometric titrations for roots (filled symbols) and cell walls (empty symbols) of wheat (squares) and tomato (circles) expressed in charge (Q) corrected by the initial charge (Q ₀).....	70
Figure 19 : ¹³ C-NMR spectra of roots (solid line) and cell walls (dotted line) of wheat (a) and tomato (b).....	71
Figure 20 : Cell wall to root signal ratios for the different ¹³ C-NMR spectra regions for wheat (filled bars) and tomato (empty bars).....	72
Figure 21 : Normalized Cu K-edge X-ray absorption near-edge spectroscopy (XANES) spectra for wheat and tomato roots (R) and cell walls (CW) and for two reference compounds, Cu(I)-cysteine and Cu(II)-malate.	94
Figure 22 : Cu K-edge k ² -weighted extended X-ray absorption fine structure (EXAFS) spectra (a) and their radial distribution function (RDF) (b) for wheat and tomato roots (R) and cell walls (CW) and for three reference compounds, Cu(II)-histidine, Cu(II)-formate and Cu(I)-cysteine.....	95
Figure 23 : Proportion for each Cu ligands resulting in the best linear combination fitting of the Cu K-edge k ² -weighted extended X-ray absorption fine structure (EXAFS) spectra of roots (R) and cell walls (CW) of wheat and tomato.	96
Figure 24 : ¹³ C-NMR spectra of (a) wheat roots containing copper bound at 0 (black line), 4855 (orange line) and 8023 (green line) mg.kg ⁻¹ dry mass and (b) tomato roots containing copper bound at 0 (black line), 832 (red line), 2785 (blue line) and 9864 (purple line) mg.kg ⁻¹ dry mass.....	98
Figure 25 : Potentiometric titrations for roots (filled symbols) and cell walls (empty symbols) of wheat (squares) and tomato (circles) expressed in charge (Q) corrected by the initial charge (Q ₀).....	99
Figure 26 : Copper binding by roots (filled symbols) and cell walls (empty symbols) of wheat (a) and tomato (b).....	103
Figure 27 : Potentiometric titrations of wheat (squares) and tomato (circles) expressed in charge (Q) corrected by the initial charge (Q ₀).....	134
Figure 28 : Copper binding on wheat (squares, a) and tomato (circles, b) roots at pH 4.7 (± 0.2) and ionic strength of 0.03 M.	137
Figure 29 : Copper binding on wheat (squares, a) and tomato (circles, b) roots at an ionic strength of 0.6 mM (blue symbols) or 0.3 M (red symbols) and at pH 4.7 (± 0.2) (see experiment 2 in section II.3).....	139
Figure 30 : Copper binding on wheat (squares, a) and tomato (circles, b) roots at pH 6.3 (± 0.1) (blue symbols) and pH 4.1 (± 0.1) (red symbols) with an ionic strength of 0.03 M (see experiment 3 in section II.3).....	141
Figure 31 : Copper binding on wheat (squares, a) and tomato (circles, b) in the presence of Ca (empty symbols) and Zn (filled symbols) at an ionic strength of 0.03 M and pH 5.1 (± 0.4) and 4.7 (± 0.1), respectively.	143
Figure S 1 : Potentiometric titrations for roots (filled symbols) and cell walls (empty symbols) of wheat (squares) and tomato (circles) expressed in charge (Q) corrected by the initial charge (Q ₀).....	113

Figure S 2 : Theoretical potentiometric titrations for wheat (triangles) and tomato (cross) plasma membranes expressed in charge (Q) corrected by the initial charge (Q_0).....	114
Figure S 3 : Theoretical copper binding (Cu_{ads}) by wheat (triangles) and tomato (cross) plasma membranes.....	115
Figure S 4 : Comparison of copper binding (Cu_{ads}) between experiment 1 (grey symbols), experiment 2 (star symbols) and 3 (colorful symbols) in wheat (a) and tomato (c) roots and wheat (b) and tomato (d) cell walls.....	116
Figure S 5 : Visible shift (arrows) in the first oscillation of the Cu K-edge k^2 -weighted extended X-ray absorption fine structure (EXAFS) spectra for wheat (black line) and tomato (grey line) roots, as similarly observed between the two reference compounds, Cu(II)-histidine (dotted black line) and Cu(II)-formate (dotted grey line).....	117
Figure S 6 : Distribution of copper between HA_I (black line) and HA_{II} (dotted line) in wheat roots (a), cell walls (c) and plasma membranes (e) and tomato roots (b), cell walls (d) and plasma membranes (f).....	118
Figure S 7 : Charge borne by wheat (squares) and tomato (circles) roots as calculated with WHAM for terrestrial higher plants parameterized independently for each species (WHAM-THPips) and parameterized for both species concomitantly (WHAM-THP).....	150
Figure S 8 : Copper adsorbed by wheat (squares) and tomato (circles) roots at pH 4.7 (± 0.2) as calculated with WHAM for terrestrial higher plants parameterized independently for each species (WHAM-THPips) and parameterized for both species concomitantly (WHAM-THP).....	151
Figure S 9 : Copper adsorbed by wheat (squares) and tomato (circles) roots at different pH (pH 4.1 (± 0.1) (red) ; and pH 6.3 (± 0.1) (blue)) as calculated with WHAM for terrestrial higher plants parameterized independently for each species (WHAM-THPips) and parameterized for both species concomitantly (WHAM-THP).....	152
Figure S 10 : Copper adsorbed by wheat (squares) and tomato (circles) roots at different ionic strength (0.3 M (red) and 0.6 mM (blue)) as calculated with WHAM for terrestrial higher plants parameterized independently for each species (WHAM-THPips) and parameterized for both species concomitantly (WHAM-THP).....	153
Figure S 11 : Copper adsorbed by wheat (squares) and tomato (circles) roots in presence of Zn (filled symbols) and Ca (empty symbols) as calculated with WHAM for terrestrial higher plants parameterized independently for each species (WHAM-THPips) and parameterized for both species concomitantly (WHAM-THP).....	154
Figure S 12 : Relationship between the cation exchange capacity (CEC) and the total binding site density (HA_T) of wheat cell walls (green), wheat roots (blue), tomato cell walls (purple), ray-grass roots (yellow), tomato roots (red) and the roots of tomato sitiens mutant (black).	155

Liste des tableaux

<i>Tableau 1 : Constantes de complexation déterminées pour l'orge</i>	39
<i>Table 2 : Acidic properties of wheat and tomato roots and cell walls</i>	69
<i>Table 3 : Acidic properties modelled from experimental data for wheat and tomato roots, cell walls (CW) and derived from theoretical potentiometric titrations for plasma membranes (PM)</i>	100
<i>Table 4 : Copper sorption properties modelled from experimental data for wheat and tomato roots, cell walls (CW) and derived from theoretical sorption data for plasma membranes (PM)</i>	102
<i>Table 5 : Total site densities (L_{Hi}, $\text{cmol}_c \cdot \text{kg}^{-1}$), proton dissociation constants ($\text{p}K_{a_i}$) and distribution terms ($\Delta \text{p}K_{a_i}$) of wheat and tomato roots parameterized in WHAM and WHAM-THP (see section III for further rationale)</i>	135
<i>Tableau 6 : Intrinsic equilibrium constants ($K_{M,i}$) and heterogeneity parameters ($\Delta \text{LK}2_{M,i}$) of copper (Cu), calcium (Ca) and zinc (Zn) binding on wheat and tomato roots parameterized in WHAM and WHAM-THP (see section III for further rationale)</i>	138
<i>Table S 1 : Initial (pCu_T) and at equilibrium (pCu_{eq}) copper concentration and pH for each data point of experiment 3</i>	111
<i>Table S 2 : Concentration of Cu bound (Cu_{ads}) and proportion for each Cu ligands resulting in the best linear fitting of the Cu K-edge extended X-ray absorption fine structure (EXAFS) spectra for wheat and tomato roots (R) and cell walls (CW), depending the initial copper concentration (pCu_T)</i>	112
<i>Table S 3 : Initial (pM_T) and final/equilibrium (pM_{eq}) concentration of copper, calcium and zinc, pH measured and ionic strength (IS) fixed in each batch experiment of copper binding on wheat roots (see section II.3 for further information)</i>	147
<i>Table S 4 : Initial (pM_T) and final/equilibrium (pM_{eq}) concentration of copper, calcium and zinc and pH measured and ionic strength (IS) fixed in each batch experiment of copper binding on tomato roots (see section II.3 for further information)</i>	148
<i>Table S 5 : Total site densities (L_{Hi}, $\text{cmol}_c \cdot \text{kg}^{-1}$), proton dissociation constants ($\text{p}K_{a_i}$) and distribution terms ($\Delta \text{p}K_{a_i}$) of wheat and tomato roots parameterized in WHAM-2HA</i>	149

INTRODUCTION

Le sol est un compartiment essentiel de notre environnement. Milieu complexe et multifonctionnel, il abrite une importante biodiversité et joue un rôle clé dans les cycles biogéochimiques (Calvet 2003). Du fait de son processus de formation extrêmement lent, le sol constitue une ressource non renouvelable à l'échelle humaine. Il est cependant sujet à de nombreux processus de dégradation dont les causes sont multiples (érosion, diminution de la matière organique, tassements, salinisation, etc.), et dont les conséquences peuvent être dramatiques pour l'Homme et l'environnement.

La conséquence des activités humaines sur la qualité des sols est une préoccupation récente. La contamination fait partie des principales menaces qui pèsent sur les sols. En 2006, le nombre de sites potentiellement contaminés dans l'Europe des 25 avait ainsi été estimé à 3,5 millions (CEE 2006). Parmi les différents contaminants répertoriés, les éléments traces (ET) sont les contaminants du sol que l'on retrouve le plus fréquemment sur ces sites. Les industries (exploitations minières, fonderies, etc.), l'agriculture (par l'emploi d'engrais, de pesticides, etc.) et le trafic urbain sont autant de sources de contamination ponctuelles ou diffuses en ET (Nagajyoti et al. 2010; Belon et al. 2012; Zhou et al. 2013).

N'étant soumis à aucun phénomène de dégradation et étant relativement peu sujets aux transferts verticaux vers les aquifères, les ET s'accumulent dans les sols où ils peuvent atteindre des concentrations toxiques pour les organismes vivants (faune, flore et microflore). En contexte agricole, la contamination des sols peut engendrer deux types de conséquences. Ayant une forte propension à s'accumuler dans la plante tout en n'altérant pas ou peu leur croissance à ces niveaux de concentration, les ET caractérisés de phyto-accumulables, tels que le cadmium (Cd) ou le plomb (Pb), peuvent entraîner une contamination de la chaîne alimentaire et atteindre l'Homme. A l'inverse, par leur caractère phytotoxique, certains ET tels que le cuivre (Cu) ou le zinc (Zn), peuvent provoquer une baisse des rendements des cultures (Adriano 2001).

Les racines des plantes sont le premier organe exposé aux contaminations métalliques des sols et sont de ce fait le premier site d'expression de la toxicité d'un ET (i.e. rhizotoxicité). Les mécanismes biochimiques entraînant une toxicité ne sont pas connus avec exactitude. Néanmoins, de nombreux travaux ont mis en évidence le fait que la toxicité d'un métal n'est pas directement reliée à sa concentration totale dans le milieu mais à une fraction dite

disponible, susceptible d'interagir avec les racines des plantes (Harmsen 2007). Cette interaction implique plusieurs étapes dont le processus-clé est l'adsorption de l'ET sur les surfaces racinaires.

L'intérêt d'étudier les mécanismes physico-chimiques de l'interaction ET – surface racinaire réside dans le fait de vouloir comprendre et prédire la conséquence d'une contamination sur une plante. Cette capacité de prédiction passe par la construction d'un formalisme mathématique modélisant les effets d'une contamination du sol sur la nutrition et la croissance d'une plante. Différents modèles ont été développés à ce jour et donnent de bons résultats. Cependant, le manque de généralité de certains de leurs paramètres et la multiplication des cas particuliers où leur application est limitée témoignent d'une nécessité de remettre en cause certaines hypothèses, initialement simplifiées pour faciliter leur développement.

Ces travaux de thèse proposent donc une nouvelle approche de modélisation, centrée sur l'étude de la complexation de l'ET au niveau des surfaces racinaires plutôt que sur l'observation d'un effet toxique, comme cela est classiquement le cas. Ils apportent des éléments de réponse sur les principaux sites d'interaction entre l'ET et la racine, problématique peu étudiée jusqu'à présent. Ils présentent également un nouvel outil de prédiction dédié à l'étude de la complexation des ET au sein des racines.

Ce manuscrit s'articule en trois parties. La première partie est dédiée à l'état de l'art sur les interactions entre les éléments traces et les racines des plantes et sur les modèles de prédiction existants. La deuxième partie est consacrée à l'étude des mécanismes de complexation racinaire. Quant à la dernière partie, elle présente le modèle de prédiction de la complexation du Cu dans les racines que j'ai développé.

Références bibliographiques

- Adriano DC (2001) Trace Elements in Terrestrial Environments : Biogeochemistry, Bioavailability, and Risks of Metals. Springer Edition:867 pp.
- Belon E, Boisson M, Deportes IZ, Eglin TK, Feix I, Bispo AO, Galsomies L, Leblond S, Guellier CR (2012) An inventory of trace elements inputs to French agricultural soils. Science of The Total Environment 439 (0):87-95. doi:<http://dx.doi.org/10.1016/j.scitotenv.2012.09.011>.
- CEE Commission des Communautés Européennes 2006 Communication de la commission au conseil, au parlement européen, au comité économique et social européen et au comité des régions - Stratégie thématique en faveur de la protection de sols, Bruxelles. 13 p.
- Calvet R (2003) Le sol : propriétés et fonctions. Tome 1 : constitution et structure, phénomènes aux interfaces. . Editions France Agricole
- Harmsen J (2007) Measuring Bioavailability: From a Scientific Approach to Standard Methods. J Environ Qual 36 (5):1420-1428. doi:10.2134/jeq2006.0492
- Nagajyoti P, Lee K, Sreekanth T (2010) Heavy metals, occurrence and toxicity for plants: a review. Environmental Chemistry Letters 8 (3):199-216. doi:10.1007/s10311-010-0297-8
- Zhou H, Zeng M, Zhou X, Liao B-H, Liu J, Lei M, Zhong Q-Y, Zeng H (2013) Assessment of heavy metal contamination and bioaccumulation in soybean plants from mining and smelting areas of southern Hunan Province, China. Environmental Toxicology and Chemistry 32 (12):2719-2727. doi:10.1002/etc.2389

Rapport-gratuit.com 
LE NUMERO 1 MONDIAL DU MÉMOIRES

1^{ÈRE} PARTIE

**SYNTHÈSE
BIBLIOGRAPHIQUE**

Synthèse bibliographique

Chapitre 1 : Phytodisponibilité des éléments traces dans les sols – généralités

Les sols sont naturellement riches en éléments qui proviennent de l'héritage géologique et de la pédogénèse. Ces éléments peuvent être classés en deux catégories : les éléments majeurs et les éléments traces. Les éléments majeurs sont au nombre de 12 (oxygène (O), silicium (Si), aluminium (Al), fer (Fe), calcium (Ca), sodium (Na), potassium (K), magnésium (Mg), titane (Ti), hydrogène (H), phosphore (P) et manganèse (Mn)) et constituent 99,4 % en masse de la croûte terrestre. Dans les sols, on les trouve généralement à des concentrations moyennes supérieures à 100 mg.kg⁻¹. Les éléments traces sont au nombre de 68 (parmi lesquels nous pouvons citer le chlore (Cl), le nickel (Ni), Cu, Pb ou encore Zn) et ne représentent, à eux tous, que 0,6 % en masse de la croûte terrestre. A l'inverse des éléments majeurs, leur concentration moyenne dans les sols n'excède pas 100 mg.kg⁻¹ (Adriano 2001; Hooda 2010; Alloway 2013).

Le terme « éléments traces » (ET) regroupe indistinctement les métaux, les métalloïdes et les non-métaux, quelle que soit leur fonction dans le système sol - plante - animal. Il se substitue depuis quelques années au terme « métaux lourds » dont la classification faisait débat étant donné son emploi pour certains métaux (potentiellement) toxiques qui ne sont pas « lourds » (comme Zn par exemple) ou pour certains éléments toxiques non métalliques (comme l'arsenic (As) qui est un métalloïde ; Miquel et al. 2001 ; Hooda 2010).

I. Origine et teneurs des éléments traces dans les sols

Dans un horizon de sol donné, les concentrations naturelles en ET constituent le fond pédogéochimique naturel local (Doelsch et al. 2006a). Diverses sources naturelles d'ET peuvent conduire à une augmentation de cette concentration. Par exemple, les éruptions volcaniques émettent de grande quantité de Cu, mercure (Hg), Ni, Pb et Zn. Quant aux vents chauds provenant des régions désertiques comme le Sahara, ils sont source de chrome (Cr), Ni, Pb et Zn (Nagajyoti et al. 2010).

D'autres sources, d'origines anthropiques, participent également à l'enrichissement des sols en ET. Les retombées atmosphériques liées aux activités industrielles (incinération de déchets, poussières industrielles, etc.) et aux trafics urbains sont sources de cadmium (Cd), Pb, étain (Sn) et Zn. Les exploitations minières constituent également des sources d'éléments variés : les stériles, générés après extraction de l'or par exemple, sont riches en

Cu, Hg, Pb et Zn. Certains intrants agricoles classiquement utilisés comme les engrais minéraux, les produits phytosanitaires ou les produits résiduaux organiques sont sources de Cd, Cr, Cu, Hg, Pb et Zn (Antwi-Agyei 2009; Nagajyoti et al. 2010; Zhou et al. 2013; Romeo et al. 2014). Une récente étude a ainsi révélé que Cu et Zn sont les deux ET les plus apportés sur les sols agricoles français, avec des apports annuels moyens de 4869 t et 15190 t respectivement (Belon et al. 2012).

Contrairement aux micropolluants organiques, les ET ne sont soumis à aucun phénomène de dégradation. Ils présentent également la particularité d'être relativement peu sujets aux transferts verticaux vers les aquifères. Ils ont donc tendance à s'accumuler dans les sols.

II. Deux catégories d'éléments traces : essentiels ou non-essentiels

Les ET peuvent être classés en deux catégories (Baize 1997; Appenroth 2010).

La première catégorie regroupe les ET essentiels pour les plantes, faisant partie de la famille des oligo-éléments. Ce sont le bore (B), Cu, le cobalt (Co) (pour les légumineuses), le molybdène (Mo), Ni et Zn. Ces ET sont dits essentiels car ils participent à de nombreux processus physiologiques (Nagajyoti et al. 2010). Le bore, par exemple, entre en jeu dans les processus de division cellulaire et de synthèse des protéines et est un acteur de la migration des sucres dans la plante. Le molybdène, quant à lui, est un élément essentiel pour la fixation de l'azote et la formation des enzymes (Moore 2001). Ces éléments sont importants pour le bon développement de la plante et doivent être apportés à une concentration optimale. En deçà d'une concentration critique basse, le métabolisme cellulaire peut être perturbé, provoquant une déficience. A l'inverse, si la concentration apportée dépasse la concentration critique haute, l'ET devient phytotoxique (*Figure 1A*). Dans les deux cas extrêmes, les conséquences sont la perte des différentes fonctions physiologiques et la mort de la plante.

La seconde catégorie est constituée d'ET uniquement toxiques. On y retrouve, entre autres, Cd, Hg, Pb et Sn. Ces éléments ne présentent aucune fonction pour l'organisme végétal et peuvent seulement être toxiques. Le cadmium par exemple, présente des similitudes avec certains éléments essentiels (Zn ou Fe entre autres) et il est supposé qu'il entre facilement dans la plante en empruntant les mêmes transporteurs que ces derniers (Krzesłowska et al. 2004; Wójcik et al. 2005). Au-delà d'une concentration seuil, ils conduisent à une inhibition de la croissance et peuvent entraîner des dommages irréversibles conduisant à la mort de la plante (*Figure 1B*; Nagajyoti et al. 2010).

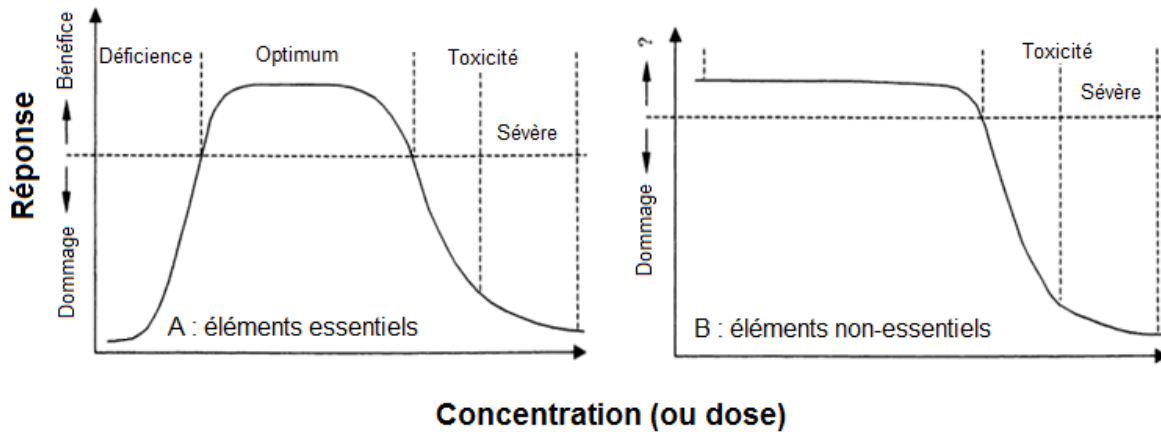


Figure 1 : Courbe dose-réponse d'un élément essentiel (A) et d'un élément uniquement toxique (B ; d'après Adriano 2001 (modifiée). Les concentrations critiques sont représentées par les lignes en pointillés, leur valeur dépend entre autre de l'ET et de la plante.

III. Toxicité des éléments traces

III.1. Fraction phytodisponible

La réponse d'une plante à une contamination en ET est, le plus souvent, mal corrélée à la concentration totale en ET dans le sol et va plutôt dépendre de la fraction biologiquement disponible de l'élément (Harmsen 2007).

En effet, une importante fraction de la concentration totale en ET d'un sol n'est pas disponible pour la plante car fortement retenue par les constituants du milieu. La fraction restante, moins énergétiquement retenue, constitue en revanche un ensemble d'ET disponible. Les différentes formes chimiques sous lesquelles va se trouver l'ET dans les différents compartiments du sol constituent sa spéciation. La spéciation d'un ET n'est pas figée. Différents facteurs liés au sol (pH, capacité d'échange cationique (CEC), quantité de matière organique, etc.) ainsi qu'à la faune et à la flore du sol (exsudation d'acides organiques par les plantes, micro-organismes, etc.) vont la conditionner (Lanno et al. 2004; Yang et al. 2005), conférant parfois à l'ET une mobilité c'est-à-dire une capacité à passer de compartiments du sol où il va être fortement retenu vers des compartiments où il le sera moins, le compartiment ultime étant la solution de sol (Juste 1988). La fraction disponible se compose d'éléments sorbés sur des phases solides du sol et d'éléments en solution (sous forme d'ions libres, de complexes inorganiques et organiques). L'ion libre ainsi que les complexes les plus labiles forment la fraction la plus disponible. Enfin, parmi ces espèces disponibles, certaines sont susceptibles d'être prélevées par la plante par l'intermédiaire de différents processus physico-chimiques d'adsorption et physiologiques d'absorption et constituent alors la fraction phytodisponible (Harmsen 2007).

C'est par les racines que la plante prélève l'eau et les ET présents dans le sol. Les surfaces racinaires présentent la particularité de pouvoir complexer les éléments. Ce processus participe à la régulation qu'opère la plante au niveau racinaire pour contrôler le transfert des ET vers les autres compartiments (pousses, feuilles, etc. ; Briat and Lebrun 1999 ; DalCorso et al. 2014).

III.2. Phytotoxicité des éléments traces

La conséquence de la contamination des sols en ET sur les plantes a fait l'objet de nombreuses études et les effets morphologiques et physiologiques ne sont plus à démontrer. Lorsqu'une plante est soumise à une contamination, la conséquence macroscopiquement observable est généralement une réduction de sa croissance (Figure 2 ; Adriano 2001 ; Panou-Filotheou et al. 2001 ; Lequeux et al. 2010). Les effets phytotoxiques sont observés dès le dépassement de la concentration optimale.

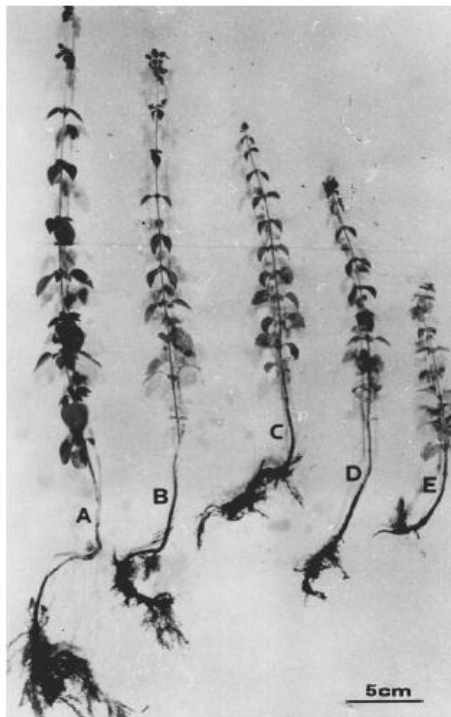


Figure 2 : Diminution de la biomasse de l'origan (*Origanum vulgare* subsp. *Hirtum*) avec l'augmentation de la concentration en Cu dans le sol, A : $0,3 \mu\text{g.g}^{-1}$, B : $13 \mu\text{g.g}^{-1}$, C : $17 \mu\text{g.g}^{-1}$, D : $22 \mu\text{g.g}^{-1}$ et E : $25,5 \mu\text{g.g}^{-1}$ (Panou-Filotheou et al. 2001).

Les racines sont le premier organe de la plante exposé à la contamination du sol. Ces dernières présentent rapidement des modifications détectables. Les symptômes de rhizotoxicité classiquement relevés sont une diminution de l'élongation racinaire, une diminution voire une inhibition de la croissance des poils absorbants, l'apparition de nombreuses ramifications, une coloration des racines (allant du brun au noir) ainsi qu'un épaissement des racines, l'apparition de gonflements localisés à l'arrière de l'apex et de ruptures au niveau du rhizoderme et du cortex externe des tissus racinaires (Figure 3 ; Wojcik *et al.* 2005 ; Sheldon et Menzies 2005 ; Kopittke et Menzies 2006 ; Michaud *et al.* 2008 ; Kopittke *et al.* 2009b ; Probst *et al.* 2009 ; Lequeux *et al.* 2010 ; Seregin *et al.* 2011).

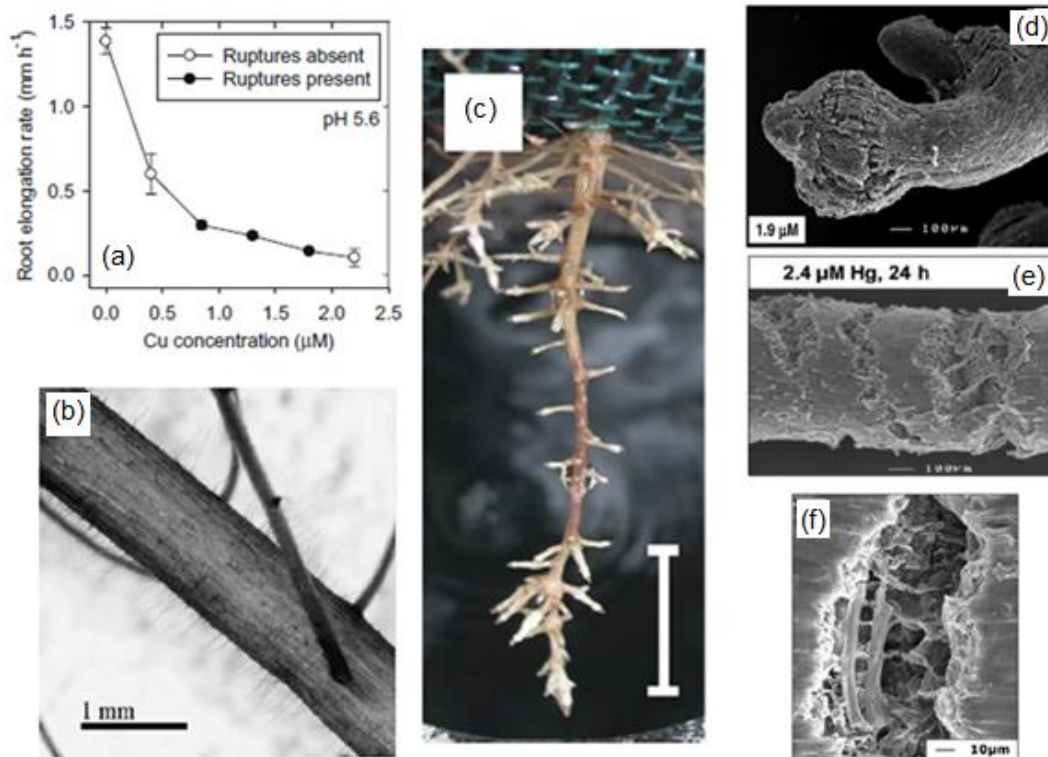


Figure 3: Symptômes de rhizotoxicité. a. diminution de l'élongation racinaire avec l'augmentation de la concentration en Cu de la solution (racines de niébé, Kopittke *et al.* 2008), b. inhibition de la croissance des poils absorbants ($0,3 \mu\text{mol.l}^{-1}$ de Cu, racines d'herbe de Rhodes (*Chloris gayana* Knuth.), Sheldon et Menzies 2005), c. système racinaire ramifié ($0,95 \mu\text{mol.l}^{-1}$ de Pb, racines de niébé, Kopittke *et al.* 2007b), d. gonflement localisé à l'arrière de l'apex ($1,9 \mu\text{mol.l}^{-1}$ de Cu, Herbe de Sabi (*Urochloa mosambicensis* H.D.), Kopittke *et al.* 2009b), e. ruptures transversales ($2,4 \mu\text{mol.l}^{-1}$ de Hg, racines de niébé, Kopittke *et al.* 2009a), f. déchirement cellulaire causé ici par un élément majeur, semblable à ce qui est observable pour les ET ($40 \mu\text{mol.l}^{-1}$ d'Al, racines de niébé, Kopittke *et al.* 2008).

Synthèse bibliographique

Tous les ET induisent des effets rhizotoxiques liés à un processus de complexation sur les surfaces racinaires. Ces effets peuvent différer d'un élément à l'autre car ils sont fonction de l'affinité de complexation de l'élément pour les surfaces (Kopittke et al. 2014b). Ainsi, d'après l'étude portant sur la rhizotoxicité de 26 éléments métalliques pour le niébé (*Vigna unguiculata* L.), Cu (troisième cation métallique le plus toxique parmi les 26) est plus toxique que Ni, qui est lui-même plus toxique que Pb (Kopittke et al. 2011a). Il a été constaté que Ni inhibe la croissance des racines latérales du niébé, contrairement à Cu et Pb qui les favorisent. Le cuivre, quant à lui, entraîne des déformations importantes des racines (formation de vrilles) et l'apparition de ruptures, symptômes qui n'ont pas été constatés avec Pb et Ni (Kopittke and Menzies 2006; Kopittke et al. 2007a; Kopittke et al. 2007b).

En résumé, à l'interface solution de sol-racines, on retrouve les deux processus suivants :

- (i) diffusion des ET (sous forme d'ion libre ou de complexe métallique) depuis la solution vers les surfaces racinaires ;
- (ii) adsorption des ET sur les surfaces racinaires, au niveau des sites de complexation.

Ce deuxième processus peut être suivi d'un processus d'absorption, l'élément traverse alors la membrane biologique. L'ensemble de ces processus conditionne la nature et l'intensité des interactions entre les racines des plantes et les ET. Néanmoins, le processus d'adsorption des ET sur les surfaces racinaires semble être un facteur clé, tant dans le déterminisme de l'absorption des ET par les cellules racinaires que de la rhizotoxicité des ET (Reid 2001; Kopittke et al. 2014b).

Chapitre 2 : Caractérisation expérimentale des interactions physico-chimiques éléments traces - racines

I. Transfert racinaire des éléments traces

I.1. Les voies apoplasmiques et symplasmiques

Au niveau racinaire, il existe deux voies de transfert des ET depuis la solution de sol vers les vaisseaux du xylème : la voie apoplasmique et la voie symplasmique (Steudle 2000; Hopkins 2003).

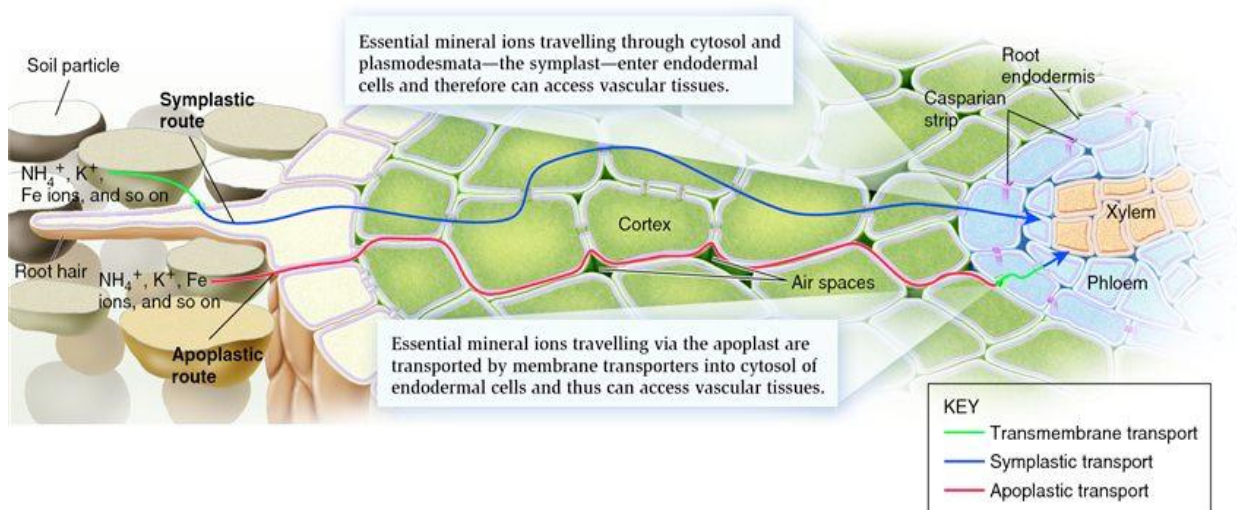


Figure 4 : Coupe d'une racine présentant les deux voies de transfert des minéraux depuis la solution de sol jusqu'au xylème ([site internet biologie-forums.com](http://site.internet.biologie-forums.com)).

La voie apoplasmique (en rose, Figure 4) est la principale voie d'absorption des éléments. Par simple diffusion, les éléments passent au travers de l'apoplasme du cortex racinaire. Ce mode de transport n'est possible que jusqu'à l'endoderme qui est constitué d'une rangée de cellules dont les parois sont principalement composées de subérine (un mélange imperméable de lipides nommé bande de Caspary) et qui constituent de ce fait une barrière empêchant le mouvement de l'eau dans l'apoplasme de l'endoderme. Dans cette zone, l'eau et les éléments sont obligés d'emprunter la voie symplasmique pour parvenir jusqu'au xylème.

La voie symplasmique (en bleu, *Figure 4*) désigne le passage de l'eau et des éléments de cellules en cellules, par l'intermédiaire des plasmodesmes (canaux traversant les parois cellulaires et reliant deux cellules entre elles). Avant de parvenir dans le symplasme racinaire, les éléments doivent d'abord traverser l'apoplasme puis les membranes plasmiques des cellules végétales grâce à des canaux ou des transporteurs membranaires.

Quelle que soit la voie empruntée, l'ET traverse à minima les parois apoplasmiques et une membrane plasmique avant d'être distribué dans la plante. Ces deux compartiments jouent donc un rôle important dans les processus de nutrition et de toxicité.

I.2. Localisation des éléments traces dans les racines

L'affinité d'un ET avec les composés racinaires va conditionner sa mobilité dans la racine. Certains éléments comme Cu et Hg vont surtout être localisés à la périphérie des racines, au niveau du rhizoderme et du cortex externe (*Figure 5*; Wang et al. 2013; Carrasco-Gil et al. 2013; Collin et al. 2014). D'autres éléments, tels que Ni et As, semblent plus mobiles et vont être trouvés respectivement dans l'ensemble du cortex racinaire et l'endoderme (*Figure 5*; Wang et al. 2013).

De même, la localisation extracellulaire ou intracellulaire des éléments va différer en fonction de leur nature. Ainsi, Pb est surtout localisé dans le compartiment extracellulaire, il est peu détecté dans les cellules (Kopittke et al. 2007b; Probst et al. 2009). De même, Cu semble avoir tendance à s'accumuler à l'extérieur des cellules : par exemple, dans les racines de *Silene paradoxa* L., la concentration en Cu mesurée dans l'espace extracellulaire était deux fois plus élevée que celle mesurée dans le milieu symplasmique (Colzi et al. 2011). A l'inverse, Cd peut être considéré comme un élément symplasmique. Il a été localisé essentiellement dans les vacuoles et le nucléole des cellules d'*Allium sativum* L. mais très peu détecté dans le compartiment extracellulaire (Liu and Kottke 2003).

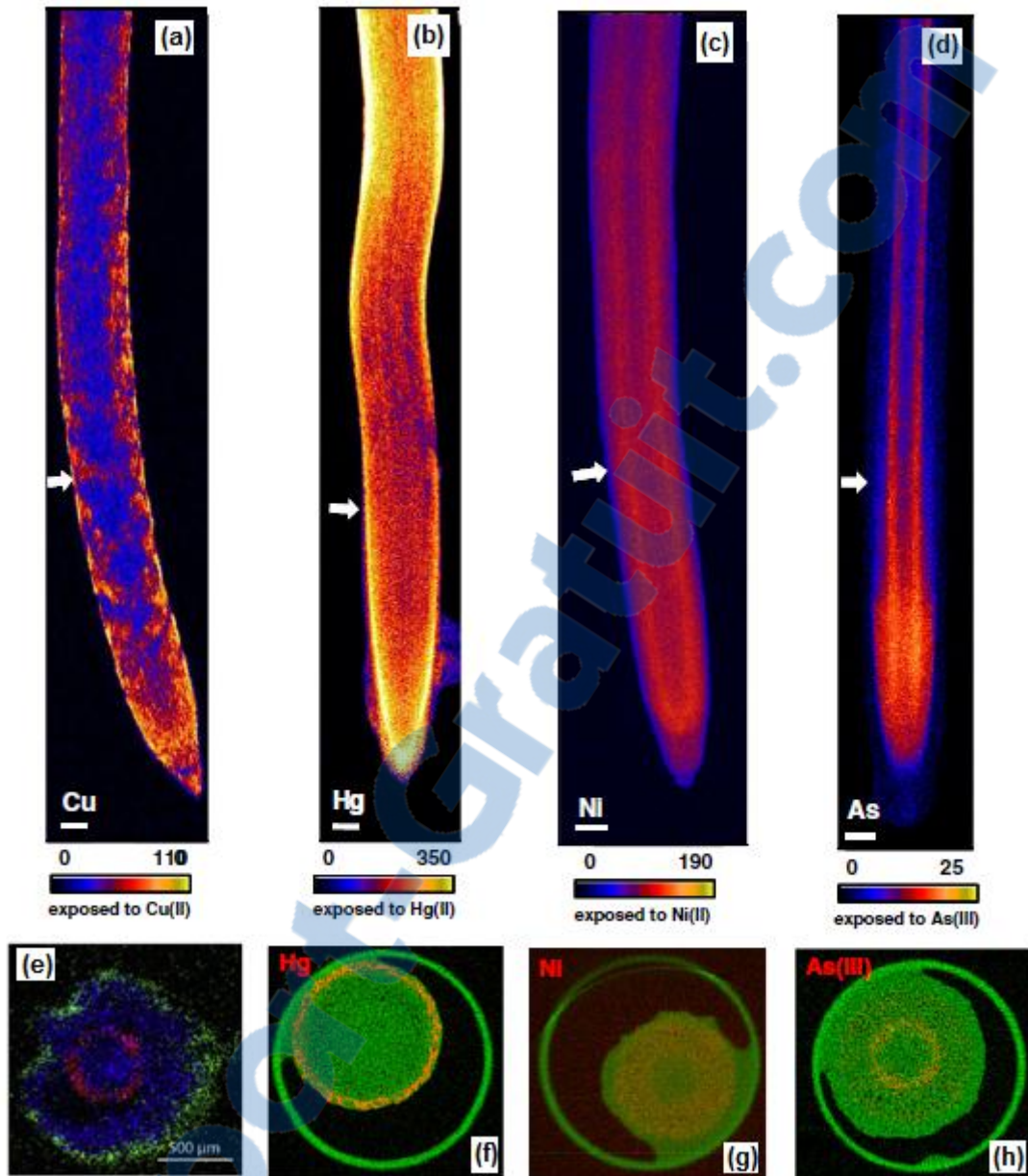


Figure 5 : Localisation des ET dans les racines. a, b, c et d. cartographies 2D des éléments présents dans des racines de niébé obtenues par micro-fluorescence à rayons X (racines exposées à $1,5 \mu\text{M}$ de Cu, $1 \mu\text{M}$ de Hg, $5 \mu\text{M}$ de Ni et $20 \mu\text{M}$ d'As ; Wang et al. 2013) ; e. cartographie élémentaire d'une section racinaire de *Phyllostachys fastuosa* exposée à $100 \mu\text{M}$ de Cu, obtenue par micro-fluorescence à rayons X (Cu en vert, K en bleu et Si en rouge ; Collin et al. 2014) ; f, g et h. tomographies de sections racinaires de niébé situées à 2 mm de l'apex (signal élémentaire en rouge, signal Compton en vert ; racines exposées à $1 \mu\text{M}$ de Hg, $5 \mu\text{M}$ de Ni et $20 \mu\text{M}$ d'As ; Wang et al. 2013).

Il est toutefois important de garder à l'esprit que les techniques employées pour localiser les ET dans les racines ont une limite de sensibilité et qu'il est possible de ne pas détecter un élément dans une région racinaire parce qu'il est présent en trop faible concentration. De plus, s'il est possible de localiser un ET à l'intérieur ou à l'extérieur de la cellule, il est difficile en revanche d'être plus précis et de faire la différence entre une localisation dans les parois

apoplasmiques et au niveau de la surface des membranes plasmiques des cellules. Une telle différenciation s'avère pourtant nécessaire pour une meilleure compréhension des mécanismes de toxicité puisqu'il semblerait que certains éléments comme Pb, qui sont supposés être localisés dans les parois apoplasmiques, sont complexés à la fois avec des composés pariétaux et avec des composés des présents sur les surfaces des membranes plasmiques (Seregin et al. 2002).

II. Le compartiment apoplasmique

Le terme apoplasme a été inventé en 1930 par le botaniste Ernst Münch et regroupe l'ensemble des compartiments situés au-delà de la membrane plasmique (Sattelmacher 2001). Etant localisé à l'interface entre le milieu extérieur et les membranes plasmiques des cellules végétales, l'apoplasme racinaire est un passage obligé pour tous les ET depuis la solution de sol vers le symplasme racinaire (Hall 2002). Ce compartiment végétal est constitué d'eau, de gaz et de parois. Ces dernières sont composées de petits polymères distincts, étroitement tissés, qui forment un maillage en 3 dimensions avec une organisation architecturale spécifique (Sarkar et al. 2009).

II.1. La lamelle moyenne et les parois apoplasmiques

On distingue 3 couches nommées lamelle moyenne, paroi primaire et paroi secondaire (Figure 6 ; Sattelmacher (2001)).

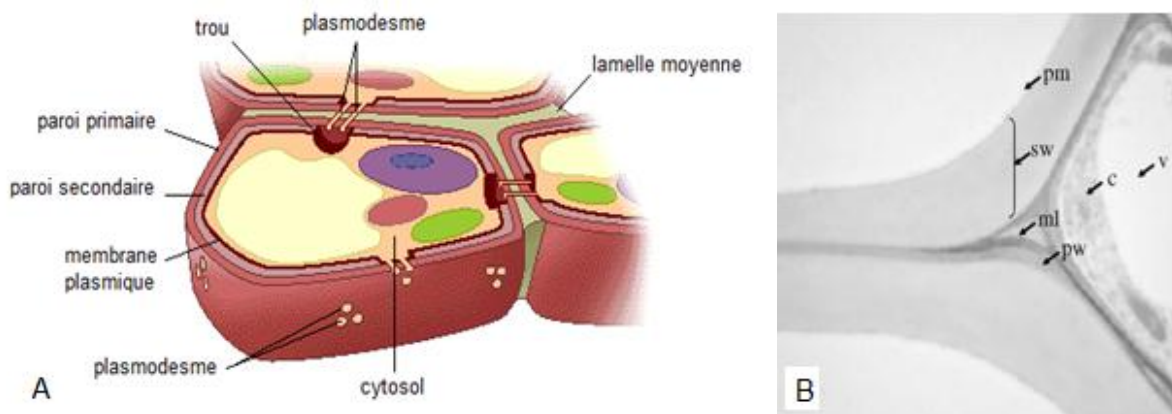


Figure 6 : Représentation schématique d'une cellule végétale entourée des parois apoplasmiques (A) ([site internet phschool.com](http://site.internet.phschool.com)) ; image MET (microscopie électronique à transmission) de parois apoplasmiques racinaires d'*Arabidopsis thaliana* (B ; membrane plasmique (pm), paroi secondaire (sw), lamelle moyenne (ml), paroi primaire (pw), cytosol (c) et vacuole (v), d'après Caffal and Mohnen 2009).

La lamelle moyenne est commune à deux cellules adjacentes et en assure la cohésion. Elle est formée lors de la mitose (processus de division cellulaire permettant l'obtention de deux cellules filles identiques à partir d'une cellule mère) et est principalement composée de pectines ayant différents degrés de méthylation (Sattelmacher 2001).

La paroi primaire est située après la lamelle moyenne. Elle est générée par les cellules méristématiques (cellules en croissance). Cette paroi est fine (moins d'un micron ; Taiz et Zeiger 2006), flexible et extensible durant la phase de croissance pour permettre l'élongation cellulaire. Elle est constituée de microfibrilles de cellulose entre lesquelles différents polysaccharides comme les pectines, les hémicelluloses, etc. ainsi que des protéines de structure s'entrelacent (Figure 7 ; Carpita et Gibeaut 1993 ; Vogel 2008).

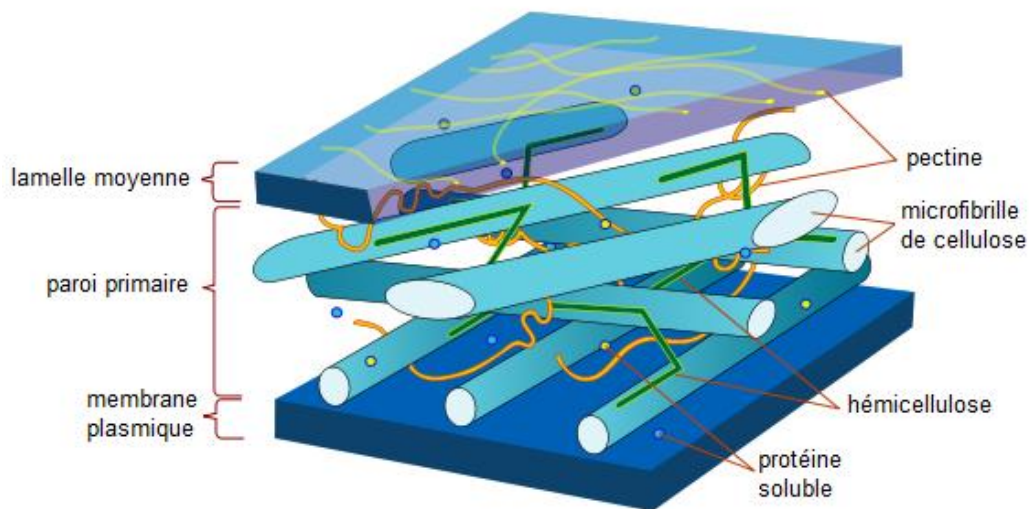


Figure 7 : Représentation 3D de l'apoplasme racinaire d'une jeune cellule (site internet : wclipart.com).

La paroi secondaire se met en place entre la paroi primaire et la membrane plasmique. Elle peut apparaître dans certains tissus lorsque la croissance cellulaire est achevée. Contrairement à la paroi primaire, la paroi secondaire est plus épaisse (Figure 6 B), rigide et inextensible. Son organisation structurale est similaire à celle de la paroi primaire mais sa composition est différente. Elle se compose principalement de cellulose, d'hémicellulose et de lignine. D'autres polysaccharides (xylans, glucomannane) peuvent être entrelacés entre les microfibrilles de cellulose (Gibeaut and Carpita 1994).

II.2. Composition chimique des parois apoplasmiques

Comme cela a été décrit dans la précédente partie, les parois apoplasmiques sont principalement formées de microfibrilles de cellulose (mesurant 30 nm de diamètre en moyenne, [Caffall and Mohnen 2009](#)), qui constituent le cadre mécanique des parois, et d'une matrice (mélange d'hémicelluloses, de pectines, de lignines, etc.) qui forme des liaisons transversales entre les microfibrilles ([Sarkar et al. 2009](#)). Tous ces composés sont synthétisés à la surface des cellules (*Figure 8* ; [Gibeaut and Carpita 1994](#)).

Les microfibrilles de cellulose sont formées par l'association de longues chaînes linéaires de résidus de β -D-glucose. La cellulose est le polysaccharide le plus abondant dans les parois cellulaires. Elle représente entre 15 et 30 % de la matière sèche des parois primaires et entre 35 et 50 % de la matière sèche des parois secondaires ([Gibeaut and Carpita 1994](#); [Vogel 2008](#)).

Les hémicelluloses sont une famille de composés chimiquement très variés qui regroupe l'ensemble des polysaccharides qui ne sont ni cellulosiques, ni pectiques. Les polymères hémicellulosiques s'associent aux microfibrilles de cellulose par des liaisons non covalentes et leur permettent d'être reliées les unes aux autres ([Caffall and Mohnen 2009](#)). Elles peuvent également se lier aux pectines. On les retrouve à la fois dans les parois primaires et secondaires.

Les pectines constituent les macromolécules pariétales les plus diversifiées ([Carpita and Gibeaut 1993](#)). Elles regroupent des polysaccharides hétérogènes complexes, riches en résidus acide galacturonique. Parmi ces polysaccharides, on trouve principalement les homogalacturonanes et les rhamnogalacturonanes de type I et II (constituants les chaînes principales) ; d'autres polysaccharides tels que les galactanes et les arabinanes forment généralement les chaînes latérales. Ces composés ont la particularité de pouvoir s'organiser en gel par l'intermédiaire de pontages (souvent réalisés par du Ca) entre deux chaînes d'acides galacturoniques (*Figure 9*). Les pectines sont essentiellement présentes dans la paroi primaire, on les trouve en très faible proportion dans la paroi secondaire. Elles vont déterminer la porosité des parois et participer à la régulation du pH et de l'équilibre ionique grâce à leurs groupements carboxyliques non méthylés ([Carpita and Gibeaut 1993](#); [Blamey 2003](#)).

Les lignines sont des polymères phénoliques formés par copolymérisation de trois types d'alcools aromatiques nommés monolignols (alcools coumarylique, coniférylique et sinapylique ; [Hatfield et Vermerris 2001](#)). Le processus de lignification se produit lors de la

Synthèse bibliographique

formation de la paroi secondaire ([Gibeaut and Carpita 1994](#)). La lignine va s'incruster dans les trois couches pariétales, assurant ainsi une rigidité à l'ensemble et empêchant la dégradation des polysaccharides pariétaux.

On trouve également dans la paroi primaire des protéines (de structure ou enzymatiques) qui participent à son élaboration, son remodelage et à la défense contre les agents pathogènes ([Cassab 1998](#); [Caffall and Mohnen 2009](#)).

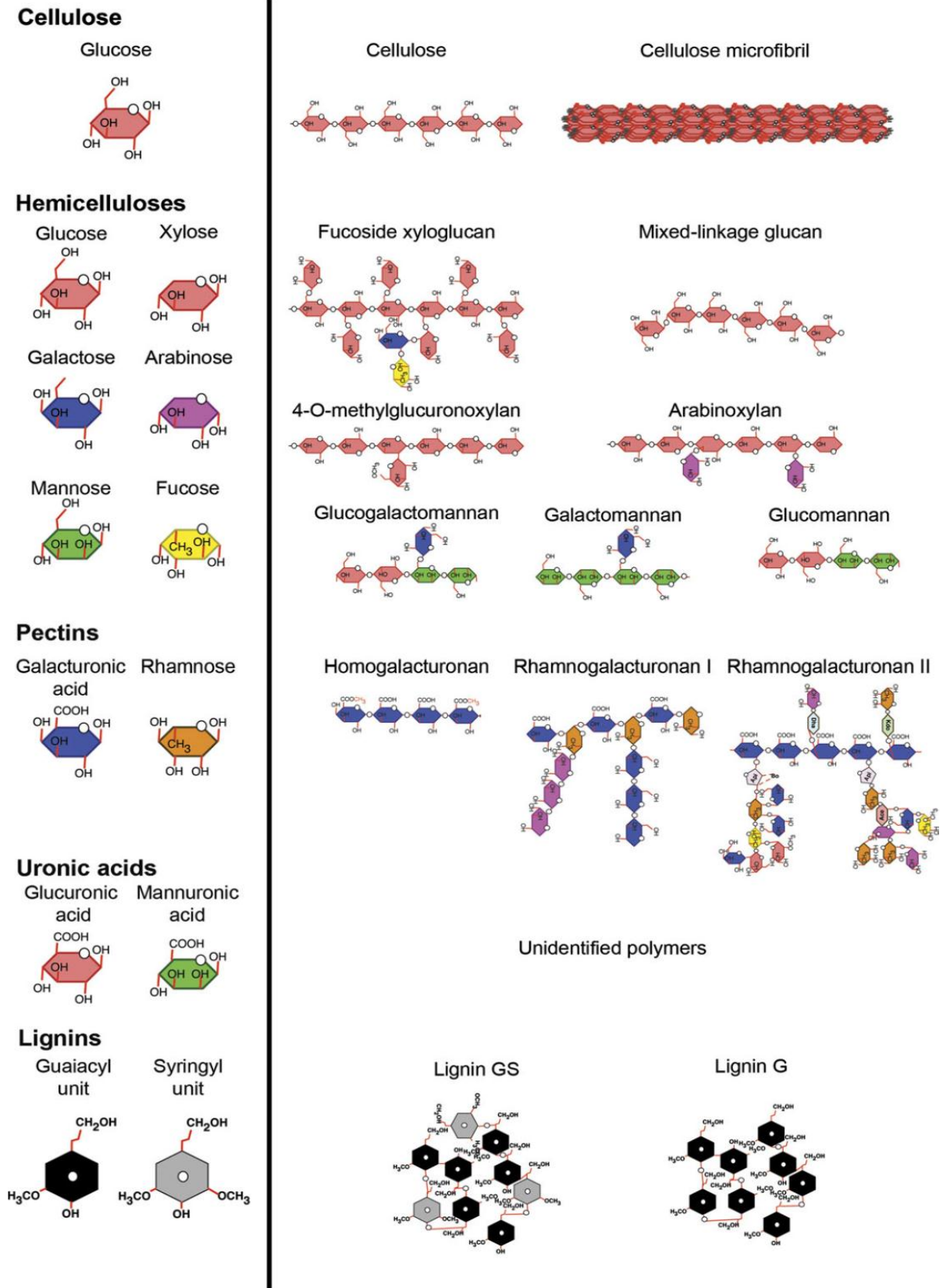


Figure 8 : Structure chimique des principaux constituants des parois apoplasmiques (monomères à gauche et polymères respectifs à droite ; Sarkar et al. 2009).

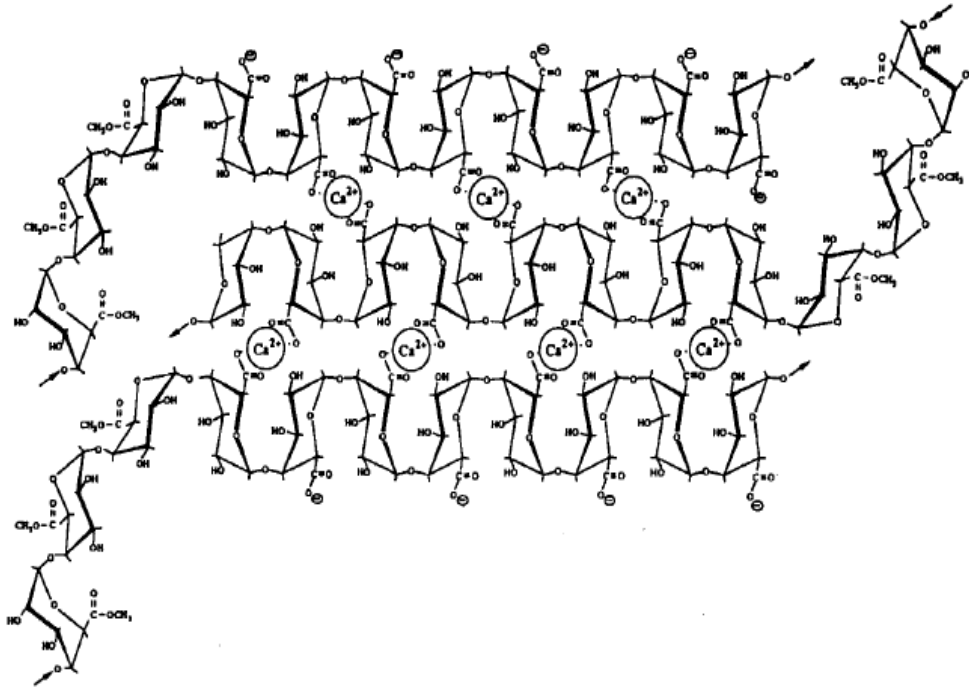


Figure 9 : Formation de gel pectique par l'intermédiaire de structures en « egg-box » (d'après [Carpita and Gibeaut 1993](#)).

Les proportions de ces différents composés ne sont pas communes chez toutes les plantes. On distingue deux modèles d'organisation de la paroi primaire ([Carpita and Gibeaut 1993](#)) : les plantes de « type I », représentatives de la plupart des dicotylédones et de quelques monocotylédones (non graminées) et les plantes de « type II », regroupant la plupart des monocotylédones ; des différences sont également visibles au niveau des parois secondaires mais elles sont moins marquées. Ainsi, les parois primaires des dicotylédones diffèrent de celles des monocotylédones par une teneur plus élevée en composés pectiques (entre 20 et 35 % de la masse sèche contre seulement 5 % pour les monocotylédones) ainsi qu'en protéines de structure (respectivement 10 % et 1 % de la masse sèche). Le type d'hémicellulose qui domine la composition est également différent : les xyloglucanes sont les hémicelluloses majoritaires chez les dicotylédones alors que les arabinoxylans prédominent chez les monocotylédones ([Vogel 2008](#)).

Les teneurs de ces différents composés varient également le long de la racine. La teneur en pectine, par exemple, est maximale au niveau de l'apex puis diminue rapidement dans la zone d'élongation racinaire (entre 2 et 5 mm après l'apex ; [Blamey 2003](#)) pour finalement être stable au-delà : [Eticha et al. 2005](#) ont constaté une diminution d'un facteur 3 dans les racines de maïs.

II.3. Capacité de complexation de l'apoplasme racinaire

L'apoplasme racinaire remplit de nombreuses fonctions chez la plante (e.g. squelette de soutien, régulateur de croissance, voie de transport pour l'eau, les nutriments, les hormones végétales, etc.) et en particulier, il joue un rôle central dans la nutrition minérale en constituant un réservoir d'ions pour la plante, permettant ainsi de temporiser leur transport (Grignon and Sentenac 1991; Sakurai 1998; Briat and Lebrun 1999; Carpita 2007).

Cette particularité provient de la composition des parois. Leur capacité de complexation est généralement associée à leurs teneurs en groupements carboxyliques non méthylés, portés entre autre par les polysaccharides acides tels que les pectines. La constante d'acidité (pK_a) de ces groupements est estimée entre 3 et 4,4 ce qui signifie qu'aux pH physiologiques de l'apoplasme (généralement 5-6) entre 80 et 97 % des groupements carboxyliques sont dissociés (Allan and Jarrell 1989; Wehr et al. 2010) et donc particulièrement disponibles pour des réactions de complexation avec des cations. Toutefois, les titrages acido-basiques de parois isolées de blé (*Triticum aestivum* L.), de pois (*Pisum sativum* L.) et de lupin (*Lupinus albus* L.) ont révélé une diversité de sites réactifs plus importante avec des pK_a plus élevés (Meychik and Yermakov 1999, 2001). D'autres composés pariétaux peuvent donc également participer à la complexation des cations. Les cations peuvent être adsorbés de manière spécifique (Cu, Mn ou Zn ; Sattelmacher 2001) ou non spécifique (Ca, K ; sous forme d'interactions électrostatiques).

La faculté d'une espèce végétale à adsorber les cations est évaluée par sa capacité d'échange cationique racinaire (CECR). La CECR est dépendante de nombreux paramètres tels que l'âge de la plante (Heintze 1961; Ram 1980). Elle est généralement plus élevée chez les dicotylédones (comprise entre 20 et 50 $\text{cmol}_c \cdot \text{kg}^{-1}$) que chez les monocotylédones (comprise entre 10 et 20 $\text{cmol}_c \cdot \text{kg}^{-1}$; Crooke et al. 1960 ; Heintze 1961 ; Straczek et al. 2008). Cette particularité provient du fait que les compositions des parois apoplasmiques sont différentes (cf. Chapitre 2 : II.2), les dicotylédones étant plus riches en composés pectiques que les monocotylédones. Les groupements carboxyliques non méthylés portés par les pectines sont généralement considérés comme étant la principale source de charges négatives des racines (Krzyszowska 2011), 70 à 90 % de la CECR leur étant attribué (Haynes 1980).

La complexation en excès des ET dans les parois apoplasmiques est l'une des principales hypothèses avancées pour expliquer les effets rhizotoxiques observés (cf. Chapitre 1 : III.2, Figure 3). Il a en effet été constaté que les propriétés physiques des parois apoplasmiques sont altérées lorsque le Ca est remplacé par un ET pour la formation des gels pectiques

(Rengel and Zhang 2003). La rigidification des parois apoplasmiques et la formation de ruptures au niveau de la zone d'élongation racinaire résulte probablement d'une augmentation de la formation de ponts entre les chaînes de polymères pariétaux telles que les chaînes pectiques (Kopittke et al. 2014b). En l'absence de contamination, ces ponts sont formés par Ca qui, en étant facilement déplacé par les protons (théorie de la croissance acide, Grignon et Sentenac 1991) n'empêche pas le glissement des chaînes lors du processus de croissance racinaire (Figure 10). A l'inverse, lorsque ces ponts sont formés par des éléments qui présentent, pour certains (e.g. Cu, Al) une affinité beaucoup plus importante que Ca pour les groupements carboxyliques des pectines (Dronnet et al. 1996; Franco et al. 2002; Horst et al. 2010) le processus se bloque, rendant les parois cellulaires plus rigides. Cette rigidité freine l'élongation racinaire et peut provoquer des ruptures au niveau des cellules du rhizoderme et du cortex externe. Ces ruptures sont probablement engendrées par des vitesses de croissances différentes entre les cellules situées dans la partie externe du cortex et celles situées dans la partie interne (Kopittke and Menzies 2006; Kopittke et al. 2009a). Cependant, le(s) mécanisme(s) exact(s) conduisant à l'inhibition de l'élongation racinaire reste(nt) encore mal connu(s). Plusieurs autres possibilités sont envisageables, par exemple un empêchement de la circulation des expansines, molécules qui contrôlent le glissement des composés pariétaux (e.g. cellulose) entre eux lors de la croissance (Kopittke et al. 2014b).

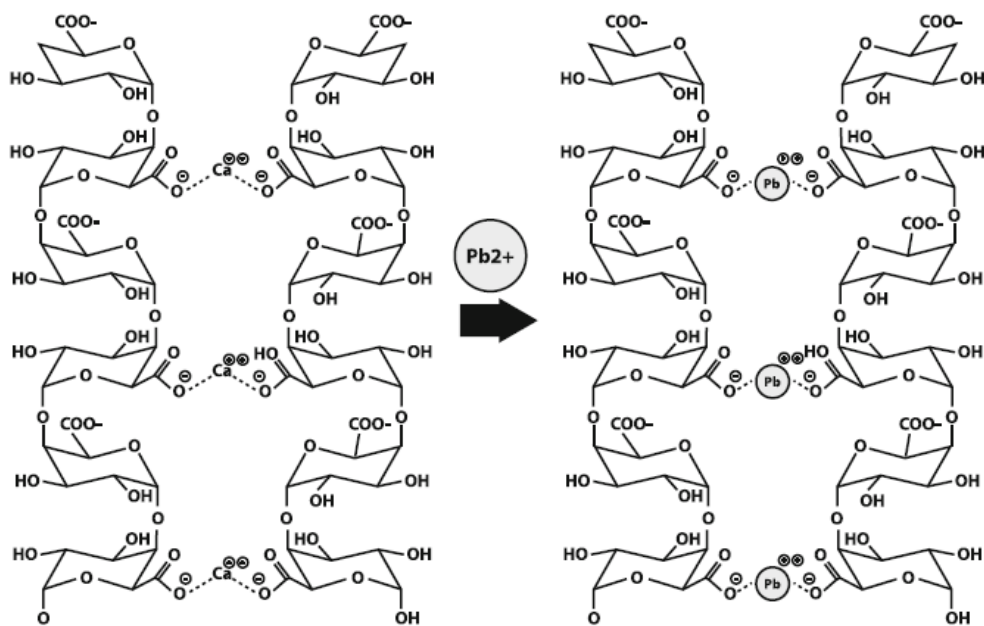


Figure 10 : Schéma représentant l'adsorption des ET (ici Pb) au sein de chaînes de polymères pectiques (Krzyszowska 2011).

D'autres hypothèses ont également été avancées pour expliquer la rhizotoxicité des ET, notamment une complexation des éléments en excès au niveau des membranes plasmiques et un effet toxique engendré par leur altération (modification de leur perméabilité ; [Ishikawa et al. 2001](#) ; [Kopittke et al. 2014b](#)).

III. Les membranes plasmiques

Les cellules végétales sont délimitées par une enveloppe appelée membrane plasmique qui permet la séparation entre le cytoplasme et le milieu extérieur (*Figure 11*).

III.1. Composition chimique des membranes plasmiques

Toutes les membranes biologiques ont la même organisation moléculaire. Elles sont formées d'une double couche de phospholipides et de protéines (*Figure 11*).

Les phospholipides sont des molécules complexes constituées de deux chaînes d'acides gras apolaires hydrophobes et d'une tête polaire hydrophile. La tête se compose d'une molécule de glycérol (faisant le lien entre les deux chaînes d'acides gras), d'un groupement phosphate et d'une molécule de tête qui peut être une molécule de choline, comme sur la figure 11, ou une autre molécule (sérine, glycérol, inositol, ethanolamine, etc. ; [Hopkins 2003](#) ; [Taiz et Zeiger 2006](#)).

Les protéines sont des macromolécules composées d'une ou plusieurs chaînes d'acides aminés liées entre eux par des liaisons peptidiques. Elles peuvent représenter jusqu'à la moitié de la masse membranaire ([Hopkins 2003](#); [Taiz and Zeiger 2006](#)). Les protéines membranaires peuvent être classées en deux catégories : les protéines intégrées (enchâssées dans la bicouche) et les protéines périphériques (liées à la surface hydrophile ; *Figure 11*).

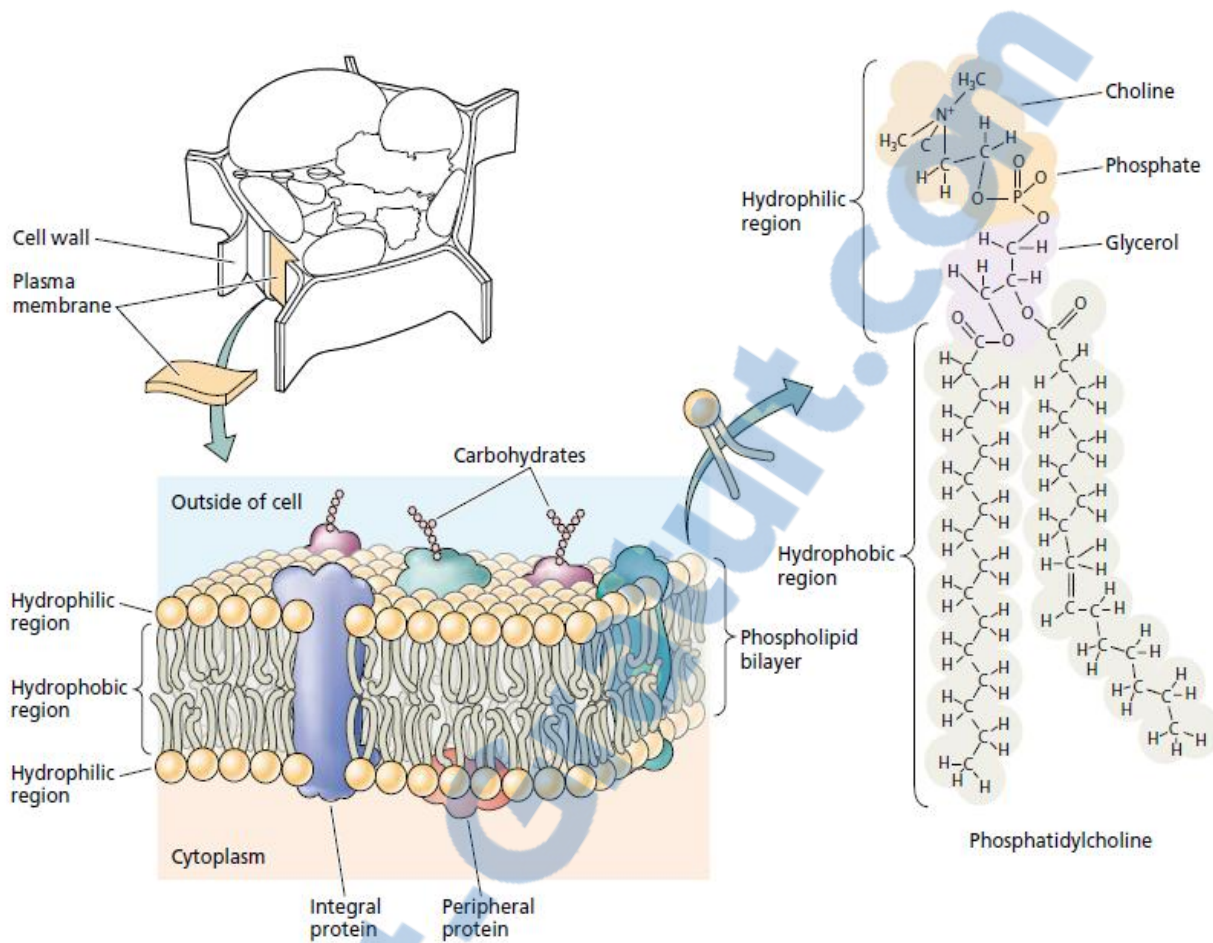


Figure 11 : Représentation schématique d'une membrane plasmique (extrait de *Taiz and Zeiger 2006*).

III.2. Capacité de complexation des membranes plasmiques

Les membranes plasmiques ont pour principales fonctions d'isoler et de protéger le cytoplasme de l'environnement extérieur ainsi que de réguler les échanges de substances et d'ions entre l'extérieur et l'intérieur de la cellule. Elles constituent également une zone de communication intercellulaire (*Gupta 2004*).

Les membranes plasmiques sont chargées négativement (*Wagatsuma and Akiba 1989*). Les charges sont principalement portées par les groupements phosphates des phospholipides et les groupements carboxyliques des protéines (*Kinraide et al. 1992; Yermiyahu et al. 1994*). Les groupements de tête des phospholipides peuvent également participer à la complexation des cations (*Cohen and Cohen 1981; McLaughlin et al. 1981*). Les groupements carboxyliques des protéines arabinogalactanes (AGPs ; *Lampport et al. 2006*) qui recouvre la surface des membranes plasmiques semblent être des sites privilégiés pour la complexation du Ca. Ils présentent d'ailleurs une affinité avec Ca plus importante que les

pectines. Il est supposé que la complexation de Ca sur les AGPs participe à la régulation du processus d'élongation racinaire, selon la même théorie de la croissance acide utilisée pour expliquer le rôle des pectines (Lamport and Várnai 2013). Par analogie, le remplacement de Ca par d'autres cations métalliques pourrait ainsi perturber le processus d'élongation racinaire et ce d'autant plus que certains cations métalliques comme Al et Cu semblent présenter une affinité élevée avec les sites réactifs présents à la surface des membranes plasmiques (Vulkan et al. 2004; Kudo et al. 2011).

IV. Spéciation des éléments traces dans les racines

Les composés racinaires impliqués dans les réactions de complexation sont de diverses natures et la spéciation peut fortement différer d'un ET à un autre.

Le plomb, préférentiellement localisé dans le milieu extracellulaire, a uniquement été trouvé en association avec des ligands oxygène dans les racines de différentes plantes (*Avena pratensis*, *Festuca ovina*, etc.). L'hypothèse d'une participation majoritaire des polysaccharides acides tels que les pectines a été retenue (Bovenkamp et al. 2013).

Le cuivre (II) est soit majoritairement trouvé en association avec des ligands oxygène (Polette et al. 2000; Kopittke et al. 2011c), soit associé à des ligands oxygène et azote (Shi et al. 2008; Collin et al. 2014). Dans le premier cas, cela suggère une complexation du Cu par les pectines (comme dans le cas du Pb, d'autant que Cu est un élément qui a tendance à s'accumuler dans le milieu extracellulaire). Cela peut aussi révéler la participation de petits acides organiques tels que le malate ou le citrate, principalement localisé dans le symplasme. Dans le second cas, cela suppose l'implication d'acides aminés présents à la fois dans le milieu extracellulaire (résidus de protéines enchâssées dans les parois apoplasmiques ou dans les membranes plasmiques) et dans le milieu intracellulaire (petits acides aminés). Une récente étude a montré que les protéines riches en résidus histidine sont le principal site de complexation du Cu dans les parois apoplasmiques de *Thlaspi arvense* (Manceau et al. 2013). Du cuivre (I) a également été détecté dans certaines racines et trouvé en association avec du soufre (Polette et al. 2000; Shi et al. 2008; Collin et al. 2014).

La réduction du Cu(II) en Cu(I) dans les racines est un processus permettant à la plante d'internaliser le Cu mais il est également supposée être un mécanisme de protection de la plante, Cu étant complexé par des protéines puis acheminé vers des tissus moins sensibles.

Synthèse bibliographique

Le cobalt semble également avoir une affinité particulière pour les acides aminés puisque de l'oxygène et de l'azote ont été détectés dans son environnement dans des racines de blé (*Triticum aestivum* L.) et de tomate (*Lycopersicon esculentum* M.) (Collins et al. 2010).

Contrairement au Cu(II) ou au Pb, Cd et Hg sont quasi-exclusivement trouvés en association avec du soufre dans les racines (Pickering et al. 1999; Isaure et al. 2006; Carrasco-Gil et al. 2013). Si pour Hg, qui est un élément plutôt extracellulaire, la présence de soufre peut être associée à des protéines riches en résidus type cystéine enchâssées dans les parois apoplasmiques ; pour Cd, élément plutôt symplasmique, cela suggère une participation de petits acides aminés tels que la cystéine ou le glutathion.

Le zinc, quant à lui, est quelque fois trouvé en association avec des ligands oxygène mais il présente la particularité d'être le plus souvent entouré de ligand oxygène et phosphore (Sarret et al. 2001; Sarret et al. 2009; Straczek et al. 2008; Kopittke et al. 2011c). Alors qu'un environnement uniquement oxygène suppose, comme pour d'autres éléments, qu'il est complexé par des acides organiques, un environnement présentant à la fois de l'oxygène et du phosphore permet de supposer qu'il y a participation de groupements phosphates et donc participation soit de petits acides caractéristiques tels que l'acide phytique, soit des groupements phosphate des phospholipides portés par les membranes plasmiques.

Synthèse bibliographique

Chapitre 3 : Modélisation des interactions éléments traces - racines

Les études menées entre 1960 et 1970 sur la toxicité de nombreux éléments traces pour les organismes aquatiques ont conduit à la formulation de deux mécanismes principaux (Erickson 2013) :

- (i) la toxicité d'un ET varie en fonction de sa spéciation chimique dans la solution baignant l'organisme ; elle est souvent étroitement corrélée à l'activité de l'ion libre, bien que d'autres espèces métalliques puissent contribuer ;
- (ii) les cations comme Ca^{2+} ou H^+ peuvent réduire la toxicité de l'élément trace.

Les modèles actuellement développés pour les plantes s'appuient sur ces deux mécanismes.

Une analyse de la littérature révèle l'existence de deux familles de modèles : certains sont centrés sur la description de la complexation de l'ET au niveau des sites réactifs et l'établissement des constantes associées, d'autres s'attachent à décrire les phénomènes électrostatiques présents au niveau de la zone d'interaction, pour lesquels l'établissement de constantes de complexation n'est pas centrale (le modèle y étant peu sensible). On constate également des divergences quant à la principale zone d'interaction entre l'ET et la plante : il peut s'agir soit des parois apoplasmiques, soit des membranes plasmiques, soit des deux.

I. Le modèle électrostatique

Le modèle électrostatique est développé depuis plus de 20 ans. Ce modèle fait l'hypothèse que les phénomènes d'absorption, les effets toxiques ainsi que les compétitions entre éléments traces et cations ou anions majeurs qui ont lieu au sein des racines sont directement reliés à la concentration en ions située à la surface des membranes plasmiques. Le formalisme mathématique employé est fondé sur le modèle de la double couche électrique (également connu sous le nom de modèle Gouy-Chapman-Stern), initialement consacré à l'étude du comportement des surfaces chargées en contact avec des solutions.

I.1. Principales hypothèses et applications

Cette partie résume les principales hypothèses du modèle électrostatique, sans description mathématique. Le lecteur est invité à consulter les articles de Kinraide et co-auteurs pour plus d'informations sur ces aspects mathématiques (Kinraide et al. 1998; Kinraide 2001).

Les principales hypothèses de ce modèle peuvent être résumées ainsi.

Les sites chargés négativement à la surface externe des membranes plasmiques vont créer un potentiel électrique de surface (noté ψ_0). Ce potentiel électrique de surface contrôle l'activité des ions à la surface des membranes plasmiques et donc les effets toxiques (Wang et al. 2009). Les parois apoplasmiques n'ont que peu d'effet sur l'activité d'un ion au niveau de la surface des membranes plasmiques (Kinraide 2004) ; elles ne sont donc pas prises en compte dans le modèle (Kopittke et al. 2014a). La description des phénomènes de complexation n'est employée que pour moduler les charges négatives à la surface des membranes plasmiques et donc moduler le potentiel électrique de surface. La qualité des simulations est donc peu sensible aux valeurs fixées pour les constantes de complexation des ET contrairement à celles des anions et cations majeurs (Kinraide 2004).

La composition ionique du milieu dans lequel se trouve les membranes plasmiques a une influence sur la densité de sites de surface chargés ainsi que sur le potentiel électrique de surface (Kinraide 2001). Par formation de liaisons covalentes ou électrostatiques, les cations tels que H^+ , Ca^{2+} et Mg^{2+} réduisent la négativité de ψ_0 (Kinraide et al. 1992). L'ampleur de la réduction de la négativité du potentiel de surface est fonction de la charge de l'ion ainsi que de sa force de liaison avec les sites de surface (Kinraide 2006). La concentration en cations métalliques à la surface des membranes plasmiques est directement liée au potentiel électrique de surface. Par conséquent, une réduction du potentiel affecte la toxicité des cations métalliques (Wang et al. 2009). Ainsi, une diminution de la toxicité de l'aluminium et du Cu pour le blé (*Triticum aestivum* L. cv Scout 66) a été constatée respectivement en présence de Ca^{2+} (Kinraide et al. 1998) et en présence de Ca^{2+} et de Mg^{2+} (Wang et al. 2008).

L'activité des cations métalliques à la surface des membranes plasmiques permet ainsi une meilleure prédiction de la diminution du taux d'élongation racinaire que l'activité des cations métalliques en solution (Figure 12 ; Kinraide 2003 ; Wang et al. 2011 ; Kopittke et al. 2011b). Ce modèle permet également de prédire la toxicité de certains métalloïdes anioniques comme l'arsenic (V) ou le sélénate (Yermiyahu 2005; Wang et al. 2008), contrairement aux autres modèles de prédiction de la toxicité qui ne sont pas paramétrés pour les anions.

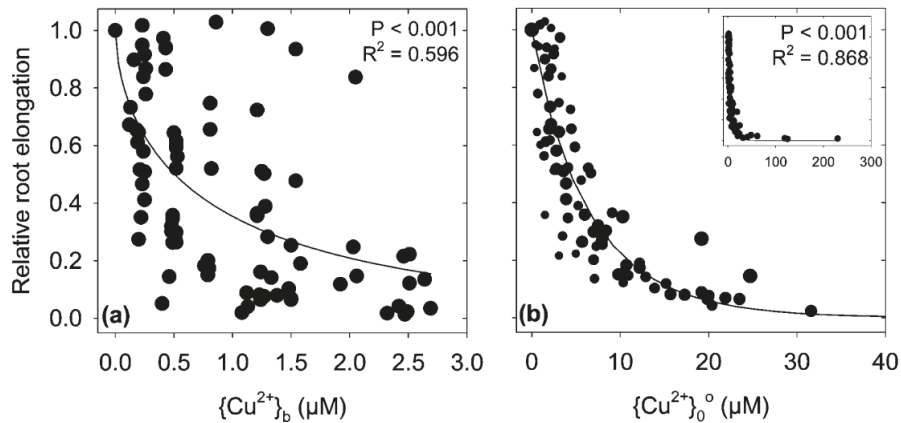


Figure 12 : Capacité de l'activité de Cu^{2+} en solution (a) et de l'activité de Cu^{2+} à la surface des membranes plasmiques (b) à décrire l'élongation racinaire relative chez *Vigna unguiculata* L. Walp (Kopittke et al. 2011b).

I.2. Principales limites

Plusieurs critiques peuvent être formulées à l'égard du modèle électrostatique.

La première porte sur le rôle non significatif de l'apoplasme sur la composition ionique du milieu à l'interface solution – membranes plasmiques. Comme nous l'avons vu dans le chapitre 2, les parois apoplasmiques sont négativement chargées dans la gamme de pH physiologique. Si, d'un point de vue purement électrostatique, elles contribuent à l'attraction des cations présents en solution vers les membranes plasmiques, elles ne sont pas pour autant inertes du point de vue de la complexation et vont potentiellement retenir un certain nombre de cations. La composition ionique du milieu à l'interface solution – membranes plasmiques n'est donc probablement pas tout à fait identique à ce qu'elle serait en l'absence de parois apoplasmiques.

L'hypothèse selon laquelle la concentration à la surface des membranes plasmiques serait un meilleur paramètre que la complexation pour la prédiction de l'absorption d'un ET ou de sa toxicité est également critiquable. Les travaux menés par Kopittke et ses co-auteurs (dont les principaux résultats ont été présentés précédemment) suggèrent que les réactions de complexation des ET au sein des racines, et en particulier au sein des parois apoplasmiques, sont à l'origine des effets rhizotoxiques observés, et notamment à l'origine de la formation de ruptures (cf. Chapitre 1 : III.2 Figure 3).

Enfin, aucune hypothèse n'est faite quant à la nature des sites réactifs situés à la surface des membranes plasmiques. Pourtant, les preuves expérimentales d'une diversité des sites de surfaces biologiques (plantes et bactéries) ne manquent pas (Meychik and Yermakov 1999, 2001; Meychik et al. 2006; Guiné et al. 2006; Wu and Hendershot 2009).

II. Les modèles de complexation

II.1. Principales hypothèses communes

Cette partie présente les principales hypothèses communes à tous les modèles de complexation. Par simplicité, les sites réactifs de surface seront nommés « ligand biotique », même si ce terme n'est pas employé de façon commune dans tous les modèles.

L'hypothèse principale des modèles de complexation est que l'ET considéré est en équilibre dans le milieu avec ses différentes formes chimiques et avec le ligand biotique (LB) (Figure 13).

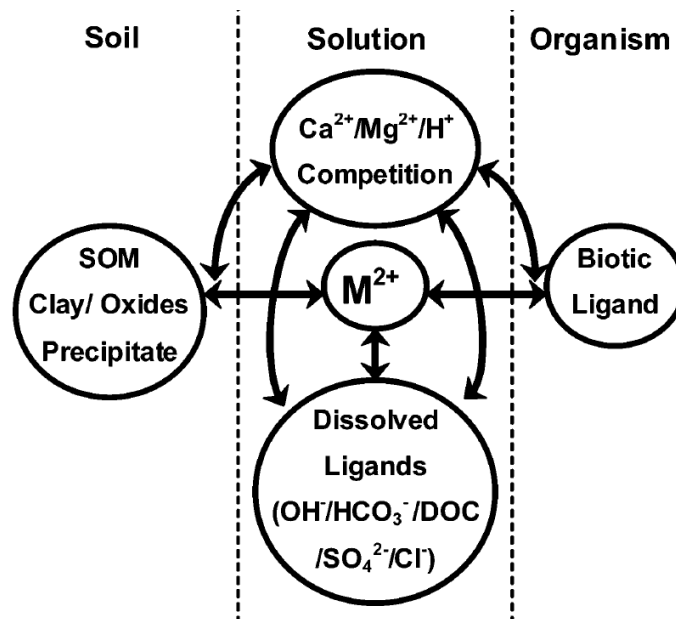
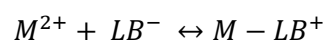


Figure 13 : Représentation schématique des équilibres chimiques qui existent entre le cation métallique, les constituants du sol et de la solution de sol et les sites réactifs situés à la surface de l'organisme (ici dénommés Biotic Ligand, [Thakali et al. 2006a](#)).

Avant d'interagir avec le LB, le métal diffuse depuis la solution vers la surface de l'organisme. Dans un système à l'équilibre, la diffusion du métal ainsi que les diverses réactions auxquelles il participe sont supposées rapides. L'interaction métal – ligand biotique (M-LB) peut être décrite de la même manière que n'importe quelle autre réaction entre le métal (M^{Z+}, sous forme d'ion libre) et un ligand organique ou inorganique à savoir :



$$K_{M-LB} = \frac{[M - LB^{+}]}{[M^{2+}][LB^{-}]}$$

Les interactions cations majeurs – ligand biotique sont également décrites de cette façon.

Le processus est simplifié : les couches de diffusion sont négligées rendant le transport à proximité de la surface de l'organisme non limitant. De même, l'étape d'adsorption du métal sur le ligand biotique est considérée comme rapide et réversible. Quant à l'étape d'internalisation du métal adsorbé, elle est considérée comme un processus limitant de façon à ce que l'hypothèse d'un équilibre entre le métal et les ligands biotiques soit validée.

Durant l'exposition, le métal n'induit pas de modification de la surface biologique. Les ligands biotiques sont considérés comme le premier site d'action du métal. Ils sont distribués de façon homogène à la surface de l'organisme cible et sont considérés comme indépendants. Certains modèles de complexation vont encore plus loin en ne faisant aucune hypothèse sur la nature des ligands biotiques et en les supposant tous chimiquement identiques. Les réactions de complexation entre le métal et les ligands biotiques sont caractérisées par une constante de complexation (K_{M-LB}).

La concentration de complexe métal – ligand biotique est directement fonction de la concentration en ions libres en solution et reste constante pour une concentration stable de métal en solution. La réponse biologique est dépendante de la concentration en complexe métal – ligand biotique sur la surface biologique. Ainsi, l'augmentation de la formation de complexes métal – ligand biotique entraîne une augmentation des effets toxiques. Dans l'exemple présenté dans la *Figure 14*, plus la quantité de Ni adsorbée est importante, plus l'élongation racinaire est réduite.

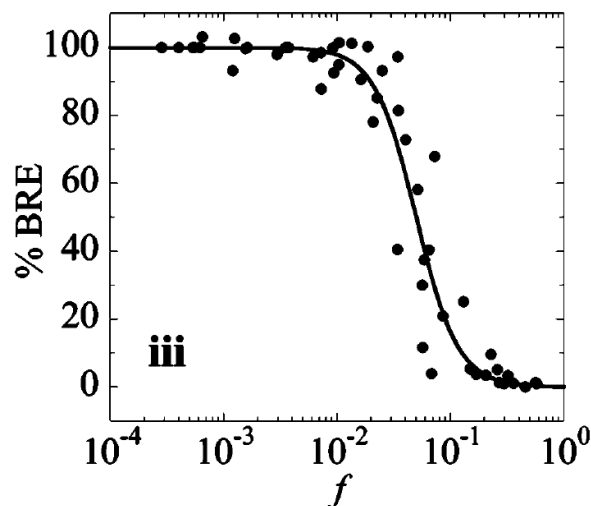


Figure 14 : Courbe dose-réponse présentant l'évolution du taux d'élongation racinaire d'*Hordeum vulgare* en fonction de la quantité de sites occupés par du Ni (Thakali et al. 2006a).

Plusieurs cations peuvent entrer en compétition avec le métal pour l'adsorption sur le ligand biotique, entraînant ainsi une atténuation de la toxicité étant donné que ces cations compétiteurs sont supposés être non toxiques pour l'organisme. Il a ainsi été montré que la présence de Ca^{2+} et de Mg^{2+} dans le milieu pouvait entraîner une diminution de la toxicité du Cu pour le blé : la CE_{50} (concentration efficace médiane) du Cu est triplée lorsque l'activité de Ca^{2+} passe de 0,14 mM à 6,41 mM et elle est quadruplée lorsque l'activité de Mg^{2+} passe de 0,04 mM à 1,61 mM (Luo et al. 2008). La prise en compte de ces cations compétiteurs permet d'améliorer la prédiction de l'élongation racinaire (Lock et al. 2007a; Lock et al. 2007b; Le et al. 2012; Chen et al. 2013).

II.2. Le TBLM

Le TBLM (Terrestrial Biotic Ligand Model) est le modèle de complexation le plus employé actuellement. Il s'agit d'une transposition du BLM au système terrestre.

En effet, le BLM (Biotic Ligand Model) est un modèle qui a été développé dans le but de prédire les effets des caractéristiques chimiques d'un milieu aquatique sur la biodisponibilité et la toxicité d'un métal pour un organisme cible (Paquin et al. 2000; Di Toro et al. 2001; Santore et al. 2001). Il fait partie des outils actuellement employés par l'USEPA (United States Environmental Protection Agency) pour évaluer la toxicité du Cu dans l'eau (Erickson 2013). Il est aujourd'hui opérationnel pour prédire la toxicité d'ET pour divers organismes aquatiques.

Le TBLM a pour vocation de prédire la toxicité des métaux pour les organismes vivants des sols. Il est en cours de développement pour une utilisation réglementaire en Europe et a déjà montré des résultats prometteurs pour la prédiction de la toxicité du Cu et du Ni sur une large gamme de sols (Antunes et al. 2006; Thakali et al. 2006a; Thakali et al. 2006b).

Le TBLM s'est avéré plus efficace que d'autres modèles (à savoir le TMM (Total Metal Model) et le FIAM (Free Ion Activity Model)) pour prédire la toxicité du Cu et du Ni pour l'orge (*Hordeum vulgare* cv Regina ; Figure 15 ; Thakali et al. 2006a) ou la toxicité du Cu pour la vigne (*Vitis vinifera* L. ; Chen et al. 2013).

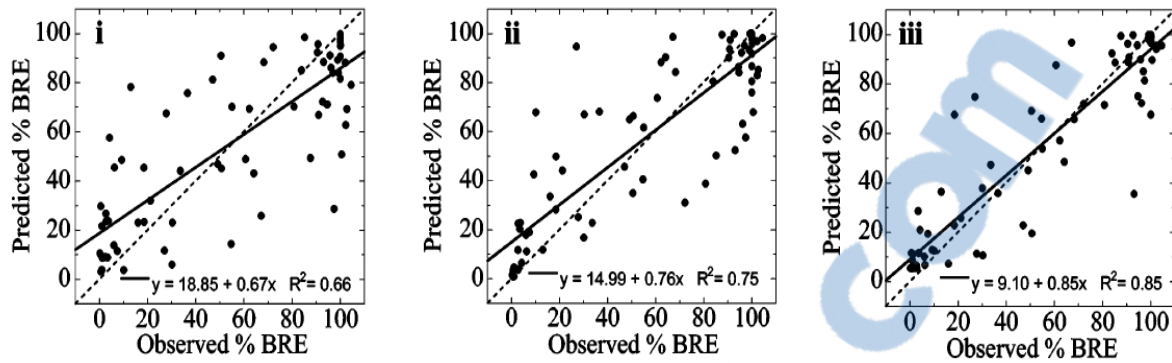


Figure 15 : Elongation racinaire prédite avec (i) le TMM (considération de la concentration totale en Cu du sol), (ii) le FIAM (considération de l'activité de Cu^{2+} libre dans la solution de sol) et (iii) le TBLM (avec prise en compte de la compétition avec le proton) en fonction de l'élongation racinaire mesurée chez l'orge (*Hordeum vulgare* cv. Regina, exposé à des sols présentant différents niveaux de contamination en Cu ainsi que des propriétés physico-chimiques variées ; [Thakali et al. 2006a](#)).

II.3. Les modèles basés sur les substances humiques

D'autres modèles de complexation, développés en parallèle du TBLM, sont utilisés pour prédire les effets toxiques des ET pour divers organismes aquatiques (plantes, bactéries, macro-invertébrés, etc.). Ces modèles emploient des formalismes mathématiques initialement développés pour étudier la complexation des ET avec les matières organiques naturelles de type substances humiques (acides fulviques et humiques).

Le formalisme mathématique le plus employé actuellement est celui de WHAM (Windermere Humic Aqueous Model). Il s'agit d'une approche de modélisation discrète. La distribution des sites est bimodale ; généralement, les sites caractérisés par des pK_a inférieurs à 7 sont dits de type « carboxylique » et les sites caractérisés par des pK_a supérieurs à 7 sont dits de type « phénolique ». Chaque type de sites regroupe 4 sites distincts, présents en égale quantité. Ce modèle permet la prise en compte d'interactions spécifiques (mono-, bi- et tri-dendates) et d'interactions non spécifiques (électrostatiques), l'accumulation de contre-ions dans la double couche de diffusion étant estimée avec une expression type Donnan. Pour de plus amples détails ainsi qu'une description mathématique complète du modèle, le lecteur est invité à consulter les deux articles suivants : [Tipping 1998](#) et [Tipping et al. 2011](#).

Dans la littérature, on trouve deux applications du formalisme mathématique de WHAM. La première, WHAM- F_{Tox} , fait l'hypothèse que la réactivité de l'organisme cible peut être directement assimilée à la réactivité d'un acide humique ; seule la densité totale de sites réactifs est ajustée. WHAM- F_{Tox} a été employé avec succès pour prédire la toxicité de différents éléments métalliques pour des macro-invertébrés ([Stockdale et al. 2010](#); [Stockdale et al. 2014a](#)), du zooplancton ([Stockdale et al. 2014b](#)) ainsi que pour des bactéries et des

organismes aquatiques (Tipping and Lofts 2013). La seconde application a permis une bonne prédiction de la toxicité du Cu pour les lentilles d'eau (*Lemna minor*; Antunes et al. 2012). Contrairement à l'application précédente, quelques paramètres ont été ajustés pour permettre au modèle WHAM de correctement représenter les données expérimentales.

L'autre formalisme mathématique employé est celui du modèle NICA-Donnan (NICA pour Non-Ideal Competitive Adsorption). Il s'agit d'une approche de modélisation continue. De même qu'avec le modèle WHAM, la distribution des sites est bimodale, il est fait la distinction entre les sites dits « type carboxylique » et les sites dits « type phénoliques ». Ce modèle permet également la prise en compte d'interactions spécifiques (monodendates) et non spécifiques (accumulation de contre-ions dans un volume de Donnan). Pour de plus amples détails ainsi qu'une description mathématique complète du modèle, le lecteur est invité à consulter les deux articles suivants : Kinniburgh et al. 1996 et Benedetti et al. 1996. Dans le cadre de l'application à l'étude des interactions ET – organismes vivants, ce formalisme mathématique a été employé une seule fois pour prédire les effets de compétition observés au niveau des parois de bactéries entre Zn, Cd, Ca et H (Plette et al. 1996).

A noter que d'autres modèles ont été ponctuellement développés et adaptés à une étude en particulier. C'est le cas par exemple, du modèle de prédiction de l'adsorption du Cu dans des parois apoplasmiques de maïs et de soja, développé par Allan et Jarrell 1989. Ce modèle est basé sur un modèle de complexation de surface initialement utilisé pour décrire la réactivité d'oxydes métalliques. Autre exemple, le modèle développé par Postma et al. 2005 qui décrit la compétition entre Al, Ca et H pour la formation de complexes au niveau des sites des parois apoplasmiques de tomate. Ce modèle est basé sur le CESS (Cation Exchange/ Specific Sorption model), un modèle généralement dédié à l'étude des réactions d'échanges cationiques dans le sol.

II.4. Limites des modèles de complexation

La critique majeure qui peut être faite au TBLM est le manque de généralité de certaines constantes de complexation, qui altère les possibilités d'application du modèle. En effet, la comparaison des constantes de complexation trouvées dans la littérature montre certains écarts importants, parfois de plusieurs ordres de grandeurs pour un même métal et pour une même plante (Tableau 1). De tels écarts sont également visibles pour un même métal entre différentes espèces végétales.

Tableau 1 : Constantes de complexation déterminées pour l'orge.

	Constantes de complexation				
	Cu-LB	Ni- LB	H- LB	Ca- LB	Mg- LB
Thakali et al. (2006a)	7,41 ± 0,23	3,60 ± 0,53	4,52 ± 0,62		3,81 ± 0,60
Lock et al. (2007b)		5,27			3,47
Antunes et al. (2009)		3,10	5,40	3,30	4,60
Li et al. (2009)		5,36 ± 0,17	4,29 ± 0,12	1,60 ± 0,15	4,01 ± 0,03
Wang et al. (2012)	6,33			1,96	2,92

De même que pour le modèle électrostatique, le TBLM présente un formalisme très simplifié ne prenant pas en compte la diversité des sites réactifs pouvant se trouver sur les surfaces biologiques. Les modèles basés sur les substances humiques présentent un formalisme mathématique un peu plus complexe, permettant de définir deux types de sites réactifs différents. Néanmoins, il n'est pas possible d'en définir de supplémentaire.

D'autre part, comme pour le modèle électrostatique, ces deux approches sont calées sur un ajustement de l'effet toxique observé et non sur des mesures effectives de complexation ou de concentration à la surface des membranes. Cela implique que l'effet toxique est proportionnel à la quantité d'ET complexés sur les surfaces racinaires ou situés aux abords des membranes plasmiques. Cette hypothèse est forte, à la vue du manque de connaissances actuelles sur les mécanismes de rhizotoxicité. Dans le cas d'une non-proportionnalité, les constantes de complexation et autres paramètres fixés à partir des courbes dose-réponse de toxicité pourraient être biaisés. Cela pourrait expliquer les écarts parfois importants constatés entre les constantes pour une même espèce, qui, dans des conditions opératoires différentes, peut présenter une sensibilité différente à l'ET.

Chapitre 4 : Objectifs et stratégies de recherche

I. Hypothèse de travail

Les racines des plantes sont le premier organe à être exposé à une contamination du sol en ET. Les mécanismes à l'origine des effets rhizotoxiques sont encore mal connus. Néanmoins, le mécanisme de sorption de l'ET semble être au cœur du processus de rhizotoxicité. En particulier, la complexation de l'ET au niveau des surfaces racinaires, première interaction entre l'élément et la plante, semble être une étape importante. Deux sites de complexation racinaires peuvent être distingués : les parois apoplasmiques d'une part et la face externe des membranes plasmiques d'autre part. Tous deux présentent une capacité élevée pour complexer les cations métalliques. Cependant, leur contribution respective dans les propriétés de complexation des racines n'est pas déterminée.

Des modèles visant à prédire l'effet toxique engendré par les ET chez les plantes se développent et donnent des résultats prometteurs. Mais la méconnaissance des mécanismes précis générant un effet toxique associée à la volonté de proposer des cadres de modélisation relativement simples entraîne la formulation de nombreuses hypothèses, pouvant paraître parfois trop simplificatrices ou non vérifiées et potentiellement limitantes pour l'application et la généralité des modèles. Il est donc nécessaire à l'heure actuelle de remettre en cause certaines de ces hypothèses de façon à dépasser ces limites.

L'hypothèse centrale de cette étude est qu'une amélioration des modèles de prédiction de la phytotoxicité passe par une modification de la démarche de modélisation employée, avec un intérêt porté sur les réactions de complexation plutôt que sur les effets toxiques observés.

II. Objectifs

Ainsi, l'objectif général de la thèse est de reconsidérer les bases mécanistiques de la complexation des ET dans les racines des plantes et de modéliser cette complexation.

Une première étape consiste à caractériser la réactivité des racines. Il s'agit :

- (i) d'identifier la nature des sites réactifs ;
- (ii) de déterminer leur localisation c'est-à-dire leur répartition entre l'apoplasme racinaire et la surface externe des membranes plasmiques des cellules.

La seconde étape est dédiée à l'étude de la complexation d'un ET modèle au sein des racines. Il s'agit :

- (i) d'identifier les sites réactifs participant à sa complexation ;
- (ii) d'étudier les effets des conditions physico-chimiques du milieu (pH, force ionique, cations compétiteurs) sur la complexation.

L'ensemble des résultats doit permettre de développer un modèle prédisant la complexation de cet ET modèle au sein des racines.

III. Modèles expérimentaux

III.1. Le cuivre : élément trace modèle

Comme cela est évoqué dans le chapitre 1, le Cu est un élément essentiel pour les plantes. Il est, avec B, Mn et Zn, l'un des éléments que l'on retrouve en grande quantité dans les tissus végétaux (Saur 1990). Il joue un rôle fondamental dans de nombreux processus physiologiques. Par exemple, Cu intervient dans le processus de photosynthèse et dans la régulation du transfert hydrique de la plante. In vivo, il peut être présent sous différents états d'oxydation (i.e. Cu^+ et Cu^{2+}) et ainsi contribuer aux réactions d'oxydoréduction des systèmes enzymatiques (Saur 1990; Marschner 1995; Yruela 2009).

Plusieurs raisons nous amènent à choisir le Cu comme élément trace modèle pour cette étude. Du point de vue de la contamination des sols, le Cu est le deuxième élément le plus apporté sur les sols agricoles français après Zn : son apport annuel moyen est estimé à 4900 t. Il provient majoritairement des effluents d'origine animale et des pesticides employés (Belon et al. 2012). Il s'agit également de l'élément essentiel le plus toxique, d'après un examen de la littérature datant de la période 1975 - 2009 sur les effets de 9 éléments essentiels et non-essentiels sur la croissance des plantes en culture hydroponique, avec une concentration toxique médiane de 2 μM (Kopittke et al. 2010). Enfin, il présente enfin une importante affinité aussi bien avec les sites des parois apoplasmiques (en particulier les pectines (Kartel et al. 1999; Franco et al. 2002)) qu'avec les sites situés sur les membranes plasmiques de cellules (Vulkan et al. 2004).

Le zinc a été sélectionné comme élément trace compétiteur modèle. Tout comme Cu, Zn est un élément essentiel, impliqué dans divers processus physiologiques comme la synthèse des hormones de croissance et la synthèse de la chlorophylle (Broadley et al. 2007). Notre choix s'est porté sur Zn car, comme évoqué précédemment, il s'agit de l'élément le plus

apporté sur les sols agricoles français, avec un apport annuel moyen estimé autour de 15190 t, principalement issu des effluents d'origine animale (Belon et al. 2012).

III.2. La tomate et le blé : espèces végétales modèles

D'après la littérature, les capacités de complexation des racines peuvent fortement différer selon l'espèce végétale (Heintze 1961). Les dicotylédones présentent généralement une capacité de complexation plus élevée (comprise entre 20 et 50 $\text{cmol}_c.\text{kg}^{-1}$) que les monocotylédones (plutôt comprise entre 10 et 20 $\text{cmol}_c.\text{kg}^{-1}$; Crooke et al. 1960; Heintze 1961; Straczek et al. 2008). Ces différences sont associées à la composition des parois apoplasmiques qui, comme nous l'avons vu au paragraphe II.2 du chapitre 2, diffère d'une espèce végétale à l'autre. En particulier, les dicotylédones sont plus riches en composés pectiques que les monocotylédones (Carpita and Gibeaut 1993).

De manière à disposer d'un large éventail de données et pouvoir ainsi développer un modèle qui soit le plus générique possible, nous avons choisi de travailler avec une dicotylédone et une monocotylédone. La tomate et le blé ont été sélectionnés parmi cinq espèces végétales pour leur capacité de complexation bien différenciées.

IV. Approches expérimentales et modélisation

Comme évoqué précédemment, plusieurs études se sont attachées à démontrer que les parois apoplasmiques et les membranes plasmiques présentent toutes deux la capacité de complexer les ET. Cependant, la contribution respective des parois apoplasmiques et des membranes plasmiques dans la réactivité des racines vis-à-vis des cations est inconnue. Dans cette étude, nous avons donc fait le choix de travailler d'une part avec des parois apoplasmiques isolées, de manière à étudier leurs propriétés de complexation, et d'autre part avec des racines entières sèches, correspondant à des racines ayant gardées à la fois les parois apoplasmiques et les membranes plasmiques mais ne présentant pas d'activité biologique. La contribution des membranes plasmiques est alors obtenue par différence entre les racines sèches et les parois isolées.

Plusieurs techniques analytiques ont été mises en œuvre sur ces deux matériaux racinaires (parois apoplasmiques et racines sèches). La spectroscopie de résonance magnétique nucléaire du carbone 13 (RMN ^{13}C) a permis d'identifier les groupements fonctionnels présents dans les apoplasmes isolés et les racines sèches. Les titrages acido-basiques ont apportés des informations sur leur réactivité. Le croisement de ces résultats a permis d'une part d'évaluer la contribution respective des parois apoplasmiques et des membranes

Synthèse bibliographique

plasmiques dans les propriétés de complexation des racines et d'autre part d'identifier les principaux sites complexant (Deuxième partie, Chapitre 5).

L'étape suivante a consisté en la caractérisation de l'adsorption du Cu au sein des racines sèches et des apoplastes isolés. La spéciation du Cu dans ces deux matériaux racinaires a été étudiée par spectroscopie d'absorption des rayons X. Quant à son affinité de complexation, il a été étudié en réalisant des expérimentations en batch et en modélisant les résultats obtenus pour chaque plante et chaque matériau racinaire (Deuxième partie, Chapitre 6).

Enfin, sur la base d'un modèle existant destiné à l'étude de la réactivité des matières organiques dissoutes, un modèle décrivant la réactivité du Cu vis-à-vis des racines a été développé (Troisième partie, Chapitre 7).

Références bibliographiques

- Adriano DC (2001) Trace Elements in Terrestrial Environments : Biogeochemistry, Bioavailability, and Risks of Metals. Springer Edition:867 pp.
- Allan DL, Jarrell WM (1989) Proton and Copper Adsorption to Maize and Soybean Root Cell Walls. *Plant Physiol* 89 (3):823-832. doi:10.1104/pp.89.3.823
- Alloway BJ (2013) Heavy Metal in Soils. Springer Edition:613 pp.
- Antunes PMC, Berkelaar EJ, Boyle D, Hale BA, Hendershot W, Voigt A (2006) The biotic ligand model for plants and metals: Technical challenges for field application. *Environmental Toxicology and Chemistry* 25 (3):875-882. doi:10.1897/04-586r.1
- Antunes PMC, Kreager NJ (2009) Development of the terrestrial biotic ligand model for predicting nickel toxicity to barley (*Hordeum Vulgare*): Ion effects at low pH. *Environmental Toxicology and Chemistry* 28 (8):1704-1710. doi:10.1897/08-387.1
- Antunes PMC, Scornaienchi ML, Roshon HD (2012) Copper toxicity to *Lemna minor* modelled using humic acid as a surrogate for the plant root. *Chemosphere* 88 (4):389-394. doi:10.1016/j.chemosphere.2012.02.052
- Antwi-Agyei P, et al. (2009) Trace elements contamination of soils around gold mine tailings dams at Obuasi, Ghana. *African Journal of Environmental Science and Technology* 3 (11):pp. 353-359
- Appenroth K-J (2010) What are “heavy metals” in Plant Sciences? *Acta Physiologiae Plantarum* 32 (4):615-619. doi:10.1007/s11738-009-0455-4
- Baize B (1997) Teneurs totales en éléments traces métalliques dans les sols : France. Editions Quae:408 pp.
- Belon E, Boisson M, Deportes IZ, Eglin TK, Feix I, Bispo AO, Galsomies L, Leblond S, Guellier CR (2012) An inventory of trace elements inputs to French agricultural soils. *Science of The Total Environment* 439 (0):87-95. doi:http://dx.doi.org/10.1016/j.scitotenv.2012.09.011
- Benedetti MF, Van Riemsdijk WH, Koopal LK (1996) Humic Substances Considered as a Heterogeneous Donnan Gel Phase. *Environmental Science & Technology* 30 (6):1805-1813. doi:10.1021/es950012y
- Blamey F (2003) A role for pectin in the control of cell expansion. *Soil Science and Plant Nutrition* 49 (6):775 - 783
- Bovenkamp GL, Prange A, Schumacher W, Ham K, Smith AP, Hormes J (2013) Lead Uptake in Diverse Plant Families: A Study Applying X-ray Absorption Near Edge Spectroscopy. *Environmental Science & Technology* 47 (9):4375-4382. doi:10.1021/es302408m
- Briat J-F, Lebrun M (1999) Plant responses to metal toxicity. *Comptes Rendus de l'Académie des Sciences - Series III - Sciences de la Vie* 322 (1):43-54. doi:10.1016/s0764-4469(99)80016-x

Synthèse bibliographique

- Broadley MR, White PJ, Hammond JP, Zelko I, Lux A (2007) Zinc in plants. *New Phytologist* 173 (4):677-702. doi:10.1111/j.1469-8137.2007.01996.x
- Caffall KH, Mohnen D (2009) The structure, function, and biosynthesis of plant cell wall pectic polysaccharides. *Carbohydrate Research* 344 (14):1879-1900. doi:10.1016/j.carres.2009.05.021
- Carpita N (2007) Cell wall-ion interactions. In: Sattelmacher, B, Horst, W, editors *The apoplast of higher plants: compartment of storage, transport, and reactions* Dordrecht: Kluwer Academic Publishers; 2007.:15-17
- Carpita NC, Gibeaut DM (1993) Structural models of primary cell walls in flowering plants: consistency of molecular structure with the physical properties of the walls during growth. *The Plant Journal* 3 (1):1-30. doi:10.1111/j.1365-313X.1993.tb00007.x
- Carrasco-Gil S, Siebner H, LeDuc DL, Webb SM, Millán R, Andrews JC, Hernández LE (2013) Mercury Localization and Speciation in Plants Grown Hydroponically or in a Natural Environment. *Environmental Science & Technology* 47 (7):3082-3090. doi:10.1021/es303310t
- Cassab GI (1998) PLANT CELL WALL PROTEINS. *Annual Review of Plant Physiology and Plant Molecular Biology* 49 (1):281-309. doi:doi:10.1146/annurev.arplant.49.1.281
- Chen B-C, Ho P-C, Juang K-W (2013) Alleviation effects of magnesium on copper toxicity and accumulation in grapevine roots evaluated with biotic ligand models. *Ecotoxicology* 22 (1):174-183. doi:10.1007/s10646-012-1015-z
- Cohen JA, Cohen M (1981) Adsorption of monovalent and divalent cations by phospholipid membranes. The monomer-dimer problem. *Biophysical journal* 36 (3):623-651
- Collin B, Doelsch E, Keller C, Cazevieille P, Tella M, Chaurand P, Panfili F, Hazemann J-L, Meunier J-D (2014) Evidence of sulfur-bound reduced copper in bamboo exposed to high silicon and copper concentrations. *Environmental Pollution* 187 (0):22-30. doi:http://dx.doi.org/10.1016/j.envpol.2013.12.024
- Collins RN, Bakkaus E, Carrière M, Khodja H, Proux O, Morel J-L, Gouget B (2010) Uptake, Localization, and Speciation of Cobalt in *Triticum aestivum* L. (Wheat) and *Lycopersicon esculentum* M. (Tomato). *Environmental Science & Technology* 44 (8):2904-2910. doi:10.1021/es903485h
- Colzi I, Doumet S, Del Bubba M, Fornaini J, Arnetoli M, Gabbrielli R, Gonnelli C (2011) On the role of the cell wall in the phenomenon of copper tolerance in *Silene paradoxa* L. *Environmental and Experimental Botany* 72 (1):77-83. doi:DOI: 10.1016/j.envexpbot.2010.02.006
- Crooke WM, Knight AH, Macdonald IR (1960) Cation exchange properties and pectin content of storage-tissue disks. *Plant and Soil* 13 (1):55-67. doi:10.1007/bf01666476
- DalCorso G, Manara A, Piasentin S, Furini A (2014) Nutrient metal elements in plants. *Metallomics*. doi:10.1039/c4mt00173g
- Di Toro DM, Allen HE, Bergman HL, Meyer JS, Paquin PR, Santore RC (2001) Biotic ligand model of the acute toxicity of metals. 1. Technical Basis. *Environmental Toxicology and Chemistry* 20 (10):2383-2396. doi:10.1002/etc.5620201034

Synthèse bibliographique

- Doelsch E, Van de Kerchove V, Saint Macary H (2006a) Heavy metal content in soils of Réunion (Indian Ocean). *Geoderma* 134 (1–2):119-134. doi:http://dx.doi.org/10.1016/j.geoderma.2005.09.003
- Dronnet VM, Renard CMGC, Axelos MAV, Thibault JF (1996) Characterisation and selectivity of divalent metal ions binding by citrus and sugar-beet pectins. *Carbohydrate Polymers* 30 (4):253-263. doi:Doi: 10.1016/s0144-8617(96)00107-5
- Erickson RJ (2013) The biotic ligand model approach for addressing effects of exposure water chemistry on aquatic toxicity of metals: Genesis and challenges. *Environmental Toxicology and Chemistry* 32 (6):1212-1214. doi:10.1002/etc.2222
- Eticha D, Stass A, Horst WJ (2005) Cell-wall pectin and its degree of methylation in the maize root-apex: significance for genotypic differences in aluminium resistance. *Plant, Cell & Environment* 28 (11):1410-1420. doi:10.1111/j.1365-3040.2005.01375.x
- Franco CR, Chagas AP, Jorge RA (2002) Ion-exchange equilibria with aluminum pectinates. *Colloids and Surfaces A: Physicochemical and Engineering Aspects* 204 (1-3):183-192. doi:Doi: 10.1016/s0927-7757(01)01134-7
- Gibeaut DM, Carpita NC (1994) Biosynthesis of plant cell wall polysaccharides. *The FASEB Journal* 8 (12):904-915
- Grignon C, Sentenac H (1991) pH and Ionic Conditions in the Apoplast. *Annual Review of Plant Physiology and Plant Molecular Biology* 42 (1):103-128. doi:doi:10.1146/annurev.pp.42.060191.000535
- Guigues S, Bravin M, Garnier C, Masion A, Doelsch E (2014) Isolated cell walls exhibit cation binding properties distinct from those of plant roots. *Plant and Soil*:1-13. doi:10.1007/s11104-014-2138-1
- Guiné V, Spadini L, Sarret G, Muris M, Delolme C, Gaudet JP, Martins JMF (2006) Zinc Sorption to Three Gram-Negative Bacteria: Combined Titration, Modeling, and EXAFS Study. *Environmental Science & Technology* 40 (6):1806-1813. doi:10.1021/es050981l
- Gupta GP (2004) *Plant Cell Biology*. Discovery Publishing House, New Delhi
- Hall JL (2002) Cellular mechanisms for heavy metal detoxification and tolerance. *Journal of Experimental Botany* 53 (366):1-11. doi:10.1093/jexbot/53.366.1
- Harmsen J (2007) Measuring Bioavailability: From a Scientific Approach to Standard Methods. *J Environ Qual* 36 (5):1420-1428. doi:10.2134/jeq2006.0492
- Hatfield R, Vermerris W (2001) Lignin Formation in Plants. The Dilemma of Linkage Specificity. *Plant Physiology* 126 (4):1351-1357. doi:10.1104/pp.126.4.1351
- Haynes RJ (1980) Ion exchange properties of roots and ionic interactions within the root apoplast: Their role in ion accumulation by plants. *Bot Rev* 46 (1):75-99. doi:10.1007/bf02860867
- Heintze SG (1961) Studies on cation-exchange capacities of roots. *Plant and Soil* 13 (4):365-383. doi:10.1007/bf01394648
- Hooda PS (2010) *Trace Elements in Soils*. Blackwell Publishing, Ltd

- Hopkins WG (2003) *Physiologie végétale*. De Boeck Université:515 pp.
- Horst WJ, Wang Y, Eticha D (2010) The role of the root apoplast in aluminium-induced inhibition of root elongation and in aluminium resistance of plants: a review. *Annals of Botany* 106 (1):185-197. doi:10.1093/aob/mcq053
- Isaure M-P, Fayard B, Sarret G, Pairis S, Bourguignon J (2006) Localization and chemical forms of cadmium in plant samples by combining analytical electron microscopy and X-ray spectromicroscopy. *Spectrochimica Acta Part B: Atomic Spectroscopy* 61 (12):1242-1252. doi:DOI: 10.1016/j.sab.2006.10.009
- Ishikawa S, Wagatsuma T, Takano T, Tawaraya K, Oomata K (2001) The Plasma Membrane Intactness of Root-Tip Cells Is a Primary Factor for Al-Tolerance in Cultivars of Five Species. *Soil Science and Plant Nutrition* 47 (3):489-501
- Juste C (1988) Appréciation de la mobilité et de la biodisponibilité des éléments en traces du sol. *Science du sol* 26 (2):103-112
- Kartel MT, Kupchik LA, Veisov BK (1999) Evaluation of pectin binding of heavy metal ions in aqueous solutions. *Chemosphere* 38 (11):2591-2596. doi:Doi: 10.1016/s0045-6535(98)00466-4
- Kinniburgh DG, Milne CJ, Benedetti MF, Pinheiro JP, Filius J, Koopal LK, Van Riemsdijk WH (1996) Metal Ion Binding by Humic Acid: Application of the NICA-Donnan Model. *Environmental Science & Technology* 30 (5):1687-1698. doi:10.1021/es950695h
- Kinraide TB (2001) Ion fluxes considered in terms of membrane-surface electrical potentials. *Australian Journal of Plant Physiology* 28 (7):605-616. doi:10.1071/pp01019
- Kinraide TB (2003) The controlling influence of cell-surface electrical potential on the uptake and toxicity of selenate (SeO₄²⁻). *Physiologia Plantarum* 117 (1):64-71. doi:10.1111/j.1365-3016.1991.tb00723.x
- Kinraide TB (2004) Possible Influence of Cell Walls upon Ion Concentrations at Plasma Membrane Surfaces. Toward a Comprehensive View of Cell-Surface Electrical Effects upon Ion Uptake, Intoxication, and Amelioration. *Plant Physiol* 136 (3):3804-3813. doi:10.1104/pp.104.043174
- Kinraide TB (2006) Plasma membrane surface potential (ψ_{pm}) as a determinant of ion bioavailability: A critical analysis of new and published toxicological studies and a simplified method for the computation of plant ψ_{pm} . *Environmental Toxicology and Chemistry* 25 (12):3188-3198. doi:10.1897/06-103r.1
- Kinraide TB, Ryan PR, Kochian LV (1992) Interactive Effects of Al³⁺, H⁺, and Other Cations on Root Elongation Considered in Terms of Cell-Surface Electrical Potential. *Plant Physiol* 99 (4):1461-1468. doi:10.1104/pp.99.4.1461
- Kinraide TB, Yermiyahu U, Rytwo G (1998) Computation of Surface Electrical Potentials of Plant Cell Membranes . Correspondence to Published Zeta Potentials from Diverse Plant Sources. *Plant Physiol* 118 (2):505-512. doi:10.1104/pp.118.2.505
- Kopittke P, Asher C, Menzies N (2007a) Toxic effects of Ni²⁺ on growth of cowpea (*Vigna unguiculata*). *Plant and Soil* 292 (1):283-289. doi:10.1007/s11104-007-9226-4

- Kopittke P, Blamey F, Menzies N (2008) Toxicities of soluble Al, Cu, and La include ruptures to rhizodermal and root cortical cells of cowpea. *Plant and Soil* 303 (1):217-227. doi:10.1007/s11104-007-9500-5
- Kopittke P, McKenna B, Blamey F, Wehr J, Menzies N (2009a) Metal-induced cell rupture in elongating roots is associated with metal ion binding strengths. *Plant and Soil* 322 (1):303-315. doi:10.1007/s11104-009-9917-0
- Kopittke P, Menzies N (2006) Effect of Cu Toxicity on Growth of Cowpea (&i>Vigna unguiculata&i>). *Plant and Soil* 279 (1):287-296. doi:10.1007/s11104-005-1578-z
- Kopittke P, Wang P, Menzies N, Naidu R, Kinraide T (2014a) A web-accessible computer program for calculating electrical potentials and ion activities at cell-membrane surfaces. *Plant and Soil* 375 (1-2):35-46. doi:10.1007/s11104-013-1948-x
- Kopittke PM, Asher CJ, Blamey FPC, Menzies NW (2009b) Toxic effects of Cu²⁺ on growth, nutrition, root morphology, and distribution of Cu in roots of Sabi grass. *Science of The Total Environment* 407 (16):4616-4621. doi:10.1016/j.scitotenv.2009.04.041
- Kopittke PM, Asher CJ, Kopittke RA, Menzies NW (2007b) Toxic effects of Pb²⁺ on growth of cowpea (*Vigna unguiculata*). *Environmental Pollution* 150 (2):280-287. doi:10.1016/j.envpol.2007.01.011
- Kopittke PM, Blamey FPC, Asher CJ, Menzies NW (2010) Trace metal phytotoxicity in solution culture: a review. *Journal of Experimental Botany* 61 (4):945-954. doi:10.1093/jxb/erp385
- Kopittke PM, Blamey FPC, McKenna BA, Wang P, Menzies NW (2011a) Toxicity of metals to roots of cowpea in relation to their binding strength. *Environmental Toxicology and Chemistry* 30 (8):1827-1833. doi:10.1002/etc.557
- Kopittke PM, Kinraide TB, Wang P, Blamey FPC, Reichman SM, Menzies NW (2011b) Alleviation of Cu and Pb Rhizotoxicities in Cowpea (*Vigna unguiculata*) as Related to Ion Activities at Root-Cell Plasma Membrane Surface. *Environmental Science & Technology* 45 (11):4966-4973. doi:10.1021/es1041404
- Kopittke PM, Menzies NW, de Jonge MD, McKenna BA, Donner E, Webb RI, Paterson DJ, Howard DL, Ryan CG, Glover CJ, Scheckel KG, Lombi E (2011c) In Situ Distribution and Speciation of Toxic Copper, Nickel, and Zinc in Hydrated Roots of Cowpea. *Plant Physiology* 156 (2):663-673. doi:10.1104/pp.111.173716
- Kopittke PM, Menzies NW, Wang P, McKenna BA, Wehr JB, Lombi E, Kinraide TB, Blamey FPC (2014b) The rhizotoxicity of metal cations is related to their strength of binding to hard ligands. *Environmental Toxicology and Chemistry* 33 (2):268-277. doi:10.1002/etc.2435
- Krzesłowska M (2011) The cell wall in plant cell response to trace metals: polysaccharide remodeling and its role in defense strategy. *Acta Physiologiae Plantarum* 33 (1):35-51. doi:10.1007/s11738-010-0581-z
- Krzesłowska M, Woźny A, Konieczna-Koperska J (2004) Calcium Ameliorates Effects of Lead in Protonema of &i>Funaria hygrometrica&i>; Hedw. *Biologia Plantarum* 48 (4):569-574. doi:10.1023/b:biop.0000047154.16119.32

- Kudo H, Kudo K, Ambo H, Uemura M, Kawai S (2011) Cadmium sorption to plasma membrane isolated from barley roots is impeded by copper association onto membranes. *Plant Science* 180 (2):300-305. doi:http://dx.doi.org/10.1016/j.plantsci.2010.09.008
- Lamport DTA, Kieliszewski MJ, Showalter AM (2006) Salt stress upregulates periplasmic arabinogalactan proteins: using salt stress to analyse AGP function*. *New Phytologist* 169 (3):479-492. doi:10.1111/j.1469-8137.2005.01591.x
- Lamport DTA, Várnai P (2013) Periplasmic arabinogalactan glycoproteins act as a calcium capacitor that regulates plant growth and development. *New Phytologist* 197 (1):58-64. doi:10.1111/nph.12005
- Lanno R, Wells J, Conder J, Bradham K, Basta N (2004) The bioavailability of chemicals in soil for earthworms. *Ecotoxicology and Environmental Safety* 57 (1):39-47. doi:http://dx.doi.org/10.1016/j.ecoenv.2003.08.014
- Le TTY, Peijnenburg WJGM, Hendriks AJ, Vijver MG (2012) Predicting effects of cations on copper toxicity to lettuce (*Lactuca sativa*) by the biotic ligand model. *Environmental Toxicology and Chemistry* 31 (2):355-359. doi:10.1002/etc.736
- Lequeux H, Hermans C, Lutts S, Verbruggen N (2010) Response to copper excess in *Arabidopsis thaliana*: Impact on the root system architecture, hormone distribution, lignin accumulation and mineral profile. *Plant Physiology and Biochemistry* 48 (8):673-682. doi:10.1016/j.plaphy.2010.05.005
- Li B, Zhang X, Wang X, Ma Y (2009) Refining a biotic ligand model for nickel toxicity to barley root elongation in solution culture. *Ecotoxicology and Environmental Safety* 72 (6):1760-1766. doi:10.1016/j.ecoenv.2009.05.003
- Liu D, Kottke I (2003) Subcellular localization of Cd in the root cells of *Allium sativum* by electron energy loss spectroscopy. *J Biosci* 28 (4):471-478. doi:10.1007/bf02705121
- Lock K, De Schamphelaere KAC, Becaus S, Criel P, Van Eeckhout H, Janssen CR (2007a) Development and validation of a terrestrial biotic ligand model predicting the effect of cobalt on root growth of barley (*Hordeum vulgare*). *Environmental Pollution* 147 (3):626-633. doi:DOI: 10.1016/j.envpol.2006.10.003
- Lock K, Van Eeckhout H, De Schamphelaere KAC, Criel P, Janssen CR (2007b) Development of a biotic ligand model (BLM) predicting nickel toxicity to barley (*Hordeum vulgare*). *Chemosphere* 66 (7):1346-1352. doi:DOI: 10.1016/j.chemosphere.2006.07.008
- Luo X-S, Li L-Z, Zhou D-M (2008) Effect of cations on copper toxicity to wheat root: Implications for the biotic ligand model. *Chemosphere* 73 (3):401-406. doi:10.1016/j.chemosphere.2008.05.031
- Manceau A, Simionovici A, Lanson M, Perrin J, Tucoulou R, Bohic S, Fakra SC, Marcus MA, Bedell J-P, Nagy KL (2013) *Thlaspi arvense* binds Cu(II) as a bis-(l-histidinato) complex on root cell walls in an urban ecosystem. *Metallomics* 5 (12):1674-1684. doi:10.1039/c3mt00215b
- Marschner H (1995) Mineral Nutrition of higher plants. Academic Press, second edition

Synthèse bibliographique

- McLaughlin S, Mulrine N, Gresalfi T, Vaio G, McLaughlin A (1981) Adsorption of divalent cations to bilayer membranes containing phosphatidylserine. *The Journal of General Physiology* 77 (4):445-473. doi:10.1085/jgp.77.4.445
- Meychik N, Nikolaeva Y, Yermakov I (2006) Ion-exchange properties of cell walls of *Spinacia oleracea* L. roots under different environmental salt conditions. *Biochemistry (Moscow)* 71 (7):781-789. doi:10.1134/s000629790607011x
- Meychik NR, Yermakov IP (1999) A new approach to the investigation on the tonogenic groups of root cell walls. *Plant and Soil* 217 (1):257-264. doi:10.1023/a:1004675309128
- Meychik NR, Yermakov IP (2001) Ion exchange properties of plant root cell walls. *Plant and Soil* 234 (2):181-193. doi:10.1023/a:1017936318435
- Michaud A, Chappellaz C, Hinsinger P (2008) Copper phytotoxicity affects root elongation and iron nutrition in durum wheat (*Triticum turgidum durum* L.). *Plant and Soil* 310 (1-2):151-165. doi:10.1007/s11104-008-9642-0
- Miquel et al. (2001) Les effets des métaux lourds sur l'environnement et la santé. Rapport pour l'office parlementaire d'évaluation des choix scientifiques et technologiques n° 261
- Moore G (2001) *Soilguide: a handbook for understanding and managing agricultural soils*. The National Library of Australia:381 pp.
- Nagajyoti P, Lee K, Sreekanth T (2010) Heavy metals, occurrence and toxicity for plants: a review. *Environmental Chemistry Letters* 8 (3):199-216. doi:10.1007/s10311-010-0297-8
- Panou-Filotheou H, Bosabalidis AM, Karataglis S (2001) Effects of Copper Toxicity on Leaves of Oregano (*Origanum vulgare* subsp. *hirtum*). *Annals of Botany* 88 (2):207-214. doi:10.1006/anbo.2001.1441
- Paquin PR, Santore RC, Wu KB, Kavvas CD, Di Toro DM (2000) The biotic ligand model: a model of the acute toxicity of metals to aquatic life. *Environmental Science & Policy* 3 (Supplement 1):175-182. doi:10.1016/s1462-9011(00)00047-2
- Pickering IJ, Prince RC, George GN, Rauser WE, Wickramasinghe WA, Watson AA, Dameron CT, Dance IG, Fairlie DP, Salt DE (1999) X-ray absorption spectroscopy of cadmium phytochelatin and model systems. *Biochimica et Biophysica Acta (BBA) - Protein Structure and Molecular Enzymology* 1429 (2):351-364. doi:http://dx.doi.org/10.1016/S0167-4838(98)00242-8
- Plette ACC, Benedetti MF, van Riemsdijk WH (1996) Competitive Binding of Protons, Calcium, Cadmium, and Zinc to Isolated Cell Walls of a Gram-Positive Soil Bacterium. *Environmental Science & Technology* 30 (6):1902-1910. doi:10.1021/es950568l
- Polette LA, Gardea-Torresdey JL, Chianelli RR, George GN, Pickering IJ, Arenas J (2000) XAS and microscopy studies of the uptake and bio-transformation of copper in *Larrea tridentata* (creosote bush). *Microchemical Journal* 65 (3):227-236. doi:10.1016/s0026-265x(00)00055-2

Synthèse bibliographique

- Postma JWM, Keltjens WG, van Riemsdijk WH (2005) Calcium-(Organo)aluminum-proton Competition for Adsorption to Tomato Root Cell Walls: Experimental Data and Exchange Model Calculations. *Environmental Science & Technology* 39 (14):5247-5254. doi:10.1021/es048138v
- Probst A, Liu H, Fanjul M, Liao B, Hollande E (2009) Response of *Vicia faba* L. to metal toxicity on mine tailing substrate: Geochemical and morphological changes in leaf and root. *Environmental and Experimental Botany* 66 (2):297-308. doi:DOI: 10.1016/j.envexpbot.2009.02.003
- Ram L (1980) Cation exchange capacity of plant roots in relation to nutrients uptake by shoot and grain as influenced by age. *Plant and Soil* 55 (2):215-224. doi:10.1007/bf02181801
- Reid RJ (2001) Mechanisms of micronutrient uptake in plants. *Functional Plant Biology* 28 (7):661-668. doi:http://dx.doi.org/10.1071/PP01037
- Rengel Z, Zhang WH (2003) Role of dynamics of intracellular calcium in aluminium-toxicity syndrome. *New Phytologist* 159 (2):295-314. doi:10.1046/j.1469-8137.2003.00821.x
- Romeo A, Vacchina V, Legros S, Doelsch E (2014) Zinc fate in animal husbandry systems. *Metallomics*. doi:10.1039/c4mt00062e
- Sakurai N (1998) Dynamic function and regulation of apoplast in the plant body. *Journal of Plant Research* 111 (1):133-148. doi:10.1007/bf02507160
- Santore RC, Di Toro DM, Paquin PR, Allen HE, Meyer JS (2001) Biotic ligand model of the acute toxicity of metals. 2. Application to acute copper toxicity in freshwater fish and *Daphnia*. *Environmental Toxicology and Chemistry* 20 (10):2397-2402. doi:10.1002/etc.5620201035
- Sarkar P, Bosneaga E, Auer M (2009) Plant cell walls throughout evolution: towards a molecular understanding of their design principles. *Journal of Experimental Botany* 60 (13):3615-3635. doi:10.1093/jxb/erp245
- Sarret G, Vangronsveld J, Manceau A, Musso M, D'Haen J, Menthonnex J-J, Hazemann J-L (2001) Accumulation Forms of Zn and Pb in *Phaseolus vulgaris* in the Presence and Absence of EDTA. *Environmental Science & Technology* 35 (13):2854-2859. doi:10.1021/es000219d
- Sarret G, Willems G, Isaure MP, Marcus MA, Fakra SC, Frérot H, Pairis S, Geoffroy N, Manceau A, Saumitou-Laprade P (2009) Zinc distribution and speciation in *Arabidopsis halleri* × *Arabidopsis lyrata* progenies presenting various zinc accumulation capacities. *New Phytologist* 184 (3):581-595. doi:10.1111/j.1469-8137.2009.02996.x
- Sattelmacher B (2001) The apoplast and its significance for plant mineral nutrition. *New Phytologist* 149 (2):167-192. doi:10.1046/j.1469-8137.2001.00034.x
- Saur E (1990) Mise au point bibliographique, au sujet de la nutrition oligo-minérale des plantes supérieures. Carences et toxicités chez les conifères. *Ann For Sci* 47 (4):367-389
- Seregin I, Kozhevnikova A, Gracheva V, Bystrova E, Ivanov V (2011) Tissue zinc distribution in maize seedling roots and its action on growth. *Russian Journal of Plant Physiology* 58 (1):109-117. doi:10.1134/s1021443711010171

- Seregin IV, Pekhov VM, Ivanov VB (2002) Plasmolysis as a Tool to Reveal Lead Localization in the Apoplast of Root Cells. *Russian Journal of Plant Physiology* 49 (2):283-285. doi:10.1023/a:1014822127865
- Sheldon A, Menzies N (2005) The Effect of Copper Toxicity on the Growth and Root Morphology of Rhodes Grass (<i>Chloris gayana</i> Knuth.) in Resin Buffered Solution Culture. *Plant and Soil* 278 (1):341-349. doi:10.1007/s11104-005-8815-3
- Shi J, Wu B, Yuan X, Yy C, Chen X, Chen Y, Hu T (2008) An X-ray absorption spectroscopy investigation of speciation and biotransformation of copper in <i>Elsholtzia splendens</i>. *Plant and Soil* 302 (1):163-174. doi:10.1007/s11104-007-9463-6
- Steudle E (2000) Water uptake by plant roots: an integration of views. *Plant and Soil* 226 (1):45-56. doi:10.1023/a:1026439226716
- Stockdale A, Tipping E, Fjellheim A, Garmo ØA, Hildrew AG, Lofts S, Monteith DT, Ormerod SJ, Shilland EM (2014a) Recovery of macroinvertebrate species richness in acidified upland waters assessed with a field toxicity model. *Ecological Indicators* 37, Part B (0):341-350. doi:http://dx.doi.org/10.1016/j.ecolind.2011.11.002
- Stockdale A, Tipping E, Lofts S, Fott J, Garmo ØA, Hruska J, Keller B, Löfgren S, Maberly SC, Majer V, Nierzwicki-Bauer SA, Persson G, Schartau A-K, Thackeray SJ, Valois A, Vrba J, Walseng B, Yan N (2014b) Metal and proton toxicity to lake zooplankton: A chemical speciation based modelling approach. *Environmental Pollution* 186 (0):115-125. doi:http://dx.doi.org/10.1016/j.envpol.2013.11.012
- Stockdale A, Tipping E, Lofts S, Ormerod SJ, Clements WH, Blust R (2010) Toxicity of proton–metal mixtures in the field: Linking stream macroinvertebrate species diversity to chemical speciation and bioavailability. *Aquatic Toxicology* 100 (1):112-119. doi:http://dx.doi.org/10.1016/j.aquatox.2010.07.018
- Straczek A, Sarret G, Manceau A, Hinsinger P, Geoffroy N, Jaillard B (2008) Zinc distribution and speciation in roots of various genotypes of tobacco exposed to Zn. *Environmental and Experimental Botany* 63 (1-3):80-90. doi:DOI: 10.1016/j.envexpbot.2007.10.034
- Taiz L, Zeiger E (2006) *Plant Physiology*, 4th Edition. Sinauer Associates Sunderland, MA
- Thakali S, Allen HE, Di Toro DM, Ponizovsky AA, Rooney CP, Zhao F-J, McGrath SP (2006a) A Terrestrial Biotic Ligand Model. 1. Development and Application to Cu and Ni Toxicities to Barley Root Elongation in Soils. *Environmental Science & Technology* 40 (22):7085-7093. doi:10.1021/es061171s
- Thakali S, Allen HE, Di Toro DM, Ponizovsky AA, Rooney CP, Zhao F-J, McGrath SP, Criel P, Van Eeckhout H, Janssen CR, Oorts K, Smolders E (2006b) Terrestrial Biotic Ligand Model. 2. Application to Ni and Cu Toxicities to Plants, Invertebrates, and Microbes in Soil. *Environmental Science & Technology* 40 (22):7094-7100. doi:10.1021/es061173c
- Tipping E (1998) Humic Ion-Binding Model VI: An Improved Description of the Interactions of Protons and Metal Ions with Humic Substances. *Aquatic Geochemistry* 4 (1):3-47. doi:10.1023/a:1009627214459

- Tipping E, Lofts S (2013) Metal mixture toxicity to aquatic biota in laboratory experiments: Application of the WHAM-FTOX model. *Aquatic Toxicology* 142–143 (0):114-122. doi:http://dx.doi.org/10.1016/j.aquatox.2013.08.003
- Tipping E, Lofts S, Sonke JE (2011) Humic Ion-Binding Model VII: a revised parameterisation of cation-binding by humic substances. *Environmental chemistry* 8 (3):225-235. doi:http://dx.doi.org/10.1071/EN11016
- Vogel J (2008) Unique aspects of the grass cell wall. *Current Opinion in Plant Biology* 11 (3):301-307. doi:http://dx.doi.org/10.1016/j.pbi.2008.03.002
- Vulkan R, Yermiyahu U, Mingelgrin U, Rytwo G, Kinraide TB (2004) Sorption of Copper and Zinc to the Plasma Membrane of Wheat Root. *Journal of Membrane Biology* 202 (2):97-104. doi:10.1007/s00232-004-0722-7
- Wagatsuma T, Akiba R (1989) Low surface negativity of root protoplasts from aluminum-tolerant plant species. *Soil Science and Plant Nutrition* 35 (3):443-452. doi:10.1080/00380768.1989.10434777
- Wang P, Kinraide TB, Zhou D, Kopittke PM, Peijnenburg WJGM (2011) Plasma Membrane Surface Potential: Dual Effects upon Ion Uptake and Toxicity. *Plant Physiol* 155 (2):808-820. doi:10.1104/pp.110.165985
- Wang P, Menzies NW, Lombi E, McKenna BA, de Jonge MD, Donner E, Blamey FPC, Ryan CG, Paterson DJ, Howard DL, James SA, Kopittke PM (2013) Quantitative determination of metal and metalloid spatial distribution in hydrated and fresh roots of cowpea using synchrotron-based X-ray fluorescence microscopy. *Science of The Total Environment* 463–464 (0):131-139. doi:http://dx.doi.org/10.1016/j.scitotenv.2013.05.091
- Wang P, Zhou D-M, Li L-Z, Li D-D (2009) What role does cell membrane surface potential play in ion-plant interactions <!--EndFragment-->. *Plant signaling & behavior* 4 (1):42-43
- Wang P, Zhou D, Kinraide TB, Luo X, Li L, Li D, Zhang H (2008) Cell Membrane Surface Potential (ψ_0) Plays a Dominant Role in the Phytotoxicity of Copper and Arsenate. *Plant Physiol* 148 (4):2134-2143. doi:10.1104/pp.108.127464
- Wang X, Hua L, Ma Y (2012) A biotic ligand model predicting acute copper toxicity for barley (*Hordeum vulgare*): Influence of calcium, magnesium, sodium, potassium and pH. *Chemosphere* 89 (1):89-95. doi:10.1016/j.chemosphere.2012.04.022
- Wehr JB, Blamey FPC, Menzies NW (2010) Comparison between Methods using Copper, Lanthanum, and Colorimetry for the Determination of the Cation Exchange Capacity of Plant Cell Walls. *Journal of Agricultural and Food Chemistry* 58 (8):4554-4559. doi:10.1021/jf100097k
- Wójcik M, Vangronsveld J, D'Haen J, Tukiendorf A (2005) Cadmium tolerance in *Thlaspi caerulescens*: II. Localization of cadmium in *Thlaspi caerulescens*. *Environmental and Experimental Botany* 53 (2):163-171. doi:DOI: 10.1016/j.envexpbot.2004.03.011
- Wu Y, Hendershot W (2009) Cation Exchange Capacity and Proton Binding Properties of Pea (<i>Pisum sativum</i> L.) Roots. *Water, Air, & Soil Pollution* 200 (1):353-369. doi:10.1007/s11270-008-9918-2

- Yang X, Feng Y, He Z, Stoffella PJ (2005) Molecular mechanisms of heavy metal hyperaccumulation and phytoremediation. *Journal of Trace Elements in Medicine and Biology* 18 (4):339-353. doi:DOI: 10.1016/j.jtemb.2005.02.007
- Yermiyahu U, Kinraide, T.B. (2005) Binding and electrostatic attraction of trace elements to plant root surfaces. *Biogeochemistry of Trace Elements in the Rhizosphere Chapter 12*
- Yermiyahu U, Nir S, Ben-Hayyim G, Kafkafi U (1994) Quantitative competition of calcium with sodium or magnesium for sorption sites on plasma membrane vesicles of melon (*Cucumis melo* L.) root cells. *J Membran Biol* 138 (1):55-63. doi:10.1007/bf00211069
- Yruela I (2009) Copper in plants: acquisition, transport and interactions. *Functional Plant Biology* 36 (5):409-430. doi:http://dx.doi.org/10.1071/FP08288
- Zhang Q, Smith A, Sekimoto H, Reid R (2001) Effect of membrane surface charge on nickel uptake by purified mung bean root protoplasts. *Planta* 213 (5):788-793. doi:10.1007/s004250100555
- Zhou H, Zeng M, Zhou X, Liao B-H, Liu J, Lei M, Zhong Q-Y, Zeng H (2013) Assessment of heavy metal contamination and bioaccumulation in soybean plants from mining and smelting areas of southern Hunan Province, China. *Environmental Toxicology and Chemistry* 32 (12):2719-2727. doi:10.1002/etc.2389

2^{ÈME} PARTIE

MÉCANISMES DE COMPLEXATION RACINAIRE

Chapitre 5 : Origine des propriétés de complexation des racines

Dans le chapitre 2, nous avons vu que les parois apoplasmiques et les membranes plasmiques portent divers groupements fonctionnels. Ces groupements sont à l'origine de leur réactivité et en particulier de leur capacité à complexer les cations. Ainsi, les propriétés de complexation des racines proviennent à la fois des parois apoplasmiques et des membranes plasmiques. Toutefois, le principal site de complexation racinaire est encore indéterminé, la contribution respective des parois apoplasmiques et des membranes plasmiques n'a jamais été clairement établie, en partie parce que ces deux compartiments ont toujours été étudiés séparément.

L'article *Isolated cell walls exhibit cation binding properties distinct from those of plant roots*, constituant ce chapitre 5, apporte un élément de réponse sur ce point en comparant les propriétés de complexation de parois apoplasmiques isolées à celles de racines sèches c'est-à-dire des racines ne présentant plus aucune activité biologique mais conservant à la fois les membranes plasmiques et les parois apoplasmiques.

Après avoir vérifié l'efficacité de la procédure sélectionnée pour l'isolation des parois apoplasmiques, nous avons montré que cette isolation est accompagnée d'une diminution de la capacité de complexation d'un facteur 2,4 pour le blé et d'un facteur 3,4 pour la tomate. Sur les spectres RMN ^{13}C de ces matériaux racinaires, nous avons constaté une diminution du signal dans certaines régions spectrales après l'isolation. Cette perte de signal est attribuable à la perte de groupements chimiques caractéristiques (groupements carboxylique, amine et phosphate), portés par le matériel racinaire ayant disparu lors de l'isolation des parois apoplasmiques à savoir les membranes plasmiques. Il a ainsi été montré que pour ces deux espèces végétales, les propriétés de complexation des racines proviennent majoritairement des groupements fonctionnels portés par les membranes plasmiques ; ces dernières contribuant à hauteur de 60 % dans les racines de blé et de 70 % dans les racines de tomate.

Cet article a été publié dans la revue *Plant and Soil*.

Isolated cell walls exhibit cation binding properties distinct from those of plant roots

Stéphanie Guigues^{1,2}, Matthieu N. Bravin³, Cédric Garnier⁴, Armand Masion
and Emmanuel Doelsch¹

¹ CIRAD, UPR Recyclage et risque, F-34398 Montpellier, France

² ADEME, 20 avenue du Grésillé, BP-90406, Angers cedex 01, France

³ CIRAD, UPR Recyclage et risque, F-97408 Saint-Denis, Réunion, France

⁴ Université de Toulon, PROTEE, EA 3819, 83957 La Garde, France

⁵ Aix-Marseille Université, CNRS, IRD, CEREGE UM34, 13545 Aix-en-Provence, France

DOI : 10.1007/s11104-014-2138-1

Abstract

The principal contributor to the cation binding properties of roots is currently considered to be the cell wall or, alternatively, the plasma membrane. The aim of this study was to highlight their respective contributions in the binding properties. Cell walls of a dicotyledon (*Solanum lycopersicum* L.) and monocotyledon (*Triticum aestivum* L.) were isolated from roots and their binding properties were compared to those of their respective roots. Cell wall and root binding capacities were evaluated by potentiometric titrations and cation exchange capacity measurements, while their biochemical composition was analyzed by ¹³C-NMR spectroscopy. The lower binding capacity of isolated cell walls compared to roots revealed that cell plasma membranes had a higher binding site density than cell walls. The significant decrease in some NMR signals, i.e. carbonyl C, N alkyl/ methoxyl C and alkyl C regions, suggested that carboxyl, amine and phosphate binding sites, borne by proteins and phospholipid plasma membranes, contribute to the binding capacity. Cell walls and plasma membranes were found to be jointly involved in root binding properties and their respective contributions seemed vary between plants.

Keywords: apoplast; cell plasma membrane; heavy metal; binding capacity; potentiometric titration; ¹³C-NMR spectroscopy.

I. Introduction

Trace elements in soil were originally derived from the weathering of parent rock (Doelsch et al. 2006a), but the development of industrial and agricultural activities and urbanization gave rise to other sources. Mining, agricultural practices such as organic waste spreading, refuse incineration and urban traffic account for substantial anthropogenic contamination (Doelsch et al. 2006b; Nagajyoti et al. 2010; Legros et al. 2013; Zhou et al., 2013).

Roots are the first plant organs exposed to trace elements in soil. Plants may show various rhizotoxicity symptoms, such as root growth inhibition, root hair damage, local swelling and ruptures in the rhizodermis and outer cortex (Sheldon and Menzies 2005; Kopittke and Menzies 2006; Kopittke et al. 2008). In recent years, root binding properties have often been put forward as a major driver of micronutrient uptake and trace element toxicity in plants (Reid 2001; Thakali et al. 2006a; Kopittke et al. 2009a). The root apoplast, i.e. the compartment consisting of water, gas and cell walls, and root cell plasma membranes are, alternatively, considered to be a major contributor to root binding properties (Sattelmacher 2001; Kinraide 2004).

Cell walls exhibit many binding sites associated with carboxylic, phenolic, amine and thiol functional groups borne by a range of chemical polymers tightly woven into the tridimensional meshwork (Sarkar et al. 2009; Kzreslowska 2011). Binding properties closely depend on the cell wall composition, which varies notably with plant age and between species. The root binding capacity is usually higher in dicots ($20\text{-}50\text{ cmol}_c\cdot\text{kg}^{-1}$ or $\text{meq}\cdot 100\text{ g}^{-1}$) than in monocots ($10\text{-}20\text{ cmol}_c\cdot\text{kg}^{-1}$) (Ram 1980; Sattelmacher 2001; Straczek et al. 2008). This difference in binding capacity is attributed to a higher pectin content in dicot cell walls (20-35% of the dry mass) than in monocot cell walls (5% of the dry mass) (Vogel 2008). Free carboxylic groups borne by pectins are usually considered to be responsible for 70-90% of the root binding properties (Haynes 1980). Experimental studies have shown that these free carboxyl groups play a crucial role in aluminum (Al) accumulation in roots and in the induction of Al rhizotoxicity (Horst et al. 2010). Beyond pH 7, phenolic groups also contribute significantly to root cell wall binding properties (Meychik and Yermakov 2001). Considering that cell wall compounds, especially pectins, seem to control root cation binding properties, model formalisms have been based on descriptions of interactions between trace elements and isolated cell walls, thus overlooking the possible contribution of other root compartments such as cell plasma membranes (Allan and Jarrell 1989; Postma et al. 2005).

However, the plasma membrane bears cation binding sites provided by phospholipid phosphate groups and protein-containing amino acids entrapped in the plasma membrane

(Kinraide et al. 1992). The negative charges provided by these sites create a negative plasma membrane electrical potential that controls the activity of ions at the plasma membrane surface (Kinraide 2006). Experimental studies on root protoplasts showed that metals such as copper (Cu), nickel (Ni) or Al have high binding affinity for root cell plasma membranes (Zhang et al. 2001; Vulkan et al. 2004; Kudo et al. 2011). The development of a plant-ion interaction model based on the binding properties of the plasma membranes while ignoring those of cell walls has markedly enhanced prediction of plant uptake and rhizotoxicity of a broad range of ions (Kopittke et al. 2011b; Wang et al. 2011). These authors have consistently suggested that plasma membranes substantially contribute to the binding properties of whole roots.

Ultimately, the respective contributions of cell walls and plasma membranes to the binding properties of whole roots have not been clearly established, especially as they are always tested separately. Studies carried out on cation distributions within whole roots using current imaging techniques have not provided any further information on this point. Elements accumulated outside and within the cells can be clearly differentiated (Liu and Kottke 2003; Kopittke et al. 2007b; Kopittke et al. 2009b), but it is much harder to distinguish between ions bound in cell walls from those bound on plasma membranes. Nanoscale secondary ion mass spectrometry (NanoSIMS), an analytical tool that provide high spatial resolution combined with high elemental sensitivity (Hermann et al. 2007), would seem to be able to make such distinctions, but to our knowledge this technique has never been used for this purpose (Smart et al. 2010; Moore et al. 2011).

The present study thus aimed to highlight the respective contributions of cell walls and plasma membranes to the binding properties of whole roots. The properties and chemical nature of cell wall and plasma membrane cation binding sites were assessed by comparing cell walls isolated from roots with cell walls and plasma membranes still in the roots. Multiple procedures using chemical or physical treatments have been previously described for isolating cell walls (Sentenac and Grignon 1981; Masion and Bertsch 1997; Bastías et al. 2010; Yang et al. 2010). All of these procedures are assumed to be capable of removing plasma membranes and the cytoplasm from roots while preserving the cell wall composition and binding properties. The isolation procedure used in this study allowed us to recover cell walls while preserving the shapes and dimensions they originally had in the roots. Experiments were performed on roots of two plant species representative of dicots i.e. *Solanum lycopersicum* L. and monocots i.e. *Triticum aestivum* L.. The cell wall and root binding properties were estimated by measuring the cation exchange capacity (CEC) and

performing potentiometric titrations. The cell wall and root compositions were characterized by solid-state ^{13}C nuclear magnetic resonance (^{13}C -NMR).

II. Material and methods

II.1. Plant growth

Bread wheat (*T. aestivum* L. cv. Premio) and tomato (*S. lycopersicum* L. cv. Moneymaker) were grown in hydroponic conditions for 21 days with an experimental procedure adapted from [Bravin et al. \(2010\)](#). Briefly, wheat and tomato seeds (5 and 20 seeds per pot, respectively) were germinated in darkness for 7 d in 600 μM CaCl_2 and 2 μM H_3BO_3 . Seedlings were then grown for 14 d in a nutrient solution (μM): $\text{Ca}(\text{NO}_3)_2$ 2000, KNO_3 2000, MgSO_4 1000, KH_2PO_4 500, $\text{NaFe}(\text{III})\text{EDTA}$ 100, H_3BO_3 10, MnCl_2 2, CuCl_2 1, ZnSO_4 1 and Na_2MoO_4 0.05. The solution was renewed every 2-3 days. The growth chamber parameters were set at (day/night): 25/20°C, 75/70% relative humidity and 16/8h with a photon flux density of 450 $\mu\text{mol photons m}^{-2} \text{s}^{-1}$ during the day. At harvest, roots were blotted with paper towels before being subdivided into homogenous subsamples and then stored frozen. After thawing, roots were subdivided into two groups: (i) root subsamples were rinsed with 1 mM $\text{Ca}(\text{NO}_3)_2$ to eliminate cytosolic compounds released during thawing and oven-dried at 50°C (until a steady mass) and are hereafter referred to as roots; and (ii) remaining root subsamples were maintained moist for subsequent analysis (see below).

II.2. Isolation of root cell walls

Cell walls were isolated from wheat and tomato roots using Triton X 100, a non-ionic detergent which enabled us to remove the cellular components by solubilizing plasma membrane phospholipids. The procedure was adapted from [Cathala et al. \(1978\)](#). Thawed wheat and tomato roots were cut into 1-2 cm long pieces, then immersed for 30 d in a solution containing 1% v/v Triton X 100 and 1 mM $\text{Ca}(\text{NO}_3)_2$. Triton X 100 was then removed by washing with a 1 mM $\text{Ca}(\text{NO}_3)_2$ solution that was renewed every day for 10 d. The whole procedure was carried out at 6 (\pm 1)°C under stirring (60 rpm). The isolated cell walls, hereafter referred as to cell walls, were stored at 4°C in 1 mM $\text{Ca}(\text{NO}_3)_2$.

To assess the efficiency of the isolation procedure, the loss of calcium (Ca), copper (Cu), iron (Fe), phosphorus (P) and potassium (K) in the cell walls during the 30-d of the procedure was determined. Initial roots and the root material obtained after 30 d of the isolation procedure was oven-dried at 50°C until a steady mass was achieved, and then ground using a porcelain mortar. A subsample of each root material was digested in a microwave oven

(March 5, CEM Corporation) for 15 min (i.e. 10 min at 600 W under 1.2 bar then 5 min at 1200 W under 10 bar) with 10 ml of aqua regia (i.e. 67% v/v of 37% HCl and 33% of 69% HNO₃). The mineral element concentration in the digest was determined by inductively coupled plasma atomic emission spectroscopy (ICP-AES, Jobin Hyvon Horiba J 38). Measurements were performed in duplicate at 0 and 30 d. Blanks, in-house reference samples and certified reference material were included in the digestions and analyses. The measurement uncertainty ranged from 6 to 15%.

II.3. Determination of the cation exchange capacity of roots and cell walls

The cation exchange capacity (CEC) of wheat and tomato roots and cell walls was determined according to the procedure of [Dufey and Braun \(1986\)](#). A 25 mg mass (dry mass basis) of roots and cell walls was shaken end-over-end in 15 ml of 10 mM CuSO₄ for 30 (± 1) min. The suspension was filtered (Whatman, grade 4) and roots and cell walls were rinsed three times with 100 ml of 0.1 mM CuSO₄ through a Büchner funnel. Roots and cell walls were then shaken end-over-end in 50 ml of 0.1 M HCl for 20 (± 1) min. The suspension was finally filtered (Whatman, grade 4) before ICP-AES determination of the Cu concentration in the filtrate. Roots and cell walls were oven-dried at 50°C and weighed. Measurements were performed in quadruplicate. Blanks were included in the measurements and analyses. Due to its high affinity for root surfaces, Cu is supposed to saturate all cation binding sites onto roots and cell walls. The CEC (cmol_c.kg⁻¹) was thus estimated from Cu concentration measured in the acidic filtrate by considering a 1:1 stoichiometric ratio between root binding sites and Cu²⁺.

II.4. Characterization of the acidic properties of roots and cell walls by potentiometric titration

To avoid analytical artefacts, roots and cell walls were first stirred in HNO₃ solution -at pH 3 - for 1 h to remove highly bound or precipitated cations (e.g. Fe and Al), then rinsed twice with ultrapure water (18.2 MΩ) for 30 min. Roots and cell walls were then oven-dried at 50°C until a steady mass was achieved.

The titration procedure was adapted from [Garnier et al. \(2004a\)](#). Briefly, titrations were performed with a Metrohm titration stand with two 719 S Titrino titrators controlled by Tinet 2.4 software. Approximately 0.2 g (dry mass basis) of roots or cell walls was placed in a thermostated cell at 25 (± 0.2)°C filled with 100 ml of 10 mM KNO₃. The solution was continuously stirred and flushed with an ultrapure nitrogen flow. Roots and cell walls were

titrated with 0.1 M KOH (Fischer chemical, titrated three times using potassium hydrogen phthalate to accurately determine the KOH concentration) and 0.2 M HNO₃ (from 69% HNO₃, trace analysis grade, Fischer Scientific, titrated three times using the freshly prepared KOH solution). The combined pH-micro-electrode (Ag/AgCl/KCl 3 M, Bioblock Scientific) was calibrated daily with pH-buffer solutions (HANNA 4.01, 7.01 and 10.01 at 25°C). Titrations were carried out in several steps. The pH was first lowered to 2.5 with HNO₃ additions. After 15 min of stirring, the solution was free from carbonates and the pH was then increased step-by-step to 11.5 with the incremental addition of KOH at two different rates: 100 µl from pH 2.5 to 3.5 and from pH 10.5 to 11.5 and 20 µl from pH 3.5 to 10.5.

The acidic properties of roots and cell walls were determined by fitting the experimental data with PROSECE software (Garnier et al. 2004b). Briefly, PROSECE is based on a discrete site distribution model where each site is defined by a site density (L_{Hi} , cmol_c.kg⁻¹) and a stability constant (pKa_i). The fitting procedure highlights the number of sites for optimal fitting as well as their optimal density and pKa.

II.5. Identification of the chemical structure of roots and cell walls by solid-state ¹³C-NMR spectroscopy

Solid-state ¹³C-¹H cross-polarization magic angle spinning nuclear magnetic resonance (¹³C CP-MAS NMR) analyses were carried out at 101.6 MHz on a Bruker Avance WB 400-MHz Spectrometer. Roots and cell walls (150-200 mg, dry mass basis) were packed into a 4 mm Zirconia rotor and spun at 10 kHz in a MAS probe. Cross-polarization was performed with ramped ¹H pulse to circumvent Hartmann-Hahn mismatches. All spectra were obtained with a 2 ms contact time and 2 s recycling time. To improve the resolution, dipolar decoupling was applied on protons during acquisition. Chemical shifts were referenced to tetramethylsilane. 12-18 k scans were conducting depending on the amount of sample.

Spectra were divided in chemical shift regions in which the chemistry of the C atoms were similar: alkyl C (0-45 ppm), N-alkyl and methoxyl C (45-60 ppm), carbohydrate C (60-90 ppm), anomeric C (90-110 ppm), Aryl C (110-145 ppm), O-aryl C (145-165 ppm) and carbonyl C (165-190 ppm) (Wershaw and Mikita 1987). For a semi-quantitative comparison between the root and cell wall spectra for each species, the anomeric region (90-110 ppm) was defined as the internal reference. The anomeric bond is a marker of polysaccharides which mostly occur in the cell walls (Vogel 2008). We therefore considered that the anomeric region was quantitatively preserved in the cell walls in comparison with the corresponding roots of each species. Spectra were thus normalized to the maximal intensity of the anomeric

region and numerical ratios between the area of each region and the area of the reference were calculated.

Spectra deconvolution was performed with IGOR PRO 5.0 software. It uses Gaussian type functions to perform the fitting. The baseline was corrected by the software. For each generated Gaussian type function, the consistency of the position, amplitude and standard deviation was thoroughly investigated.

III. Results

III.1. Loss of mineral elements during the isolation procedure

The mineral element loss patterns during wheat and tomato cell wall isolation were very similar (Fig. 16). Potassium was no longer detected after the 30-day isolation procedure. P, Ca and Fe losses were 90-95, 86-80 and 77-80% for tomato and wheat, respectively. The weakest loss was noted for Cu, with 52 and 62% for tomato and wheat, respectively.

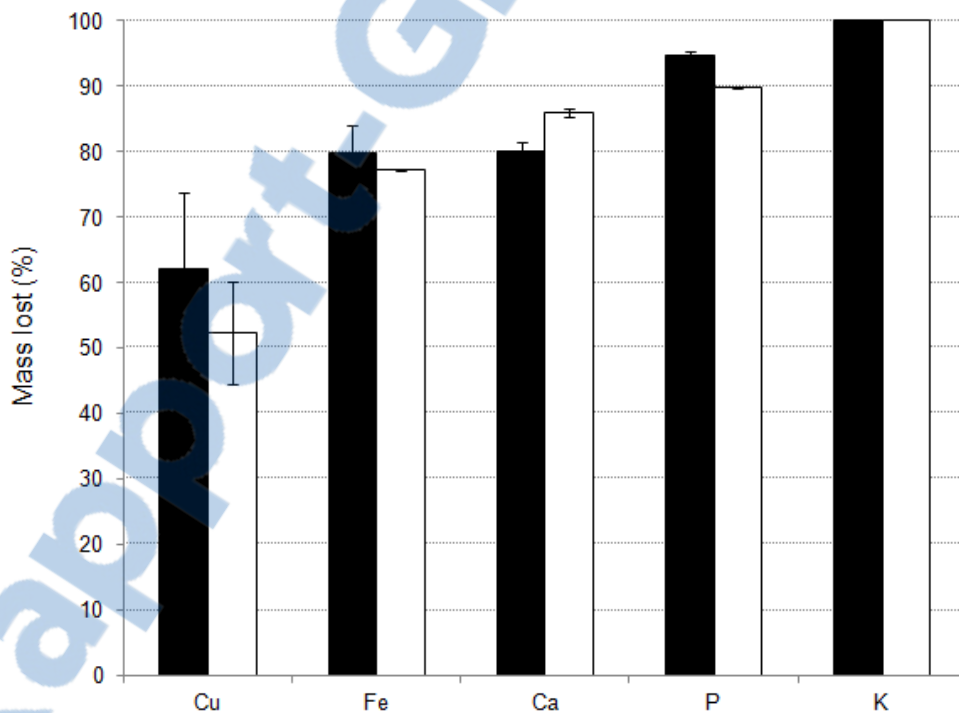


Figure 16 : Percentage of the mass of copper (Cu), iron (Fe), calcium (Ca), phosphorus (P) and potassium (K) in roots lost in cell walls after the 30-d isolation procedure, for wheat (filled bars) and tomato (empty bars). Error bars stand for the standard deviation (n=2).

III.2. Cation exchange capacity of roots and cell walls

For wheat and tomato, the root CEC was threefold higher than that of the respective cell walls when expressed on an initial root mass basis (Fig. 17). The CEC of tomato roots ($73 \pm 2 \text{ cmol}_c.\text{kg}^{-1}$) and cell walls ($23 \pm 3 \text{ cmol}_c.\text{kg}^{-1}$) was ca. 2.5-fold higher than that of wheat roots ($29 \pm 4 \text{ cmol}_c.\text{kg}^{-1}$) and cell walls ($10 \pm 1 \text{ cmol}_c.\text{kg}^{-1}$), respectively.

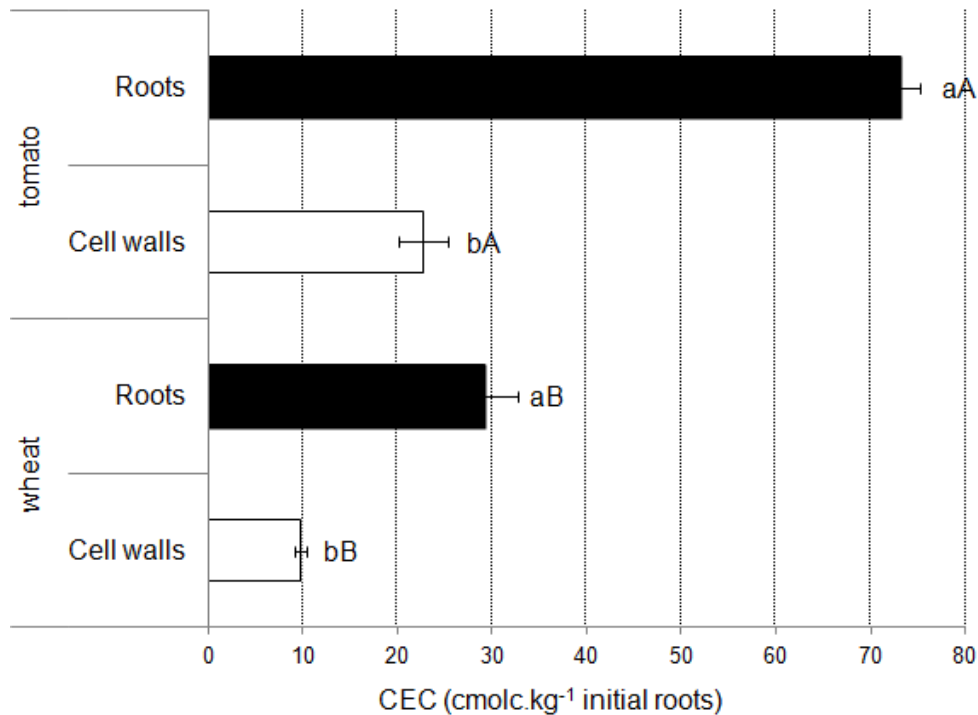


Figure 17 : Cation exchange capacity (CEC) of roots (filled bars) and cell walls (empty bars) of wheat and tomato. Error bars stand for the standard deviation ($n=4$). Different lower case letters stand for a significant difference between roots and cell walls of a given species, while different upper case letters stand for a significant difference between roots and cell walls of wheat and tomato ($P \leq 0.05$, Mann-Whitney U test).

III.3. Acidic properties of roots and cell walls

The experimental potentiometric titration data for wheat and tomato roots and cell walls were accurately fitted with PROSECE by parameterising four proton binding functional groups for wheat and tomato roots and cell walls (Fig. 18; Table 2). These sites were characterised by distinct pKa. The pKa of site 1 (L_1) were fitted at 3.4 and 3.6 for wheat and tomato cell walls and 4.1 and 4.4 for roots. The pKa of site 2 (L_2) ranged from 5.0 to 5.3 for wheat and tomato cell walls and tomato roots, while it was fitted at 7.2 for wheat roots. The pKa of site 3 (L_3) were fitted at 7.4 and 8.1 for tomato cell walls and roots and at 8.7 and 9.1 for wheat cell

walls and roots. The pKa of site 4 (L₄) consistently ranged from 9.8 to 10.1 for all samples. The estimated site density markedly differed depending on the root material (Table 2). For tomato, the site density was consistently distributed for cell walls and roots, with L_{H4T} > L_{H1T} > L_{H2T} > L_{H3T}. For wheat, no consistent pattern was observed in the site density distribution for cell walls and roots. The total site density estimated for wheat and tomato roots was respectively 2.4- and 3.4-times higher than those estimated for cell walls (Table 2).

Table 2 : Acidic properties of wheat and tomato roots and cell walls. The density of acidic sites (L_{HIT}, cmol_c.kg⁻¹ initial dry roots) and their stability constants (pKa_i) were obtained by fitting the experimental data with PROSECE software (as described in the Material and Methods).

		L ₁		L ₂		L ₃		L ₄		Total
		L _{H1T}	pKa ₁	L _{H2T}	pKa ₂	L _{H3T}	pKa ₃	L _{H4T}	pKa ₄	sites
Wheat	Roots	7.0	4.4	5.4	7.2	10.1	9.1	14.0	10.1	36.5
	Cell walls	6.2	3.4	2.1	5.3	3.1	8.7	3.8	9.9	15.2
Tomato	Roots	30.2	4.1	15.2	5.2	13.3	8.1	38.5	9.9	97.2
	Cell walls	10.4	3.6	3.1	5.0	2.4	7.4	12.8	9.8	28.7

These results are consistent with the total site density estimated on the basis of CEC, as the CEC measured in wheat and tomato cell walls and roots was linearly correlated with the total site density estimated on the basis of potentiometric titration data (R²=0.98, data not shown). The total site density estimated by potentiometric titration was slightly higher than that estimated on the basis of the CEC (regression slope: 1.25).

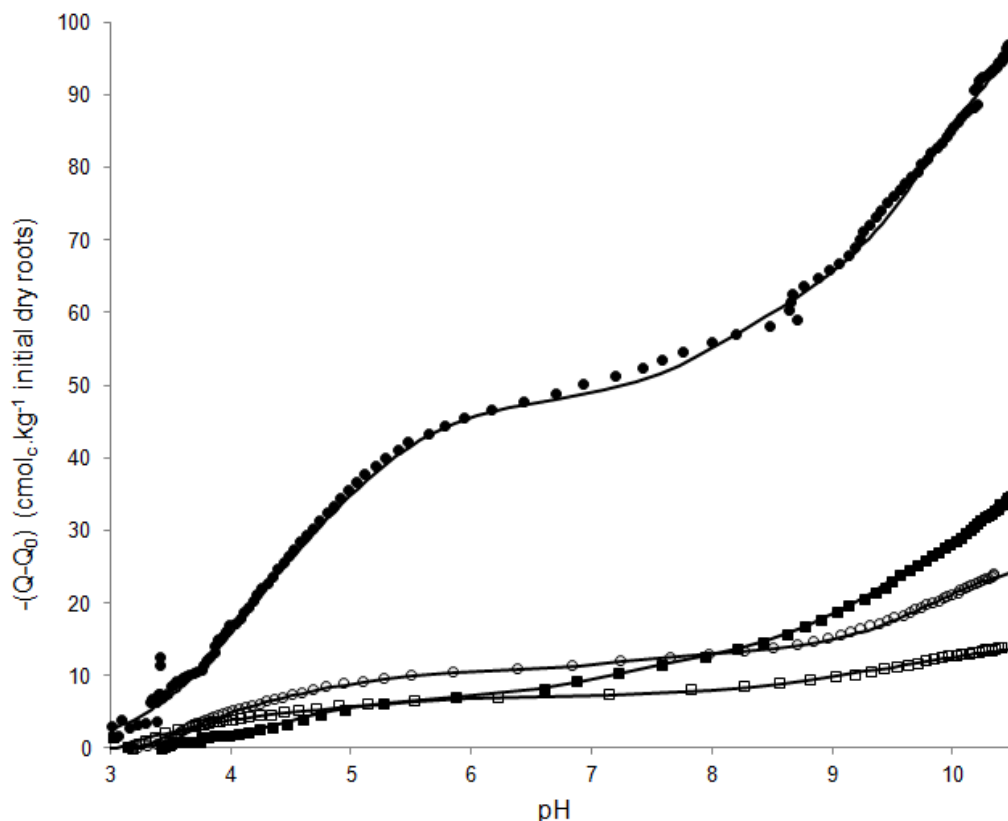


Figure 18 : Potentiometric titrations for roots (filled symbols) and cell walls (empty symbols) of wheat (squares) and tomato (circles) expressed in charge (Q) corrected by the initial charge (Q_0). Solid lines refer to the fitting curves obtained with PROSECE software as described in the Material and Methods.

III.4. ^{13}C -NMR spectra of roots and cell walls

Overall, the spectra shape was very similar for wheat and tomato cell walls and roots (Fig. 19a and b). All spectra exhibited a quantitatively substantial carbohydrate region (between ca. 60 and 110 ppm). The NMR spectra intra-species comparison revealed that the total area of the cell wall spectra accounted for 76 and 85% of the total area of the root spectra for tomato and wheat, respectively (Fig. 19). For both species, the area of the cell wall carbohydrate region was very similar to that of the roots, i.e. the cell wall to root signal ratio was over 90% (Fig. 20). The carbonyl C and the N alkyl-/methoxyl C regions exhibited a cell wall to root signal ratio ranging from 39 to 44% in wheat and from 55 to 65% in tomato. The lowest cell wall to root signal ratio was obtained for the alkyl C region, with a cell wall to root signal of only 35%. The aryl C and O-aryl C regions were not studied because the signal intensity was too weak to be confidently distinguished from the baseline.

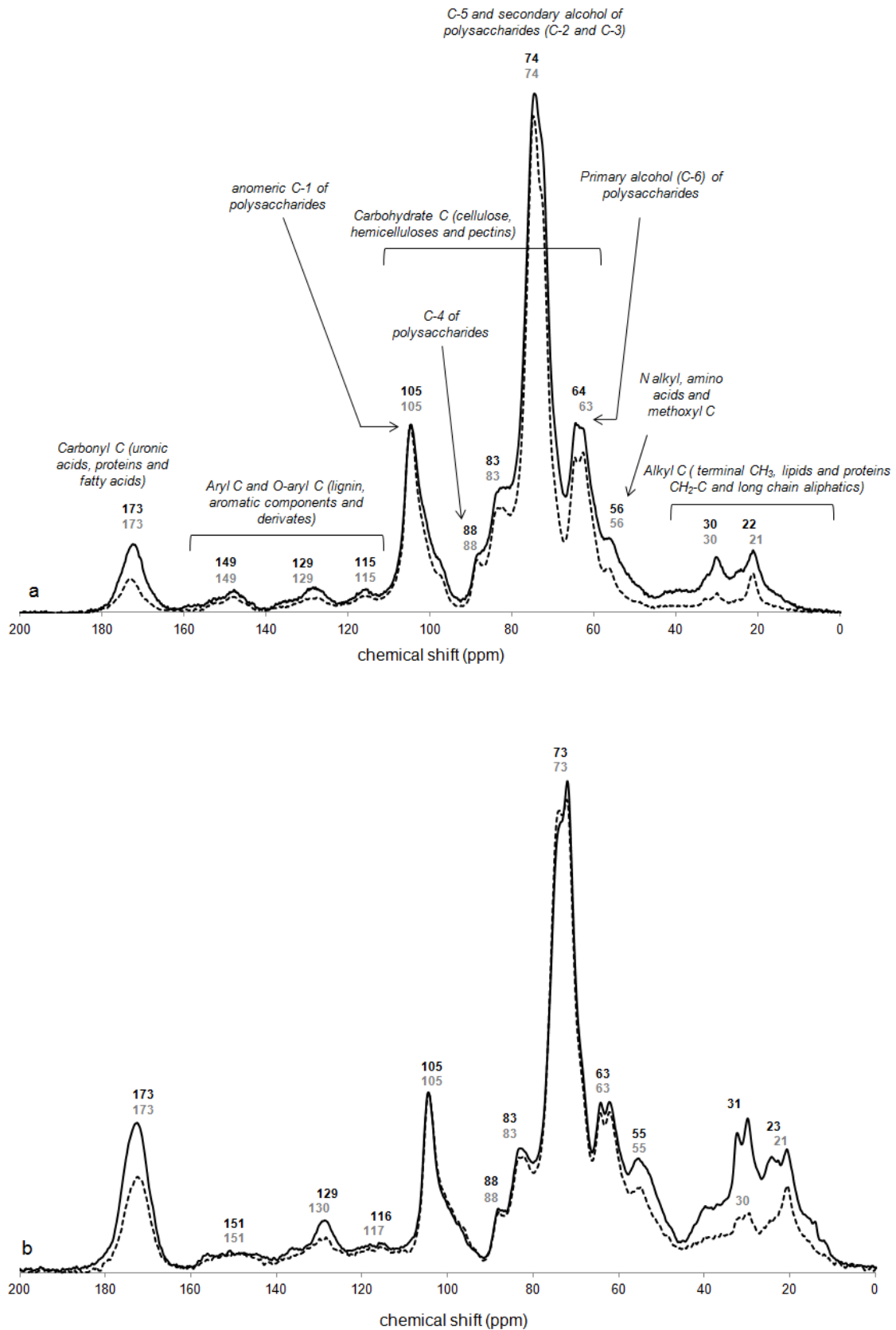


Figure 19 : ^{13}C -NMR spectra of roots (solid line) and cell walls (dotted line) of wheat (a) and tomato (b).

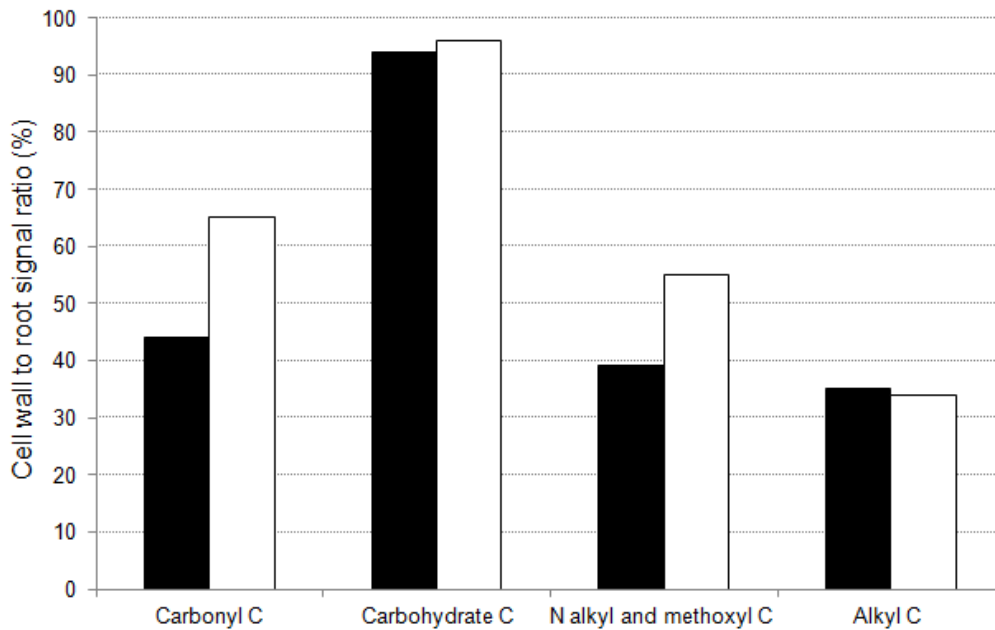


Figure 20 : Cell wall to root signal ratios for the different ^{13}C -NMR spectra regions for wheat (filled bars) and tomato (empty bars).

IV. Discussion

Root cation binding properties are alternatively attributed to the properties of cell walls, particularly pectins, or of root cell plasma membranes. To assess the respective contributions of these two root materials, we investigated the properties and chemical nature of cation binding sites of isolated cell walls compared to those of whole roots still containing cell walls and plasma membranes.

IV.1. Efficiency of the cell wall isolation procedure

Theoretically, an efficient root cell wall isolation procedure should: (i) entirely remove the root symplasm by solubilization of cell plasma membranes, and (ii) quantitatively and qualitatively preserve the cell wall compounds. Although the quality of the isolation procedure is seldom checked, this aspect can be assessed in various ways, e.g. electronic microscopy observation (Sentenac and Grignon 1981) or measurement of ATPase and Cyt C activities (Masion and Bertsch 1997). We assessed the efficiency of the isolation procedure by probing the loss of mineral elements in isolated cell walls compared to the roots (Fig. 16).

The removal of 90-95% of P, which is a representative membrane phospholipid constituent, in tomato and wheat cell walls compared to their respective roots suggested that the plasma membranes were efficiently solubilized by our isolation procedure using Triton X 100

(Fig. 16). The low percentage of P remaining in cell walls could be attributed to the P-containing proteins embedded in the cell walls (Kaida et al. 2010). The loss of almost 70% of the alkyl-C NMR signal, presumably largely corresponding to the long aliphatic chains of membrane phospholipids, in tomato and wheat cell walls compared to their respective roots further suggests that plasma membranes were efficiently solubilized and removed from isolated cell walls (Figs. 19 and 20). Cathala et al. (1978) also reported that optical and microscopic observations of root cell walls (isolated with a Triton X 100 procedure very similar to the one we used) did not show any remaining plasma membrane fragments.

Following the removal of plasma membranes, the cell wall isolation procedure should allow removal of the cytoplasmic content. The complete loss of K, a soluble cation almost entirely contained in the cytoplasm (Marschner 1995), during the cell wall isolation procedure illustrated efficient removal of the cytoplasmic content of root cells (Fig. 16). Cathala et al. (1978) similarly reported that K recovered in cell walls isolated using Triton X 100 represented less than 3% of the K initially measured in the roots of several dicots and monocots.

The partial recovery of Ca, Fe and Cu contrasted with the loss of P and K from the isolated cell walls (Fig. 16). Calcium, Fe and even more so Cu are well-known to highly interact and accumulate in root cell walls. Bravin et al. (2010) reported a percentage of apoplastic Cu ranging between 50 to 80% for durum wheat grown under hydroponic conditions very similar to those we used to grow tomato and wheat. Strasser et al. (1999) reported a percentage of apoplastic Fe ranging from 10 to 50% for both dicots and monocots. The recovery of Ca in isolated cell walls was harder to accurately interpret as it depends concomitantly on the initial distribution of Ca between the root symplast and apoplast and the desorption of Ca from cell walls during the isolation procedure following the decrease in Ca concentration from the hydroponic solution (i.e. 2 mM) to the isolation solution (i.e. 1 mM).

Finally, the ¹³C-NMR determination allows us to assess the qualitative preservation of cell wall compounds (Fig. 19 and 20). We noted that the peak observed in the anomeric C region conserved a maximum intensity of close to 105 ppm, which corresponds to inter-chain glycosidic bonds (Fig. 20). This highlighted the absence of any pecto-cellulosic chain degradation.

The above-cited results concomitantly suggested that the major components of the material isolated from roots were preserved, even though the absence of any loss of quantitatively minor cell wall components could not be definitely ascertained. In comparison with isolated cell walls, the roots did contain both cell walls and plasma membranes. Isolated cell walls

and roots were consequently adequate for evaluating the respective contributions of cell walls and plasma membranes to the root cation binding properties.

IV.2. Limited contribution of cell walls to the total binding capacity of roots

The binding capacity of wheat and tomato cell walls, when expressed as a function of the initial root mass, was 2.4- and 3.4-fold lower than the binding capacity of wheat and tomato roots, respectively (Fig. 17 and 18 ; Table 2). These results mean that root material removed during cell wall isolation, i.e. cell plasma membranes and cytosolic compounds, accounted for 60 and 70% of the total binding capacity of wheat and tomato roots, respectively. Determination of the concentration of major organic acids extracted from frozen-thawed roots showed that their global contributions to the CEC of tomato and wheat roots were lower than 5% (results not shown). As these organic acids were mainly found within the cytosol, this suggests that the difference in the binding capacity of roots and cell walls could be mainly attributed to plasma membranes. These results contradict those generally reported in the literature, i.e. indicating that 70-90% of the cation binding capacity of roots is mainly provided by carboxylic groups borne by cell wall pectins (Haynes 1980; Sattelmacher 2001; Krzesłowska 2011). In contrast, our results suggest that root cell plasma membranes are the main contributors to the total binding capacity of roots. This hypothesis is supported by the reported measurements of significant surface charge densities and ion binding affinities of plasma membranes as reviewed by Kinraide (2001).

The limited contribution of the cell walls to the root binding capacity could thus be partly explained by the loss of root material bearing binding sites during the cell wall isolation procedure, as 48-50% of the initial root mass was lost (results not shown). However, it is noteworthy that this loss of root material was still lower than the 60 and 70% decrease in the binding capacity of cell walls compared to that of wheat and tomato roots, respectively (Table 2). This means that the binding site density in cell walls, i.e. 29.2 and 57.7 $\text{cmol}_c \cdot \text{kg}^{-1}$ of dry cell walls for wheat and tomato, was lower than that of the root material lost during this isolation procedure, i.e. presumably plasma membranes, i.e. 44.5 and 136.2 $\text{cmol}_c \cdot \text{kg}^{-1}$ of dry mass for wheat and tomato. The result was particularly striking for tomato roots as it suggested that the cell wall binding site density was 2-fold lower than that of plasma membranes.

Cathala et al. (1978) reported very similar CEC in roots and the corresponding cell walls of maize and sunflower. Although the percentage of root material lost during the cell wall isolation procedure was not specified, the findings of that study suggested, like our results,

that cell walls do not contribute to more than 50% of the total binding capacity of roots with a substantial concomitant contribution of plasma membranes. Based on a comparison of the electrical potentials of root cell walls and plasma membranes, [Shomer et al. \(2003\)](#) also suggested that the ion-binding strength of plasma membranes is higher than that of cell walls.

IV.3. Distinct acidic properties of roots and cell walls related to the chemical nature of binding sites

While the total binding capacity of cell walls was shown to be substantially lower than the total binding capacity of roots, it remains unclear whether the acidic properties of cell walls and roots differed and whether these acidic properties could be related to the chemical nature of the binding sites in cell walls and roots.

As already mentioned, the ^{13}C -NMR spectra of roots and cell walls were qualitatively identical, i.e. the same chemical C-bonds were detected (Fig. 19). Nevertheless, the quantity of chemical C-bonds differed significantly between cell walls and roots. The substantial (i.e. 35-55%) decrease in the carbonyl C signal, visible ca. 173 ppm (Fig. 19 and 20), is particularly noteworthy. This spectral region consists of contributions from uronic acids, proteins and fatty acids of phospholipids. Uronic acid, which is a component of cell wall pectins that bears cation binding sites, is considered to be a major source of carboxyl groups in plant roots ([Grignon and Sentenac 1991](#)). As the spectral contributions of pectins were also noted in the carbohydrate C region (60-110 ppm, Fig. 19), which presented an NMR signal close to that of the roots, it was unlikely that there was any loss of carboxyl groups from uronic acid during the isolation procedure. Alternatively, the disappearance of carbonyl groups from isolated cell walls could be attributed to the removal of proteins embedded in plasma membranes. Indeed, proteins are composed of one or more chains of amino acids linked by peptide bonds and ending by both carboxyl and amine groups. These proteins can represent as much as half of the plasma membrane mass ([Gupta 2004](#); [Taiz and Zeiger 2006](#)). [Lampport and Várnai \(2013\)](#) recently reported on the binding capacity towards Ca of carboxyl groups borne by periplasmic arabinogalactan glycoproteins (AGPs). These AGPs may contribute significantly to the binding capacity of plasma membranes. The spectral contribution of proteins was also noted at 56 ppm (N alkyl/ methoxyl C) and between 0 and 40 ppm (alkyl C), i.e. two other NMR regions also presenting a signal loss (Fig. 19). Consequently, the lower binding capacity of cell walls was likely partly associated to the substantial loss of carboxyl and amine binding sites borne by proteins embedded in plasma membranes.

The disappearance of 65% of the alkyl-C signal in cell walls compared to that in roots could also have been partly associated with the removal of phospholipids, i.e. the primary constituent of plasma membranes, during the cell wall isolation procedure. The chemical structure of phospholipids consists of a phosphate group covalently linked to a glycerol molecule which in turn is covalently linked to two fatty acids. A variable head group is further attached to the phosphate group. Phospholipids of the outer part of the plasma membrane can therefore exhibit two to three cation binding sites borne by the head group and phosphate group. For instance, phosphatidylserine contains a serine as head group, a molecule having one carboxyl group and one amine group (Taiz and Zeiger 2006). Cohen and Cohen (1981) and McLaughlin et al. (1981) showed that these functional groups were responsible for the adsorption of monovalent and divalent cations by membrane phospholipids. Consequently, the lower binding capacity of cell walls is likely partly associated with the substantial loss of phosphate, carboxyl and amine binding sites borne by plasma membrane phospholipids.

The potentiometric titrations coupled with PROSECE modeling generated further insight into the identification of functional groups responsible for the binding properties of roots and cell walls. Four types of binding sites were identified for each root material with specific acidic properties, i.e. a stability constant (pKa) and a site density (Table 2). The pKa ranges of carboxylic, phosphate, amine and phenolic groups are respectively 3.4 to 7.5, 5.7 to 7.2 and 8 to 11 for the two latter groups (Meychik and Yermakov 1999; Guiné et al. 2006; Ahmady-Asbchin et al. 2008). Binding sites were consequently grouped into two distinct families, i.e. the carboxyl/-phosphate-like (C-P) sites and the phenolic/-amine-like (Φ -A) sites, with pKa respectively lower and higher than ca. 7.5. The C-P/ Φ -A ratio was respectively 0.5 and 1.2 in wheat roots and cell walls, indicating that Φ -A sites were the most abundant in roots and that C-P sites were the most abundant in cell walls. The C-P/ Φ -A ratio was respectively 0.9 and 1.2 in tomato roots and cell walls, revealing a similar although less marked site dominance pattern than noted in wheat. The switch in the dominance between Φ -A and C-P sites from roots to cell walls could be explained by a higher loss of Φ -A sites as compared to the loss of C-P sites during the cell wall isolation procedure.

The assignment of a chemical nature to each type of binding site identified by potentiometric titration is still, however, complicated. C-P and Φ -A site denominations are only indicative of the actual reactivity of roots and cell walls as the chemical environment of a functional group may substantially alter its pKa. For example, the pKa of a low molecular acid such as acrylic acid is 4.3 but the pKa of ionogenic groups of acrylic acid in the cross-linked polymer structure may range from 5 to 7.5 (Meychik and Yermakov 1999). Likewise, polygalacturonic

acid carboxylic groups may have a pKa in the range of that of Φ -A sites (Lenoble et al. 2008). Accurate knowledge on the chemical structure is thus necessary. The NMR signal loss effectively reflected the decrease in the total site density observed by both potentiometric titration and CEC measurement. However, due to the substantial chemical heterogeneity in the roots and cell walls, the NMR spectra did not generate more accurate results or highlight a straightforward link between the identified functional groups and the pKa.

V. Conclusion

While, based on previous reports, it is often commonly considered that root binding properties are mainly dependent on the cell wall composition, our results conversely suggest that cell walls does not contribute to more than 50% of the total binding capacity of roots. Because of the apparent efficiency of the cell wall isolation procedure in removing plasma membranes, we noted that binding sites borne by plasma membranes contributed markedly to the total binding capacity of roots.

The distinct binding properties of isolated cell walls and roots should no longer be neglected and should be considered carefully in studies focused on root-ion interactions. Cell walls and plasma membranes should be separated especially to gain insight into processes taking place within cell walls, such as root elongation mechanisms. Conversely, cell walls and plasma membranes have to be seen as a continuum in the overall issue of rhizotoxicity because of their respective contributions in the binding properties of roots. From a more operational standpoint, the biotic ligand model will be more effective if cell walls and plasma membranes are considered as separate cation binding sites. Further in-depth studies are nevertheless required to investigate the binding of trace elements by each type of root material in order to identify the extents of participation of their respective binding sites.

Acknowledgements

The authors are grateful to French Environment and Energy Management Agency (ADEME) and the French Centre of Agricultural Research for Development (CIRAD) for funding the PhD scholarship of Stéphanie Guigues and INSU (CNRS) for funding the study via the EC2CO-CYTRIX call. The authors thank Patrick Cazevaille and Claire Chevassus-Rosset (CIRAD) for their technical support during the plant growth phase, Hélène Miche (CEREGE) for providing access to ICP-AES and Jean-Claude Davidian (Montpellier SupAgro) for his advice on root cell wall isolation.

Références bibliographiques

- Ahmady-Asbchin S, Andrès Y, Gérente C, Cloirec PL (2008) Biosorption of Cu(II) from aqueous solution by *Fucus serratus*: Surface characterization and sorption mechanisms. *Bioresource Technology* 99 (14):6150-6155. doi:10.1016/j.biortech.2007.12.040
- Allan DL, Jarrell WM (1989) Proton and Copper Adsorption to Maize and Soybean Root Cell Walls. *Plant Physiol* 89 (3):823-832. doi:10.1104/pp.89.3.823
- Bastías E, Alcaraz-López C, Bonilla I, Martínez-Ballesta MC, Bolaños L, Carvajal M (2010) Interactions between salinity and boron toxicity in tomato plants involve apoplastic calcium. *Journal of Plant Physiology* 167 (1):54-60. doi:http://dx.doi.org/10.1016/j.jplph.2009.07.014
- Bravin M, Merrer B, Denaix L, Schneider A, Hinsinger P (2010) Copper uptake kinetics in hydroponically-grown durum wheat (*Triticum turgidum durum* L.) as compared with soil's ability to supply copper. *Plant and Soil* 331 (1-2):91-104. doi:10.1007/s11104-009-0235-3
- Brunner I, Luster J, Günthardt-Goerg MS, Frey B (2008) Heavy metal accumulation and phytostabilisation potential of tree fine roots in a contaminated soil. *Environmental Pollution* 152 (3):559-568. doi:DOI: 10.1016/j.envpol.2007.07.006
- Cathala N, Ghorbal, M. H., Lamant, A., Salsac, L. (1978) Obtention de parois cellulosiques à l'aide d'un détergent : étude préliminaire de leur composition minérale. *C R Acad Sc Paris t. 286*:1025-1027
- Cohen JA, Cohen M (1981) Adsorption of monovalent and divalent cations by phospholipid membranes. The monomer-dimer problem. *Biophysical journal* 36 (3):623-651
- Crooke WM, Knight AH, Macdonald IR (1960) Cation exchange properties and pectin content of storage-tissue disks. *Plant and Soil* 13 (1):55-67. doi:10.1007/bf01666476
- Doelsch E, Deroche B, Van de Kerchove V (2006b) Impact of sewage sludge spreading on heavy metal speciation in tropical soils (Réunion, Indian Ocean). *Chemosphere* 65 (2):286-293. doi:http://dx.doi.org/10.1016/j.chemosphere.2006.02.046
- Doelsch E, Van de Kerchove V, Saint Macary H (2006a) Heavy metal content in soils of Réunion (Indian Ocean). *Geoderma* 134 (1-2):119-134. doi:http://dx.doi.org/10.1016/j.geoderma.2005.09.003
- Dufey JE, Braun R (1986) Cation Exchange Capacity of Roots : Tirtation Sum of Exchangeable Cations, Copper Adsorption. *Journal of Plant Nutrition* 9 (8):1147-1155
- Garnier C, Mounier S, Benaïm JY (2004a) Influence of dissolved organic carbon content on modelling natural organic matter acid-base properties. *Water Research* 38 (17):3685-3692. doi:http://dx.doi.org/10.1016/j.watres.2004.05.019
- Garnier C, Pižeta I, Mounier S, Benaïm JY, Branica M (2004b) Influence of the type of titration and of data treatment methods on metal complexing parameters determination of single and multi-ligand systems measured by stripping voltammetry. *Analytica Chimica Acta* 505 (2):263-275. doi:http://dx.doi.org/10.1016/j.aca.2003.10.066

- Grignon C, Sentenac H (1991) pH and Ionic Conditions in the Apoplast. *Annual Review of Plant Physiology and Plant Molecular Biology* 42 (1):103-128. doi:10.1146/annurev.pp.42.060191.000535
- Guiné V, Spadini L, Sarret G, Muris M, Delolme C, Gaudet JP, Martins JMF (2006) Zinc Sorption to Three Gram-Negative Bacteria: Combined Titration, Modeling, and EXAFS Study. *Environmental Science & Technology* 40 (6):1806-1813. doi:10.1021/es050981I
- Gupta GP (2004) *Plant Cell Biology*. Discovery Publishing House, New Delhi
- Haynes RJ (1980) Ion exchange properties of roots and ionic interactions within the root apoplast: Their role in ion accumulation by plants. *Bot Rev* 46 (1):75-99. doi:10.1007/bf02860867
- Heintze SG (1961) Studies on cation-exchange capacities of roots. *Plant and Soil* 13 (4):365-383. doi:10.1007/bf01394648
- Herrmann AM, Ritz K, Nunan N, Clode PL, Pett-Ridge J, Kilburn MR, Murphy DV, O'Donnell AG, Stockdale EA (2007) Nano-scale secondary ion mass spectrometry — A new analytical tool in biogeochemistry and soil ecology: A review article. *Soil Biology and Biochemistry* 39 (8):1835-1850. doi:http://dx.doi.org/10.1016/j.soilbio.2007.03.011
- Horst WJ, Wang Y, Eticha D (2010) The role of the root apoplast in aluminium-induced inhibition of root elongation and in aluminium resistance of plants: a review. *Annals of Botany* 106 (1):185-197. doi:10.1093/aob/mcq053
- Kaida R, Serada S, Norioka N, Norioka S, Neumetzler L, Pauly M, Sampedro J, Zarra I, Hayashi T, Kaneko TS (2010) Potential Role for Purple Acid Phosphatase in the Dephosphorylation of Wall Proteins in Tobacco Cells. *Plant Physiology* 153 (2):603-610. doi:10.1104/pp.110.154138
- Kinraide TB (2001) Ion fluxes considered in terms of membrane-surface electrical potentials. *Australian Journal of Plant Physiology* 28 (7):605-616. doi:10.1071/pp01019
- Kinraide TB (2004) Possible Influence of Cell Walls upon Ion Concentrations at Plasma Membrane Surfaces. Toward a Comprehensive View of Cell-Surface Electrical Effects upon Ion Uptake, Intoxication, and Amelioration. *Plant Physiol* 136 (3):3804-3813. doi:10.1104/pp.104.043174
- Kinraide TB (2006) Plasma membrane surface potential (ψ_{pm}) as a determinant of ion bioavailability: A critical analysis of new and published toxicological studies and a simplified method for the computation of plant ψ_{pm} . *Environmental Toxicology and Chemistry* 25 (12):3188-3198. doi:10.1897/06-103r.1
- Kinraide TB, Ryan PR, Kochian LV (1992) Interactive Effects of Al^{3+} , H^{+} , and Other Cations on Root Elongation Considered in Terms of Cell-Surface Electrical Potential. *Plant Physiol* 99 (4):1461-1468. doi:10.1104/pp.99.4.1461
- Kopittke P, Blamey F, Menzies N (2008) Toxicities of soluble Al, Cu, and La include ruptures to rhizodermal and root cortical cells of cowpea. *Plant and Soil* 303 (1):217-227. doi:10.1007/s11104-007-9500-5

- Kopittke P, McKenna B, Blamey F, Wehr J, Menzies N (2009a) Metal-induced cell rupture in elongating roots is associated with metal ion binding strengths. *Plant and Soil* 322 (1):303-315. doi:10.1007/s11104-009-9917-0
- Kopittke P, Menzies N (2006) Effect of Cu Toxicity on Growth of Cowpea (&i>Vigna unguiculata&i>). *Plant and Soil* 279 (1):287-296. doi:10.1007/s11104-005-1578-z
- Kopittke PM, Asher CJ, Blamey FPC, Menzies NW (2009b) Toxic effects of Cu²⁺ on growth, nutrition, root morphology, and distribution of Cu in roots of Sabi grass. *Science of The Total Environment* 407 (16):4616-4621. doi:10.1016/j.scitotenv.2009.04.041
- Kopittke PM, Asher CJ, Kopittke RA, Menzies NW (2007) Toxic effects of Pb²⁺ on growth of cowpea (*Vigna unguiculata*). *Environmental Pollution* 150 (2):280-287. doi:10.1016/j.envpol.2007.01.011
- Kopittke PM, Kinraide TB, Wang P, Blamey FPC, Reichman SM, Menzies NW (2011) Alleviation of Cu and Pb Rhizotoxicities in Cowpea (*Vigna unguiculata*) as Related to Ion Activities at Root-Cell Plasma Membrane Surface. *Environmental Science & Technology* 45 (11):4966-4973. doi:10.1021/es1041404
- Krzyszowska M (2011) The cell wall in plant cell response to trace metals: polysaccharide remodeling and its role in defense strategy. *Acta Physiologiae Plantarum* 33 (1):35-51. doi:10.1007/s11738-010-0581-z
- Kudo H, Kudo K, Ambo H, Uemura M, Kawai S (2011) Cadmium sorption to plasma membrane isolated from barley roots is impeded by copper association onto membranes. *Plant Science* 180 (2):300-305. doi:http://dx.doi.org/10.1016/j.plantsci.2010.09.008
- Lampart DTA, Várnai P (2013) Periplasmic arabinogalactan glycoproteins act as a calcium capacitor that regulates plant growth and development. *New Phytologist* 197 (1):58-64. doi:10.1111/nph.12005
- Legros S, Doelsch E, Feder F, Moussard G, Sansoulet J, Gaudet JP, Rigaud S, Doelsch IB, Macary HS, Bottero JY (2013) Fate and behaviour of Cu and Zn from pig slurry spreading in a tropical water–soil–plant system. *Agriculture, Ecosystems & Environment* 164 (0):70-79. doi:http://dx.doi.org/10.1016/j.agee.2012.09.008
- Lenoble V, Garnier C, Masion A, Ziarelli F, Garnier JM (2008) Combination of ¹³C/¹¹³Cd NMR, potentiometry, and voltammetry in characterizing the interactions between Cd and two models of the main components of soil organic matter. *Analytical and Bioanalytical Chemistry* 390 (2):749-757. doi:10.1007/s00216-007-1678-0
- Liu D, Kottke I (2003) Subcellular localization of Cd in the root cells of *Allium sativum* by electron energy loss spectroscopy. *J Biosci* 28 (4):471-478. doi:10.1007/bf02705121
- Marschner H (1995) Mineral Nutrition of higher plants. Academic Press, second edition
- Masion A, Bertsch PM (1997) Aluminium speciation in the presence of wheat root cell walls: a wet chemical study. *Plant, Cell & Environment* 20 (4):504-512. doi:10.1046/j.1365-3040.1997.d01-86.x

- McLaughlin S, Mulrine N, Gresalfi T, Vaio G, McLaughlin A (1981) Adsorption of divalent cations to bilayer membranes containing phosphatidylserine. *The Journal of General Physiology* 77 (4):445-473. doi:10.1085/jgp.77.4.445
- Meychik NR, Yermakov IP (1999) A new approach to the investigation on the tonogenic groups of root cell walls. *Plant and Soil* 217 (1):257-264. doi:10.1023/a:1004675309128
- Meychik NR, Yermakov IP (2001) Ion exchange properties of plant root cell walls. *Plant and Soil* 234 (2):181-193. doi:10.1023/a:1017936318435
- Moore KL, Schröder M, Wu Z, Martin BGH, Hawes CR, McGrath SP, Hawkesford MJ, Feng Ma J, Zhao F-J, Grovenor CRM (2011) High-Resolution Secondary Ion Mass Spectrometry Reveals the Contrasting Subcellular Distribution of Arsenic and Silicon in Rice Roots. *Plant Physiology* 156 (2):913-924. doi:10.1104/pp.111.173088
- Nagajyoti P, Lee K, Sreekanth T (2010) Heavy metals, occurrence and toxicity for plants: a review. *Environmental Chemistry Letters* 8 (3):199-216. doi:10.1007/s10311-010-0297-8
- Postma JWM, Keltjens WG, van Riemsdijk WH (2005) Calcium-(Organo)aluminum-proton Competition for Adsorption to Tomato Root Cell Walls: Experimental Data and Exchange Model Calculations. *Environmental Science & Technology* 39 (14):5247-5254. doi:10.1021/es048138v
- Ram LC (1980) Cation exchange capacity of plant roots in relation to nutrients uptake by shoot and grain as influenced by age. *Plant and Soil* 55 (2):215-224. doi:10.1007/bf02181801
- Reid RJ (2001) Mechanisms of micronutrient uptake in plants. *Functional Plant Biology* 28 (7):661-668. doi:http://dx.doi.org/10.1071/PP01037
- Sarkar P, Bosneaga E, Auer M (2009) Plant cell walls throughout evolution: towards a molecular understanding of their design principles. *Journal of Experimental Botany* 60 (13):3615-3635. doi:10.1093/jxb/erp245
- Sattelmacher B (2001) The apoplast and its significance for plant mineral nutrition. *New Phytologist* 149 (2):167-192. doi:10.1046/j.1469-8137.2001.00034.x
- Sentenac H, Grignon C (1981) A Model for Predicting Ionic Equilibrium Concentrations in Cell Walls. *Plant Physiol* 68:415-419
- Sheldon A, Menzies N (2005) The Effect of Copper Toxicity on the Growth and Root Morphology of Rhodes Grass (&i>Chloris gayana&i> Knuth.) in Resin Buffered Solution Culture. *Plant and Soil* 278 (1):341-349. doi:10.1007/s11104-005-8815-3
- Shomer I, Novacky AJ, Pike SM, Yermiyahu U, Kinraide TB (2003) Electrical Potentials of Plant Cell Walls in Response to the Ionic Environment. *Plant Physiology* 133 (1):411-422. doi:10.1104/pp.103.024539
- Smart KE, Smith JAC, Kilburn MR, Martin BGH, Hawes C, Grovenor CRM (2010) High-resolution elemental localization in vacuolate plant cells by nanoscale secondary ion mass spectrometry. *The Plant Journal* 63 (5):870-879. doi:10.1111/j.1365-313X.2010.04279.x

- Straczek A, Sarret G, Manceau A, Hinsinger P, Geoffroy N, Jaillard B (2008) Zinc distribution and speciation in roots of various genotypes of tobacco exposed to Zn. *Environmental and Experimental Botany* 63 (1-3):80-90. doi:DOI: 10.1016/j.envexpbot.2007.10.034
- Strasser O, Köhl K, Römheld V (1999) Overestimation of apoplastic Fe in roots of soil grown plants. *Plant and Soil* 210 (2):179-189. doi:10.1023/a:1004650506592
- Taiz L, Zeiger E (2006) *Plant Physiology*, 4th Edition. Sinauer Associates Sunderland, MA
- Thakali S, Allen HE, Di Toro DM, Ponizovsky AA, Rooney CP, Zhao F-J, McGrath SP (2006) A Terrestrial Biotic Ligand Model. 1. Development and Application to Cu and Ni Toxicities to Barley Root Elongation in Soils. *Environmental Science & Technology* 40 (22):7085-7093. doi:10.1021/es061171s
- Vogel J (2008) Unique aspects of the grass cell wall. *Current Opinion in Plant Biology* 11 (3):301-307. doi:http://dx.doi.org/10.1016/j.pbi.2008.03.002
- Vulkan R, Yermiyahu U, Mingelgrin U, Rytwo G, Kinraide TB (2004) Sorption of Copper and Zinc to the Plasma Membrane of Wheat Root. *Journal of Membrane Biology* 202 (2):97-104. doi:10.1007/s00232-004-0722-7
- Wang P, Kinraide TB, Zhou D, Kopittke PM, Peijnenburg WJGM (2011) Plasma Membrane Surface Potential: Dual Effects upon Ion Uptake and Toxicity. *Plant Physiol* 155 (2):808-820. doi:10.1104/pp.110.165985
- Wershaw R, Mikita M (1987) *NMR of humic substances and coal*. Lewis Publishers, Chelsea, MI
- Yang Z-B, Eticha D, Rao IM, Horst WJ (2010) Alteration of cell-wall porosity is involved in osmotic stress-induced enhancement of aluminium resistance in common bean (*Phaseolus vulgaris* L.). *Journal of Experimental Botany* 61 (12):3245-3258. doi:10.1093/jxb/erq146
- Zhang Q, Smith A, Sekimoto H, Reid R (2001) Effect of membrane surface charge on nickel uptake by purified mung bean root protoplasts. *Planta* 213 (5):788-793. doi:10.1007/s004250100555
- Zhou H, Zeng M, Zhou X, Liao B-H, Liu J, Lei M, Zhong Q-Y, Zeng H (2013) Assessment of heavy metal contamination and bioaccumulation in soybean plants from mining and smelting areas of southern Hunan Province, China. *Environmental Toxicology and Chemistry* 32 (12):2719-2727. doi:10.1002/etc.2389

Chapitre 6 : Rôle des acides aminés dans la complexation du cuivre au sein du continuum parois apoplasmiques – membranes plasmiques

Dans le chapitre précédent (chapitre 5), nous avons vu que les parois apoplasmiques et les membranes plasmiques présentent toutes deux des propriétés de complexation vis-à-vis des cations métalliques, les membranes plasmiques portant d'ailleurs une densité de sites complexant plus élevée que les parois apoplasmiques. Néanmoins, l'induction par les cations métalliques d'une rhizotoxicité est généralement associée à leur complexation par les groupements carboxyliques portés par les pectines. Le cuivre fait cependant partie des cations métalliques qui présentent une rhizotoxicité particulièrement élevée, au-delà de ce qui est prédit par l'affinité du cuivre pour les groupements carboxyliques ([Kopittke et al. 2014](#)). Cela suggère que le cuivre pourrait être complexé par d'autres groupements réactifs des parois apoplasmiques.

L'article *Implication of amino acids in high-affinity copper complexation in the apoplast of tomato and wheat roots: spectroscopic and thermodynamic evidences*, constituant ce chapitre 6, est une étude de la complexation du cuivre au sein du compartiment extracellulaire racinaire à savoir le continuum parois apoplasmiques – membranes plasmiques. Comme dans le chapitre précédent (chapitre 5), les contributions respectives des parois apoplasmiques et des membranes plasmiques sont déduites de la comparaison parois apoplasmiques isolées – racines sèches.

Contrairement aux résultats attendus d'après les conclusions du chapitre 5, les parois apoplasmiques semblent contribuer au moins autant, voire plus (entre 50 et 60% du cuivre total complexé), que les membranes plasmiques à la complexation du cuivre sur les surfaces racinaires. En croisant différentes techniques analytiques (spectroscopie d'absorption des rayons X et RMN ^{13}C) avec la modélisation de la réactivité des racines de blé et de tomate vis-à-vis du cuivre, nous avons mis en évidence une spéciation du cuivre partagée, de façon presque égale, entre des ligands oxygènes présentant une faible affinité, et des ligands oxygène / azote présentant une affinité élevée. Ces deux familles de ligands traduisent respectivement la contribution des groupements carboxyliques et des acides aminés portés à la fois au niveau des parois apoplasmiques et des membranes plasmiques.

Chapitre 6 : Implication of amino acids in high-affinity copper complexation in the apoplast of tomato and wheat roots : spectroscopic and thermodynamic evidences

Implication of amino acids in high-affinity copper complexation in the apoplast of tomato and wheat roots : spectroscopic and thermodynamic evidences

Stéphanie Guigues^{1,2}, Matthieu N. Bravin³, Cédric Garnier⁴, Armand Masion⁵, Claire Chevassus-Rosset¹, Patrick Cazevieille¹ and Emmanuel Doelsch¹

¹ CIRAD, UPR Recyclage et risque, F-34398 Montpellier, France

² ADEME, 20 avenue du Grésillé, BP-90406, Angers cedex 01, France

³ CIRAD, UPR Recyclage et risque, F-97408 Saint-Denis, Réunion, France

⁴ Université de Toulon, PROTEE, EA 3819, 83957 La Garde, France

⁵ Aix-Marseille Université, CNRS, IRD, CEREGE UM34, 13545 Aix-en-Provence, France

Abstract

Carboxylic groups located in plant cell walls (CW) are generally considered as the main copper binding sites in plant roots, despite the presence of other functional groups which contribute to root binding properties. The aim of this study was to investigate sites responsible of copper binding in root apoplast i.e. the cell walls – outer surface of plasma membranes (PM) continuum. The apoplastic localization of binding sites was investigated by comparing isolated CW of a monocotyledon (*Triticum aestivum* L.) and dicotyledon (*Solanum lycopersicum* L.) with their respective whole roots. Copper speciation was examined by X-ray absorption and ¹³C-nuclear magnetic resonance spectroscopies while the affinity of ligands involved in copper binding was investigated by modeling copper sorption isotherms. Homogeneous speciation of copper was found in root apoplast. Nitrogen/oxygen ligands associated to CW and PM amino acids were identified in slightly higher proportion than single oxygen ligand assimilated to CW polysaccharides. Furthermore, low- and high-affinity binding sites almost contributed in equivalent proportion to copper complexation in the root apoplast of wheat and tomato. Jointly to CW polysaccharides, amino acids embedded in CW and PM participate in copper binding on roots.

Keywords: cell walls; plasma membrane; trace metal; modeling; binding site; X-ray absorption spectroscopy

I. Introduction

As seven other micronutrients, copper (Cu) is essential for the development of plants (Marschner 1995). Copper is a redox-active transition metal that exists as Cu^{2+} and Cu^+ depending on physiological conditions. It participates in many biological processes such as photosynthesis, mitochondrial respiration, perception of ethylene and cell wall (CW) remodeling. The optimum range of Cu concentration in plant is narrow, as deficiency and toxicity are usually expected below 5 and above $20 \mu\text{g}\cdot\text{g}^{-1}$ dry weight in shoots respectively. Consequently, plants must regulate finely Cu uptake and homeostasis (Burkhead 2009). The substantial and repetitive inputs of Cu on agricultural areas (fungicides, organic waste spreading, etc.) associated with the low mobility of Cu in soil lead to large-scale Cu contamination of soils that questions the potential occurrence of Cu phytotoxicity (Belon et al. 2012). Due to their location within soil, roots are primarily exposed to Cu contamination and are thus known to be particularly sensitive to Cu rhizotoxicity. Indeed, Cu(II) (hereafter referred as to Cu) was found to be the third most rhizotoxic metal cation out of 26 (Kopittke et al. 2011a).

Kopittke et al. (2014) suggested that the minimum rhizotoxicity of metal cations, including Cu, would mainly be based on a non-specific mechanism related to the binding strength of metal cations to hard ligands (e.g. carboxyl, phosphate, carbonyl, phenolic and amine groups) in the CW, especially to the carboxylic groups of galacturonic acids located within the pectic matrix. As other metal cations showing a large affinity for hard ligands, Cu accumulates almost entirely within the rhizodermis and the outer cortex of roots (Kopittke et al. 2011c; Collin et al. 2014) and is mainly located in the apoplastic compartment (Bravin et al. 2010; Colzi et al. 2011). Measurements in X-ray absorption spectroscopy (XAS) and pectinase treatment independently suggest that Cu was mainly bound to polygalacturonate-like groups located in CW (Konno et al. 2005; Kopittke et al. 2011c). Taken together, these experimental considerations support the hypothesis of an increased rigidity of CW of outer root tissues due to the substantial and strong binding of Cu to pectins, which results in a slower elongation rate of outer cells compared to the cells located in the stele and inner cortex and finally to the appearance of ruptures in the rhizodermis and the outer cortex of roots. However, Cu belongs to the four metal cations exhibiting “an unexpectedly high rhizotoxicity”, i.e. a rhizotoxicity higher than that estimated from the binding strength of Cu to the hard ligand scale (HLScale) mainly represented by carboxyl groups, that requires further investigation (Kopittke et al. 2014). Reexamining this theory involving hard ligands, we intended to investigate the speciation and the sorption of Cu in root apoplast to evaluate the two following hypotheses: (i) Cu ligands such as phosphate and amine groups in CW and the

outer surface of plasma membranes (PM; that we consider herein as the inner borderline of apoplast) significantly contribute to Cu binding in addition to carboxyl groups borne by pectins and (ii) the Cu binding strength of root apoplast is under-estimated by the current HLScale owing to the under-representation of amine groups as high-affinity Cu binding sites.

To evaluate the relevance of the two above-stated hypotheses, we combine the determination of the speciation and the sorption of Cu in root apoplast. Tomato (*Solanum lycopersicum* L.) and wheat (*Triticum aestivum* L.) were chosen as the model species of dicots and monocots respectively as it is well known that dicots exhibit a higher pectin concentration and a higher total density of binding sites than monocots. Copper sorption experiments were carried out both on CW isolated from roots and on the whole roots still containing CW and PM, to evaluate the respective contribution of CW and PM to the whole root Cu binding ability. The affinity of root materials for Cu were estimated by fitting sorption data with a geochemical model dedicated to the binding of metal cations on humic substances. The main functional groups involved in Cu sorption within the root were further identified by XAS and nuclear magnetic resonance (NMR).

II. Material and methods

II.1. Plant growth and isolation of root cell walls

The procedures followed to get healthy plants and isolated root CW were already detailed by [Guigues et al. \(2014\)](#). Briefly, seeds of bread wheat (cv. Premio) and tomato (cv. Moneymaker) were grown in hydroponic conditions for 21 days. At harvest, roots were subdivided into homogenous subsamples and then stored frozen. After thawing, a portion of roots were rinsed with 1 mM $\text{Ca}(\text{NO}_3)_2$ to eliminate the cytosolic compounds related to membrane leakage during thawing and oven-dried at 50°C (until a steady mass). Dried roots, hereafter referred as to roots, did contain both CW and PM. The remaining subsamples of rinsed roots were maintained moist for the isolation of CW.

Cell walls were isolated from wheat and tomato roots by using Triton X 100 (1% v/v) for 30 d. Isolated CW were then washed for 10 d in 1 mM $\text{Ca}(\text{NO}_3)_2$ and finally stored at 4 °C. The efficiency of the isolation procedure was checked by measuring the loss of calcium, Cu, iron, phosphorus and potassium and by performing NMR measurements on roots and CW ([Guigues et al. 2014](#)).

II.2. Experimental batches of copper sorption on roots and cell walls

Before copper sorption experiments, roots and CW were stirred in HNO₃ solution – at pH 3 – for 1 h to remove highly bound or precipitated cations (e.g. iron and aluminium), then rinsed twice with ultrapure water (18.2 M Ω) for 30 min and finally oven-dried at 50°C until a steady mass was achieved.

II.2.a. Experiment 1

An equivalent of 50 mg (dry mass basis) of roots or CW of wheat and tomato was shaken end-over-end during 24h at 25 °C in 250 ml of 0.05 M NaNO₃ at pH 4.7 (\pm 0.3) with an initial Cu concentration varying from pCu_T 6.2 to 4.8 (pCu_T = -log₁₀ [Cu_T]). The suspension was filtered (Whatman, grade 4) and roots and CW were rinsed 3 times with 100 ml of 0.05 NaNO₃ through a Büchner funnel. Sorption experiments were performed in triplicate. The replicate reserved for XAS analysis were immediately frozen in liquid N₂ and stored at -18°C. The two remaining replicates were oven-dried at 50 °C until a steady mass was achieved, ground using a porcelain mortar and digested for Cu analysis using hot mixing of 69% HNO₃ and 30% H₂O₂ (TraceSELECT ultra, Sigma-Aldrich). Copper concentration in the digest was determined by ICP-MS. Blanks and certified reference materials (rye-grass roots ERM-CD 281, EnviroMAT Drinking water EP-L-3 and groundwater ES-H-2) were included in the digestions and analyses procedures. The measurement uncertainty was lower than 15%.

II.2.b. Experiment 2

An equivalent of 50 mg (dry mass basis) of wheat and tomato roots was shaken end-over-end during 24h at 25°C in 250 ml of 0.05 M NaNO₃ at pH 4.5 (\pm 0.2) with an initial Cu concentration varying from pCu_T 5.1 to 3. The suspension was filtered (Whatman, grade 4) and roots were rinsed 3 times with 100 ml of 0.05 NaNO₃ through a Büchner funnel. Copper concentration in initial and at equilibrium solution was determined by inductively coupled plasma atomic emission spectroscopy (ICP-AES, Jobin Hyvon Horiba J 38). Blanks and in-house reference samples were included in the analyses. The measurement uncertainty was lower than 15%. The amount of Cu bound to wheat and tomato roots was calculated by making difference in the quantity of Cu recovered in the initial solution and the solution in chemical equilibrium with roots.

II.2.c. Experiment 3

A dry mass of 10 (\pm 0.5) mg of roots or CW of wheat and tomato was shaken end-over-end during 24h at 25°C in 25 ml of 0.03 M NaNO₃ at pH 4.5 (\pm 0.3) with an initial Cu concentration varying from pCu_T 7.3 to 3. Sorption experiments were performed in duplicate. After a short sedimentation time of plant material (few minutes), the supernatant was taken off for analysis. Copper concentration in initial and at equilibrium solution was determined by inductively coupled plasma mass spectrometry (ICP-MS, NexION 300X Perkin Elmer). For each data point, a summary of initial and equilibrium Cu concentration and pH measured was presented in Table S1. Blanks and certified reference material (EnviroMAT Drinking water EP-L-3 and groundwater ES-H-2) were included in the analyses. The measurement uncertainty was lower than 10%. The amount of Cu bound to roots or CW of wheat and tomato was calculated by making difference in the quantity of Cu recovered in the initial solution and the solution in chemical equilibrium with roots or CW.

II.3. Copper speciation in roots and cell walls by X-ray absorption spectroscopy

Copper K-edge X-ray absorption spectra for reference compounds and plant samples from the experiment 1 were collected on the FAME Beamline at the ESRF ([Hazemann et al. 2009](#)). Frozen roots and CW were ground and compacted into pellets in liquid N₂ (77K), with special care taken to keep the pellets frozen in liquid N₂ until the XAS analysis in order to avoid artificial speciation changes. Pellets of frozen-hydrated samples and reference compounds were transferred to a He cryostat and cooled to 10K ([Proux et al. 2006](#)) to prevent radiation. The spectra for the root and CW samples are the sum of 1 to 12 scans of 45 min each, depending on the Cu concentration recorded in fluorescence mode using a 30-element solid-state Ge detector (Canberra). Each scan was focused on a different specimen position to reduce the risk of beam damage and obtain representative spectra. The procedure of normalization and analyses of the data are reported in supporting information (Methods S1).

II.4. Identification of Cu binding functional groups by NMR

Root samples from the experiment 2 were analyzed by solid state ¹³C CP-MAS NMR spectroscopy. Since Cu(II) is paramagnetic, the C atoms in its vicinity will have their resonance broadened beyond detection. This property can be used to identify the binding sites of Cu on the root material by monitoring the functional groups experiencing signal loss upon addition of Cu(II). It should be noted that, due to the lack of sensitivity of conventional

pulse NMR, the quantities of Cu necessary to observe a significant effect are well above the concentrations to be expected in a natural environment. However, these experiments can help identify trends and differences in behavior between the root material samples. Spectra were obtained with a Bruker Avance WB 400-MHz spectrometer at 101.6 MHz. Typical acquisition parameters include spin rate of 10kHz, 2 ms contact time and 2 s recycling delays. Depending on the sample, 10-18k scans were recorded. The FIDs were processed with the MestReNova software; data treatment consisted in a 50 Hz line broadening and standard baseline and phase correction. Semi quantitative analysis was performed by spectra decomposition into gaussian peaks using the IGOR PRO 5.0 software.

In parallel, attempts to obtain usable ^{15}N NMR data failed because N accounts for only 5% and 3% weight of the root material of tomato and wheat respectively (results not shown), which, considering the low sensitivity of the ^{15}N nucleus, leads to unreasonably long acquisition times.

II.5. Modeling copper sorption on roots, cell walls and plasma membranes

The sorption of Cu on roots and CW of wheat and tomato was characterized by simulating the data from the experiment 3 (see Methods S2 for details on the modelling procedure) with the Humic Ion-Binding Model VII, hereafter referenced as to Model VII (Tipping (1998) and Tipping et al. 2011). Model VII was originally designed to simulate the sorption properties of two humic substances, namely a fulvic and a humic acid, depicted as a regular array of binding sites of type 1 and 2. The density (L_{Hi} , $\text{cmol}_c.\text{kg}^{-1}$) of type-1 sites is arbitrarily fixed as twice higher than the density of the type-2 sites (i.e. $L_{H1} = 2 \times L_{H2}$). Protons and metal ions compete for sorption on these sites with metal ions being able to form mono-, bi- and tri-dentate complexes. Electrostatic effects are accounted for in Model VII by approximating the diffuse layer/bulk solution system with a Donnan model. As roots and CW are solid organic matters, we parameterized their sorption properties on the basis of the default conformation parameters defined for the humic acid (HA) in Model VII. The partial pressure of CO_2 was assumed to be that of the ambient atmosphere ($10^{-3.5}$ atm) and the temperature was fixed at 25 °C for calculations. The modelling procedure (Methods S2) was further implemented on the theoretical potentiometric titrations and Cu sorption isotherms of the outer surface of root cell PM for wheat and tomato that were calculated by making the difference between roots and CW data (Figs. S2 and S3).

III. Results

III.1. Copper speciation in roots and cell walls

The sorption of Cu on roots and CW of wheat and tomato measured in the batch experiments 1 and 3 were similar (Fig. S4), thus demonstrating that Cu speciation studied by XAS can be related to Cu sorption characterized with Model VII.

The analyses of samples from experiment 1 indicated that the Cu sorbed (Cu_{ads}) on wheat (roots or CW) and tomato (roots or CW) ranged from 61 to 891 $mg.kg^{-1}$ (Table S2) as a function of initial Cu concentration (pCu_T 6.2 to 4.8). For a same pCu_T , Cu_{ads} for tomato was equal or slightly higher than Cu_{ads} for wheat.

The shape of XANES and EXAFS spectra and Fourier Transforms (FT) of wheat and tomato roots were very similar to those of CW (Fig. 21 and 22), regardless of the concentration of adsorbed Cu (Table S2). All XANES spectra gave an intense absorption maximum at 8997 eV (feature A) and a weak feature at 8978 eV (feature B) as XANES spectrum of Cu(II)-malate (Fig. 21), indicating that Cu was predominantly bound as Cu(II) on the roots and CW of wheat and tomato. All EXAFS spectra exhibited a shoulder at 5.6 \AA^{-1} , more or less pronounced depending on the sample (Fig. 22a, feature C). This shoulder was also observed on Cu(II)-histidine spectrum but not on that of Cu(II)-formate. Wheat spectra can be differentiated from those of tomato by a shift of the first oscillation (between 2.9 and 3.7 \AA^{-1}) of 0.12 \AA^{-1} (Fig. S5). This shift is also observed between Cu(II)-histidine and Cu(II)-formate. All FT presented a first peak at around 1.5 \AA (feature D, distance uncorrected for phase shift) representing the first coordination shell Cu-O which can be easily distinguished from Cu-S (feature E, at 1.8 \AA as observed for the FT of Cu(I)-cysteine, Fig. 22b). Furthermore, the FT of wheat and tomato roots and CW exhibited a signal close to that of Cu(II)-histidine (features F and G). A characteristic peak (feature H), visible on spectrum of Cu(II)-formate was also visible on the FT of tomato roots and CW (Fig. 22b).

No significant differences in Cu speciation in roots and CW of wheat or tomato were found with LCF (Fig. 22 and 23 and Table S2). With the exception of one sample, the best fits were obtained by combining Cu(II)-histidine with one or more reference compounds. In wheat samples, Cu(II)-histidine represented between 37 and 73% of the EXAFS spectra and from 42 to 57% of the EXAFS spectra of tomato samples (Fig. 23, Table S2). Tomato CW_61 was the only exception with the best fit combining 65% Cu(II)-galacturonate and 35% Cu(II)-formate. In tomato roots and CW, Cu(II)-formate was identified as the second compound of spectra, between 35 and 49%, except for tomato R_658 where a best fit was obtained with

Cu(II)-acetate. In addition of Cu(II)-histidine, reference compounds used in the LCF of wheat roots and CW spectra included Cu(II)-galacturonate, Cu(II)-malate or Cu(II)-malonate whatever the pCu_T .

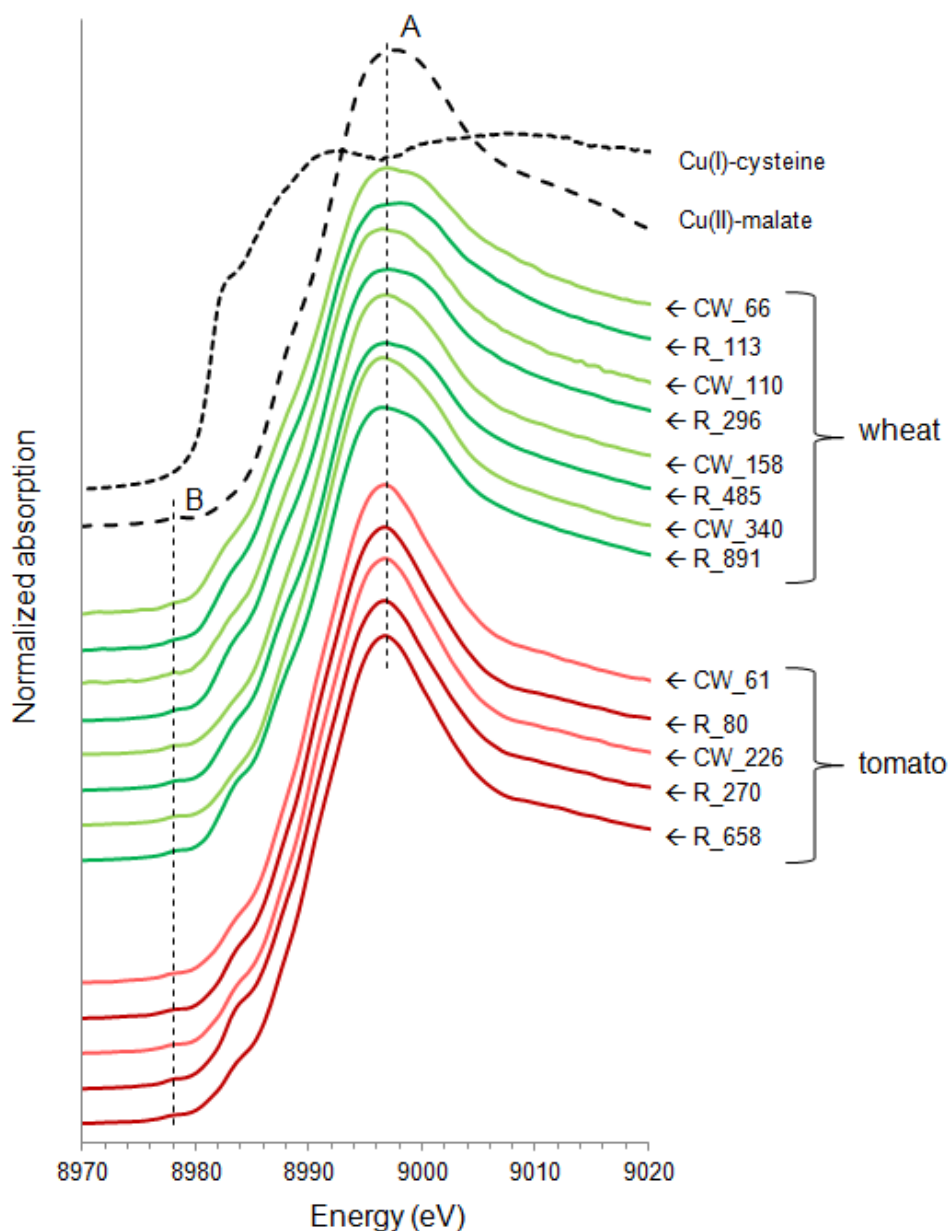


Figure 21 : Normalized Cu K-edge X-ray absorption near-edge spectroscopy (XANES) spectra for wheat and tomato roots (R) and cell walls (CW) and for two reference compounds, Cu(I)-cysteine and Cu(II)-malate. The number presents in the name of the sample refers to the concentration of Cu bound to the plant material ($mg.kg^{-1}$ initial dry roots).

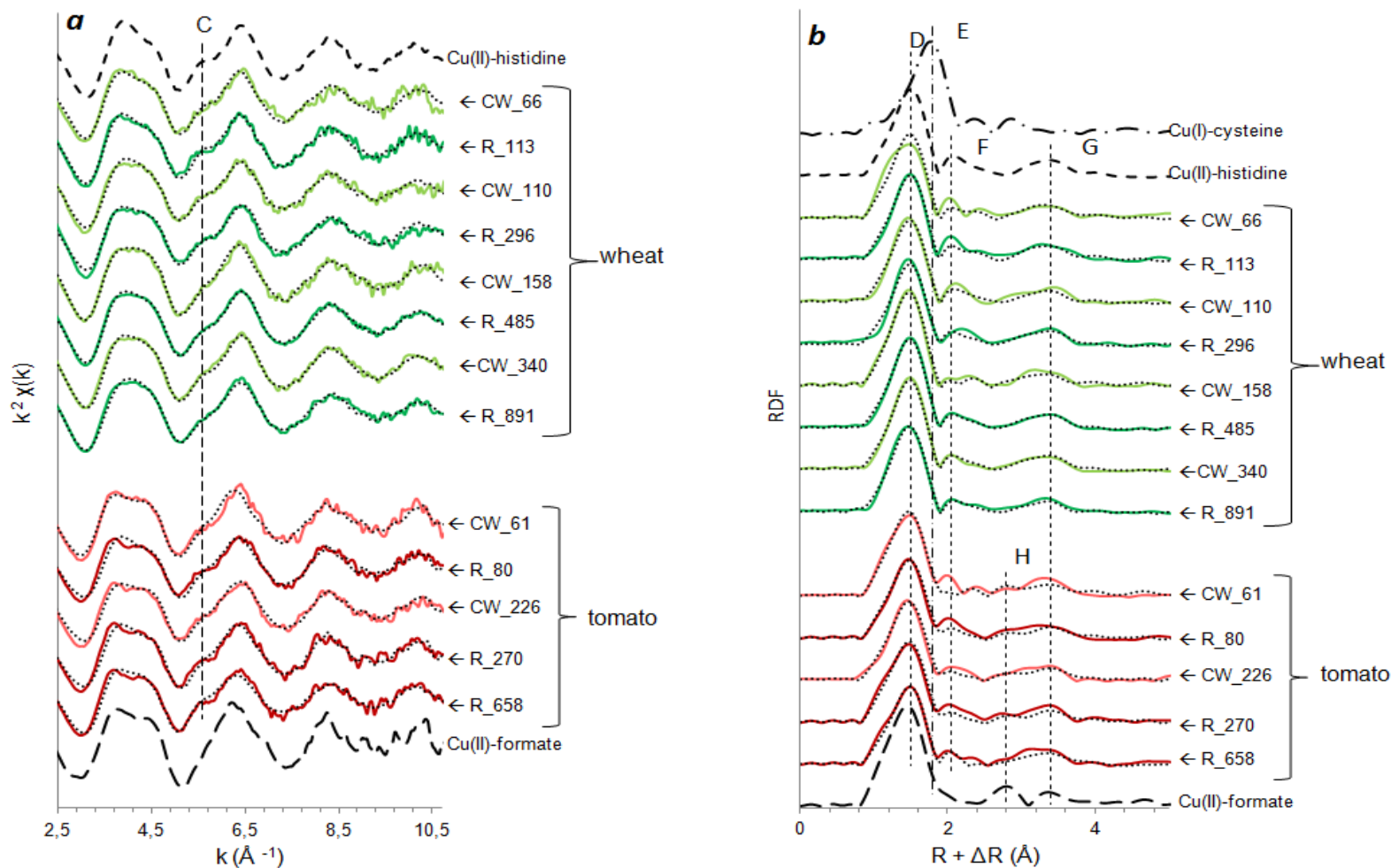


Figure 22 : Cu K-edge k^2 -weighted extended X-ray absorption fine structure (EXAFS) spectra (a) and their radial distribution function (RDF) (b) for wheat and tomato roots (R) and cell walls (CW) and for three reference compounds, Cu(II)-histidine, Cu(II)-formate and Cu(I)-cysteine. Solid lines represent experimental spectra and dotted lines are the best linear combination fits. The distances are uncorrected for phase shift. The number presents in the name of the sample refers to the Cu adsorbed in the plant material (in mg.kg^{-1} initial dry roots).

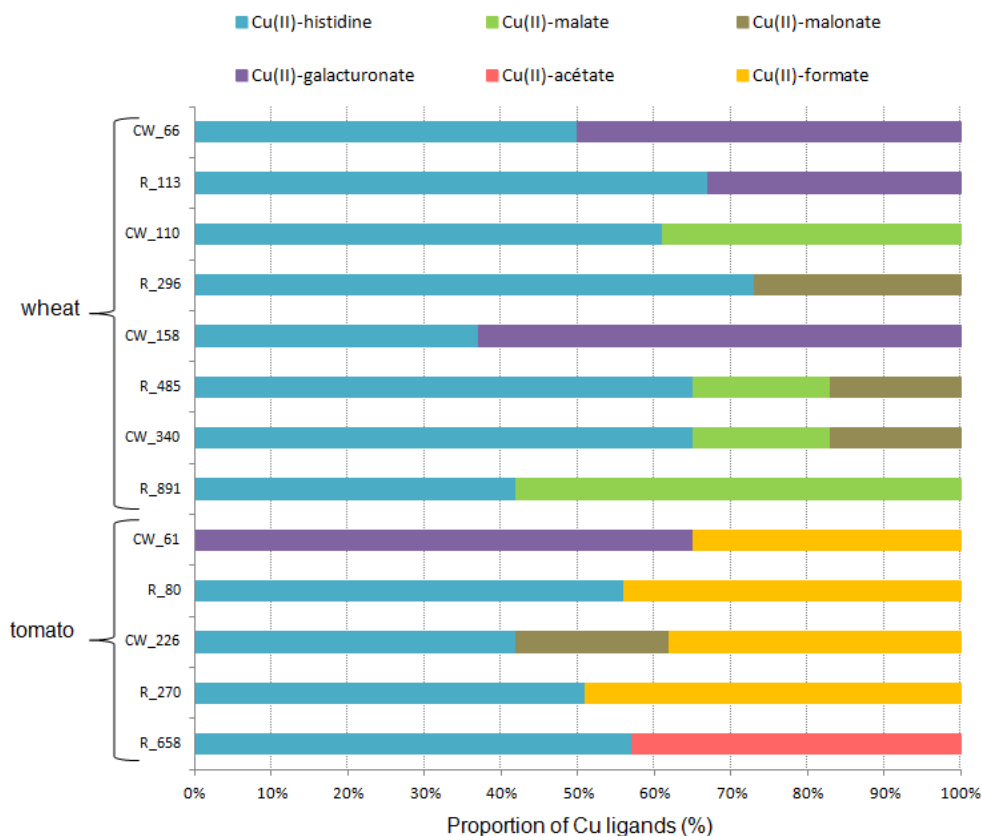


Figure 23 : Proportion for each Cu ligands resulting in the best linear combination fitting of the Cu K-edge k^2 -weighted extended X-ray absorption fine structure (EXAFS) spectra of roots (R) and cell walls (CW) of wheat and tomato.

III.2. Identification of functional groups involved in Cu binding by ^{13}C -NMR

The sorption of Cu on wheat and tomato roots measured in the batch experiments 2 and 3 looked similar (Fig. S4), thus demonstrating that the functional groups involved in Cu binding as identified by ^{13}C -NMR can be related to Cu binding site affinity characterized with Model VII.

As expected, the ^{13}C -NMR signal for all samples is dominated by the carbohydrates in the roots, i.e. the resonances between 60 and 110 ppm (cellulose, hemicellulose, pectin, etc.) which account for 60% of the detected C in tomato and 80% in wheat, and the line around 172 ppm (carboxyls/amide of uronates and proteins) (Fig. 24a and b). Aromatic compounds, which include lignins and aromatic amino acids, represent a combined proportion below 5% in all cases and are negligible. Total phenols account for ca. 1-2 % of the detected C. The major difference in root composition between the tomato and wheat sample is the proportion of alkyl C, presumably proteins. This fraction of aliphatic C accounts for approximately 30%

in the tomato roots (Fig. 24b) whereas this proportion is only ca. 15% in the case of wheat (Fig. 24a). It should be kept in mind however that these are rough estimates since aliphatic amino acids such as valine (Val), threonine (Thr), proline (Pro) and isoleucine (Ile) have resonances between 60 and 70 ppm, i.e. the carbohydrate region, and under our experimental conditions cannot be distinguished from cellulose type material.

In the case of the tomato roots, the addition of increasing amount of Cu leads to diminished intensities of the peaks in the alkyl- and carbonyl/carboxyl regions (Fig. 24b). The intensity variations observed between 0 and approximately 60 ppm cannot be converted with sufficient confidence into variations of proportions since, assuming that they are due to Cu binding by proteins, only a limited fraction of C is potentially impacted; also there is an overlap between the contribution around 55 and 60 ppm which complicates the determination of alkyl- vs. carbohydrate compounds. Semi-quantitative analysis is possible however for the variations of the carboxyl resonance around 172 ppm: when the Cu concentration is increased from 0 to 9864 mg.kg⁻¹ (dry mass), the surface area of the peak is diminished by approximately 30%. In the case of wheat, equivalent amount of added Cu(II) caused only a ca. 10% reduction of the contribution around 172 ppm showing that for this material Cu binding to carboxyl is less prevalent (Fig. 24a). Similarly to the case of tomato, the intensity variations in the alkyl region are difficult to translate into meaningful variations of proportions. An interesting feature is the decrease in intensity of the line around 62 ppm. As it seems unlikely that the primary alcohol of a hexose moiety specifically binds Cu, this decrease can be attributed to the loss of signal of the amino acids Val, The, Pro and Ile, thereby pointing to a specific composition of root proteins.

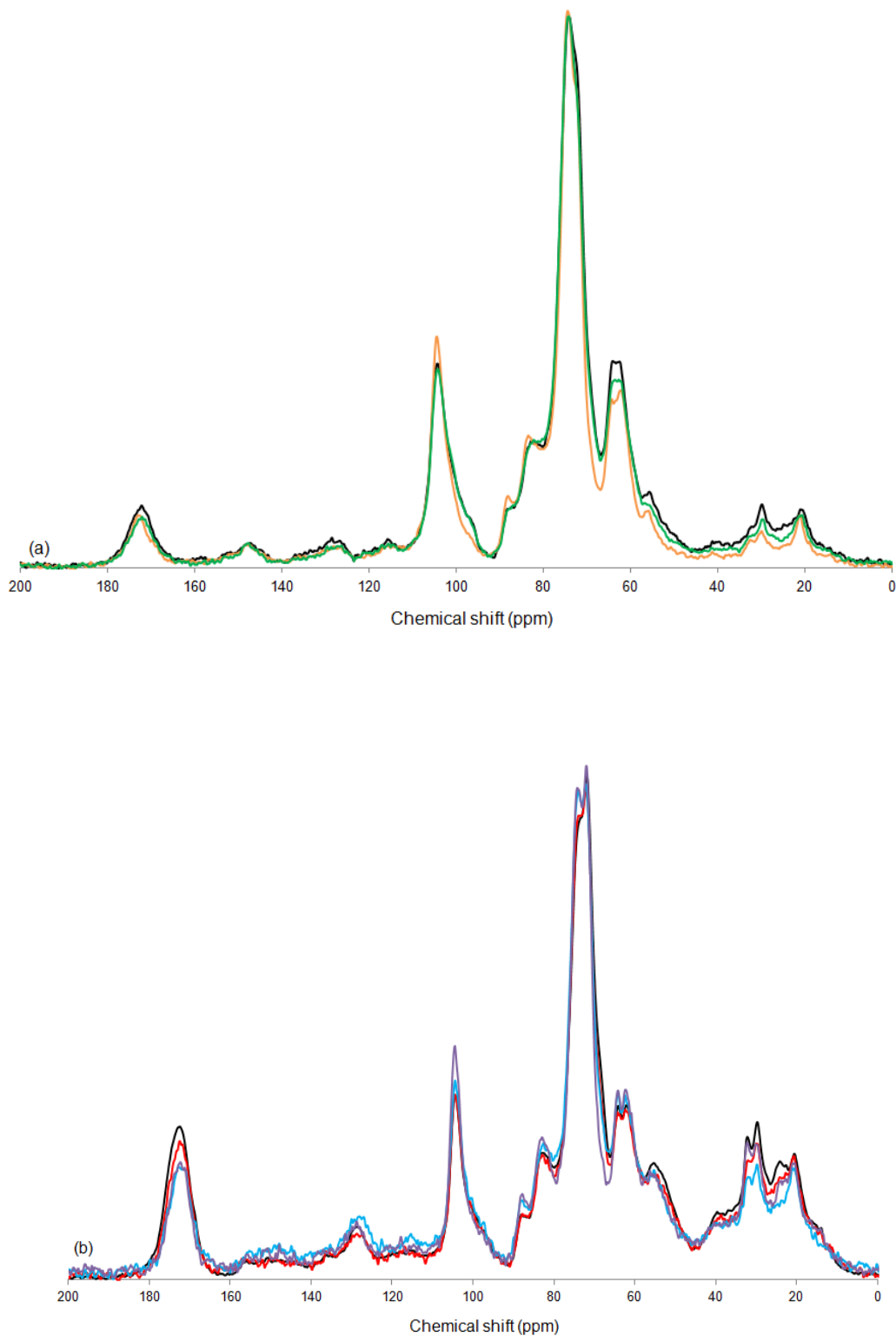


Figure 24 : ¹³C-NMR spectra of (a) wheat roots containing copper bound at 0 (black line), 4855 (orange line) and 8023 (green line) mg.kg⁻¹ dry mass and (b) tomato roots containing copper bound at 0 (black line), 832 (red line), 2785 (blue line) and 9864 (purple line) mg.kg⁻¹ dry mass.

III.3. Modeling the acidic properties of roots, cell walls and plasma membranes

The parameterization of the two HA model enabled to fit almost neatly ($RMSR < 1.9 \text{ cmol}_c \cdot \text{kg}^{-1}$) the potentiometric titrations obtained experimentally for roots and CW and theoretically for PM of wheat and tomato (Table 3, fig. 25 and fig. S2). The goodness of the fit for PROSECE (Guigues et al. 2014) and two HA models are similar, thus strengthening the relevance of the parameterization used herein. Roots and PM of wheat and tomato as well as wheat CW were each described by four pK_a (Table 3). For HA_I - and HA_{II} -borne sites, pK_a ranged from 3.4 to 7.5 and from 7.2 to 10.0, respectively. Tomato CW were characterized by only three pK_a amounted to 3.6 and 6.0 for HA_I -borne sites and 9.75 for HA_{II} -borne sites. Only one out of the four distribution terms, ΔpK_a was set at a value different from zero to fit adequately the data for each root material. The relationship between the acidic properties and the chemical nature of binding sites of CW and PM were further discussed by Guigues et al. 2014.

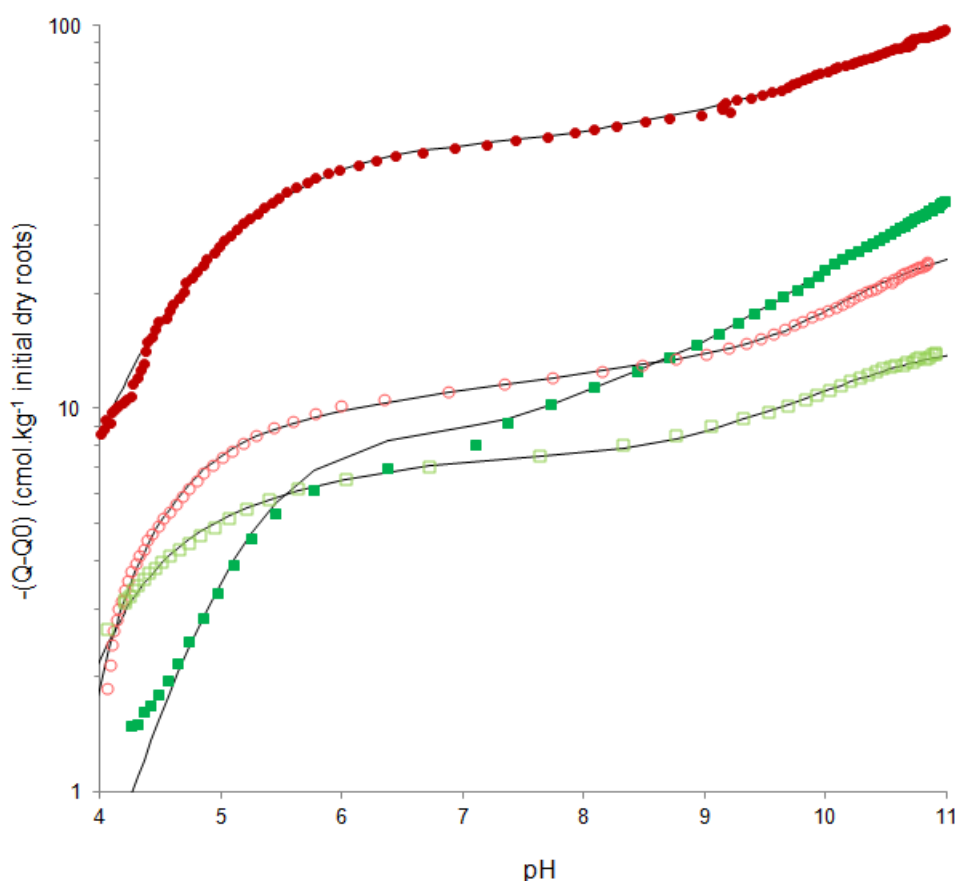


Figure 25 : Potentiometric titrations for roots (filled symbols) and cell walls (empty symbols) of wheat (squares) and tomato (circles) expressed in charge (Q) corrected by the initial charge (Q_0). Solid lines refer to the fitting curves obtained with the two humic-acid model as described in the Material and Methods.

Table 3 : Acidic properties modelled from experimental data for wheat and tomato roots, cell walls (CW) and derived from theoretical potentiometric titrations for plasma membranes (PM). The total site density of roots and CW ($\text{cmol}_c.\text{kg}^{-1}$ initial dry roots) were obtained by fitting the experimental data with PROSECE software (Guigues et al. 2014), that of PM were derived from this last results. The acidic site density of type 1 (L_{H1}) was equal to twice that of type 2 (L_{H2}). The stability constants ($\text{p}K_{a_i}$) and the distribution terms ($\Delta\text{p}K_{a_i}$) were obtained by fitting the experimental data with the two humic-acid model as described in the Material and Methods.

		HA _I						HA _{II}						Total site density
		Type 1			Type 2			Type 1			Type 2			
		L_{H1}	$\text{p}K_{a1}$	$\Delta\text{p}K_{a1}$	L_{H2}	$\text{p}K_{a2}$	$\Delta\text{p}K_{a2}$	L_{H1}	$\text{p}K_{a1}$	$\Delta\text{p}K_{a1}$	L_{H2}	$\text{p}K_{a2}$	$\Delta\text{p}K_{a2}$	
	Roots	8.2	4.6	1.5	4.1	7.4	0	16.1	10.0	0	8.1	9.1	0	36.5
Wheat	CW	5.5	3.4	0	2.8	4.9	2.0	2.3	9.8	0	4.6	8.6	0	15.2
	PM	6.4	5.2	2.5	3.2	7.5	0	3.9	10.0	0	7.8	9.5	0	21.3
	Roots	30.3	4.0	0	15.1	5.1	0	34.5	9.8	0	17.3	8.3	1.8	97.2
Tomato	CW	10.6	3.6	0	5.3	6.0	3.5	8.5	9.75	0	4.3	9.75	0	28.7
	PM	20.4	4.1	0	10.1	4.6	0	25.3	9.6	0	12.7	7.2	1.8	68.5

III.4. Copper sorption on roots, cell walls and plasma membranes

Whatever the root material considered in the batch experiment 3, the concentration of Cu adsorbed increased with the increasing total Cu concentration in solution (Fig. 26). When expressed in dry mass of roots and CW respectively, the quantity of Cu bound to roots and CW was the same, reflecting an identical binding behavior of these two plant materials (results not shown). In accordance with binding site density (Table 3), roots and CW of wheat bound less Cu at a given Cu concentration in equilibrated solution and were more rapidly saturated in Cu than roots and CW of tomato (Fig. 26). Very similar observations can be done for the theoretical Cu sorption data calculated for PM (Fig. S3).

III.5. Modeling copper sorption on roots, cell walls and plasma membranes

The two HA model was able to fit almost neatly the sorption of Cu on roots, CW and PM of wheat ($RMSR = 76 \text{ mg.kg}^{-1}$) over the entire range of Cu concentration in solution and of tomato ($RMSR = 4.5 \text{ mg.kg}^{-1}$) for $pCu_T > 4.5$ (Fig. 26, Fig. S3). For $pCu_T < 4.5$, the two HA model deviated from the experimental data points for roots, CW and PM of tomato. While the two HA model can be specifically parameterized to fit the tomato data for $pCu_T < 4.5$ in solution (data not shown), the modeling results were discussed below on the basis of the parameterization used to fit the data for $pCu_T > 4.5$ that corresponds to the environmentally-relevant range of root-exposed Cu concentrations in solution (Table 4). For HA_I sites, $\log K_{Cu,1}$ and $\log K_{Cu,2}$ ranged from 1.9 to 2.45 and from 2.1 to 3.9, respectively (Table 4). The intraspecific comparison revealed that the HA_I sites of PM had lower intrinsic equilibrium constants than those of roots and CW for both wheat and tomato. For HA_{II} sites, $\log K_{Cu,1}$ and $\log K_{Cu,2}$ ranged from 6.0 to 7.5 and from 4.5 to 6.7, respectively. For the HA_{II} sites of tomato, intrinsic equilibrium constants obtained for PM were lower than those of roots and CW. For the HA_{II} sites of wheat, the $\log K_{Cu,1}$ of PM was equal to those of roots and CW and the $\log K_{Cu,2}$ of PM was slightly higher than those of roots and CW. Interspecific comparison revealed that equilibrium constants of roots and PM were higher for wheat than for tomato. Contrarily, equilibrium constants of CW were higher for tomato than for wheat. The heterogeneity parameters (ΔLK_{2Cu}) for both HA_I and HA_{II} sites were fairly low, i.e. equals to 0.8 for wheat roots or not different from zero for all other root material of wheat and tomato.

Chapitre 6 : Implication of amino acids in high-affinity copper complexation in the apoplast of tomato and wheat roots : spectroscopic and thermodynamic evidences

Copper repartition between HA_I and HA_{II} sites obtained with the two HA model revealed a slightly higher contribution of HA_{II} sites to Cu binding in wheat roots and a similar contribution between HA_I and HA_{II} sites for tomato roots (Fig. S6). While HA_I sites were preponderant in wheat and tomato CW and tomato PM, HA_{II} sites were preponderant in wheat PM.

Table 4 : Copper sorption properties modelled from experimental data for wheat and tomato roots, cell walls (CW) and derived from theoretical sorption data for plasma membranes (PM). The intrinsic equilibrium constant ($\log K_{Cu}$) and the heterogeneity parameter ($\Delta LK2_{Cu}$) were obtained by fitting the experimental data with the two humic-acid model as described in the Material and Methods. The intrinsic equilibrium constant ($\log K_{Cu,2}$) were derived from $\log K_{Cu,1}$ as given in equation (1) .

		HA _I			HA _{II}		
		Type 1		Type 2	Type 1		Type 2
		$\log K_{Cu,1}$	$\log K_{Cu,2}$	$\Delta LK2_{Cu,I}$	$\log K_{Cu,1}$	$\log K_{Cu,2}$	$\Delta LK2_{Cu,II}$
Wheat	Roots	2.45	3.9	0.8	7.0	6.4	≤ 0.2
	CW	2.1	3.0	≤ 0.1	7.0	6.1	≤ 0.5
	PM	2.0	2.9	≤ 0.4	7.0	6.7	≤ 0.1
Tomato	Roots	2.1	2.7	≤ 0.2	7.0	5.9	≤ 0.1
	CW	2.3	3.8	≤ 0.2	7.5	7.5	≤ 0.2
	PM	1.9	2.1	≤ 0.1	6.0	4.5	0

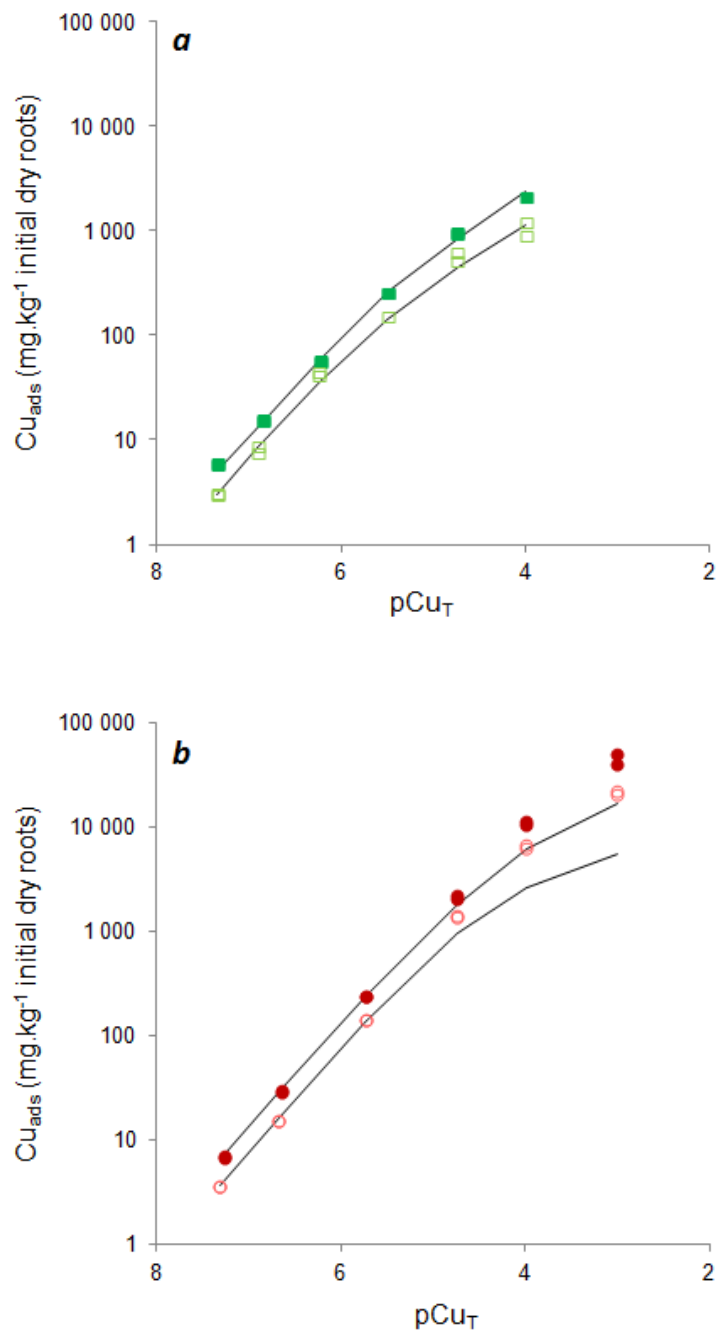


Figure 26 : Copper binding by roots (filled symbols) and cell walls (empty symbols) of wheat (a) and tomato (b). Solid lines refer to the fitting curves obtained with the two humic-acid model as described in the Material and Methods.

IV. Discussion

IV.1. Dual copper coordination with carboxyl and amine groups

There is increasing evidences that hard ligands other than carboxylic groups could be significantly involved in metal sorption within root apoplast. The potentiometric titrations of root CW enabled to identify the occurrence of cation binding sites with pK_a higher than ca. 7.5, i.e. presumably attributed to phenolic and amine groups (Meychik and Yermakov 2001). Complementary to CW, the role of cation binding sites borne by the outer surface of root PM can be also evoked. Based on the investigation of the paramagnetic effect of cobalt (Co) on the ^{31}P - and ^{13}C -NMR signals of phosphatidylserine, McLaughlin (1982) estimated that Co(II) was bound to the surface of the model membrane as phosphate complex for 13 %, amine-carboxyl chelate complex for 32 % and carboxyl complex for 54 %. Hence, it is conceivable that a significant amount of the Cu binding sites borne by root-cell plasma membranes may involve not only carboxyl groups but also phosphate, phenolic and amine groups.

For both tomato and wheat, roots and CW, and whatever the level of Cu loading, the chemical environment of Cu revealed by XAS analysis looked very similar, thus suggesting that Cu speciation was rather homogeneous in root apoplast (Fig. 22a and b). While it is usually assumed that the distinction between Cu-N and Cu-O coordinations for biomolecules is difficult to make with XAS, Manceau et al. (2013) recently succeed in showing that Cu was mainly bound to histidine residue in the root CW of *T. arvense*. In line with this result, we found that Cu(II)-histidine like species were ubiquitous in all the samples but one and (co-)dominated Cu speciation in 10 out of the 13 samples of roots and CW (Fig. 23, Table S2). In the Cu(II)-histidine reference compound, Cu was simultaneously bound to oxygen and nitrogen atoms carried by carboxylic and amine groups (Evertson 1969). This reflects the involvement of amino acid residues, embedded in CW (Cassab 1998) and at the outer surface of PM (Taiz and Zeiger 2006). Copper was also associated with O atoms in roots and CW of wheat and tomato (Fig. 23, Table S2). While the Cu-O local environment was ubiquitous in all samples, it (co-)dominated Cu speciation in only 6 out of the 13 samples. Copper was likely bound to both carboxyl and alcohol groups, as in Cu(II)-galacturonate and Cu(II)-malate. Such environment most likely reflects the participation of CW polysaccharides as pectins in Cu complexation. Such CW sites had already been identified as Cu binding sites in roots of cowpea exposed to Cu during 24h (Kopittke et al. 2011c). Beyond the contribution of Cu-N and Cu-O first coordination shells, no other Cu ligand was detected by XAS analysis in roots and CW of wheat and tomato. The absence of Cu-phosphate bond suggests that the PM phospholipids were not involved in Cu binding or in too low proportion

to be detected (i.e. below 10%). Indeed, Cu has a low affinity for phosphate groups, in contrast to zinc (Sarret et al. 2001; Kopittke et al. 2011c). We have not detected Cu-sulfur bond either. This bond has been detected for plants which cope with Cu by internal sequestration via several S-rich ligands (e.g. metallothioneins) or by biomineralization of copper sulfide (Collin et al. 2014). As the dry roots and CW we studied were metabolically-inactive, these physiologically-driven processes were likely not active.

The homogeneity in Cu speciation whatever the plant species, the root apoplastic compartment and the level of apoplastic Cu loading considered is further supported by the values fitted for $\Delta LK2_{Cu}$ in the two HA model. This parameter was designed to account for the occurrence at low concentration of binding sites exhibiting a very high affinity for metals in humic substances, thus enabling to simulate strong binding behaviors at low metal concentration (Tipping et al. 2011). The $\Delta LK2_{Cu}$ values fitted in the two HA model (≤ 0.8 ; Table 4) were much lower than the values reported for humic substances (2.34 for Cu), suggesting that this kind of sites is either almost absent from root apoplast or can be neglected.

IV.2. High-affinity copper complexation

XAS analysis showed that Cu is coordinated in root apoplast either with a single O ligand mainly involving carboxyl groups or with both O and N ligands involving carboxyl and amine groups of amino acids. Copper has a much higher affinity for synthetic and natural ligands with both carboxylic and amine groups (e.g. ethylenediaminetetraacetic acid, histidine, nicotianamine) than for ligands with carboxyl groups only (Fry et al. 2002; Karlsson et al. 2008). In line with these considerations, the two HA model was parameterized for wheat and tomato roots by considering that 34 to 47 % of binding sites were low-pKa sites (i.e. type 1 and 2 in HA_I) presumably corresponding to carboxyl-like groups and exhibiting low-affinity Cu binding constants ranging from $\log K_{Cu}$ 2.1 to 3.9, whereas 53 to 66 % of binding sites were high-pKa sites (i.e. type 1 and 2 in HA_{II}) presumably corresponding to amine-like groups and exhibiting high-affinity Cu binding constants ranging from $\log K_{Cu}$ 5.9 to 7 (Tables 3 and 4). It is noteworthy that these high-affinity Cu binding sites presumably corresponding to amine sites exhibit Cu binding constants even higher than those (i.e. $\log K_{Cu}$ 4.8-5.6) of similar high-pKa sites usually described in humic substances that presumably correspond to phenolic sites (Tipping et al. 2011). The two HA model further suggested that the high-affinity Cu binding sites significantly contributed to the actual complexation of Cu, especially when considering the whole root surfaces where these high-affinity sites bound 40 to 60 % of total Cu complexed (Fig. S6a and b).

IV.3. Relative contribution of cell walls and plasma membranes

The comparison of Cu sorption in roots and CW revealed that PM bound only 38 to 44% of Cu in wheat and tomato roots. This lower quantitative contribution of PM over CW to Cu complexation is surprising at first sight as PM bore 60 to 70% of the total density of binding sites in wheat and tomato roots (Guigues et al. 2014). This first suggests that cation binding sites in CW exhibit a much higher affinity for Cu than those located at the outer surface of PM. This hypothesis works for tomato for which the $\log K_{Cu}$ of CW sites were higher by 0.4 to 3 units than the $\log K_{Cu}$ of PM sites (Table 4). However, for wheat the $\log K_{Cu}$ of CW sites were either weakly higher by 0 to 0.1 unit (for HA_I sites and type-1 sites of HA_{II}) or lower by 0.6 unit than the $\log K_{Cu}$ of PM sites. The weak Cu binding strength of PM in wheat roots could be alternatively related to electrostatic effects that were showed to strongly influence ion concentration at PM surfaces (Wang et al. 2010; Kopittke et al. 2011). Indeed, the net negative charge of isolated CW was higher than that of roots for wheat when solution pH was lower than 5.5 (Fig. 25), thus leading to calculate that PM were positively charged in sorption experiments performed at pH 4.5-5. Plasma membranes in wheat roots may hence have exerted a repulsive effect on Cu²⁺ that lowered their Cu binding strength. An additional hypothesis that may explain the greater contribution of CW over PM to Cu complexation is the spatial arrangement of these two compartments. By design, any metal cation interacting with roots first interacts and binds within CW and after passing through the remaining non-bound metal cation then interacts and binds on the outer surface of PM. Consequently, we hypothesize that Cu which exhibits a high affinity for binding sites in root apoplast first and thus mainly accumulates in CW even if CW have a lower density and Cu-affinity of their binding sites than PM. The larger contribution of CW to Cu complexation we observed in root apoplast apparently contradict the previous findings of Shomer et al. (2003) and Kinraide (2004) who suggested that metal cations would bind much more strongly to PM sites than to CW sites and that CW would have a negligible influence on the metal cation concentration at PM surfaces. However, these authors did not effectively measure the binding of metal cations to CW and PM but measured the electrical potential in CW and at PM surfaces. The modeling approach then implemented was thus very sensitive to the binding site density of CW but conversely almost insensitive to the binding strength of metal cations in CW (Kinraide 2004; Kinraide et al. 2004). Consequently, the electrostatic model developed by Kinraide and co-workers is likely relevant to calculate the ion concentration at PM surfaces but would most likely fail to calculate the effective binding of metal cations in root apoplast that as we showed involves the substantial contribution of CW.

IV.4. Interspecific comparison

Tomato roots exhibited a 2.7-fold higher site density than wheat roots (Guigues et al. 2014). Calculations performed with the two HA model suggest that binding sites were exhibiting a higher affinity for Cu (i.e. higher $\log K_{Cu}$) in wheat roots than in tomato roots (Table 4). The higher mean contribution of the Cu(II)-histidine reference in the LCF of EXAFS spectra (Fig. 23) for wheat ($62 \pm 14\%$) than for tomato ($55 \pm 3\%$) consistently suggest a higher contribution of amino acids to root Cu complexation in wheat over tomato. This preferential binding to N groups in wheat is also supported by the NMR data. Indeed, the addition of Cu(II) leads to modification primarily in the spectral region below 60 ppm, i.e. where signal from amino acids is expected, even though the modifications are difficult to quantify ($N < 3\%$ weight, results not shown), whereas the resonance of carboxyl C around 172 ppm remains largely unaffected (Fig. 24a and b). Although the amount of N in tomato roots is approximately twice as high as in wheat (result not shown), the present spectroscopic data does not support a preferential binding of Cu to N-groups. This suggests that the nature and thus the affinity for Cu, and/or (steric) accessibility of N binding sites are different in tomato and wheat roots.

IV.5. The HLScale under-estimates the contribution of amino acids

It is questionable how the HLScale which is defined with a single value is able to account for both low- and high-affinity sites we identified in root apoplast? The HLScale may correlate both with low- and high-affinity sites defined for a range of metal cations. However, this assertion cannot be tested as we focused our investigation on Cu only. Alternatively, a look on the classification of Cu binding strength in the HLScale shows that Cu^{2+} is one of the divalent cations exhibiting the highest binding strength toward hard ligands but that it remains (much) lower than the binding strength of trivalent cations (Kinraide 2009). This behavior is typical from the binding strength of Cu to most hard ligands with the notable exception of some amino acids that are known to play an important role in metal transport to and within plants. For instance, Cu exhibits an exceptionally high affinity for phyto siderophores exudated by the roots of monocots and some histidine-rich sequences of metal-transport proteins located at the outer surface of PM (Murakami et al. 1989; Grosseohme et al. 2006). In comparison with synthetic N ligands, Cu exhibits with these biologically-relevant amino acids a binding strength that approaches or even exceeds that of trivalent cations such as Fe^{3+} . Owing to the substantial contribution of amino acid residue in Cu binding in root apoplast, we may infer that the HLScale likely under-estimates the high affinity of these

binding sites for Cu, which may partly explain the under-prediction of the unexpectedly high Cu rhizotoxicity underlined by [Kopittke et al. \(2014\)](#).

V. Conclusion

By crossing modeling and spectroscopic investigations, we found a dual local environment of Cu in the root apoplast of wheat and tomato roots. As expected, CW pectins were identified as one of the major Cu binding sites. We found no evidence of the involvement of PM phospholipids. More surprisingly, Cu speciation was (co)-dominated by amino acids embedded in CW and PM. These amino acids exhibited a high affinity for Cu and hence significantly contributed to the actual Cu complexation in root apoplast. We further infer that a re-evaluation of the HLScale to better account for the contribution of amino acids may help to explain the unexpectedly high rhizotoxicity exhibited by Cu.

Although this study gives a consistent and updated picture of Cu binding in root apoplast, we investigated only non-metabolically-active materials. Hence, it would be interesting to confirm these results with fresh plants.

Acknowledgments

The authors are grateful to French Environment and Energy Management Agency (ADEME) and the French Centre of Agricultural Research for Development (CIRAD) for funding the PhD scholarship of Stéphanie Guigues and INSU (CNRS) for funding the study via the EC2CO-CYTRIX call. The authors thank Hélène Miche (CEREGE) for providing access to ICP-AES and Bernard Angeletti (CEREGE) for ICP-MS analyses. The authors also acknowledge support from Spectropole, the Analytical Facility of Aix-Marseille University, by allowing a special access to the instruments purchased with European Funding (FEDER OBJ2142-3341) and especially Fabio Ziarelli for his assistance with the NMR experiments.

VI. Supporting information

Methods S1: Procedure of normalization and analyses of the X-ray absorption spectroscopy data

A Cu foil was used to calibrate the X-ray energy (threshold energy taken at the zero-crossing point of the second derivative spectrum).

The data were normalized using Athena software ([Ravel and Newville 2005](#)). The k^2 -weighted EXAFS (2.5 to 10.7 Å⁻¹) recorded on plant samples were fitted by linear combination fitting (LCF) using a library of Cu reference compounds consisting of organic and mineral species.

Principal component analysis (PCA) was applied to EXAFS spectra to determine the number of species contained in the samples, but the PCA indicator value failed to reach a minimum. Thus, for each plant spectrum, LCFs using one, two and three reference compounds were tested successively. The LCFs with $n + 1$ components was retained if the normalized sum-squares residual (Table S2) was decreased by more than 20% compared to the fit with n components. Satisfactory fits were obtained with a combination of two or three references. A part of the reference compound database used was described previously in [Collin et al. \(2014\)](#) and compounds described below were added. Cu(II)-gluconate, Cu(II)-phthalocyanine and libethenite (Cu₂PO₄OH) were purchased from Sigma-Aldrich. Cu(II)-galacturonate was synthesized according to the procedure of [Synytsya et al. \(2004\)](#). Cu(II)-methionine and Cu(II)-phenylalanine were prepared in compliance with the protocol of [Stanila et al. \(2004\)](#). And Cu(II)-phytate was obtained in the same way as described in [Kopittke et al. \(2011c\)](#).

Methods S2: Modeling procedure (Model VII)

In a first step, Model VII was used to fit the potentiometric titrations previously done by [Guigues et al. \(2014\)](#) on roots and cell walls of wheat and tomato. These titrations were previously interpreted with the dedicated software PROSECE ([Guigues et al. 2014](#)) which enabled for each root material to fix the total site density as an input parameter and to give indicative values to fit the intrinsic proton dissociation constant, pK_{a_i} , and the corresponding distribution term, ΔpK_{a_i} , for sites of type 1 and 2. Preliminary investigations showed that it was not possible to fit adequately the titration data of tomato roots and wheat and tomato cell walls when considering a single HA. This was mainly due to the following condition imposed by Model VII: $L_{H1} = 2 \times L_{H2}$ (Fig. S1). To relax the consequences of this condition, we fit the titration data by representing each root material with two HA independently parameterized (HA_I and HA_{II}) that stand for the low-and the high- pK_a sites respectively. In a second step, the data of Cu sorption from the experiment 2 were simulated for roots and cell walls of wheat and tomato with the two HA model by fitting the intrinsic equilibrium constant, $\log K_{Cu,1}$, for the type-1 sites and the heterogeneity parameter, $\Delta LK_{Cu,1}$. The intrinsic equilibrium constant for the type-2 sites, $\log K_{Cu,2}$, was derived from $\log K_{Cu,1}$ ([Tipping et al. 2011](#)) :

$$\log K_{Cu,2} = \log K_{Cu,1} \times \frac{pK_{a_2}}{pK_{a_1}} \quad (1)$$

While Model VII can account for the complexation of the free ionic form and the first hydrolysis product of each metal, we accounted for Cu^{2+} only as a preliminary speciation calculation showed that Cu^{2+} stood for > 99 % of total Cu in solution at $pH \leq 5$.

The best fit was determined by minimizing the root mean square residual (*RMSR*), calculated as follows:

$$RMSR = \sqrt{\frac{\sum_{i=1}^n (x_{i,exp} - x_{i,model})^2}{n}} \quad (2)$$

where $x_{i,exp}$ is an experimental data point, $x_{i,model}$ its corresponding calculated point with the two humic-acid model and n the total number of experimental data points.

This modelling procedure was further implemented on the theoretical potentiometric titrations and Cu sorption isotherms of the outer surface of root cell plasma membranes for wheat and tomato that were calculated by making the difference between roots and cell walls data (Figs. S2 and S3).

Chapitre 6 : Implication of amino acids in high-affinity copper complexation in the apoplast of tomato and wheat roots : spectroscopic and thermodynamic evidences

Table S 1 : Initial (pCu_T) and at equilibrium (pCu_{eq}) copper concentration and pH for each data point of experiment 3.

Wheat roots			Wheat cell walls			Tomato roots			Tomato cell walls		
pCu_T	pCu_{eq}	pH	pCu_T	pCu_{eq}	pH	pCu_T	pCu_{eq}	pH	pCu_T	pCu_{eq}	pH
7.3	8.0	4.9	7.3	8.1	4.5	7.3	8.0	4.5	7.3	8.5	4.4
7.3	8.1	4.9	7.3	8.0	4.6	7.3	8.0	4.6	7.3	8.6	4.4
6.8	7.4	4.9	6.9	7.7	4.5	6.6	7.3	4.6	6.7	8.2	4.5
6.8	7.3	4.9	6.9	7.5	4.3	6.6	7.4	4.6	6.7	8.2	4.4
6.2	6.6	4.9	6.2	7.5	4.6	5.7	6.5	4.5	5.7	7.4	4.4
6.2	6.6	4.8	6.2	7.1	4.6	5.7	6.5	4.6	5.7	7.4	4.5
5.5	5.8	4.8	5.5	5.9	4.5	4.7	5.3	4.6	4.7	6.2	4.4
5.5	5.8	4.9	4.7	5.0	4.6	4.7	5.4	4.5	4.7	6.8	4.3
4.7	4.9	4.8	4.7	4.9	4.5	4.0	4.5	4.4	4.0	4.8	4.2
4.7	4.9	4.7	4.0	4.0	4.5	4.0	4.5	4.4	4.0	4.7	4.2
4.0	4.1	4.8	4.0	4.1	4.5	3.0	3.1	4.3	3.0	3.1	3.9
						3.0	3.2	4.1	3.0	3.1	3.9

Chapitre 6 : Implication of amino acids in high-affinity copper complexation in the apoplast of tomato and wheat roots : spectroscopic and thermodynamic evidences

Table S 2 : Concentration of Cu bound (Cu_{ads}) and proportion for each Cu ligands resulting in the best linear fitting of the Cu K-edge extended X-ray absorption fine structure (EXAFS) spectra for wheat and tomato roots (R) and cell walls (CW), depending the initial copper concentration (pCu_T). The goodness of fit was assessed with the normalized sum-square (NSS) equation:

$$NSS = 100 \times \left(\sum_{i=1}^N [k^2\chi(k_i)_{measured} - k^2\chi(k_i)_{fitted}]^2 \right) / \left(\sum_{i=1}^N [k^2\chi(k_i)_{measured}]^2 \right)$$

where N is the number of points, $k^2\chi(k_i)_{measured}$ is the EXAFS spectrum of the sample in the k -space and $k^2\chi(k_i)_{fitted}$ is the EXAFS fit in the k -space.

		pCu_T	Cu_{ads} (mg.kg ⁻¹ initial dry roots)	Cu(II)- histidine	Cu(II)- malate	Cu(II)- malonate	Cu(II)- galacturonate	Cu(II)- acétate	Cu(II)- formate	sum	NSS (%)
Wheat	CW	6.2	66 ± 16	50			50			100	6.4
	R	6.2	113 ± 4	67			33			100	4.4
	CW	5.6	110 ± 50	61	39					100	4.2
	R	5.6	296 ± 93	73		27				100	4.7
	CW	5.2	158 ± 31	37			63			100	3.5
	R	5.2	485 ± 55	65	18	17				100	1.0
	CW	4.8	340 ± 57	65	18	17				100	1.8
	R	4.8	891 ± 20	42	58					100	2.3
Tomato	CW	6.2	61 ± 1				65		35	100	7.3
	R	5.9	80 ± 24	56					44	100	6.9
	CW	5.6	226 ± 27	42		20			38	100	5.5
	R	5.6	270 ± 40	51					49	100	7.0
	R	5.2	658 ± 88	57				43		100	5.3

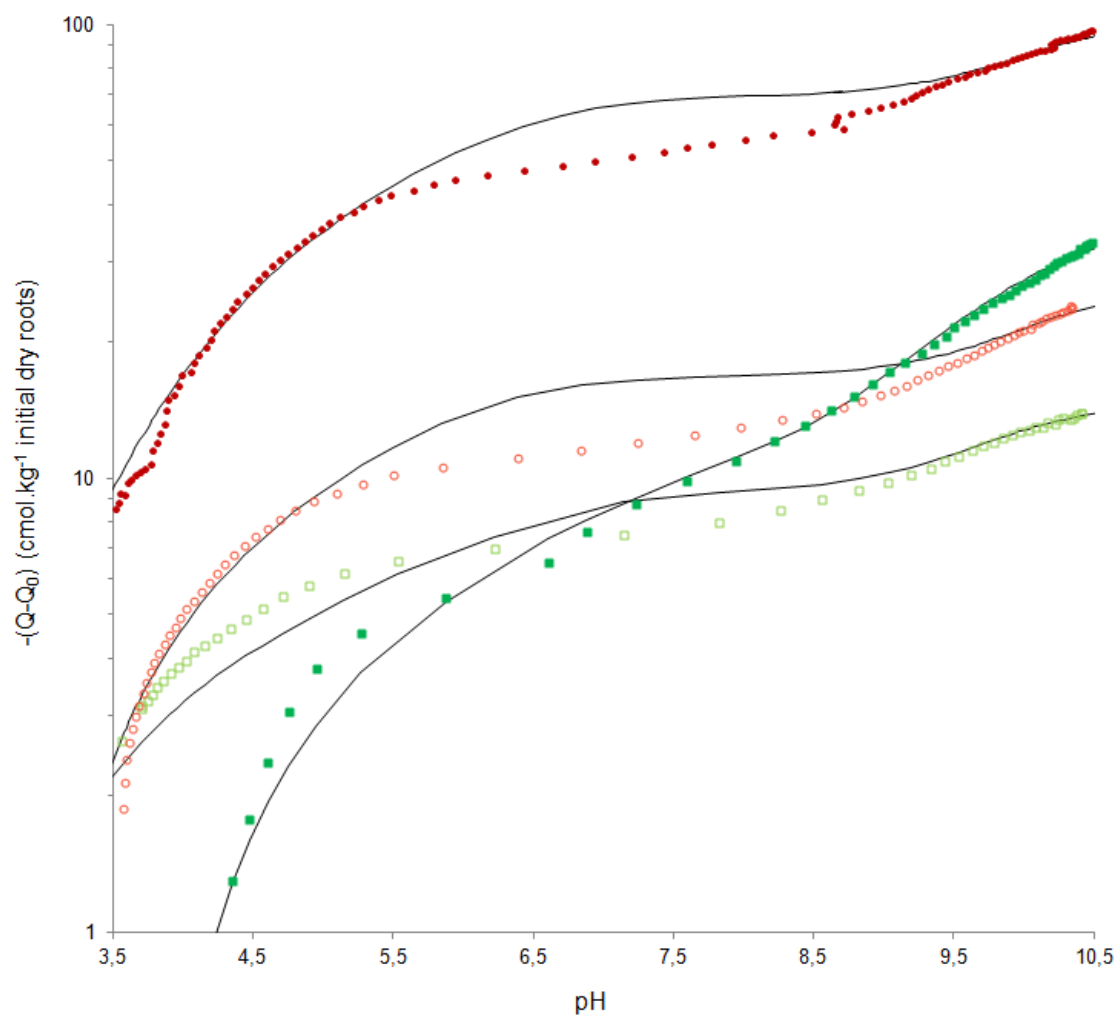


Figure S 1 : Potentiometric titrations for roots (filled symbols) and cell walls (empty symbols) of wheat (squares) and tomato (circles) expressed in charge (Q) corrected by the initial charge (Q_0). Solid lines refer to the fitting curves obtained with model VII using one humic-acid as described in the Material and Methods.

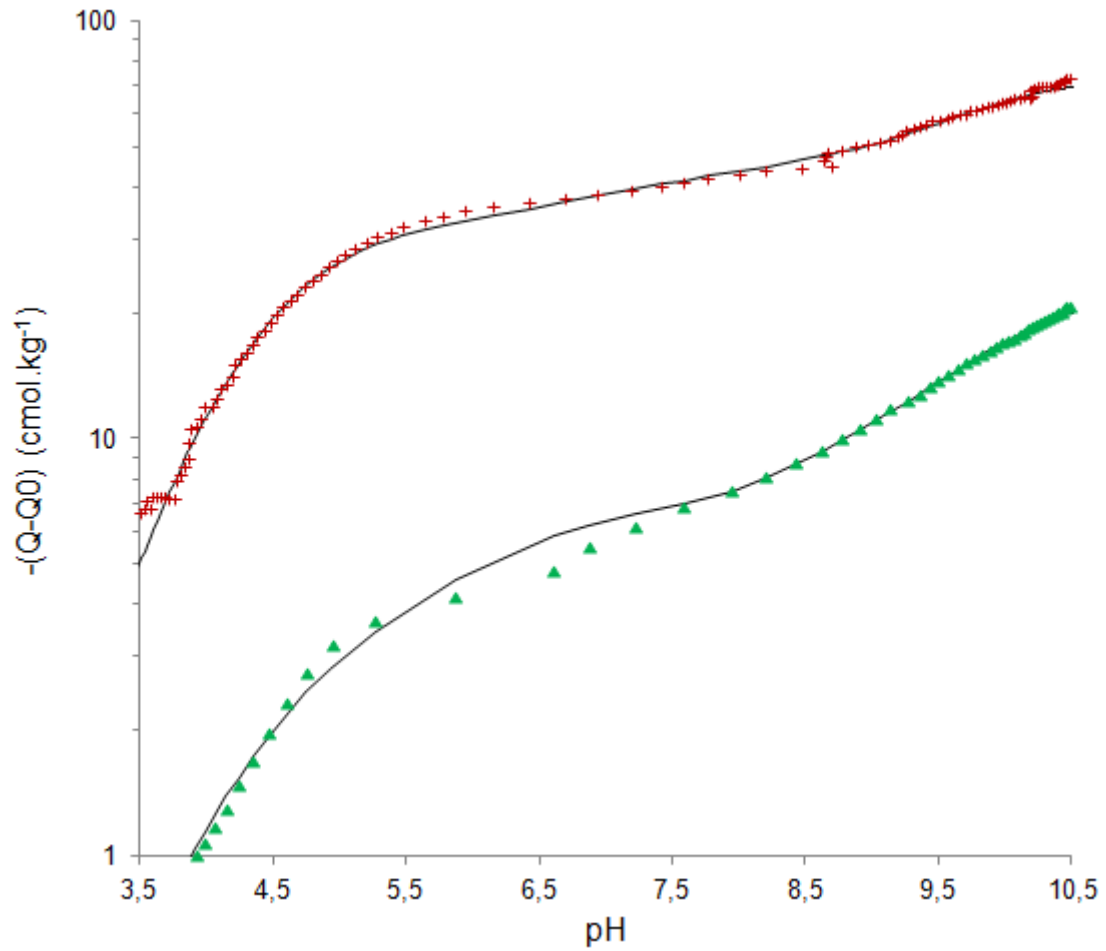


Figure S 2 : Theoretical potentiometric titrations for wheat (triangles) and tomato (cross) plasma membranes expressed in charge (Q) corrected by the initial charge (Q_0). Solid lines refer to the fitting curves obtained with model VII using the two HA model as described in the Material and Methods.

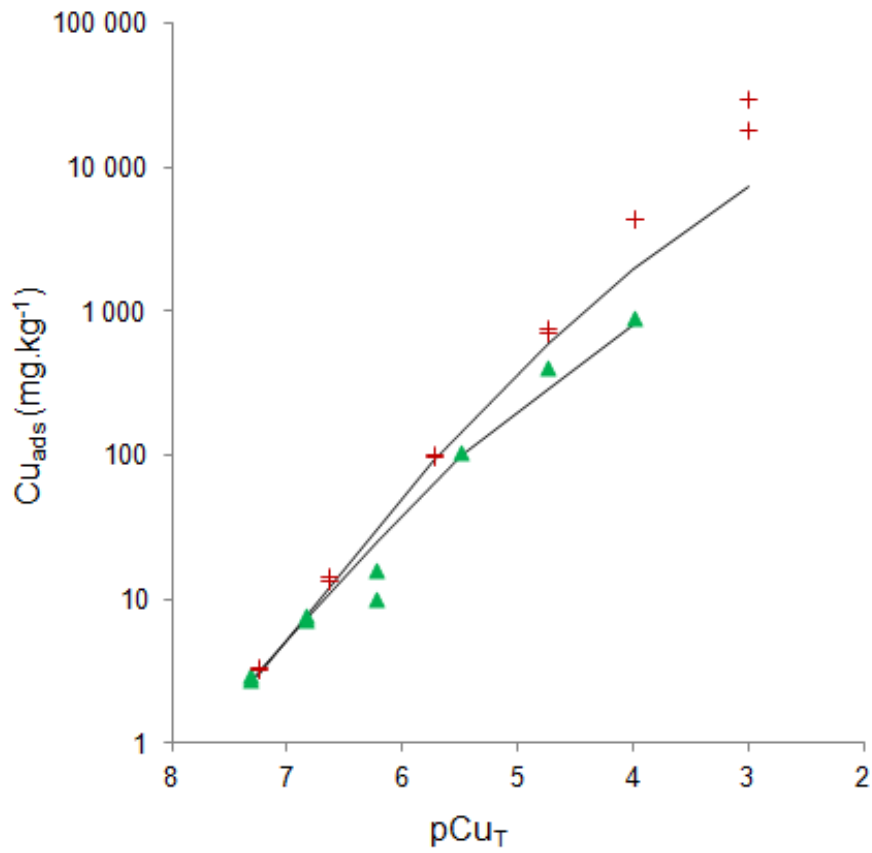


Figure S 3: Theoretical copper binding (Cu_{ads}) by wheat (triangles) and tomato (cross) plasma membranes. Solid lines refer to the fitting curves obtained with the two HA model as described in the Material and Methods.

Chapitre 6 : Implication of amino acids in high-affinity copper complexation in the apoplast of tomato and wheat roots : spectroscopic and thermodynamic evidences

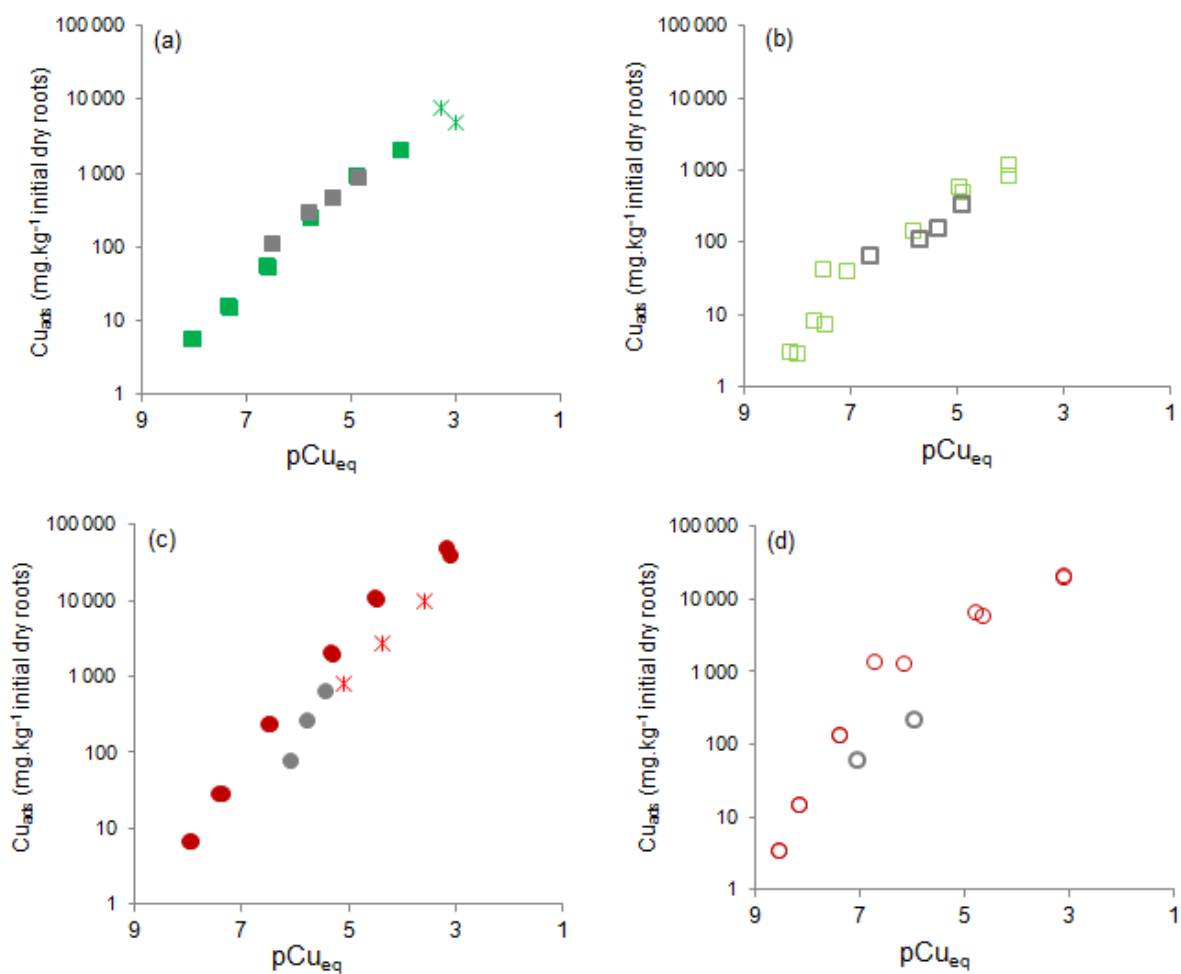


Figure S 4 : Comparison of copper binding (Cu_{ads}) between experiment 1 (grey symbols), experiment 2 (star symbols) and 3 (colorful symbols) in wheat (a) and tomato (c) roots and wheat (b) and tomato (d) cell walls.

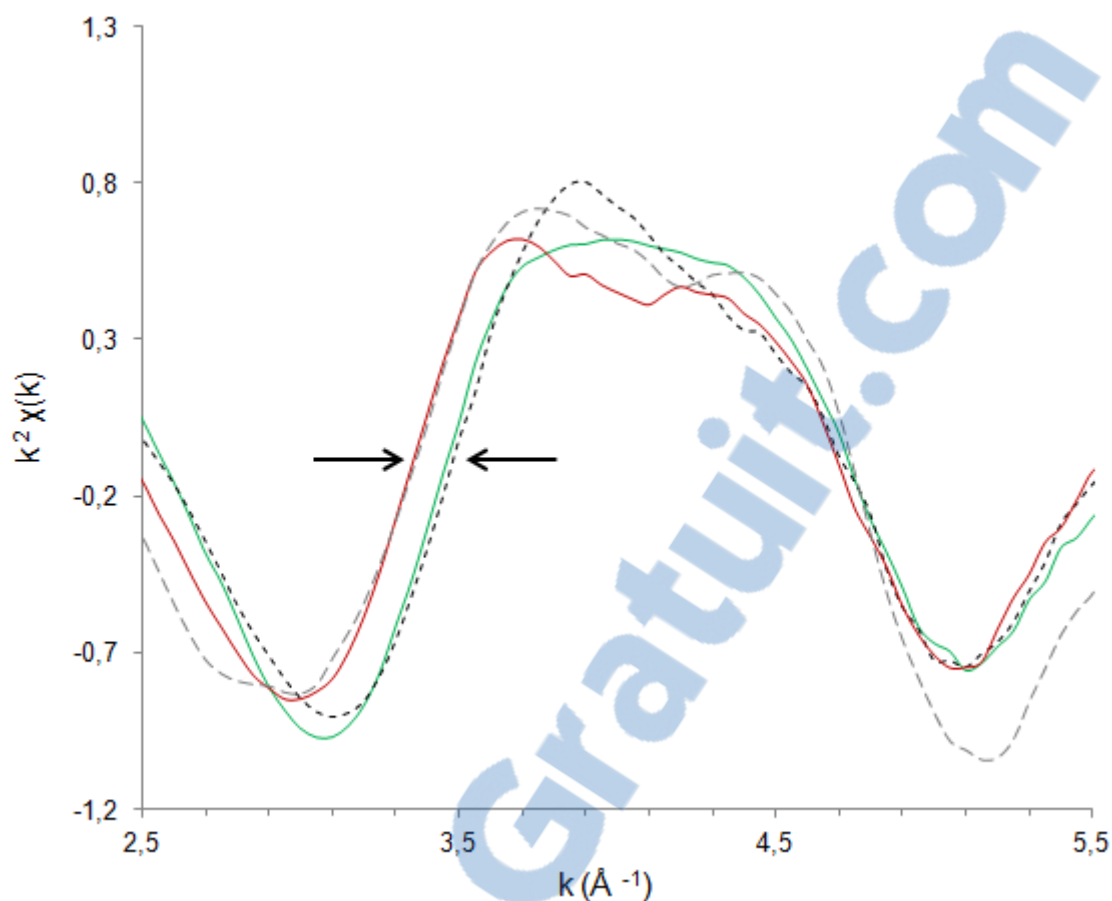


Figure S 5: Visible shift (arrows) in the first oscillation of the Cu K-edge k^2 -weighted extended X-ray absorption fine structure (EXAFS) spectra for wheat (black line) and tomato (grey line) roots, as similarly observed between the two reference compounds, Cu(II)-histidine (dotted black line) and Cu(II)-formate (dotted grey line).

Chapitre 6 : Implication of amino acids in high-affinity copper complexation in the apoplast of tomato and wheat roots : spectroscopic and thermodynamic evidences

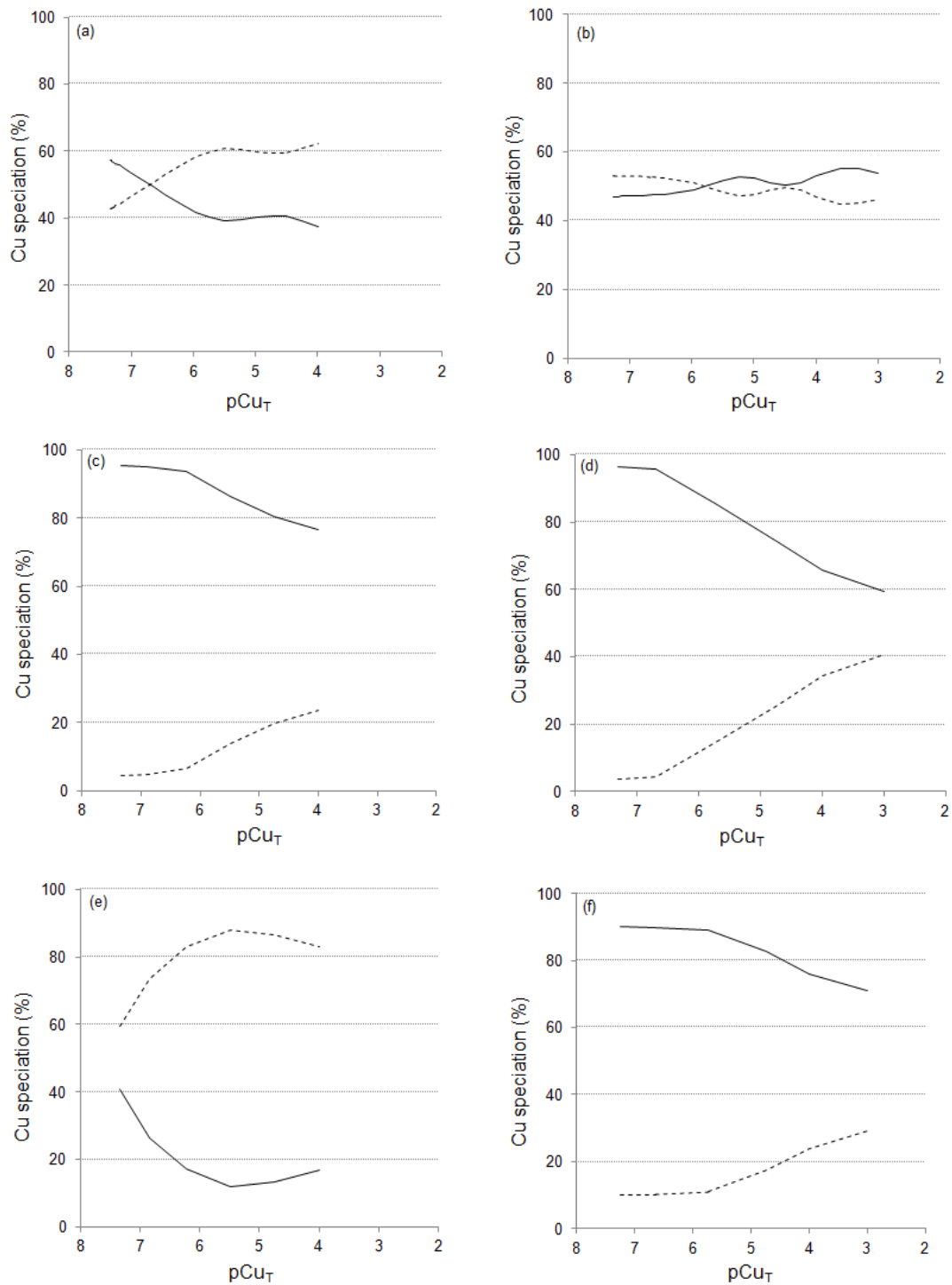


Figure S 6 : Distribution of copper between HA_I (black line) and HA_{II} (dotted line) in wheat roots (a), cell walls (c) and plasma membranes (e) and tomato roots (b), cell walls (d) and plasma membranes (f).

Références bibliographiques

- Belon E, Boisson M, Deportes IZ, Eglin TK, Feix I, Bispo AO, Galsomies L, Leblond S, Guellier CR (2012) An inventory of trace elements inputs to French agricultural soils. *Science of The Total Environment* 439 (0):87-95. doi:http://dx.doi.org/10.1016/j.scitotenv.2012.09.011
- Bravin M, Merrer B, Denaix L, Schneider A, Hinsinger P (2010) Copper uptake kinetics in hydroponically-grown durum wheat (*Triticum turgidum durum* L.) as compared with soil's ability to supply copper. *Plant and Soil* 331 (1-2):91-104. doi:10.1007/s11104-009-0235-3
- Burkhead JL, Gogolin Reynolds KA, Abdel-Ghany SE, Cohu CM, Pilon M (2009) Copper homeostasis. *New Phytologist* 182 (4):799-816. doi:10.1111/j.1469-8137.2009.02846.x
- Cassab GI (1998) PLANT CELL WALL PROTEINS. *Annual Review of Plant Physiology and Plant Molecular Biology* 49 (1):281-309. doi:doi:10.1146/annurev.arplant.49.1.281
- Collin B, Doelsch E, Keller C, Cazevieille P, Tella M, Chaurand P, Panfili F, Hazemann J-L, Meunier J-D (2014) Evidence of sulfur-bound reduced copper in bamboo exposed to high silicon and copper concentrations. *Environmental Pollution* 187 (0):22-30. doi:http://dx.doi.org/10.1016/j.envpol.2013.12.024
- Colzi I, Doumett S, Del Bubba M, Fornaini J, Arnetoli M, Gabbrielli R, Gonnelli C (2011) On the role of the cell wall in the phenomenon of copper tolerance in *Silene paradoxa* L. *Environmental and Experimental Botany* 72 (1):77-83. doi:DOI: 10.1016/j.envexpbot.2010.02.006
- Evertsson B (1969) The crystal structure of bis-l-histidinecopper(II) dinitrate dihydrate. *Acta Crystallographica Section B* 25 (1):30-41. doi:doi:10.1107/S0567740869001737
- Fry SC, Miller JG, Dumville JC (2002) A proposed role for copper ions in cell wall loosening. *Plant and Soil* 247 (1):57-67. doi:10.1023/a:1021140022082
- Grossoehme NE, Akilesh S, Guerinot ML, Wilcox DE (2006) Metal-Binding Thermodynamics of the Histidine-Rich Sequence from the Metal-Transport Protein IRT1 of *Arabidopsis thaliana*. *Inorganic Chemistry* 45 (21):8500-8508. doi:10.1021/ic0606431
- Guigues S, Bravin M, Garnier C, Masion A, Doelsch E (2014) Isolated cell walls exhibit cation binding properties distinct from those of plant roots. *Plant and Soil*:1-13. doi:10.1007/s11104-014-2138-1
- Hazemann J-L, Proux O, Nassif V, Palancher H, Lahera E, Da Silva C, Braillard A, Testemale D, Diot M-A, Alliot I, Del Net W, Manceau A, Gelebart F, Morand M, Dermigny Q, Shukla A (2009) High-resolution spectroscopy on an X-ray absorption beamline. *Journal of Synchrotron Radiation* 16 (2):283-292. doi:doi:10.1107/S0909049508043768
- Karlsson T, Elgh-Dalgren K, Skyllberg U (2008) Modeling Copper(II) Complexation in a Peat Soil Based on Spectroscopic Structural Information All rights reserved. *Soil Sci Soc Am J* 72 (5):1286-1291. doi:10.2136/sssaj2007.0390

Chapitre 6 : Implication of amino acids in high-affinity copper complexation in the apoplast of tomato and wheat roots : spectroscopic and thermodynamic evidences

- Kinraide TB (2004) Possible Influence of Cell Walls upon Ion Concentrations at Plasma Membrane Surfaces. Toward a Comprehensive View of Cell-Surface Electrical Effects upon Ion Uptake, Intoxication, and Amelioration. *Plant Physiol* 136 (3):3804-3813. doi:10.1104/pp.104.043174
- Kinraide TB (2009) Improved scales for metal ion softness and toxicity. *Environmental Toxicology and Chemistry* 28 (3):525-533. doi:10.1897/08-208.1
- Kinraide TB, Pedler JF, Parker DR (2004) Relative effectiveness of calcium and magnesium in the alleviation of rhizotoxicity in wheat induced by copper, zinc, aluminum, sodium, and low pH. *Plant and Soil* 259 (1):201-208. doi:10.1023/b:plso.0000020972.18777.99
- Konno H, Nakato T, Nakashima S, Katoh K (2005) *Lygodium japonicum* fern accumulates copper in the cell wall pectin. *Journal of Experimental Botany* 56 (417):1923-1931. doi:10.1093/jxb/eri187
- Kopittke PM, Blamey FPC, McKenna BA, Wang P, Menzies NW (2011a) Toxicity of metals to roots of cowpea in relation to their binding strength. *Environmental Toxicology and Chemistry* 30 (8):1827-1833. doi:10.1002/etc.557
- Kopittke PM, Kinraide TB, Wang P, Blamey FPC, Reichman SM, Menzies NW (2011b) Alleviation of Cu and Pb Rhizotoxicities in Cowpea (*Vigna unguiculata*) as Related to Ion Activities at Root-Cell Plasma Membrane Surface. *Environmental Science & Technology* 45 (11):4966-4973. doi:10.1021/es1041404
- Kopittke PM, Menzies NW, de Jonge MD, McKenna BA, Donner E, Webb RI, Paterson DJ, Howard DL, Ryan CG, Glover CJ, Scheckel KG, Lombi E (2011c) In Situ Distribution and Speciation of Toxic Copper, Nickel, and Zinc in Hydrated Roots of Cowpea. *Plant Physiology* 156 (2):663-673. doi:10.1104/pp.111.173716
- Kopittke PM, Menzies NW, Wang P, McKenna BA, Wehr JB, Lombi E, Kinraide TB, Blamey FPC (2014) The rhizotoxicity of metal cations is related to their strength of binding to hard ligands. *Environmental Toxicology and Chemistry* 33 (2):268-277. doi:10.1002/etc.2435
- Legros S, Doelsch E, Feder F, Moussard G, Sansoulet J, Gaudet JP, Rigaud S, Doelsch IB, Macary HS, Bottero JY (2013) Fate and behaviour of Cu and Zn from pig slurry spreading in a tropical water-soil-plant system. *Agriculture, Ecosystems & Environment* 164 (0):70-79. doi:http://dx.doi.org/10.1016/j.agee.2012.09.008
- Manceau A, Marcus MA, Tamura N (2002) Quantitative Speciation of Heavy Metals in Soils and Sediments by Synchrotron X-ray Techniques. *Reviews in Mineralogy and Geochemistry* 49 (1):341-428. doi:10.2138/gsrmg.49.1.341
- Manceau A, Simionovici A, Lanson M, Perrin J, Tucoulou R, Bohic S, Fakra SC, Marcus MA, Bedell J-P, Nagy KL (2013) *Thlaspi arvense* binds Cu(II) as a bis-(l-histidinato) complex on root cell walls in an urban ecosystem. *Metallomics* 5 (12):1674-1684. doi:10.1039/c3mt00215b
- Marschner H (1995) *Mineral Nutrition of higher plants*. Academic Press, second edition
- Meychik NR, Yermakov IP (2001) Ion exchange properties of plant root cell walls. *Plant and Soil* 234 (2):181-193. doi:10.1023/a:1017936318435

Chapitre 6 : Implication of amino acids in high-affinity copper complexation in the apoplast of tomato and wheat roots : spectroscopic and thermodynamic evidences

- Moore KL, Schröder M, Wu Z, Martin BGH, Hawes CR, McGrath SP, Hawkesford MJ, Feng Ma J, Zhao F-J, Grovenor CRM (2011) High-Resolution Secondary Ion Mass Spectrometry Reveals the Contrasting Subcellular Distribution of Arsenic and Silicon in Rice Roots. *Plant Physiology* 156 (2):913-924. doi:10.1104/pp.111.173088
- Murakami T, Ise K, Hayakawa M, Kamei S, Takagi S-i (1989) Stabilities of Metal Complexes of Mugineic Acids and Their Specific Affinities for Iron(III). *Chemistry Letters* 18 (12):2137-2140. doi:10.1246/cl.1989.2137
- Proux O, Nassif V, Prat A, Ulrich O, Lahera E, Biquard X, Menthonnex J-J, Hazemann J-L (2006) Feedback system of a liquid-nitrogen-cooled double-crystal monochromator: design and performances. *Journal of Synchrotron Radiation* 13 (1):59-68. doi:doi:10.1107/S0909049505037441
- Ravel B, Newville M (2005) ATHENA, ARTEMIS, HEPHAESTUS : data analysis for X-ray absorption spectroscopy using IFEFFIT. *Journal of Synchrotron Radiation* 12:537 - 541.
- Sarret G, Vangronsveld J, Manceau A, Musso M, D'Haen J, Menthonnex J-J, Hazemann J-L (2001) Accumulation Forms of Zn and Pb in *Phaseolus vulgaris* in the Presence and Absence of EDTA. *Environmental Science & Technology* 35 (13):2854-2859. doi:10.1021/es000219d
- Shomer I, Novacky AJ, Pike SM, Yermiyahu U, Kinraide TB (2003) Electrical Potentials of Plant Cell Walls in Response to the Ionic Environment. *Plant Physiology* 133 (1):411-422. doi:10.1104/pp.103.024539
- Stanila A, Marcu A, Rusu D, Rusu M, David L (2007) Spectroscopic studies of some copper(II) complexes with amino acids. *Journal of Molecular Structure* 834–836 (0):364-368. doi:10.1016/j.molstruc.2006.11.048
- Synytsya A, Urbanová M, Setnička V, Tkadlecová M, Havlíček J, Raich I, Matějka P, Synytsya A, Čopíková J, Volka K (2004) The complexation of metal cations by d-galacturonic acid: a spectroscopic study. *Carbohydrate Research* 339 (14):2391-2405. doi:10.1016/j.carres.2004.07.008
- Taiz L, Zeiger E (2006) *Plant Physiology*, 4th Edition. Sinauer Associates Sunderland, MA
- Tipping E (1998) Humic Ion-Binding Model VI: An Improved Description of the Interactions of Protons and Metal Ions with Humic Substances. *Aquatic Geochemistry* 4 (1):3-47. doi:10.1023/a:1009627214459
- Tipping E, Lofts S, Sonke JE (2011) Humic Ion-Binding Model VII: a revised parameterisation of cation-binding by humic substances. *Environmental chemistry* 8 (3):225-235. doi:http://dx.doi.org/10.1071/EN11016
- Vulkan R, Yermiyahu U, Mingelgrin U, Rytwo G, Kinraide TB (2004) Sorption of Copper and Zinc to the Plasma Membrane of Wheat Root. *Journal of Membrane Biology* 202 (2):97-104. doi:10.1007/s00232-004-0722-7

3^{ÈME} PARTIE

DÉVELOPPEMENT D'UN MODÈLE DE COMPLEXATION RACINAIRE

Chapitre 7 : Développement d'un modèle de prédiction de la complexation du cuivre dans les racines

Comme présenté dans le chapitre 3, divers modèles de prédiction sont actuellement disponibles dans la littérature. Parmi ces modèles, le TBLM (Terrestrial Biotic Ligand Model) est le plus communément employé. Les études utilisant le TBLM présentent des résultats encourageants lorsqu'elles sont individuellement considérées. Cependant, leur comparaison révèle un manque de généralité de certains paramètres et la multiplication des cas particuliers où l'application du TBLM est limitée témoigne d'une nécessité de remettre en cause certaines hypothèses du formalisme mathématique sous-jacent.

L'article *Predicting copper competitive binding on terrestrial plant roots using a two humic-acid model*, constituant ce chapitre 7, présente le modèle de prédiction de la complexation du cuivre dans les racines que j'ai développé. Ce nouveau modèle est fondé sur un formalisme mathématique plus élaboré que celui du modèle TBLM (différentes natures de sites réactifs, prise en compte des effets électrostatiques, etc.). Il remet également en cause la démarche de modélisation classiquement employée puisqu'il n'a pas été paramétré par l'ajustement de données expérimentales de toxicité mais par l'ajustement de données expérimentales concernant le processus effectivement modélisé, c'est à dire la complexation du Cu sur les racines.

Ainsi, nous avons montré que la complexation du cuivre dans les racines des deux plantes modèles ne peut pas être décrite de manière simple. L'inaptitude de WHAM (Windermere Humic Acid Model) paramétré par défaut à représenter cette complexation se traduit comme une impossibilité d'assimiler la réactivité des racines des plantes à celle des substances humiques, comme cela a pu être fait pour les organismes aquatiques. A partir du formalisme mathématique de WHAM, nous avons donc développé un modèle plus élaboré, adapté aux plantes supérieures terrestres : le WHAM-Terrestrial Higher Plants (WHAM-THP). Grâce à une prédiction fine des propriétés acides des racines, ce nouveau modèle a été capable de prédire l'adsorption du cuivre sur les racines de blé et de tomate, et pour des environnements chimiques très variables (force ionique, pH et cations compétiteurs). Malgré les différences de réactivité qui existent entre les racines de blé et de tomate (cf. chapitre 6), nous avons réussi à proposer un jeu de paramètres communs pour les deux espèces. Dans un souci de simplicité d'utilisation, nous avons également proposé, sur la base d'une

comparaison entre des mesures de capacité d'échange cationique racinaire (CECR) et des titrages acido-basiques, une relation qui permettra au futur utilisateur d'estimer assez précisément la densité totale de sites racinaires à partir d'une simple mesure de CECR pouvant être réalisée en routine.

Predicting copper competitive binding on terrestrial plant roots using a two humic-acid model

Stéphanie Guigues ^{1,2}, Matthieu N. Bravin ³, Cédric Garnier ⁴ and Emmanuel Doelsch ¹

¹ CIRAD, UPR Recyclage et risque, F-34398 Montpellier, France

² ADEME, 20 avenue du Grésillé, BP-90406, Angers cedex 01, France

³ CIRAD, UPR Recyclage et risque, F-97408 Saint-Denis, Réunion, France

⁴ Université de Toulon, PROTEE, EA 3819, 83957 La Garde, France

Abstract

The Terrestrial Biotic Ligand Model (TBLM) is widely used to predict the toxic effect of trace metals for various soil organisms including higher plants. However, its formalism remains based on strong assumptions that may partly explain inconsistent results observed in the fitted binding constants of trace metals to plant roots. To improve this, we aimed at adapting the parameterization of the humic acid defined in the Windermere Humic Aqueous Model (WHAM) for terrestrial higher plants (THP). Contrary to WHAM parameterized by default, WHAM-THP was able with a unique set of parameters to predict adequately the acidic properties and the binding of copper on the root surfaces of wheat (*Triticum aestivum* L.) and tomato (*Solanum lycopersicum* L.), while accounting for the electrostatic effect and the competition with proton, calcium and zinc.

Keywords: WHAM; complexation; trace element; modeling; heavy metal

I. Introduction

Soil contamination still remains a major environmental concern. Among contaminants, the particular case of trace metals is worrying as e.g. they exhibit the highest occurrence in European soils (European Environmental Agency 2007). Atmospheric deposition related to industrial activities, urban traffic, mining activities and agricultural practices (organic waste spreading, use of pesticides and fungicides) contribute to the enrichment of trace metals in soils (Hooda 2010). Hence, a major challenge for the environmental risk assessment of trace metals in soil is the development of predictive ecotoxicological tools able to estimate the toxic effect of trace metals on soil organisms. Toxicity to soil organisms is usually poorly correlated to the total concentration of trace metals in soil but rather depends on the speciation of trace metals, especially in the soil solution where trace metals are taken up (Harmsen 2007). The toxic effect is further determined by the interaction of trace metals with the outer surface of soil organisms. This interaction is strongly influenced by the chemical parameters of the soil solution such as pH, ionic strength and the concentrations of other competitive metal cations (Brown and Markich 2000).

Among existing models, the biotic ligand model (BLM) is increasingly used in predictive ecotoxicology. Based on the determination of trace metals speciation in solution, the BLM is designed to estimate trace metal toxicity as a function of site-specific competitions between cations (e.g. H^+ , Ca^{2+} and Mg^{2+}) and trace metals for binding to the biotic ligand borne by the outer surface of an organism (Di Toro et al. 2001). Initially dedicated to the prediction of trace element toxicity to aquatic organisms (Paquin et al. 2002), a terrestrial BLM (TBLM) was developed in the past decades for soil organisms such as plants, invertebrates and microorganisms (Thakali et al. 2006; Ardestani et al. 2014). Among these soil organisms, the TBLM seems to be an approach particularly promising for plants for which the mechanistic basis is particularly consistent with the major mechanism involved in the occurrence of trace metal toxicity to plant roots, i.e. rhizotoxicity. Indeed, Kopittke et al. (2014) recently contended “*that the primary mechanism of rhizotoxicity of many metal cations is nonspecific and that the magnitude of toxic effects is positively related to the strength with which they bind to hard ligands, especially carboxylate ligands of the cell-wall pectic matrix*”. Consequently, the ability of the TBLM formalism to describe accurately the binding of trace metals on plant root surface is a crucial issue.

However, the mathematical formalism of the TBLM is based on several strong assumptions that question its relevancy for application in predictive ecotoxicological risk assessment (Slaveykova and Wilkinson 2005; Erickson 2013). The TBLM notably assumes (i) the homogeneity of the nature, the distribution and the affinity of the binding sites, (ii) that

electrostatic effects do not significantly alter trace metal binding and (iii) that trace metals bind to the biotic ligand only with a 1:1, i.e. monodentate, coordination stoichiometry. The validity of these three assumptions are clearly questionable since they were all rejected and reconsidered in the current modeling approaches of trace metal binding on humic substances, i.e. another kind of complex and natural organic matters (Milne et al. 2003; Tipping et al. 2011). An additional concern in the implementation of the TBLM is the widespread practice of fitting binding constants from the measurements of toxic endpoints rather than actual binding. It is therefore not surprising to find binding constants varying over several orders of magnitude, even when restricting the comparison to the same plant species, exposure condition and toxic endpoint (Ardestani et al. 2014). For example, the binding constant of Cu to the biotic ligand determined for the root elongation of *Hordeum vulgare* in hydroponics ranged between $\log K \leq 3.9$ (Antunes et al. 2007) and $\log K = 6.3$ (Wang et al. 2012b). The considerable variability in the parameterization and the apparent weaknesses in the underlying hypothesis of the mathematical formalism concomitantly suggest the necessity to revisit and likely to further improve the implementation of the TBLM (Erickson 2013).

Accordingly, geochemical models initially designed to predict trace metal binding on humic substances were applied in predictive ecotoxicology (Plette et al. 1996; Tipping et al. 2008). The Windermere Humic Aqueous Model (WHAM) more particularly was used successfully in the past few years to predict the binding and toxicity of trace metals to a range of aquatic organisms including bacteria, algae, invertebrates and lower and higher plants (Tipping et al. 2008; Antunes et al. 2012; Iwasaki et al. 2013). We recently characterized the Cu binding properties of the root surface of two higher plants, namely wheat (*Triticum aestivum* L.) and tomato (*Solanum lycopersicum* L.), by implementing a two humic-acid (HA) model based on WHAM (Chapter 6). Consistently with spectroscopic investigations, this two-HA model enabled us to demonstrate that Cu binding on plant roots was driven by two types of sites occurring in ca. equivalent amount, i.e. low- and high-affinity sites corresponding to carboxylic and amine functional groups respectively. Foreshadowing potential improvement of the current TBLM formalism, the application of WHAM for terrestrial higher plants, hereafter called WHAM-THP, should deserve further attention.

Consequently, the present study aimed at developing a generic WHAM-THP for Cu by parameterizing its complexation on the root surface of wheat and tomato under varying chemical conditions (i.e. ionic strength, pH and competitive cations). Wheat and tomato were chosen as the two model plant species to be respectively representative of monocots and dicots which are known to differ substantially in the composition and the cation binding properties of their root surfaces (Sattelmacher 2001; Vogel 2008).

II. Experimental approach

II.1. Plant root material

Wheat (cv. Premio) and tomato (cv. Moneymaker) were grown in hydroponics for 21 days, i.e. 7 days of germination in darkness and 14 days of growth (see [Guigues et al. \(2014\)](#) for additional information). The growth chamber parameters were set at (day/night): 25/20°C, 75/70% relative humidity and 16/8h with a photon flux density of 450 $\mu\text{mol photons m}^{-2} \text{s}^{-1}$ during the day. At harvest, roots were separated from shoots, then blotted with paper towels before being subdivided into homogenous subsamples and finally stored frozen.

After thawing, roots were rinsed with 1 mM $\text{Ca}(\text{NO}_3)_2$ to eliminate vacuolar compounds released during thawing. Therefore, the root material (hereafter are referred to as roots) obtained was assumed to do not exhibit any biological activity, allowing us to overcome cellular absorption phenomena and to study only binding reactions. Furthermore, these roots did contain both cell walls and plasma membranes, i.e. two plant compartments that give to roots their binding properties ([Guigues et al. 2014](#); [Chapter 6](#)). Before any further experiment, roots were stirred in HNO_3 solution at pH 3 for 1 h to remove highly bound or precipitated cations (e.g. Fe and Al), then rinsed twice with ultrapure water (18.2 M Ω) for 30 min. Roots were then oven-dried at 50°C until a steady mass was achieved.

II.2. Potentiometric titration

Potentiometric titration experiments were extensively described by [Guigues et al. \(2014\)](#). Briefly, ca. 0.2 g (dry mass basis) of roots was placed in 100 ml of 10 mM KNO_3 . During titrations, pH was first lowered to 2.5 with 0.2 M HNO_3 additions and was then increased step-by-step to 11.5 with the incremental additions of 0.2 M KOH of either 100 μl in the pH ranges 2.5-3.5 and 10.5-11.5 or 20 μl in the pH range 3.5-10.5.

II.3. Copper sorption experiments

A dry mass of 10 (± 0.5) mg of wheat and tomato roots was shaken end-over-end for 24 h at 25°C in 25 ml of solution of varying chemical composition (Tables S3 and S4). In the experiment 1, the solution contained an initial, total Cu concentration varying from pCu_T 7.3 to 3.0 ($\text{pCu}_T = -\log_{10}[\text{Cu}]_T$) with an ionic strength and a pH fixed at 0.03 M with NaNO_3 and 4.7 (± 0.2), respectively.

In the experiment 2, the solution contained an ionic strength fixed at 0.6 mM or 0.3 M with NaNO_3 , an initial, total Cu concentration fixed at pCu_T 4.2, 5.2 or 6.2 and a pH fixed at 4.7 (± 0.2).

In the experiment 3, the solution contained a pH fixed at 4.1 (± 0.1) or 6.3 (± 0.1), an initial, total Cu concentration fixed at pCu_T 4.2, 5.2 or 6.2 and an ionic strength fixed at 0.03 M with NaNO_3 .

In the experiment 4, the solution contained an initial, total Ca concentration varying from pCa_T 2.0 to 4.0 but with an initial, total Cu concentration, an ionic strength and a pH fixed at pCu_T 6.3, 0.03 M with NaNO_3 and 5.1 (± 0.4), respectively.

In the experiment 5, the solution contained an initial, total Zn concentration varying from pZn_T 4.5 to 7.2 but with an initial, total Cu concentration, an ionic strength and a pH fixed at pCu_T 6.3, 0.03 M with NaNO_3 and 4.7 (± 0.1), respectively.

The pH was buffered with 1 mM 2-[N-morpholino] ethane sulfonic acid and adjusted by NaOH or HNO_3 . Sorption experiments were performed in duplicate and blanks were included in the measurements. Copper concentration in initial and final (i.e. at equilibrium) solution was determined by inductively coupled plasma mass spectrometry (ICP-MS, NexION 300X Perkin Elmer). Blanks and certified reference material (EnviroMAT Drinking water EP-L-3 and groundwater ES-H-2) were included in the analyses. The measurement uncertainty was lower than 10%. The amount of Cu bound to wheat and tomato roots was calculated by subtracting the final to the initial Cu concentration measured in each batch.

III. Modeling approach

The modeling approach was based on the formalism of the Humic Ion-Binding Model included in WHAM VII. This formalism was extensively described by [Tipping \(1998\)](#) and [Tipping et al. \(2011\)](#). To summarize, WHAM is able to simulate the sorption properties of humic substances depicted as a regular array of binding sites of type 1 and 2. The density (L_{Hi} , $\text{cmol}_c.\text{kg}^{-1}$) of type-1 sites is arbitrarily fixed as twice higher than the density of the type-2 sites (i.e. $L_{H1} = 2 \times L_{H2}$). Protons and metal ions compete for sorption on these sites with metal ions being able to form mono-, bi- and tri-dentate complexes. Proton sorption to humic substances were characterized by one intrinsic proton dissociation constant for each type of sites, i.e. pKa_1 and pKa_2 , and the corresponding distribution terms, ΔpKa_1 and ΔpKa_2 . Metal sorption to humic substances was characterized by one intrinsic equilibrium constant for each type of sites, i.e. $K_{M,1}$ and $K_{M,2}$, and a heterogeneity parameter, $\Delta\text{LK}2_M$.

The parameter $K_{M,2}$ was calculated as follows (Tipping et al. 2011) :

$$\text{Log}K_{M,2} = \text{Log}K_{M,1} \times \frac{pKa_2}{pKa_1} \quad (1)$$

Electrostatic effects are accounted for in WHAM by approximating the diffuse layer/bulk solution system with a Donnan model. While WHAM can account for the complexation of the free ionic form and the first hydrolysis product of each metal, we only accounted for Cu^{2+} as a preliminary speciation calculation showed that Cu^{2+} stood for > 95 % of total Cu in solution with $\text{pH} \leq 6.3$. The partial pressure of CO_2 was assumed to be that of the ambient atmosphere ($10^{-3.5}$ atm) and the temperature was fixed at 25 °C for calculations.

Toward the development of a predictive tool, our modeling approach aimed at fitting the experimental data as accurately as possible with the most squeezed and generic set of parameters for the two plant species tested. Accordingly, WHAM was firstly implemented by representing root binding properties with a single HA exhibiting the default parameterization given in WHAM except for the total site density of wheat and tomato roots that was derived from a previous work (Guigues et al. 2014). WHAM was also configured with two HA (configuration hereafter referred as to WHAM-2HA) to agree with the actual distribution of low- and high-pKa sites on wheat and tomato roots. In WHAM-2HA (table S5), the first HA represented the low-pKa sites while the second HA represented the high-pKa sites, each HA respectively exhibiting the same parameterization as the type-1 and type-2 sites defined in WHAM. Some unsatisfactory fits (see Results and discussion section for rationale) led however to develop a more complex model.

WHAM-THP was thus implemented by representing root binding properties with two concomitant HA (HA_I and HA_{II}) independently parameterized and that stand for the low-and the high-pKa sites, respectively. The total density of HA_I and HA_{II} sites was derived from a previous work (Guigues et al. 2014). The implementation of WHAM-THP started with the parameterization of pKa_1 , pKa_2 , ΔpKa_1 and ΔpKa_2 for HA_I and HA_{II} by fitting experimental titration curves of wheat and tomato roots. Then, $K_{Cu,1}$, $K_{Cu,2}$ and $\Delta LK2_{Cu}$ was parameterized by fitting Cu sorption data from experiment 1. The ability of WHAM-THP to predict ionic strength and pH effects on Cu binding was tested by fitting Cu sorption data from experiments 2 and 3. Finally, the ability of WHAM-THP to account for the competitive effect of Ca and Zn was assessed by parameterizing $K_{Ca,1}$, $K_{Ca,2}$, $\Delta LK2_{Ca}$, $K_{Zn,1}$, $K_{Zn,2}$ and $\Delta LK2_{Zn}$ using Cu sorption data from experiments 4 and 5.

WHAM, WHAM-2HA and WHAM-THP best fits were determined by minimizing the root mean square residual.

IV. Results and discussion

Initially developed to simulate trace metal binding on humic substances, WHAM was applied in the past few years in predictive ecotoxicology by suggesting humic acid as a relevant surrogate of the biotic ligand. On this principle, the present study was focused on the development of WHAM for terrestrial higher plants (i.e. WHAM-THP) to predict Cu binding on root surfaces under varying chemical conditions.

IV.1. Ability of WHAM-THP to predict root acidic properties

WHAM failed to fit the experimental data for both wheat and tomato. WHAM overestimated the binding site density depicted by experimental data over the major part of the pH range investigated (up to 9 $\text{cmol}_c.\text{kg}^{-1}$ for wheat and 14 $\text{cmol}_c.\text{kg}^{-1}$ for tomato) with a shape that differed substantially from that of experimental data (Fig. 27; table 5). This inadequacy of WHAM partly came from the imposed relationship between the density of type-1 and type-2 sites, i.e. $L_{H1} = 2 \times L_{H2}$. Indeed, the distribution of low- and high-pKa sites on wheat and tomato roots did not meet this requirement as low to high-pKa sites ratio was equal to 0.4 and 0.9, respectively (Guigues et al. 2014). Similarly, other biotic ligands from other plant roots and bacteria cell walls exhibited low to high-pKa sites ratio different from 2, ranging from 1.4 to 3 (Plette et al. 1995; Ginn et al. 2008; Wu and Hendershot 2009; Mishra et al. 2010). Such results mean that the nature of binding sites borne by biotic ligands differs substantially from the nature of binding sites borne by humic substances.

WHAM-2HA only improved satisfactorily the fit of potentiometric data for tomato roots at $\text{pH} \leq 6$ while potentiometric data for tomato roots at $\text{pH} > 6$ and wheat roots remained very poorly fitted (Fig. 27). Hence, the parameters describing proton dissociation (i.e. pKa and ΔpKa) of HA in WHAM were also inadequate for wheat and tomato roots. This led us to conclude that the acidic properties of plant roots are much different from those of HA and thus require to be specifically parameterized for terrestrial higher plants.

Accordingly, WHAM-THP was specifically parameterized and thus allowed to precisely represent potentiometric titration of wheat and tomato roots with a unique set of parameters for both plant species (Fig. 27, table 5). Beyond its specific parameterization, the better fits obtained with WHAM-THP also partly came from the larger number of parameters fitted, which resulted in a more flexible model. Indeed, while eight different pKa were defined in WHAM and WHAM-2HA, thirteen different pKa were defined in WHAM-THP (tables 5 and S5).

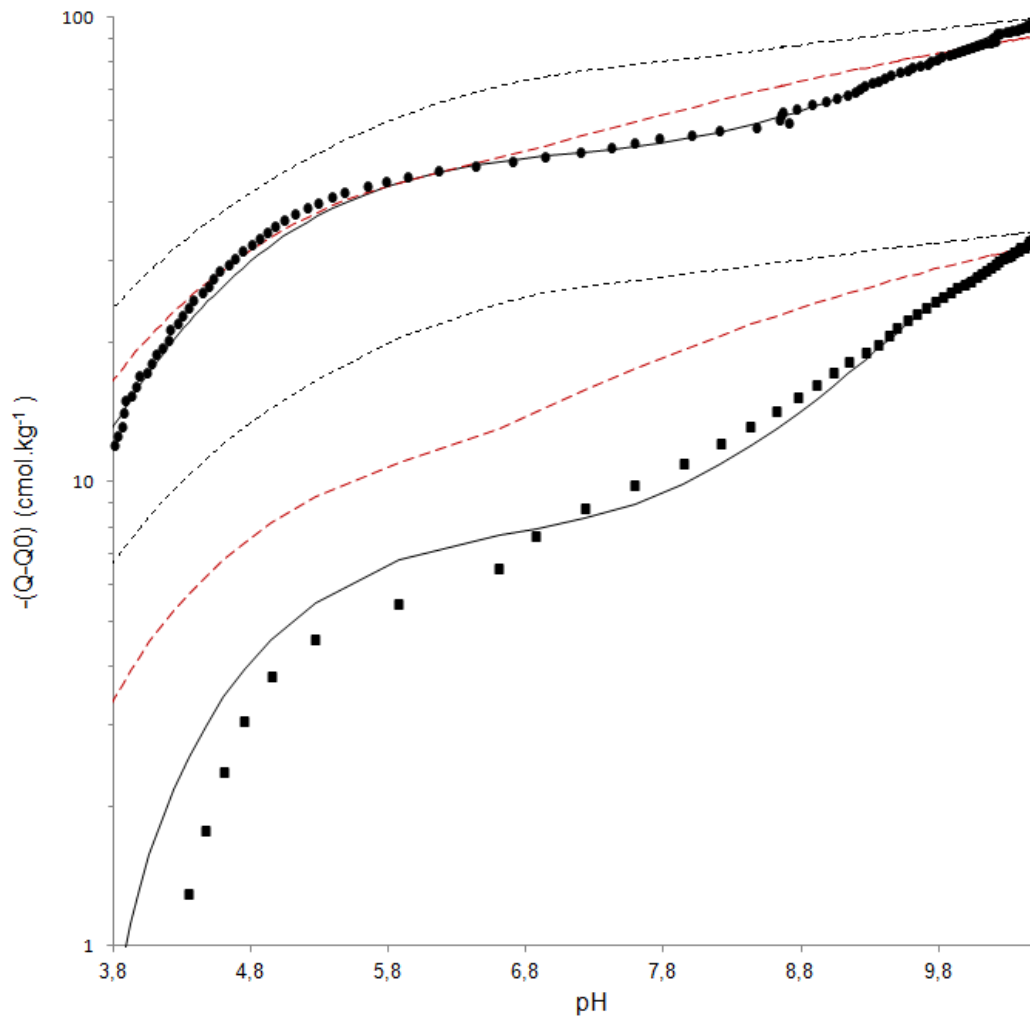


Figure 27 : Potentiometric titrations of wheat (squares) and tomato (circles) expressed in charge (Q) corrected by the initial charge (Q0). Black dashed and solid lines refer to simulations obtained with WHAM parameterized by default or specifically for terrestrial higher plants (WHAM-THP), respectively (see section III). Red dashed lines refer to simulations obtained with WHAM parameterized with two humic acids defined by default.

Table 5 : Total site densities (L_{Hi} , $\text{cmol}_c.\text{kg}^{-1}$), proton dissociation constants (pKa_i) and distribution terms (ΔpKa_i) of wheat and tomato roots parameterized in WHAM and WHAM-THP (see section III for further rationale).

		HA_I						HA_{II}						Total site density	
		Type 1			Type 2			Type 1			Type 2				
		L_{H1}	pKa_1	ΔpKa_1	L_{H2}	pKa_2	ΔpKa_2	L_{H1}	pKa_1	ΔpKa_1	L_{H2}	pKa_2	ΔpKa_2		
WHAM	Wheat	24.4			12.2										36.6
	Tomato	64.9	4.1	2.1	32.5	8.8	3.6	–	–	–	–	–	–	–	97.4
WHAM-THP	Wheat	6.3			3.2			18.0			9.0				36.5
	Tomato	31.3	4.2	1.5	15.7	5.2	2.0	33.5	9.8	0	16.8	8.8	1.5		97.3

IV.2. Ability of WHAM-THP to predict copper binding on roots

IV.2.a. Root copper binding affinity

Although Cu sorption on wheat and tomato roots was contrasted, WHAM fitted Cu sorption data for both species (Fig. 28) much better than it fitted potentiometric data (Fig. 27). However, WHAM overestimated Cu bound on wheat roots by 67% on average, with an increase of the overestimation as Cu concentration in solution increases (Fig. 28a). WHAM-THP fitted very precisely (deviation $< \pm 10\%$) Cu binding on wheat roots. Both WHAM and WHAM-THP fitted adequately Cu binding on tomato roots (i.e. with an average deviation of 20% and $< 10\%$, respectively) for $pCu_T > 4.5$ (i.e. $pCu_{eq} > 5$; table S4), a concentration range relevant for Cu rhizotoxicity as it encompasses the usual concentration (equivalent to $pCu_{eq} > 5$) that was shown to cause a 50% reduction in the elongation rate of cowpea roots (Kopittke et al. 2010). However, a two-fold gap with experimental data was observed for WHAM and WHAM-THP at $pCu_T < 4.5$ (Fig. 28b; Chapter 6). Similar trends were also observed for WHAM-2HA (Fig. 28). However, the fit obtained with WHAM-2HA at elevated concentrations of Cu in solution was better than that obtained with WHAM (but not than that obtained with WHAM-THP) for wheat roots. For tomato roots, the fit obtained with WHAM-2HA was worse than that obtained with WHAM and WHAM-THP with a higher underestimation of Cu binding.

The $\log K_{Cu,1}$ of HA_I sites (i.e. 2.4) fixed by default in WHAM was intermediate between the $\log K_{Cu,1}$ (i.e. 2.2) and the $\log K_{Cu,2}$ (i.e. 2.7) of HA_I sites specifically defined for WHAM-THP (table 6). However, the $\log K_{Cu,2}$ (i.e. 5.1) of HA_I sites fixed by default in WHAM was much lower than the $\log K_{Cu,1}$ (i.e. 6.0) and the $\log K_{Cu,2}$ (i.e. 6.7) of HA_{II} sites specifically defined for WHAM-THP (table 6). This difference between WHAM and WHAM-THP can be attributed to the nature of the binding sites exhibiting a high affinity for Cu which are typically phenolic groups on HA (Tipping 1998), while they were shown to be amine groups on wheat and tomato roots (chapter 6). Even if both phenolic and amines groups have a higher Cu affinity than carboxylic groups, amine groups presented a particularly high Cu affinity (Fry et al. 2002), even higher than that of phenolic groups. The heterogeneity parameter, $\Delta LK2_{Cu,I}$ (i.e. 2.3) defined by default in WHAM is however much higher than the two $\Delta LK2_{Cu}$ specifically defined in WHAM-THP as they were both fixed at zero (table 6). This heterogeneity parameter is used in WHAM to account for the occurrence of binding sites typically corresponding to sulfhydryl and amine groups borne by HA that occurred at low concentration but that exhibited a high affinity towards Cu (Tipping 1998). Whereas amine groups is a major type of binding sites on wheat and tomato roots accounted for in WHAM-THP by the parameterization of the HA_{II} , sulfhydryl groups would not participate significantly

to Cu binding on plant roots as concomitantly supported by spectroscopic investigations (Chapter 6).

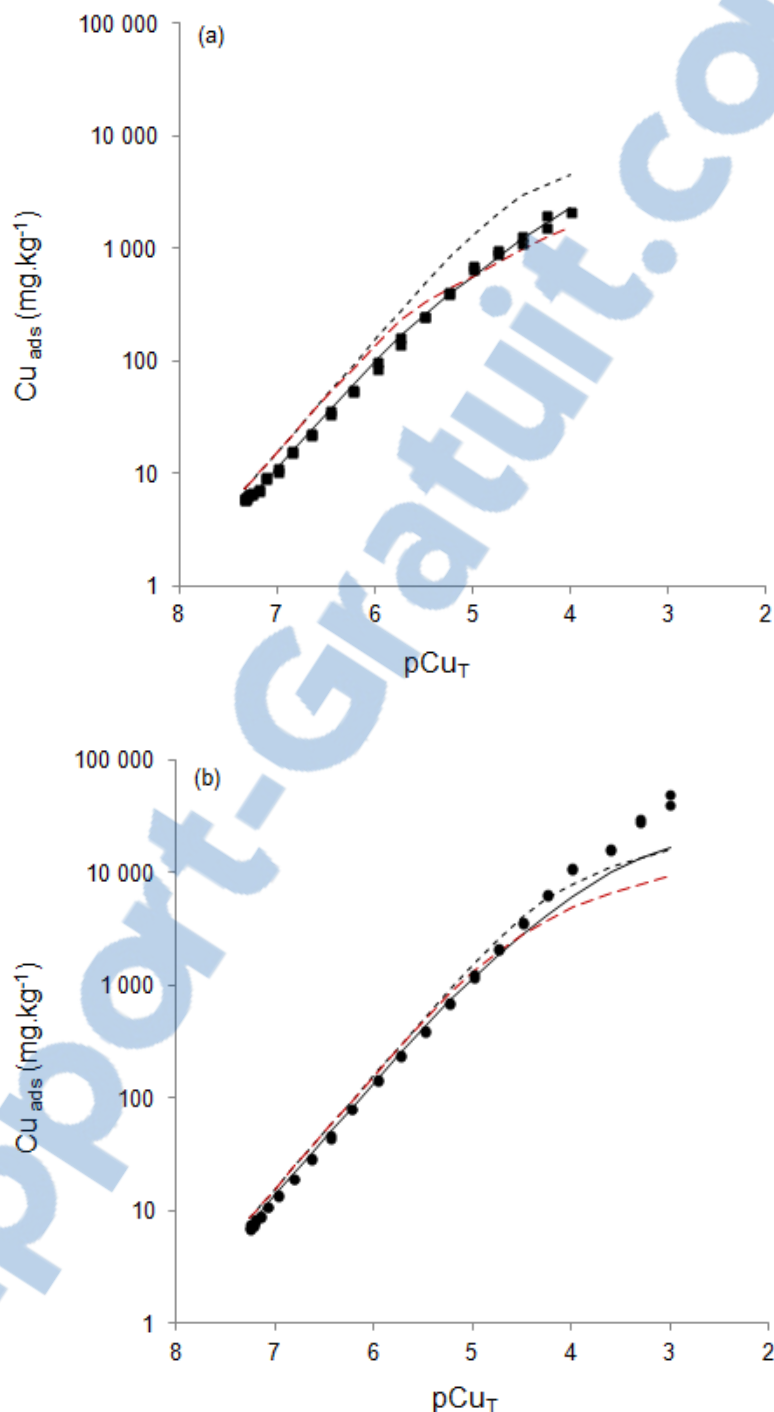


Figure 28 : Copper binding on wheat (squares, a) and tomato (circles, b) roots at pH 4.7 (\pm 0.2) and ionic strength of 0.03 M. Black dashed and solid lines refer to simulations obtained with WHAM parameterized by default or specifically for terrestrial higher plants (WHAM-THP), respectively (see section III). Red dashed lines refer to simulations obtained with WHAM parameterized with two humic acids defined by default.

Tableau 6 : Intrinsic equilibrium constants ($K_{M,i}$) and heterogeneity parameters ($\Delta LK2_{M,i}$) of copper (Cu), calcium (Ca) and zinc (Zn) binding on wheat and tomato roots parameterized in WHAM and WHAM-THP (see section III for further rationale).

		HA _I			HA _{II}		
		Type 1	Type 2		Type 1	Type 2	
		Log $K_{M,1}$	Log $K_{M,2}$	$\Delta LK2_{M,I}$	Log $K_{M,1}$	Log $K_{M,2}$	$\Delta LK2_{M,II}$
Cu	WHAM	2.4	5.1	2.3	–	–	–
	WHAM-THP	2.2	2.7	0	6.7	6.0	0
Ca	WHAM	1.3	2.3	0	–	–	–
	WHAM-THP	1.2	1.5	0	4.5	4.0	0
Zn	WHAM	1.9	4.1	1.3	–	–	–
	WHAM-THP	2.0	2.5	0	6.7	6.0	0

IV.2.b. Influence of ionic strength

An increase of the ionic strength in solution is assumed to lead to a decrease of Cu binding on roots. Indeed, the higher the ionic strength is, the higher the counter-ions are abundant in the diffuse layer. The accumulation of counter-ions thus weakens the ability of binding sites to attract and bind Cu (Wang et al. 2008; Vidali et al. 2011). In the case of wheat and tomato roots, an increase in ionic strength led to a decrease of 43% in Cu binding on average (Fig. 29).

WHAM and WHAM-2HA exhibited very similar predictions (Fig. 29). At the low ionic strength (i.e. 0.6 mM), WHAM and WHAM-THP did the same predictions for both plant species (Fig. 29), even if WHAM-THP prediction for wheat roots was a little more precise than that of WHAM (Fig. 29a). However, at the high ionic strength (i.e. 0.3 M), WHAM overestimated Cu binding on wheat and tomato roots, except at the highest Cu concentration (i.e. pCu_T 4.2). In contrast, WHAM-THP was able to well describe Cu binding on the roots of both plant species. The higher predictive power of WHAM-THP over WHAM under varying ionic strength is directly linked to the specific set of parameters describing proton and Cu binding in WHAM-THP since the default value of the electrostatic parameter P fixed in WHAM was conserved in WHAM-THP. From a modeling point of view, this suggests that the parameterization of the electrostatic effect in WHAM is generic enough to describe electrostatic interactions on plant roots and can thus be used in WHAM-THP without specific parameterization. From a mechanistic point of view, these results show that Cu binding on roots is more sensitive to the modification of ionic strength than Cu binding on HA under the chemical conditions tested.

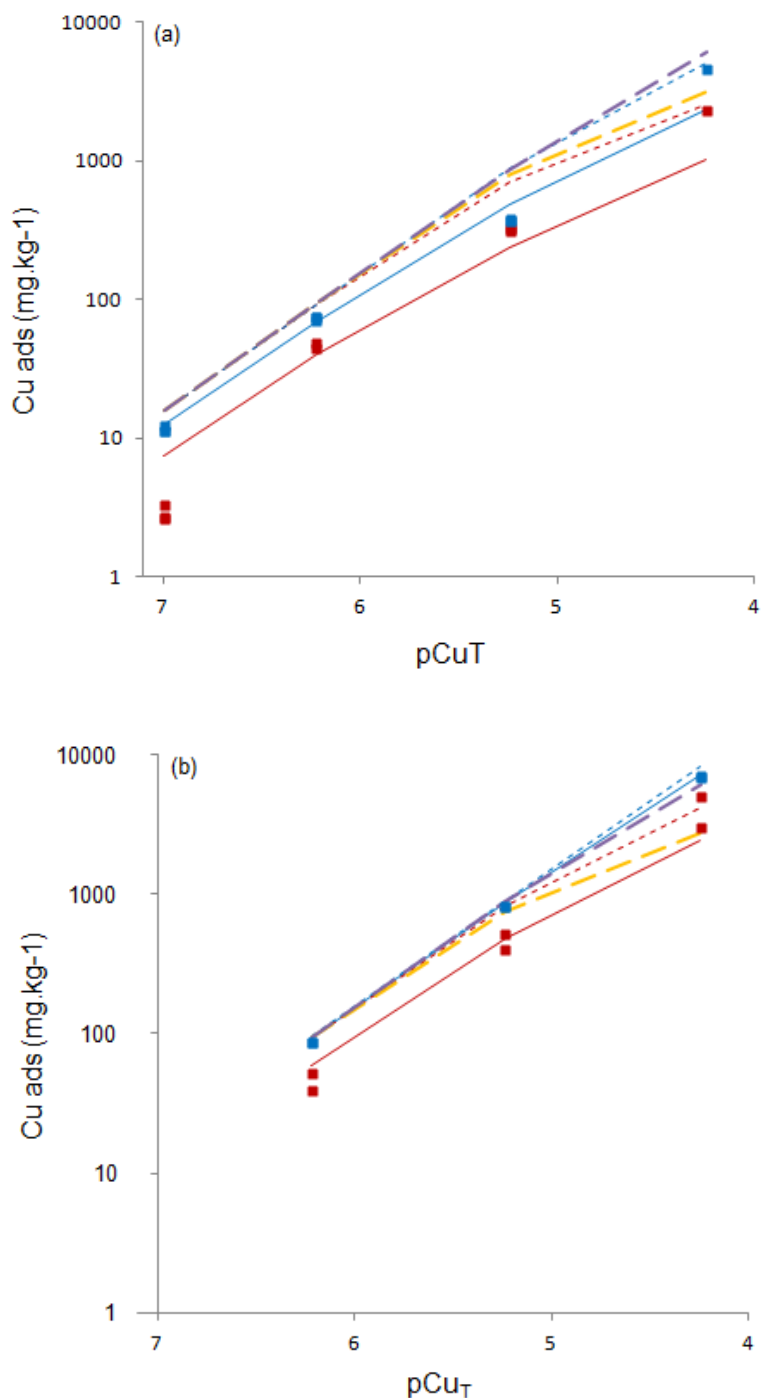


Figure 29 : Copper binding on wheat (squares, a) and tomato (circles, b) roots at an ionic strength of 0.6 mM (blue symbols) or 0.3 M (red symbols) and at pH 4.7 (± 0.2) (see experiment 2 in section II.3). Red and blue solid lines refer to simulations obtained with WHAM parameterized specifically for terrestrial higher plants (WHAM-THP). Red and blue dashed lines refer to simulations obtained with WHAM parameterized by default. Yellow and purple dashed lines refer to simulations obtained with WHAM parameterized with two humic acids defined by default.

IV.2.c. Proton competition

As pH increases, amount of Cu bound to roots would increase because root surfaces become more negatively charged, thus resulting in a lower competition between H^+ and Cu^{2+} for binding on roots (Haque et al. 2007; Bulgariu and Bulgariu 2012). Indeed, the quantity of Cu bound on wheat and tomato roots increased on average by 41% (Fig. 30a) and 16% (Fig. 30b), respectively, when pH increased. The competition between H^+ and Cu^{2+} was more pronounced for highest Cu concentration in solution and for wheat roots than for tomato roots.

At pH 6, WHAM, WHAM-2HA and WHAM-THP similarly overestimated Cu binding on wheat and tomato roots by 30% on average (Fig. 30). At pH 4, WHAM and WHAM-2HA overestimated Cu binding on wheat and tomato roots by 37% on average, except for WHAM-2HA at the highest Cu concentration in solution that adequately fit the experimental data. In comparison, WHAM-THP tended to underestimated Cu binding on wheat and tomato roots by 33% on average. Consequently, WHAM and WHAM-2HA predicted a very weak competition between H^+ and Cu^{2+} for binding on wheat and tomato roots in the range of pH 4 to 6, thus leading to a consistent overestimation of the amount of Cu bound as determined experimentally. Conversely, WHAM-THP accounted for a substantial competition between H^+ and Cu^{2+} for binding on wheat and tomato roots, even if the simulated changes in Cu bound between pH 4 and 6 overestimated the changes observed experimentally. Similarly, Wu and Hendershot (2010) had to lower the logK of Cu binding on roots of *Pisum sativum* L. by ca. 1 unit to fit the proton competitive effect from pH 4 to 6.

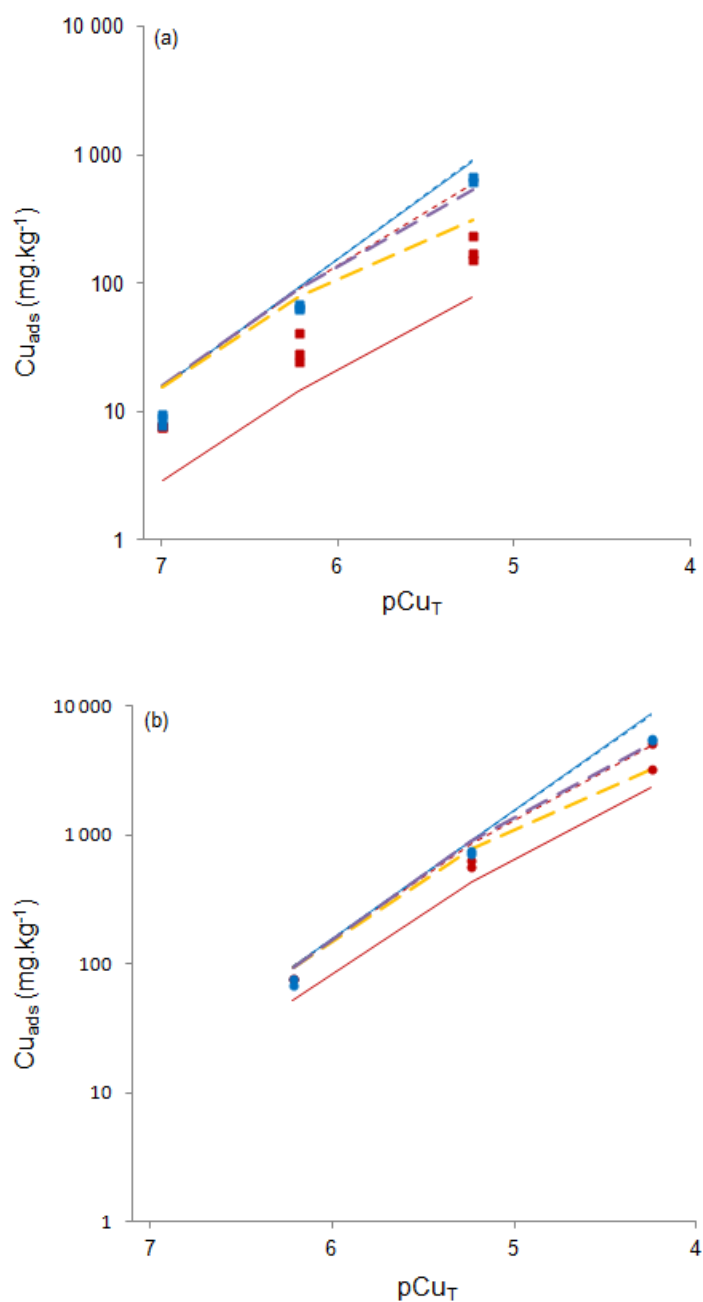


Figure 30 : Copper binding on wheat (squares, a) and tomato (circles, b) roots at pH 6.3 (± 0.1) (blue symbols) and pH 4.1 (± 0.1) (red symbols) with an ionic strength of 0.03 M (see experiment 3 in section II.3). Red and blue solid lines refer to simulations obtained with WHAM parameterized specifically for terrestrial higher plants (WHAM-THP). Red and blue dashed lines refer to simulations obtained with WHAM parameterized by default. Yellow and purple dashed lines refer to simulations obtained with WHAM parameterized with two humic acids defined by default.

IV.2.d. Calcium and zinc competition

The presence of competitor cations in solution is expected to cause a decrease in Cu binding on roots, as some binding sites would partly complex these competitor cations instead of Cu (Luo et al. 2008). While Ca concentration range exceeded Cu concentration by more than four orders of magnitude, Ca had only a low competitive effect on Cu binding on roots, as no significant decrease was observed in the amount of Cu bound to tomato roots while the decrease in the amount of Cu bound to wheat roots did not exceed 15% (Fig. 31). Zinc had a higher competitive effect than Ca on Cu binding on roots, as the quantity of Cu bound to roots decreased by ca. 30% and 18% for wheat and tomato, respectively (Fig. 31).

WHAM failed to fit correctly Cu binding on wheat and tomato roots (Fig. 31). WHAM did not predict any competition between Cu and Ca or Zn and hence overestimated Cu binding on roots in the presence of Ca or Zn by 45% and 21 % for wheat and tomato, respectively. Accounting for the actual distribution of low- vs. high-pKa sites in WHAM-2HA did not improve the fit of experimental data for tomato roots and only slightly enabled the ability of WHAM-2HA to predict Ca and Zn competitive effect for wheat roots (Fig. 31). Conversely, WHAM-THP was able to fit correctly Cu binding on wheat and tomato roots both in the presence of Ca and Zn (Fig. 31). The specific parameterization of Ca and Zn binding to wheat and tomato roots (table 6) thus enabled WHAM-THP to account for the competitive effect of Ca and Zn towards Cu, a competitive effect to which the HA parameterized by default in WHAM seems to be insensitive under the chemical conditions tested. As similarly observed for Cu binding (table 6), the major difference between the parameterization of WHAM and WHAM-THP to adequately account for the competitive effect of Ca and Zn is the value of the $\log K_{Cu,2}$ of HA_I sites (i.e. 2.3 and 4.1 for Ca and Zn, respectively) fixed by default in WHAM that was much lower than the $\log K_{Cu,1}$ and $\log K_{Cu,2}$ of HA_{II} sites (i.e. 4 and 4.5 for Ca and 6 and 6.7 for Zn) specifically defined for WHAM-THP (table 6).

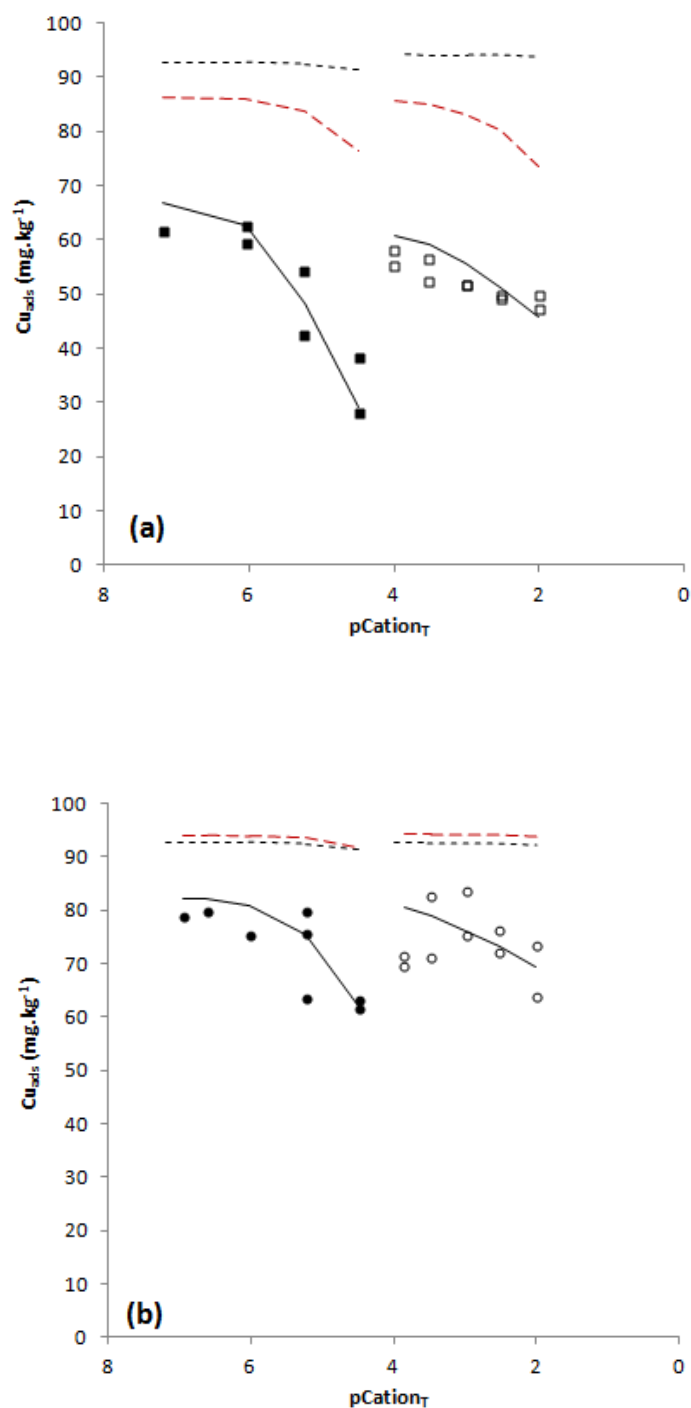


Figure 31 : Copper binding on wheat (squares, a) and tomato (circles, b) in the presence of Ca (empty symbols) and Zn (filled symbols) at an ionic strength of 0.03 M and pH 5.1 (± 0.4) and 4.7 (± 0.1), respectively. Black dashed and solid lines refer to simulations obtained with WHAM parameterized by default or specifically for terrestrial higher plants (WHAM-THP), respectively (see section III). Red dashed lines refer to simulations obtained with WHAM parameterized with two humic acids defined by default.

IV.3. Perspectives for the application of WHAM-THP in predictive ecotoxicology

In line with theoretical considerations about biotic ligands, the present study demonstrated that Cu binding on plant roots is sensitive to variations in the ionic strength, pH and the concentration of competitive metal cations such as Ca and Zn in solution. Although WHAM as configured by default was shown to be able to account satisfactorily for electrostatic effect as well as the competitive effect of proton and cations on trace metal binding on aquatic organisms (Tipping et al. 2008; Tipping and Lofts 2013), similar conclusion cannot be reached for plant roots. If WHAM was grossly able to predict Cu binding to wheat and tomato roots at a fixed pH ca. 4.5 and an ionic strength of 0.03 M, WHAM was however unable to predict Cu binding on plant roots under varying ionic strength or pH. Moreover, WHAM did not account at all for the competitive effect of Ca and Zn. These results concomitantly evidenced that the HA defined in WHAM cannot be used as a straightforward surrogate for terrestrial plant roots. Alternatively, the mathematical formalism used in WHAM can serve as a basis for the specific parameterization of HA to predict the Cu binding properties of terrestrial plant roots. Accordingly, we developed WHAM Terrestrial Higher Plants independently parameterize species model (WHAM-THP_{ips}) by parameterizing independently two HA for each plant (see chapter 6 for additional information and for model parameters). The similarity of parameters obtained for the two plants allowed to define a unique set of parameters without degrading the quality of predictions (Fig. S7 to S11). Thus, we developed WHAM-THP and then demonstrated the ability of WHAM-THP to predict adequately proton and Cu binding on wheat and tomato roots under varying ionic strength, pH and concentration of competitive Ca and Zn that were representative of the usual chemical properties of soil solution. A similar approach was implemented by Plette et al. (1995 and 1996) who successfully reparameterized the NICA-Donnan model for predicting the competitive binding of protons, calcium, cadmium and Zn on the cell walls of a soil bacterium. The main interest of WHAM-THP is to suggest a unique parameterization for both wheat and tomato. These plant species were respectively representative of monocots and dicots and accordingly their roots exhibited distinct composition and binding properties (Guigues et al. 2014). This leads to suggest that WHAM-THP could be the first step toward a more generic TBLM for plants. Nonetheless, the application of WHAM-THP in predictive ecotoxicology is still constraints by several limitations.

The main difficulty that can appear upon application of WHAM-THP relates to the parameterization of the density and the distribution of binding sites. As exemplify by tomato and wheat roots, the density of binding sites was specific to each plant species.

Potentiometric titration is the referenced procedure to finely measure the density of binding sites. However, potentiometric titration remains a laborious and time-consuming methodology in the perspective of predictive ecotoxicology. To facilitate the parameterization of WHAM-THP, we propose to determine the density of root binding sites through the determination of the root cation exchange capacity (CEC) measured with a routine procedure based on the adsorption and desorption of Cu from roots (Dufay and Braun 1986). We found a highly significant, linear relationship (Fig. S12) between the density of binding sites determined from root CEC and that determined from potentiometric titration that works for three plant species (i.e. wheat, ray-grass and tomato) and two types of root material (i.e. roots and isolated cell walls). Thus, by performing a CEC measurement and applying the proposed relationship, it is possible to estimate fairly accurately the density of root binding sites. Beyond the density of binding sites, the distribution of low- and high-pKa sites was also different for wheat and tomato roots and our attempt to parameterize WHAM-THP with a single low- to high-pKa sites ratio led to unsatisfactory fits (results not shown). If the distribution of low- and high-pKa sites may differ for each plant species, it likely also depends on the composition of root tissues, particularly that of the cell walls. The composition of root cell walls is known to be particularly different between dicots and monocots (Vogel 2008). In a first approximation, we may suggest to parameterize the low- to high-pKa sites ratio in WHAM-THP by using the ratio determined in tomato roots for dicots and in wheat roots for monocots.

To date, WHAM-THP was only tested in solution with pH below 6.5. Above this pH, Cu speciation will be progressively dominated by Cu hydroxyl species and then Cu carbonates that were not parameterized in WHAM-THP but that were suspected to be significantly involved in the induction of Cu rhizotoxicity (Wang et al. 2012a; Wang et al. 2012b). In addition, WHAM-THP was only tested for the competitive effect of proton, calcium and zinc while recent implementations of the BLM suggested that magnesium could be also an efficient competitor towards Cu (Luo et al. 2008; Wang et al. 2012a; Chen et al. 2013). A more complete parameterization of WHAM-THP for Cu and even more so for other trace metals should thus deserve further attention.

Finally, the next step in the implementation of WHAM-THP relies on its application in ecotoxicological studies related to Cu rhizotoxicity.

Acknowledgments

The authors are grateful to French Environment and Energy Management Agency (ADEME) and the French Centre of Agricultural Research for Development (CIRAD) for funding the PhD scholarship of Stéphanie Guigues and INSU (CNRS) for funding the study via the EC2CO-CYTRIX call. The authors thank Patrick Cazeveille and Claire Chevassus-Rosset (CIRAD) for their technical support during the plant growth phase, Bernard Angeletti (CEREGE) for ICP-MS analyzes.

V. Supporting information

Table S 3 : Initial (pM_T) and final/equilibrium (pM_{eq}) concentration of copper, calcium and zinc, pH measured and ionic strength (IS) fixed in each batch experiment of copper binding on wheat roots (see section II.3 for further information).

Experiment 1	pCu_T	7.3	7.3	7.3	7.3	7.3	7.3	7.3	7.3	7.3	7.2	7.2	7.1	7.1	7.0	7.0	6.8	6.8	6.7	6.7	6.4
	pCu_{eq}	8.0	8.1	8.1	8.1	8.0	8.0	8.0	7.9	7.9	7.8	7.7	7.8	7.7	7.6	7.5	7.4	7.3	7.1	7.1	6.9
	pH	5.0	4.9	4.9	4.9	4.9	4.7	4.9	4.9	4.7	4.9	4.9	4.9	4.8	4.9	4.9	4.9	4.9	4.9	4.9	4.9
	IS (M)	0.03	0.03	0.03	0.03	0.03	0.03	0.03	0.03	0.03	0.03	0.03	0.03	0.03	0.03	0.03	0.03	0.03	0.03	0.03	0.03
	pCu_T	6.4	6.2	6.2	6.0	6.0	5.7	5.7	5.5	5.5	5.2	5.2	5.0	5.0	4.7	4.7	4.5	4.5	4.2	4.2	4.0
	pCu_{eq}	6.9	6.6	6.6	6.3	6.3	6.0	6.1	5.8	5.8	5.5	5.5	5.2	5.2	4.9	4.9	4.6	4.6	4.3	4.4	4.1
	pH	4.9	4.9	4.9	4.9	4.8	4.7	4.9	4.8	4.8	4.8	4.9	4.8	4.8	4.8	4.8	4.8	4.7	4.8	4.8	4.8
	IS (M)	0.03	0.03	0.03	0.03	0.03	0.03	0.03	0.03	0.03	0.03	0.03	0.03	0.03	0.03	0.03	0.03	0.03	0.03	0.03	0.03
Experiment 2	pCu_T	7.0	7.0	7.0	6.2	6.2	5.2	5.2	5.2	4.2	7.0	7.0	7.0	6.2	6.2	6.2	5.2	5.2	5.2		
	pCu_{eq}	7.1	7.1	7.1	6.5	6.5	5.4	5.4	5.4	4.4	7.5	7.6	7.5	6.9	6.8	6.9	5.5	5.5	5.5		
	pH	4.8	4.8	4.8	4.8	4.9	4.8	4.9	5.0	4.8	4.7	4.8	4.8	4.8	4.7	/	4.8	4.7	4.8		
	IS	0.3	0.3	0.3	0.3	0.3	0.3	0.3	0.3	0.3	0.6	0.6	0.6	0.6	0.6	0.6	0.6	0.6	0.6		
Experiment 3	pCu_T	7.0	7.0	7.0	6.2	6.2	6.2	5.2	5.2	5.2	7.0	7.0	7.0	6.2	6.2	6.2	5.2	5.2			
	pCu_{eq}	7.3	7.3	7.3	6.4	6.4	6.5	5.3	5.4	5.3	7.4	7.3	7.4	6.7	6.8	6.7	5.7	5.8			
	pH	4.0	4.0	4.0	4.0	4.0	4.0	4.0	4.0	4.0	6.3	6.4	6.3	6.4	6.3	6.3	6.3	6.3			
	IS (M)	0.03	0.03	0.03	0.03	0.03	0.03	0.03	0.03	0.03	0.03	0.03	0.03	0.03	0.03	0.03	0.03	0.03			
Experiment 4 and 5	pCu_T		6.2	6.2	6.2	6.2	6.2	6.2	6.2	6.2	6.2			6.2	6.2	6.2	6.2	6.2	6.2	6.2	
	pCu_{eq}		6.6	6.6	6.6	6.6	6.6	6.6	6.5	6.6	6.5	6.6			6.7	6.7	6.7	6.6	6.5	6.4	6.5
	pM_T	Ca	4.0	4.0	3.5	3.5	3.0	3.0	2.5	2.5	2.0	2.0	Zn	7.2	6.0	6.0	5.2	5.2	4.5	4.5	
	pM_{eq}	(exp. 4)	4.7	4.7	4.2	4.2	3.7	3.7	3.1	3.1	2.2	2.3	(exp. 5)	7.2	6.0	6.0	6.0	6.0	4.6	4.6	
	pH		4.9	4.9	4.8	4.9	4.9	4.9	4.8	4.8	4.6	4.8			4.8	4.9	4.9	4.9	4.9	4.8	4.9
	IS (M)		0.03	0.03	0.03	0.03	0.03	0.03	0.03	0.03	0.03	0.03			0.03	0.03	0.03	0.03	0.03	0.03	0.03

Table S 4 : Initial (pM_T) and final/equilibrium (pM_{eq}) concentration of copper, calcium and zinc and pH measured and ionic strength (IS) fixed in each batch experiment of copper binding on tomato roots (see section II.3 for further information).

Experiment 1	pCu _T	7.3	7.3	7.3	7.3	7.2	7.2	7.2	7.2	7.2	7.2	7.1	7.1	7.1	7.1	7.0	7.0	6.8	6.8	6.6	6.6	
	pCu _{eq}	8.0	8.1	8.1	8.0	8.0	8.0	8.0	7.9	8.0	7.9	7.8	7.8	7.8	7.8	7.6	7.7	7.5	7.6	7.3	7.4	
	pH	4.5	4.6	4.6	4.7	4.6	4.6	4.6	4.6	4.6	4.6	4.6	4.6	4.6	4.5	4.5	4.5	4.6	4.6	4.6	4.6	
	IS (M)	0.03	0.03	0.03	0.03	0.03	0.03	0.03	0.03	0.03	0.03	0.03	0.03	0.03	0.03	0.03	0.03	0.03	0.03	0.03	0.03	0.03
	pCu _T	6.4	6.4	6.2	6.2	6.0	6.0	5.7	5.7	5.5	5.5	5.2	5.2	5.0	5.0	4.7	4.7	4.5	4.5	4.2	4.2	
	pCu _{eq}	7.2	7.1	7.1	7.1	6.7	6.8	6.5	6.5	6.1	6.2	5.9	5.9	5.7	5.6	5.3	5.4	5.1	5.0	4.8	4.8	
	pH	4.6	4.6	4.5	4.5	4.6	4.5	4.5	4.6	4.6	4.6	4.5	4.5	4.5	4.6	4.6	4.5	4.5	4.5	4.6	4.5	
	IS (M)	0.03	0.03	0.03	0.03	0.03	0.03	0.03	0.03	0.03	0.03	0.03	0.03	0.03	0.03	0.03	0.03	0.03	0.03	0.03	0.03	0.03
	pCu _T	4.0	4.0	3.6	3.6	3.3	3.3	3.0	3.0													
	pCu _{eq}	4.5	4.5	3.8	3.8	3.5	3.5	3.1	3.2													
pH	4.4	4.4	4.7	4.6	4.2	4.4	4.3	4.1														
IS (M)	0.03	0.03	0.03	0.03	0.03	0.03	0.03	0.03														
Experiment 2	pCu _T	6.2	6.2	5.2	5.2	4.2	4.2	6.2	6.2	5.2	5.2	4.2	4.2									
	pCu _{eq}	6.6	6.4	5.6	5.5	4.4	4.6	7.4	7.3	6.3	6.3	4.9	4.9									
	pH	5.0	5.0	4.9	4.9	4.8	4.8	4.5	4.6	4.6	4.3	4.2	4.2									
	IS	0.3	0.3	0.3	0.3	0.3	0.3	0.6	0.6	0.6	0.6	0.6	0.6									
Experiment 3	pCu _T	6.2	6.2	5.2	5.2	4.2	4.2	6.2	6.2	5.2	5.2	4.2	4.2									
	pCu _{eq}	6.9	6.9	5.7	5.8	4.6	4.4	6.8	6.9	6.0	5.9	4.7	4.7									
	pH	4.2	4.2	4.2	4.2	4.1	4.1	6.3	6.2	6.2	6.3	6.1	6.2									
	IS (M)	0.03	0.03	0.03	0.03	0.03	0.03	0.03	0.03	0.03	0.03	0.03	0.03									
Experiments 4 and 5	pCu _T		6.2	6.2	6.2	6.2	6.2	6.2	6.2	6.2	6.2			6.2	6.2	6.2	6.2	6.2	6.2	6.2	6.2	
	pCu _{eq}		6.8	6.8	6.8	7.1	7.2	6.9	6.9	6.8	6.7	6.9			7.0	7.0	6.9	7.0	6.9	6.7	6.7	
	pM _T	Ca	3.9	3.9	3.5	3.5	3.0	3.0	2.5	2.5	2.0	2.0	Zn	6.9	6.6	6.0	5.2	5.2	5.2	4.5	4.5	
	pM _{eq}	(exp. 4)	3.9	4.0	4.1	4.0	3.4	3.4	2.8	2.8	2.2	2.2	(exp. 5)	7.1	6.9	6.4	5.6	5.6	5.6	4.9	5.0	
	pH		5.2	4.9	4.7	4.6	5.5	5.6	5.5	5.8	5.6	5.7			4.7	4.7	4.6	4.6	4.6	4.6	4.5	
	IS (M)		6.2	6.2	6.2	6.2	6.2	6.2	6.2	6.2	6.2	6.2			6.2	6.2	6.2	6.2	6.2	6.2	6.2	

Table S 5 : Total site densities (L_{Hi} , $\text{cmol}_c.\text{kg}^{-1}$), proton dissociation constants (pKa_i) and distribution terms (ΔpKa_i) of wheat and tomato roots parameterized in WHAM-2HA.

	HA _I						HA _{II}						Total site density
	Type 1			Type 2			Type 1			Type 2			
	L_{H1}	pKa_1	ΔpKa_1	L_{H2}	pKa_2	ΔpKa_2	L_{H1}	pKa_1	ΔpKa_1	L_{H2}	pKa_2	ΔpKa_2	
Wheat	6.3			3.2			18.0			9.0			36.5
Tomato	31.3	4.1	2.1	15.7	4.1	2.1	33.5	8.8	3.6	16.8	8.8	3.6	97.3

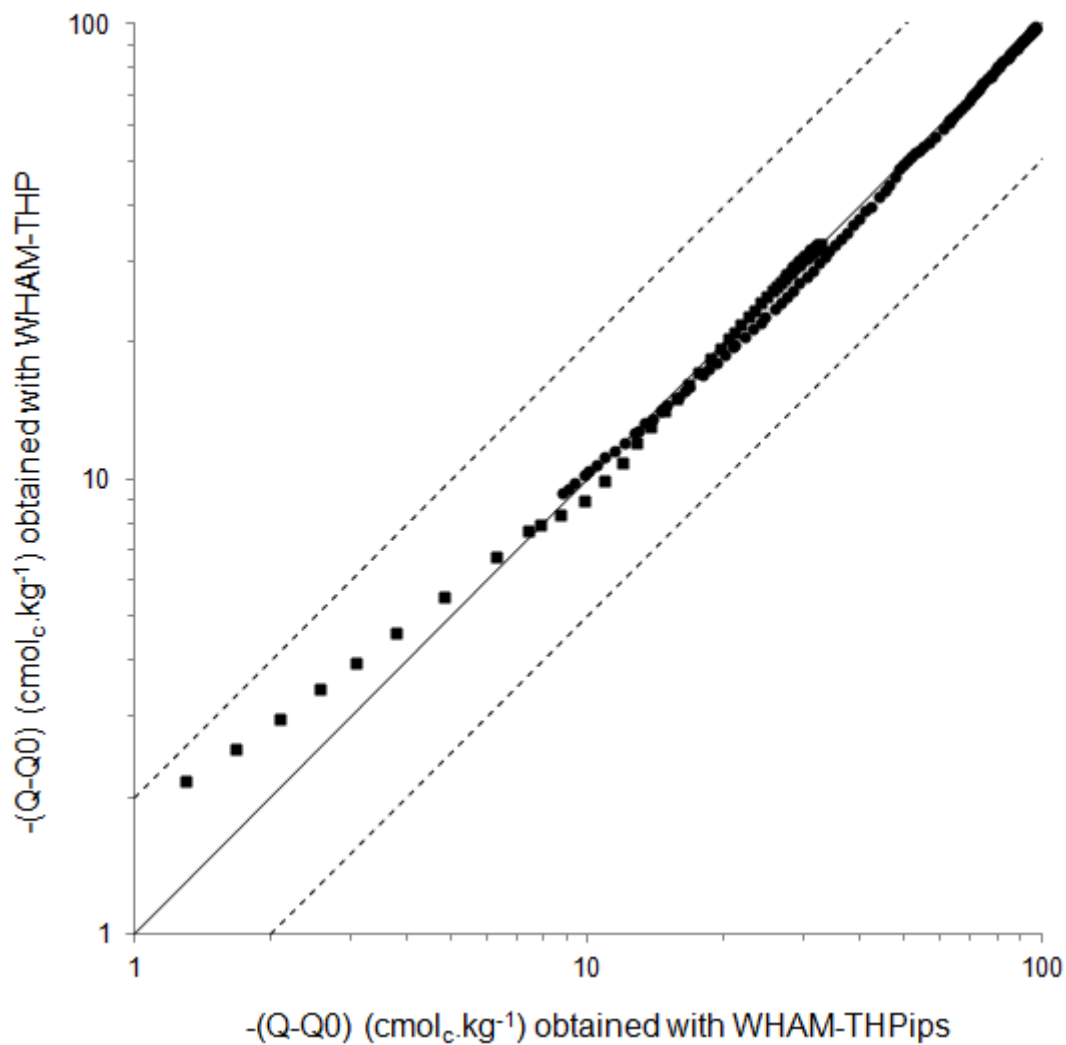


Figure S 7 : Charge borne by wheat (squares) and tomato (circles) roots as calculated with WHAM for terrestrial higher plants parameterized independently for each species (WHAM-THPips) and parameterized for both species concomitantly (WHAM-THP). Solid line refers to 1:1 line and dotted lines refer to a factor ± 2 .

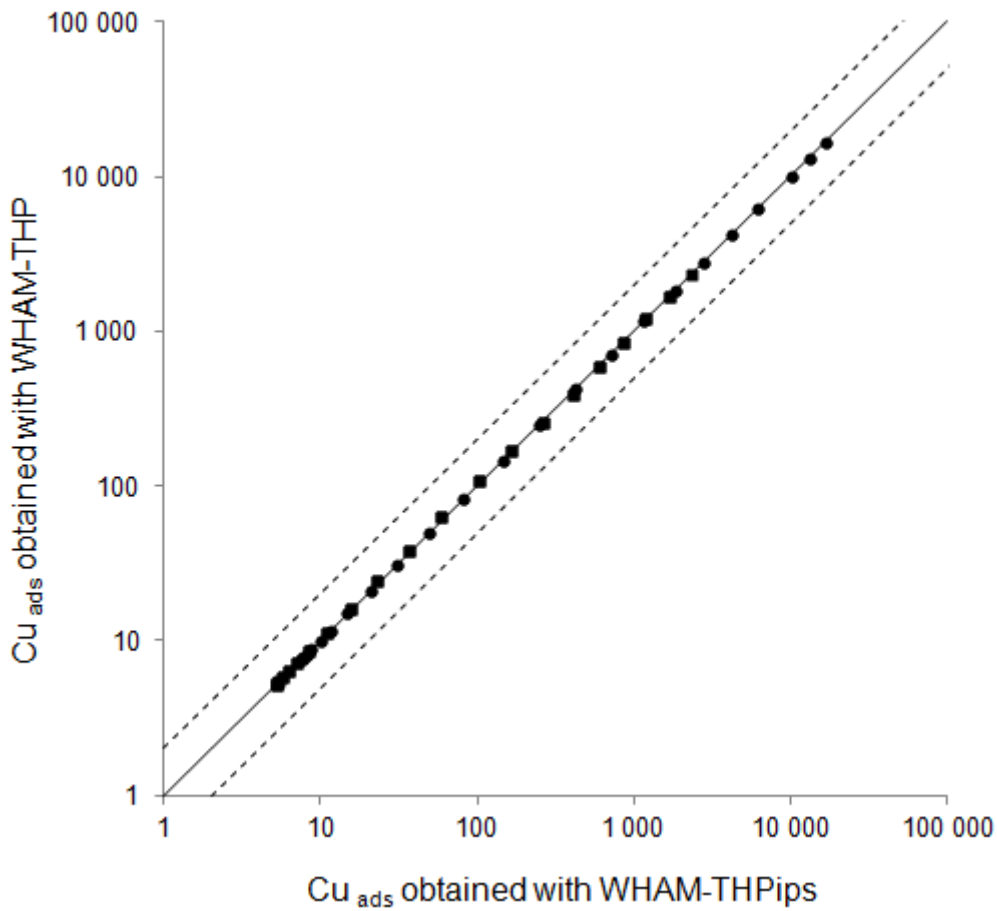


Figure S 8 : Copper adsorbed by wheat (squares) and tomato (circles) roots at pH 4.7 (± 0.2) as calculated with WHAM for terrestrial higher plants parameterized independently for each species (WHAM-THPips) and parameterized for both species concomitantly (WHAM-THP). Solid line refers to 1:1 line and dotted lines refer to a factor ± 2 .

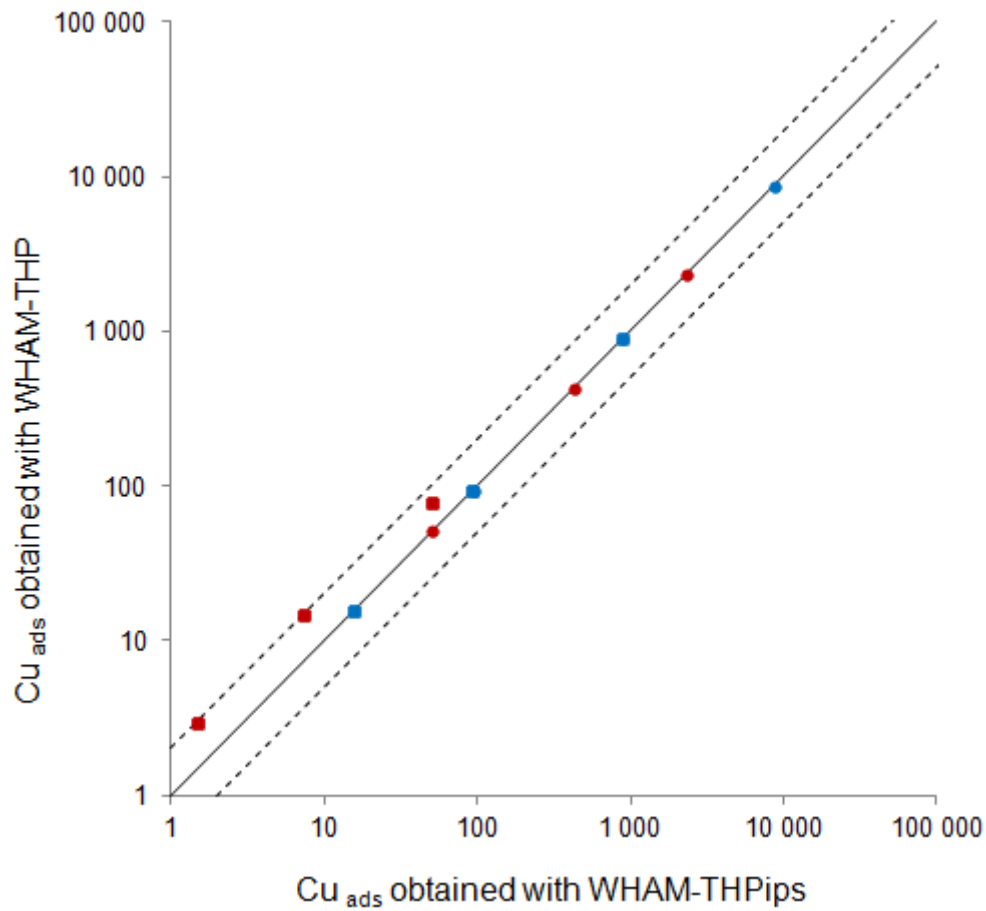


Figure S 9 : Copper adsorbed by wheat (squares) and tomato (circles) roots at different pH (pH 4.1 (± 0.1) (red) ; and pH 6.3 (± 0.1) (blue)) as calculated with WHAM for terrestrial higher plants parameterized independently for each species (WHAM-THPips) and parameterized for both species concomitantly (WHAM-THP). Solid line refers to 1:1 line and dotted lines refer to a factor ± 2 .

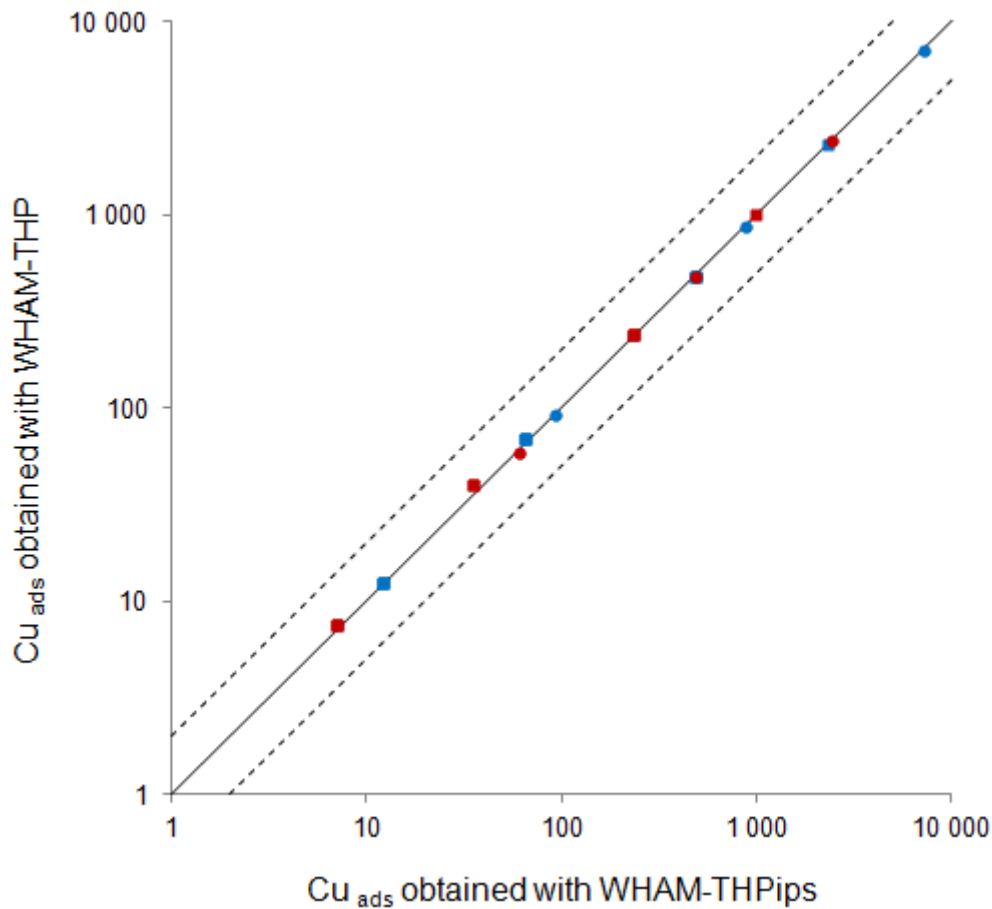


Figure S 10 : Copper adsorbed by wheat (squares) and tomato (circles) roots at different ionic strength (0.3 M (red) and 0.6 mM (blue)) as calculated with WHAM for terrestrial higher plants parameterized independently for each species (WHAM-THPips) and parameterized for both species concomitantly (WHAM-THP). Solid line refers to 1:1 line and dotted lines refer to a factor ± 2 .

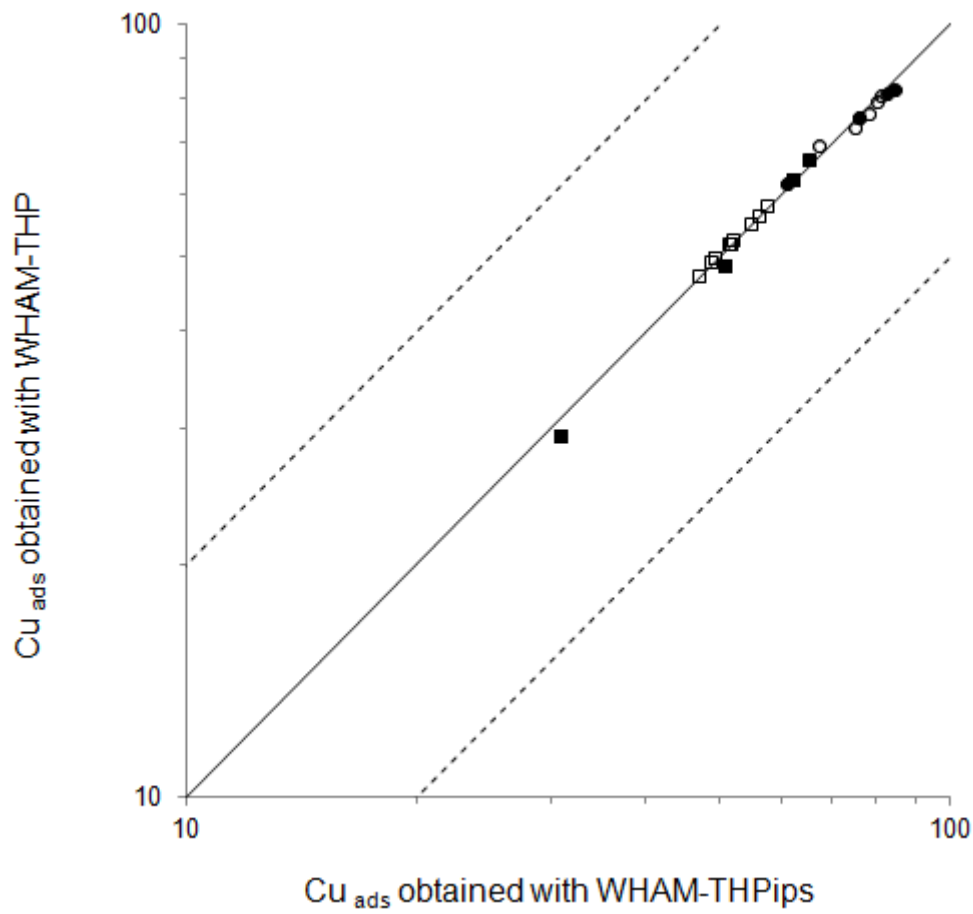


Figure S 11 : Copper adsorbed by wheat (squares) and tomato (circles) roots in presence of Zn (filled symbols) and Ca (empty symbols) as calculated with WHAM for terrestrial higher plants parameterized independently for each species (WHAM-THPips) and parameterized for both species concomitantly (WHAM-THP). Solid line refers to 1:1 line and dotted lines refer to a factor ± 2 .

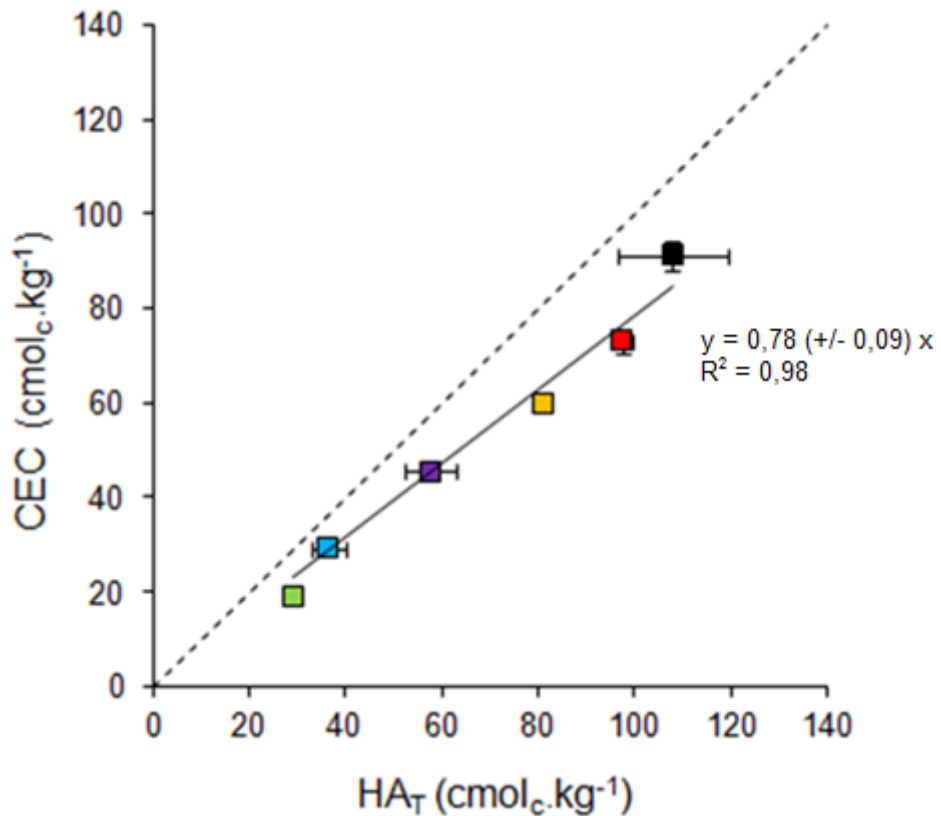


Figure S 12 : Relationship between the cation exchange capacity (CEC) and the total binding site density (HA_T) of wheat cell walls (green), wheat roots (blue), tomato cell walls (purple), ray-grass roots (yellow), tomato roots (red) and the roots of tomato sitiens mutant (black). The procedures used to isolate cell walls, to determine CEC by saturating plant materials with copper and to determine HA_T by potentiometric titration were detailed by Guigues et al. 2014. The number in parenthesis represents the 99% confidence interval.

Références bibliographiques

- Antunes PMC, Hale BA, Ryan AC (2007) Toxicity versus accumulation for barley plants exposed to copper in the presence of metal buffers: Progress towards development of a terrestrial biotic ligand model. *Environmental Toxicology and Chemistry* 26 (11):2282-2289. doi:10.1897/06-641r.1
- Antunes PMC, Scornaienchi ML, Roshon HD (2012) Copper toxicity to *Lemna minor* modelled using humic acid as a surrogate for the plant root. *Chemosphere* 88 (4):389-394. doi:10.1016/j.chemosphere.2012.02.052
- Ardestani MM, van Straalen NM, van Gestel CAM (2014) The relationship between metal toxicity and biotic ligand binding affinities in aquatic and soil organisms: A review. *Environmental Pollution* 195 (0):133-147. doi:http://dx.doi.org/10.1016/j.envpol.2014.08.020
- Brown PL, Markich SJ (2000) Evaluation of the free ion activity model of metal-organism interaction: extension of the conceptual model. *Aquatic Toxicology* 51 (2):177-194. doi:Doi: 10.1016/s0166-445x(00)00115-6
- Bulgariu D, Bulgariu L (2012) Equilibrium and kinetics studies of heavy metal ions biosorption on green algae waste biomass. *Bioresource Technology* 103 (1):489-493. doi:10.1016/j.biortech.2011.10.016
- Chen B-C, Ho P-C, Juang K-W (2013) Alleviation effects of magnesium on copper toxicity and accumulation in grapevine roots evaluated with biotic ligand models. *Ecotoxicology* 22 (1):174-183. doi:10.1007/s10646-012-1015-z
- Di Toro DM, Allen HE, Bergman HL, Meyer JS, Paquin PR, Santore RC (2001) Biotic ligand model of the acute toxicity of metals. 1. Technical Basis. *Environmental Toxicology and Chemistry* 20 (10):2383-2396. doi:10.1002/etc.5620201034
- Dufey JE, Braun R (1986) Cation Exchange Capacity of Roots : Tirtation Sum of Exchangeable Cations, Copper Adsorption. *Journal of Plant Nutrition* 9 (8):1147-1155
- Erickson RJ (2013) The biotic ligand model approach for addressing effects of exposure water chemistry on aquatic toxicity of metals: Genesis and challenges. *Environmental Toxicology and Chemistry* 32 (6):1212-1214. doi:10.1002/etc.2222
- Fry SC, Miller JG, Dumville JC (2002) A proposed role for copper ions in cell wall loosening. *Plant and Soil* 247 (1):57-67. doi:10.1023/a:1021140022082
- Ginn BR, Szymanowski JS, Fein JB (2008) Metal and proton binding onto the roots of *Fescue rubra*. *Chemical Geology* 253 (3-4):130-135. doi:10.1016/j.chemgeo.2008.05.001
- Guigues S, Bravin M, Garnier C, Masion A, Doelsch E (2014) Isolated cell walls exhibit cation binding properties distinct from those of plant roots. *Plant and Soil*:1-13. doi:10.1007/s11104-014-2138-1
- Haque MN, Morrison GM, Perrusquía G, Gutierréz M, Aguilera AF, Cano-Aguilera I, Gardea-Torresdey JL (2007) Characteristics of arsenic adsorption to sorghum biomass. *Journal of Hazardous Materials* 145 (1-2):30-35. doi:10.1016/j.jhazmat.2006.10.080

- Harmsen J (2007) Measuring Bioavailability: From a Scientific Approach to Standard Methods. *J Environ Qual* 36 (5):1420-1428. doi:10.2134/jeq2006.0492
- Hooda PS (2010) Trace Elements in Soils. Blackwell Publishing, Ltd
- Iwasaki Y, Cadmus P, Clements WH (2013) Comparison of different predictors of exposure for modeling impacts of metal mixtures on macroinvertebrates in stream microcosms. *Aquatic Toxicology* 132–133 (0):151-156. doi:http://dx.doi.org/10.1016/j.aquatox.2013.02.007
- Kopittke PM, Blamey FPC, Asher CJ, Menzies NW (2010) Trace metal phytotoxicity in solution culture: a review. *Journal of Experimental Botany* 61 (4):945-954. doi:10.1093/jxb/erp385
- Kopittke PM, Menzies NW, Wang P, McKenna BA, Wehr JB, Lombi E, Kinraide TB, Blamey FPC (2014) The rhizotoxicity of metal cations is related to their strength of binding to hard ligands. *Environmental Toxicology and Chemistry* 33 (2):268-277. doi:10.1002/etc.2435
- Luo X-S, Li L-Z, Zhou D-M (2008) Effect of cations on copper toxicity to wheat root: Implications for the biotic ligand model. *Chemosphere* 73 (3):401-406. doi:10.1016/j.chemosphere.2008.05.031
- Milne CJ, Kinniburgh DG, van Riemsdijk WH, Tipping E (2003) Generic NICA–Donnan Model Parameters for Metal-Ion Binding by Humic Substances. *Environmental Science & Technology* 37 (5):958-971. doi:10.1021/es0258879
- Mishra B, Boyanov M, Bunker BA, Kelly SD, Kemner KM, Fein JB (2010) High- and low-affinity binding sites for Cd on the bacterial cell walls of *Bacillus subtilis* and *Shewanella oneidensis*. *Geochimica et Cosmochimica Acta* 74 (15):4219-4233. doi:http://dx.doi.org/10.1016/j.gca.2010.02.019
- Paquin PR, Gorsuch JW, Apte S, Batley GE, Bowles KC, Campbell PGC, Delos CG, Di Toro DM, Dwyer RL, Galvez F, Gensemer RW, Goss GG, Hogstrand C, Janssen CR, McGeer JC, Naddy RB, Playle RC, Santore RC, Schneider U, Stubblefield WA, Wood CM, Wu KB (2002) The biotic ligand model: a historical overview. *Comparative Biochemistry and Physiology Part C: Toxicology & Pharmacology* 133 (1-2):3-35. doi:10.1016/s1532-0456(02)00112-6
- Plette ACC, Benedetti MF, van Riemsdijk WH (1996) Competitive Binding of Protons, Calcium, Cadmium, and Zinc to Isolated Cell Walls of a Gram-Positive Soil Bacterium. *Environmental Science & Technology* 30 (6):1902-1910. doi:10.1021/es950568l
- Plette ACC, van Riemsdijk WH, Benedetti MF, van der Wal A (1995) pH Dependent Charging Behavior of Isolated Cell Walls of a Gram-Positive Soil Bacterium. *Journal of Colloid and Interface Science* 173 (2):354-363. doi:DOI: 10.1006/jcis.1995.1335
- Sattelmacher B (2001) The apoplast and its significance for plant mineral nutrition. *New Phytologist* 149 (2):167-192. doi:10.1046/j.1469-8137.2001.00034.x
- Slaveykova VI, Wilkinson KJ (2005) Predicting the Bioavailability of Metals and Metal Complexes : Critical Review of the Biotic Ligand Model. *Environmental chemistry* 2:9-24

- Thakali S, Allen HE, Di Toro DM, Ponizovsky AA, Rooney CP, Zhao F-J, McGrath SP (2006) A Terrestrial Biotic Ligand Model. 1. Development and Application to Cu and Ni Toxicities to Barley Root Elongation in Soils. *Environmental Science & Technology* 40 (22):7085-7093. doi:10.1021/es061171s
- Tipping E (1998) Humic Ion-Binding Model VI: An Improved Description of the Interactions of Protons and Metal Ions with Humic Substances. *Aquatic Geochemistry* 4 (1):3-47. doi:10.1023/a:1009627214459
- Tipping E, Lofts S (2013) Metal mixture toxicity to aquatic biota in laboratory experiments: Application of the WHAM-FTOX model. *Aquatic Toxicology* 142–143 (0):114-122. doi:http://dx.doi.org/10.1016/j.aquatox.2013.08.003
- Tipping E, Lofts S, Sonke JE (2011) Humic Ion-Binding Model VII: a revised parameterisation of cation-binding by humic substances. *Environmental chemistry* 8 (3):225-235. doi:http://dx.doi.org/10.1071/EN11016
- Tipping E, Vincent CD, Lawlor AJ, Lofts S (2008) Metal accumulation by stream bryophytes, related to chemical speciation. *Environmental Pollution* 156 (3):936-943. doi:http://dx.doi.org/10.1016/j.envpol.2008.05.010
- Vidali R, Remoundaki E, Tsezos M (2011) An Experimental and Modelling Study of Cu²⁺ Binding on Humic Acids at Various Solution Conditions. Application of the NICA-Donnan Model. *Water, Air, & Soil Pollution* 218 (1-4):487-497. doi:10.1007/s11270-010-0662-z
- Vogel J (2008) Unique aspects of the grass cell wall. *Current Opinion in Plant Biology* 11 (3):301-307. doi:http://dx.doi.org/10.1016/j.pbi.2008.03.002
- Wang P, Menzies N, Wang Y-M, Zhou D-M, Zhao F-J, Kopittke P (2012a) Identifying the species of copper that are toxic to plant roots in alkaline nutrient solutions. *Plant and Soil* 361 (1-2):317-327. doi:10.1007/s11104-012-1260-1
- Wang P, Zhou D, Kinraide TB, Luo X, Li L, Li D, Zhang H (2008) Cell Membrane Surface Potential (ψ_0) Plays a Dominant Role in the Phytotoxicity of Copper and Arsenate. *Plant Physiol* 148 (4):2134-2143. doi:10.1104/pp.108.127464
- Wang X, Hua L, Ma Y (2012b) A biotic ligand model predicting acute copper toxicity for barley (*Hordeum vulgare*): Influence of calcium, magnesium, sodium, potassium and pH. *Chemosphere* 89 (1):89-95. doi:10.1016/j.chemosphere.2012.04.022
- Wu Y, Hendershot W (2009) Cation Exchange Capacity and Proton Binding Properties of Pea (<i>Pisum sativum</i> L.) Roots. *Water, Air, & Soil Pollution* 200 (1):353-369. doi:10.1007/s11270-008-9918-2
- Wu Y, Hendershot WH (2010) The effect of calcium and pH on nickel accumulation in and rhizotoxicity to pea (*Pisum sativum* L.) root—empirical relationships and modeling. *Environmental Pollution* 158 (5):1850-1856. doi:10.1016/j.envpol.2009.10.046

Rapport-gratuit.com 
LE NUMERO 1 MONDIAL DU MÉMOIRES

Rapport-gratuit.com 
LE NUMERO 1 MONDIAL DU MÉMOIRES

CONCLUSION ET PERSPECTIVES

Depuis quelques années, les études développant ou employant un modèle de prédiction de la toxicité se multiplient. Parmi les formalismes mathématiques actuellement disponibles, le Biotic Ligand Model (BLM, ou Terrestrial BLM lorsqu'il est utilisé pour des études de toxicité menées sur des organismes terrestres) fait figure de référence et est, de ce fait, le plus utilisé. En particulier, le TBLM s'avère être un modèle adapté à l'étude d'effets toxiques chez les plantes. En effet, dans ce modèle, la réponse biologique observée est supposée être engendrée par la complexation de l'élément trace avec les ligands biotiques situés à la surface de l'organisme cible ([Thakali et al. 2006](#)), tout comme les effets rhizotoxiques observés sont supposés être engendrés par la complexation de l'élément trace sur les surfaces racinaires ([Kopittke et al. 2014](#)).

Lorsqu'elles sont considérées individuellement, les études employant le TBLM donnent des résultats prometteurs. Cependant, leur comparaison révèle souvent un manque de généralité de certains des paramètres et les cas particuliers où l'application du TBLM est limitée se multiplient. Ces limites trouvent leur origine dans la formulation d'hypothèses trop simplificatrices, résultant d'une connaissance encore incomplète des mécanismes générant l'effet toxique. La solution, pour dépasser ces limites et ainsi améliorer les modèles de prédiction, est de ne pas se contenter d'une simple application du formalisme mathématique classique du BLM pour l'ajustement de données expérimentales de toxicité mais de revenir à l'étude des mécanismes ([Erickson 2013](#)).

C'est dans ce contexte que s'inscrivent mes travaux de recherche dont l'objectif principal était de proposer une démarche de modélisation différente, centrée sur les réactions de complexation se produisant à la surface de l'organisme cible plutôt que sur l'effet toxique observé. Cette approche a été employée pour prédire l'adsorption du cuivre sur les racines de deux plantes modèles, le blé et la tomate, sélectionnées pour la capacité contrastée de leurs racines à complexer les cations métalliques. L'étude de la nature et des propriétés des sites de complexation du Cu des racines a permis de valider les paramètres obtenus par modélisation.

Complexation du cuivre dans les racines

D'après la littérature, les propriétés de complexation des racines peuvent être attribuées aux groupements fonctionnels portés principalement soit par les parois apoplasmiques (et en particulier par les polysaccharides pectiques) soit par les membranes plasmiques (Kinraide 2004 ; Krzeslowska 2011). Les études portant sur ce sujet sont peu nombreuses et uniquement consacrées à l'un ou à l'autre de ces compartiments de sorte que leur contribution respective dans les propriétés de complexation des surfaces racinaires n'a jamais été définie.

La première étape a donc été de caractériser la réactivité des racines des deux plantes modèles, c'est-à-dire localiser et identifier les sites réactifs racinaires. Nous avons ainsi montré que l'isolement des parois apoplasmiques entraîne une diminution de la capacité de complexation des racines, d'un facteur 2,4 pour le blé et d'un facteur 3,4 pour la tomate. Ces résultats révèlent une contribution majoritaire du matériel racinaire ayant disparu lors de l'isolation des parois apoplasmiques, à savoir les membranes plasmiques, dans les propriétés de complexation racinaire. Cette contribution a été évaluée à hauteur de 60 % dans les racines de blé et de 70 % dans les racines de tomate. Cette diminution de capacité de complexation après isolement a été accompagnée de la perte de groupements chimiques caractéristiques tels que des groupements carboxyliques, amines et phosphates. Ces groupements, portés par les protéines et les phospholipides des membranes plasmiques, sont donc impliqués dans les propriétés de complexation des racines. Ainsi, contrairement à ce qui est communément supposé, les groupements carboxyliques des polysaccharides pectiques, et d'une façon générale l'ensemble des groupements portés par les parois apoplasmiques, contribue pour moins de 50 % dans la capacité de complexation des racines des deux plantes étudiées.

Toutefois, les contributions respectives des parois apoplasmiques et des membranes plasmiques dans les propriétés de complexation des racines que nous avons déterminées sont fondées sur l'hypothèse que la réactivité des parois apoplasmiques est similaire en présence et en l'absence de membranes plasmiques. Il serait intéressant de vérifier cette hypothèse, en étudiant d'une part les parois apoplasmiques et les membranes plasmiques séparément et d'autre part, en étudiant les racines « entières ». Le protocole employé dans ces travaux pour isoler les parois apoplasmiques semble convenir et pourrait donc être à nouveau utilisé. En effet, nous avons montré qu'il ne restait plus aucune trace des membranes plasmiques après la procédure d'isolation et que le protocole n'entraînait pas de dégradation des polysaccharides pariétaux. L'isolation des membranes plasmiques est

également possible ; il s'agit d'ailleurs du matériel végétal classiquement employé pour le développement du modèle électrostatique (Wang et al. 2008).

Une autre possibilité, pour étudier la contribution respective des parois apoplasmiques et des membranes plasmiques dans les propriétés de complexation racinaire, est de procéder à une localisation de l'élément cible (par exemple Cu) au sein des racines grâce à une technique d'imagerie. Une étude aussi fine devrait pouvoir être réalisée grâce à la nanoSIMS (nano-scale Secondary Ion Mass Spectrometry), une technique analytique qui offre une résolution spatiale élevée combinée à une analyse élémentaire très sensible (Herrmann et al. 2007). A ce jour, les études nano-SIMS sont surtout employées pour étudier la distribution des éléments entre le compartiment apoplasmique et le compartiment symplasmique, néanmoins la distinction entre parois apoplasmiques et membranes plasmiques semble possible (Moore et al. 2011).

La seconde étape de ces travaux a été dédiée à l'étude de la complexation du cuivre au sein des racines. Même s'il est parfois détecté dans le milieu symplasmique, le cuivre est connu pour être un élément s'accumulant préférentiellement dans le compartiment extracellulaire à savoir le continuum parois apoplasmiques – faces externes des membranes plasmiques (Colzi et al. 2011). Nous avons donc cherché, parmi les sites réactifs identifiés précédemment, ceux qui participent à la complexation du cuivre. Nous avons montré que plus de 50 % des sites participant à sa complexation sont situés dans les parois apoplasmiques. Etant donné que la densité de sites des parois apoplasmiques est moins élevée que celle des membranes plasmiques, cette contribution majoritaire des parois apoplasmiques dans la complexation du Cu peut provenir d'une plus grande affinité du Cu pour les sites pariétaux des racines de blé et de tomate que pour les sites membranaires. Une autre explication pourrait être directement liée à la géométrie des racines, Cu rencontrant en premier lieu les parois apoplasmiques et, seulement après avoir traversé ces dernières, les membranes plasmiques. L'organisation spatiale des tissus racinaires serait, dans ce cas, déterminante. Il n'est pas exclu, cependant, qu'il s'agisse d'une action conjointe de ces deux hypothèses. Nous avons également montré que plus de la moitié des sites racinaires participant à la complexation du Cu ont une réactivité assimilable à un groupement amine, seulement 40 % environ présentent une réactivité proche de celle d'un acide carboxylique. Cette constatation a été confortée par la spéciation du cuivre identifiée dans les racines. En effet, Cu a été trouvé sous la forme de Cu(II)-O/N organique de façon très légèrement prépondérante par rapport à la forme Cu(II)-O organique c'est-à-dire associé à des acides aminés pouvant être enchâssés soit dans les parois apoplasmiques en association avec des polysaccharides pariétaux, soit au niveau des membranes plasmiques.

De tels résultats modifient significativement la vision actuelle du mécanisme conduisant à la génération d'effets rhizotoxiques. En effet, il est communément admis que la complexation des éléments traces avec les groupements carboxyliques portés par les polysaccharides pariétaux en est la principale cause, les autres groupements fonctionnels présents dans les racines étant supposés avoir une contribution minoritaire (Krzeslowska 2011). Une contribution significative d'autres composés, tels que les protéines, dans la complexation du Cu au sein de racines pourrait expliquer l'incohérence entre la rhizotoxicité observée pour Cu et l'échelle d'affinité avec les ligands forts proposée par Kopittke et al. 2014.

Validité du modèle WHAM-THP pour prédire l'adsorption du cuivre dans les racines

Développés en parallèle du BLM, d'autres modèles de complexation sont utilisés pour prédire les effets toxiques des éléments traces pour les organismes aquatiques. Ces modèles emploient des formalismes mathématiques initialement développés pour étudier la complexation des éléments traces avec les matières organiques naturelles de type substances humiques. Le formalisme mathématique du modèle WHAM est le plus employé actuellement. Ce modèle semble être un outil adéquat pour prédire la toxicité des éléments traces pour les organismes aquatiques (Tipping et al. 2008 ; Antunes et al. 2012) mais il n'avait encore jamais été employé pour des études de complexation menées avec des plantes supérieures.

Contrairement au cas des organismes aquatiques, le modèle WHAM tel qu'initialement paramétré ne s'est pas avéré efficace pour prédire la réactivité des racines. Nous avons montré que cela provenait d'une part de la distribution imposée des sites réactifs (ratio de sites présentant un pK_a faible et un pK_a élevé fixe) et d'autre part de la valeur des constantes, définies initialement pour des substances humiques. Le développement d'un modèle plus complexe a donc été nécessaire pour prédire correctement la complexation du Cu dans les racines de blé et de tomate. Le modèle WHAM-Terrestrial Higher Plants (WHAM-THP) a été capable de prédire l'adsorption du Cu dans les racines de blé et de tomate pour différents pH, différentes forces ioniques et en présence des deux cations compétiteurs que sont Ca et Zn. Malgré les différences de propriétés de complexation observées entre les racines de blé et de tomate, il a été possible d'établir un jeu de paramètres commun pour ces deux espèces. Nous avons également cherché à rendre l'application du modèle la plus simple possible en proposant une relation mathématique permettant de déterminer, rapidement et sans équipement spécifique, la densité totale de sites racinaire.

Le modèle WHAM-THP a donné des résultats prometteurs pour modéliser des réactions de complexation du Cu au sein des racines de blé et tomate. Cependant, son usage reste encore très limité et il serait intéressant d'étendre son domaine d'application. En premier lieu, il serait intéressant de compléter le modèle existant pour Cu. En effet, WHAM-THP ne permet, à ce jour, que de représenter l'adsorption du Cu sur une gamme de pH allant jusqu'à 6,5. Au-delà, la spéciation du Cu est plus diversifiée (CuOH^+ , CuHCO_3 , CuOH_2 , etc.) et les constantes de complexation de ces espèces de Cu n'ont pas été déterminées. L'hypothèse d'une participation d'autres espèces métalliques que l'ion libre dans l'induction d'un effet toxique tend à se confirmer au travers de différentes études (Wang et al. 2009 ; Wang et al. 2012). L'ajout de nouvelles constantes de complexation pour d'autres espèces de Cu permettra une application plus étendue du modèle. De même, Cu avait été sélectionné comme élément modèle dans cette étude mais le modèle WHAM-THP doit être développé pour d'autres éléments traces (par exemple, Pb, Ni ou Cd) et testé sur d'autres espèces végétales (par exemple l'orge, qui est une plante modèle souvent employée dans les études TBLM). Le protocole employé pour réaliser les expérimentations en batch est simple et efficace et devrait permettre l'acquisition rapide de nouveaux jeux de données. La description des propriétés acides, communes au blé et à la tomate, doit pouvoir être appliquée à n'importe quelle autre plante, l'utilisateur n'ayant qu'à déterminer la densité totale de sites. De même, le logiciel WHAM, à partir duquel sont obtenus les résultats de modélisation, permet de définir d'autres espèces chimiques très simplement.

Il serait également nécessaire d'éprouver la capacité du modèle WHAM-THP à prédire l'adsorption de Cu dans les racines de blé et de tomate lorsque ces plantes sont exposées à une contamination en cuivre. En effet, la principale critique qui peut être faite à ces travaux de recherche est l'absence de résultats *in vivo*. En effet, ces travaux ont été menés avec du matériel végétal racinaire ne présentant pas d'activité biologique. Une telle configuration nous a permis d'axer notre étude sur les réactions de complexation se produisant dans les racines tout en nous affranchissant des phénomènes d'absorption. Mais le modèle WHAM-THP doit pouvoir être employé pour prédire la fraction de Cu adsorbé dans les racines d'une plante exposée à une contamination. Cela nécessite donc de réaliser une étape intermédiaire qui est de valider les constantes de complexation pour le blé et la tomate ou d'estimer un écart entre les prédictions et les observations expérimentales de façon à affiner le modèle. Pour commencer, une culture hydroponique devrait permettre de contrôler assez finement les conditions expérimentales. La quantité de Cu adsorbée dans les racines de blé et de tomate, après exposition à une contamination, pourra directement être comparée à la prédiction du modèle WHAM-THP.

Références bibliographiques

- Antunes PMC, Scornaienchi ML, Roshon HD (2012) Copper toxicity to *Lemna minor* modelled using humic acid as a surrogate for the plant root. *Chemosphere* 88 (4):389-394. doi:10.1016/j.chemosphere.2012.02.052
- Colzi I, Doumett S, Del Bubba M, Fornaini J, Arnetoli M, Gabbrielli R, Gonnelli C (2011) On the role of the cell wall in the phenomenon of copper tolerance in *Silene paradoxa* L. *Environmental and Experimental Botany* 72 (1):77-83. doi:DOI: 10.1016/j.envexpbot.2010.02.006
- Erickson RJ (2013) The biotic ligand model approach for addressing effects of exposure water chemistry on aquatic toxicity of metals: Genesis and challenges. *Environmental Toxicology and Chemistry* 32 (6):1212-1214. doi:10.1002/etc.2222
- Herrmann AM, Ritz K, Nunan N, Clode PL, Pett-Ridge J, Kilburn MR, Murphy DV, O'Donnell AG, Stockdale EA (2007) Nano-scale secondary ion mass spectrometry — A new analytical tool in biogeochemistry and soil ecology: A review article. *Soil Biology and Biochemistry* 39 (8):1835-1850. doi:http://dx.doi.org/10.1016/j.soilbio.2007.03.011
- Kinraide TB (2004) Possible Influence of Cell Walls upon Ion Concentrations at Plasma Membrane Surfaces. Toward a Comprehensive View of Cell-Surface Electrical Effects upon Ion Uptake, Intoxication, and Amelioration. *Plant Physiol* 136 (3):3804-3813. doi:10.1104/pp.104.043174
- Kopittke PM, Menzies NW, Wang P, McKenna BA, Wehr JB, Lombi E, Kinraide TB, Blamey FPC (2014) The rhizotoxicity of metal cations is related to their strength of binding to hard ligands. *Environmental Toxicology and Chemistry* 33 (2):268-277. doi:10.1002/etc.2435
- Krzyszowska M (2011) The cell wall in plant cell response to trace metals: polysaccharide remodeling and its role in defense strategy. *Acta Physiologiae Plantarum* 33 (1):35-51. doi:10.1007/s11738-010-0581-z
- Moore KL, Schröder M, Wu Z, Martin BGH, Hawes CR, McGrath SP, Hawkesford MJ, Feng Ma J, Zhao F-J, Grovenor CRM (2011) High-Resolution Secondary Ion Mass Spectrometry Reveals the Contrasting Subcellular Distribution of Arsenic and Silicon in Rice Roots. *Plant Physiology* 156 (2):913-924. doi:10.1104/pp.111.173088
- Thakali S, Allen HE, Di Toro DM, Ponizovsky AA, Rooney CP, Zhao F-J, McGrath SP (2006) A Terrestrial Biotic Ligand Model. 1. Development and Application to Cu and Ni Toxicities to Barley Root Elongation in Soils. *Environmental Science & Technology* 40 (22):7085-7093. doi:10.1021/es061171s
- Tipping E, Vincent CD, Lawlor AJ, Lofts S (2008) Metal accumulation by stream bryophytes, related to chemical speciation. *Environmental Pollution* 156 (3):936-943. doi:http://dx.doi.org/10.1016/j.envpol.2008.05.010
- Wang P, Menzies N, Wang Y-M, Zhou D-M, Zhao F-J, Kopittke P (2012) Identifying the species of copper that are toxic to plant roots in alkaline nutrient solutions. *Plant and Soil* 361 (1-2):317-327. doi:10.1007/s11104-012-1260-1

- Wang P, Zhou D, Kinraide TB, Luo X, Li L, Li D, Zhang H (2008) Cell Membrane Surface Potential (ψ_0) Plays a Dominant Role in the Phytotoxicity of Copper and Arsenate. *Plant Physiol* 148 (4):2134-2143. doi:10.1104/pp.108.127464
- Wang X, Ma Y, Hua L, McLaughlin MJ (2009) Identification of hydroxyl copper toxicity to barley (*Hordeum vulgare*) root elongation in solution culture. *Environmental Toxicology and Chemistry* 28 (3):662-667. doi:10.1897/07-641.1

Rapport-Gratuit.com

RÉSUMÉ

Cette étude a été consacrée au développement d'une nouvelle approche de modélisation de la phytodisponibilité des éléments traces, basée sur leurs réactions de complexation au sein des racines des plantes. Cette approche a été développée pour prédire l'adsorption du cuivre (Cu) sur les racines de deux plantes, le blé et la tomate. Plusieurs techniques analytiques (titrages acido-basiques, résonance magnétique nucléaire du carbone 13, spectroscopie d'absorption des rayons X) ont été employées et croisées avec les résultats de modélisation. Dans un premier temps, la réactivité des racines a été caractérisée. Les racines étant constituées de parois apoplasmiques et de membranes plasmiques, la contribution respective de ces deux compartiments aux propriétés de complexation des racines a été évaluée. L'étude a ensuite été focalisée sur la complexation du Cu au sein des racines et sur l'évolution de cette complexation en fonction des conditions physico-chimiques du milieu (pH, force ionique, cations compétiteurs). Grâce aux résultats obtenus sur la caractérisation des racines et à l'acquisition d'un jeu varié de données expérimentales sur la complexation du Cu, le modèle a pu être paramétré. Il a été montré que les propriétés de complexation des racines de blé et de tomate proviennent conjointement des membranes plasmiques et des parois apoplasmiques. La spéciation du Cu au sein des racines était partagée, de façon presque égale, entre les composés pectiques des parois apoplasmiques et les protéines enchâssées à la fois dans les parois apoplasmiques et les membranes plasmiques. Un modèle propre aux racines a pu être développé sur la base d'un modèle existant dédié à la réactivité des substances humiques. Le modèle WHAM-Terrestrial Higher Plants, présenté dans cette étude, est un premier pas vers un nouvel outil d'évaluation de la disponibilité des éléments traces pour les plantes.

SUMMARY

This study has been dedicated to the development of a new modeling approach of trace element phytoavailability, focusing on binding reactions between trace element and plant roots. This approach was used to predict copper (Cu) adsorption on wheat and tomato roots. Several analytical techniques (acid-base titrations, nuclear magnetic resonance of carbon 13, X-ray absorption spectroscopy) were used and crossed with modeling results. At first, plant root reactivity was characterized. Because plant roots consist of cell walls and plasma membranes, the relative contribution of these two compartments in root binding properties was evaluated. The study was then focused on Cu binding reactions on roots and the effects of physico-chemical conditions (pH, ionic strength, presence of cations) on copper binding. The model has been set thanks to results on root characterization obtained and the acquisition of a set of experimental data on Cu binding. It has been shown that binding properties of wheat and tomato roots came from both cell walls and plasma membranes. Copper speciation in roots was shared, almost evenly, between cell wall pectic compounds and proteins embedded in cell walls and plasma membranes. A model, specific to plant roots, has been developed on the basis of a current model dedicated to the humic substances reactivity. The WHAM-Terrestrial Higher Plants model presented in this study is a first step towards a new tool for assessing the availability of trace elements for plants.